Dissertation zur Erlangung des akademischen Grades des Doktors der Naturwissenschaften (Dr.rer.nat.) im Fachbereich 18 der Universität Kassel

Synthesis and Characterization of Novel Spiro-Starburst-Structures as Blue Light Emitters and Zeolites

Dissertation

Submitted in the fulfilment of the requirement for the degree

Doctor of Natural Science (Dr. rer. nat.)

in the field of Natural Science "Macro Molecular Chemistry and Molecular Materials" in Fachbereich 18 of Kassel University

by

Mandira Devi Shrestha Saiju

Kathmandu, Nepal

Dissertation Day: 14.04.2009

Kassel

Declaration / Erklärung

“I herewith certify that I made this thesis independently, without any disallowed assistance and I did not use others than the aid as indicated in this thesis. I marked all places, which are literally or in a general manner taken out of published or unpublished books or articles. No part of this thesis has been previously submitted in support of an application for any other degree or qualification in this or other university.”

„Hiermit versichere ich, daß ich die vorliegende Dissertation selbständig und ohne unerlaubte Hilfe angefertigt und andere als die in der Dissertation angegebenen Hilfsmittel nicht benutzt habe. Alle Stellen, die wörtlich oder sinngemäß aus veröffentlichten oder unveröffentlichten Schriften entnommen sind, habe ich als solche kenntlich gemacht. Kein Teil dieser Arbeit ist in einem anderen Promotions- oder Habilitationsverfahren verwendet worden.“

Kassel, 19.12.2008

First Supervisor: Prof. Dr. J. Salbeck
Second Supervisor: Prof. Dr. U. Siemeling

Acknowledgement

I would like to express my gratitude towards all the persons who have helped me or stayed along my side during this work.

First, I would like to thank Prof. Dr. Josef Salbeck for giving me this great opportunity to work in his research group and encouraging me with his valuable suggestions.

I express my gratitude to Dr. Martin Maurer for NMR-spectroscopic measurements, Dr. Sven Fuehrmeier for mass spectroscopic analysis of all the substances that have been synthesized in this work.

I thank my colleagues Achim Siebert for helping me to handle HPLC and with softwares of DSC and TGA, worthy suggestion for some synthesises and Mrs. Ayna Schaefler for CV measurements.

Special thanks to Dr. Rainer Bausch, Herrn Priv.-Doz. Dr. Thomas Fuhrmann-Lieker, Dipl.-Chem. Thomas Ebert and Maria Kiuski for a friendly cooperation during practical supervision.

This work was of course not possible without the kind help, friendly atmosphere and warm hospitality from my fellow co-workers of research groups of Prof. Dr. Siemeling and Prof. Dr. Faust and collaborators.

I appreciate the help from Dr. Christoph Ayasse, Dr. Manfred Kussler, and Dr. Tobat Saragi for fruitful discussions and company for lunch during this work.

Thanks to Dr. Clemens Bruhn for crystal structure analysis and Herrn H. Schüller (University of Regensburg) for CH-analysis.

I am grateful to Dr. Bjoern Pampuch and Dr. Kirstin Kahlke (solving the problem faced during fly back to Germany from Poland!!) for being very kind, nice and helping to me and working extra for correcting my thesis!

I am in debt of Prof. Dr. Nikolaos Risch and all friends in Paderborn University who supported my confidence to achieve this destination.

I admire the support given to me from all my teachers, friends of my whole academic life who contributed one way or the other in fulfilling this task.

I sincerely thank to Mrs. Helga Walter (Oma) and Mr. Werner Walter (Opa) for being like own grandparents to our son Raymond. Their very caring and homely atmosphere made my further study possible.

I owe a great deal to my family. My father Govinda Lal Shrestha, mother Ram Sundari, elder brother Sagar and younger brother anand, who supported me in every situation in life, provided me with the best things they have and took a good care of me. I hope I live up to their expectation and make them proud.

I feel immensely grateful to my husband Dr. Eng. Rajesh Saiju for inspiring and bolstering me to make my dream true.

A hearty thank you to……

……our lovely son Raymond for making us always happy.

Thank you!

Abstract

Spiro-starburst-structures with symmetric globular structures in forms of first and second generations that readily form stable amorphous glasses have been synthesized and then characterised in this work. During the synthesis of these materials, possibilities of the extension of the chains of the phenyl rings in 2,2',7 and 7'-positions of the central core of the spirobifluorene as well as the 2',7 and 7'-positions of the terminal spirobifluorene units of the spiro-starburst-structures have been investigated so that solubilities and morphologies of the compounds are not negatively influenced. Their morphological properties have been explored by recording their decomposition temperature and glass transition temperature. These compounds possessing two perpendicular arrangement of the two molecular halves show high glass transition temperature (T_g), which is one of the most important parameter indicating the stability of the amorphous state of the material for optoelectronic devices like organic light emitting diodes. Within the species of second generation compounds, for example, 4-spiro[3] shows the highest T_g (330 °C) and the highest branching degree. When one [4B(SBF)SBF-SBF **84**] or two [4SBFSBF-SBF **79**] terminal spirobifluorene units are removed, the T_g decreases to 318 °C and 307 °C respectively. Photo absorption and fluorescence spectra and cyclic voltammetry measurements are taken in account to characterize the optoelectronic properties of the compounds. Spiro-starburst-structures emit radiation in the blue region of the visible spectrum. The peak maxima of absorption and emission spectra are observed to be at higher wavelength in the molecules with longer chromophore chains than in the molecules with shorter chromophore chains. Excitation spectra are monitored with their emission peak maxima. The increasing absorbing species in molecule leads to increasing molar extinction coefficient. In the case of 4B(TP)SBF-SBF **53** and 4B(SBF)SBF-SBF **84**, the greater values of the molar extinction coefficients ($43*10^4$ and $44*10^4$ L mol^{-1} cm^{-1} respectively) are the evidences of the presence of four times octiphenyl conjugation rings and eight times terminal fluorene units respectively. The optical properties of solid states of these compounds in the form of thin film indicate that the intermolecular interaction and aggregation of individual molecules in neat amorphous films are effectively hindered by their sterically demanding structures. Accordingly, in solid state, they behave like isolated molecules in highly dilute solution. Cyclic voltammetry measurements of these compounds show electrochemically reversibility and stability. Furthermore, the zeolitic nature (host-guest) of the molecular sieve of the synthesized spiro-starburst-structures has been analysed by thermogravimetric analysis method.

Full Forms of

(I) Abbreviated Subjective Expression

• APCI	Atmospheric Pressure Chemical Ionization
• ATR	Attenuated Total Reflection
• CV	Cyclic Voltammetry
• DSC	Differential Scanning Calorimetry
• ESI	Electro Spray Ionisation
• KPG	Kerngezogenes Präzisions-Glasgerät
• HOMO	Highest Occupied Molecular Orbital
• LUMO	Lowest Unoccupied Molecular Orbital
• h	hour
• HPLC	High Performance Liquid Chromatography
• IR	Infra Red
• *J*	Coupling constant (^{1}H-NMR)
• MALDI	Matrix Assisted Laser Desorption Ionisation
• min	Minute
• MS	Mass Spectroscopy
• NMR	Nuclear Magnetic Resonance
• OLED	Organic Light Emitting Diode
• RT	Room Temperature
• r. b.	round bottom
• TGA	Thermo Gravimetric Analysis
• T_{cry}	Crystallization Temperature
• T_d	Decomposition Temperature
• T_g	Glass Transition Temperature
• T_m	Melting Temperature (point)
• UV-Vis	Ultraviolett-Visible Spectroscopy

(II) Abbreviated Chemical Substances

- DCM — Dichloromethane
- DMSO — Dimethylsulfoxide
- EtOH — Ethanol
- Fc/Fc^{+} — Ferrocene/Ferrocenium
- HCl — Hydrochloric Acid
- KCN — Kaliumcyanide
- NMP — N-Methyl-2-pyrrolidone
- $Pd(OAc)_2$ — Palladium(II)acetate
- $P(Ph)_3$ — Triphenylphosphine
- THF — Tetrahydrofurane

1 Introduction

The scope of organic electronics has become almost unlimited in the fields of physics and chemistry. Up to only a short time ago, organic electronic and its optical phenomena have been the domain of "pure research", somewhat removed from practical application.[1] This situation changed dramatically in the mid 1980s, when Tang and van Slyke at Kodak[2] demonstrated a low voltage and efficient thin film light emitting diode. Since that first demonstration, organic electronics have proven useful in a number of applications. The most successful electronic and optoelectronic devices are, for example, OLEDs (Organic Light Emitting Diodes), low cost and effective organic photovoltaic devices, organic field-effect transistors (OFETS) and so on. Compared to inorganic semiconductors (Si, Ge, As, GaN or SiC) organic materials offer several advantages such as light weight, potentially low cost and capability of thin-film, large-area, flexible plastic substrate-like device fabrication. OLEDs have found practical applications in small displays as in mobile phones, digital camera finders and car audios. Current research aims at replacing liquid crystal displays (LCD) in flat panel televisions. Furthermore, OLEDs are promising candidates for future lighting applications.

All the devices described above involve charge transport as an essential operating process and hence require charge-transporting materials. Charge transporting materials are mostly based on π-electron systems, which are characterized by properties such as light absorption and emission in the ultraviolet- to visible- wavelength region, charge-carrier generation and transport, and so forth. Organic charge transporting materials include both small molecules, that is, molecular materials and polymers. Recent development has acquired small organic molecules that readily form stable amorphous glasses. This has enabled the studies of charge transport in the amorphous glassy state of these molecules without any binder polymers.

Charge transporting materials with different morphologies have been used depending on the kind of devices. Single crystal growth on the plane of a large substrate for device applications is not easy. However, grain size, grain boundaries, and molecular orientations of micro-crystalline materials affect the devices' performance. Amorphous materials are preferable to crystalline materials in device fabrication because of their transparency and homogeneity. An important group of small amorphous molecules like 2,2',7,7'-Tetrakis-(N,N-diphenylamino)-9,9'-spirobifluorene (spiro-TAD) known as charge–transporting material has been synthesized

by Salbeck and his research team in 1996. Introduction of a spiro-linkage into this molecule reduces its crystallization tendency and improves the morphological stability of the material.[3, 4, 5, 6]

The spiro compounds consist of two individual π-systems, which are connected to each other by an sp^3-hybridized spiro carbon atom. These π-systems are independent to one another, although an orbital interaction, so-called spiro conjugation, takes place in the excited state.[7, 8] The simplest representative example of such spiro compound is spirobifluorene (figure 1.1), which is formed by two biphenyl systems.

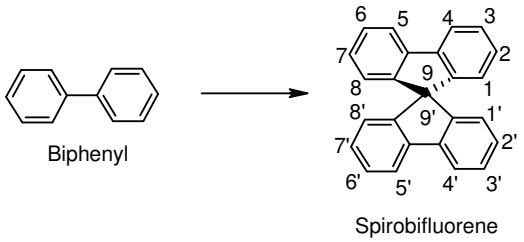

Figure 1.1 Spirobifluorene; Numbering of the ring system.

Compared to the non-spiro-linked parent compounds, the corresponding spiro compounds offer benefits like rigidity of structure and higher solubility. These are results of the high steric demand which is caused by the perpendicular arrangement of the two molecular halves. Furthermore, spiro compounds show high glass transition temperature (T_g), which is one of the most important parameter indicating the stability of the amorphous state of the material for optoelectronic devices. High T_gs prevent amorphous materials from crystallizing caused by the heat generated during the devices' application. Thus, they reduce the degradation of devices.

2 Problem Formulation

When an amorphous film is heated above T_g, molecular motion increases rapidly, allowing the transition into the crystalline state. Therefore it is of utmost importance to design the molecular structure in such a way that a high T_g is achieved. A relationship between molecular structure and stability of the amorphous state was shown by Naito and Miura.[9,10] They found that molecules with a symmetric globular structure, large molecular weight and small intermolecular cohesion result in a high stability of the amorphous state. Several concepts addressing this issue have been proposed, including the development of dendritic architectures[11] and tetrahedral structures.[12]

A focusing point of this work is to synthesize and characterize low molecular amorphous materials, their various derivatives with symmetric globular structures in the form of spiro-starburst-structures to further investigate their high T_g.

The aim of this work is also to investigate the possibility of the extension of the chains of the phenyl rings in 2,2',7 and 7'-positions of the central core of the spirobifluorene as well as the 2',7 and 7'-positions of the terminal spirobifluorene units of the spiro-starburst-structures (figure 2.1) so that the solubilities and morphologies of the compounds are not negatively influenced.

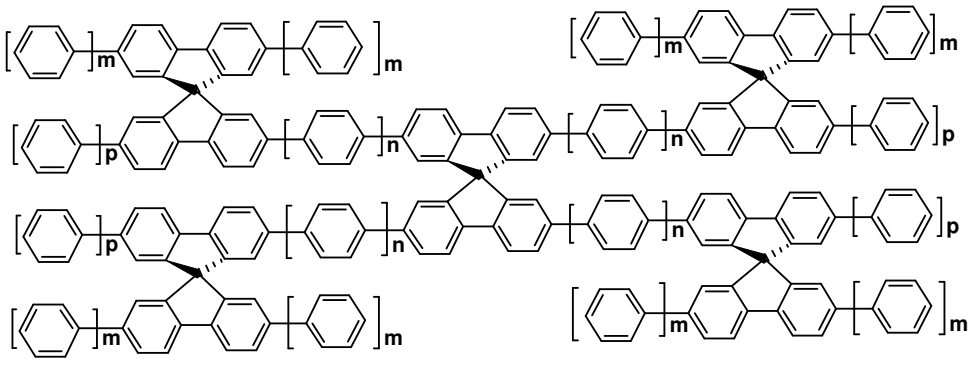

Figure 2.1 Spiro-starburst-structures with variously extended phenyl rings in the terminal spirobifluorene units as well as between terminal spirobifluorene and the central core spirobifluorene.

The synthesized products are to be characterized by Nuclear Magnetic Resonance (NMR) and Mass Spectrometry (MS). The organic glasses are further characterized by analyzing their morphology. To explore their morphological properties, decomposition temperature and glass transition temperature are measured. Photo absorption and fluorescence spectra and cyclic voltammetry measurements are methods to characterize the optoelectronic properties of the compounds.

Furthermore, the zeolitic nature of the molecular sieve of the synthesized spiro-starburst-structures is to be analysed.

3 General Parts

3.1 Optoelectronics

The term “optoelectronic devices” is by now used for devices in which both electrons and photons are essential for their operation, as a natural evolution from the definitions of electronic devices that involved only electrons and holes in their operation and of photonic devices that involved only photons in their operation.[13]

In its simplest form, an optoelectronic device consists of a light emitting diode (LED), for signal transmission, and a photo sensor for signal reception. The transmitter takes the electrical signal and converts it into a beam of modulated visible light or infrared. This beam travels across a transparent gap and is picked up by the “receiver” which converts the modulated light or IR back into an electrical signal.

3.2 Organic Glass

The material glass is very old, well known and a type of material that is neither stable nor metastable. The glassy state is a non-equilibrium state of matter. There is still much about the molecular physics and thermodynamics of glass which is not well understood but a general account of glass is thought to be the following case:

Many solids have a crystalline structure on microscopic scales. The molecules are arranged in a regular lattice. As the solid is heated the molecules vibrate about their position in the lattice until, at the melting point, the crystal breaks down and the molecules start to flow. There is a sharp distinction between the solid and the liquid state, which is separated by a first order phase transition, i. e. a discontinuous change in the properties of the material such as density and heat capacity. Freezing is marked by a release of heat known as the heat of fusion.

A liquid has viscosity, a measure of its resistance to flow. The viscosity of water at room temperature is about 0.01 poises. Thick oil might have a viscosity of about 1.0 poise. As a liquid is cooled, its viscosity normally increases, but viscosity also has a tendency to prevent crystallization. Usually when a liquid is cooled to below its melting point, crystals form and it

solidifies but sometimes it can become super cooled and remain liquid below its melting point because there are no nucleation sites to initiate the crystallization. If the viscosity rises enough as it is cooled further, it may never crystallize. The viscosity rises rapidly and continuously, forming thick syrup and eventually an amorphous solid. The molecules then have a disordered arrangement but sufficient cohesion to maintain some rigidity. In this state, it is often called an amorphous solid or glass. The term "amorphous", consistent with its Greek roots, is descriptive of any condensed phase. "Glassy" is considered to be descriptive of a very restricted class of amorphous materials. A useful definition of what constitutes a glass has been given by the National Research Council Ad Hoc Committee on Infrared Transmitting Materials. It suggests a glass is an x-ray amorphous solid which exhibits glass transition. [14]

3.3 Glass Transition Temperature

Glass transition is defined as that phenomenon in which a solid amorphous phase exhibits with changing temperature a more or less sudden change in the derivative thermodynamic properties, such as heat capacity and expansion coefficient, from crystal-like to liquid-like values. The temperature of the transition is called the glass (transition) temperature and denoted by T_g.[15]

The exact temperature at which these changes are observed depends on the type of measurement used to detect them. If the measurement is performed slowly, e. g. over a period of several minutes, then the property changes will be detected at a significantly lower temperature than if the measurement is performed very quickly. This is because the changes of thermodynamic properties depend on changes in the internal structure of the amorphous phase, which occur slowly near T_g. The glass transition phenomenon is observed when this "structural relaxation time" becomes commensurate with the time scale of the experiment. Because this structural relaxation time also determines the magnitude of the liquid state viscosity, the glass transition temperature is usually associated with a particular value of the viscosity. The popular idea that T_g is the temperature at which the liquid viscosity reaches 10^{13} poise is based on thermodynamic measurements (density, refractive index) carried out on time scales of many minutes.[14]

Above the glass temperature, the amorphous phase has the thermodynamic properties of the liquid state, hence is referred to as being in the "supercooled liquid" as distinct from the

"glassy" state. In fact, there is a second order transition between the supercooled liquid state and the glass state. The transition is not as dramatic as the phase change which occurs from liquid to crystalline solids (figure 3.1). There is no discontinuous change of density and no latent heat of fusion. The transition can be detected as a marked change in the thermal expansivity and heat capacity of the material.

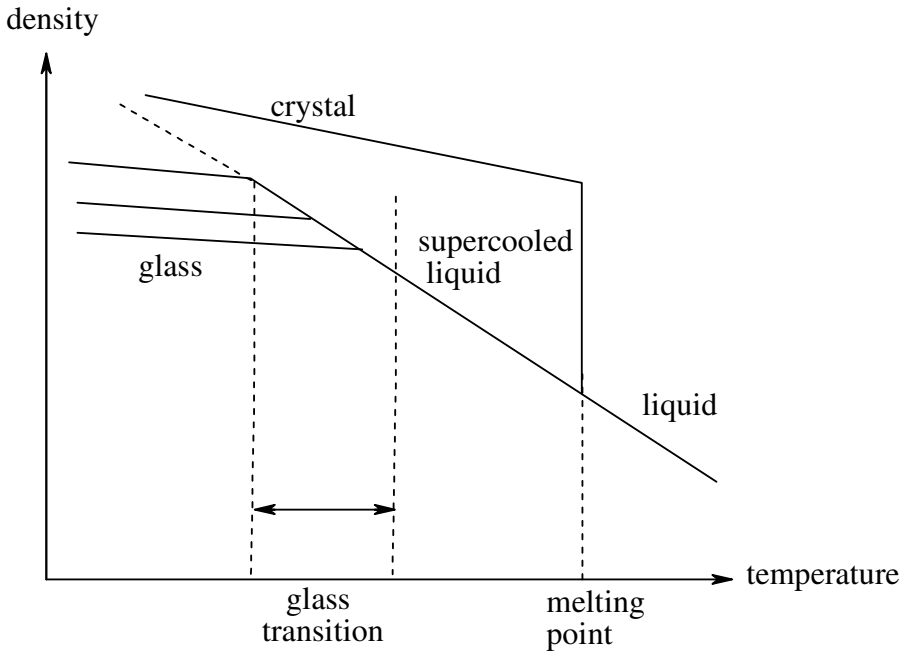

Figure 3.1 Density as a function of temperature in the phases of glassy materials.[14]

3.3.1 Conditions for Glass Formation

The relation between crystallization, kinetics and glass forming ability and a new lattice energy based interpretation of why certain compounds and not others fulfil these conditions can be explained as below:

Whether or not a given liquid crystallizes during cooling before T_g is reached is strictly a kinetic problem involving the rate of nucleation and growth of crystals on the one hand and the rate at which thermal energy may be extracted from the cooling liquid on the other hand.

At least two types of energy barrier may be involved in the metastability of the supercooled liquid. These two types of barrier consist of :

(1) The energy barrier to crystal nucleus formation arises essentially because the melting point of small crystals is lower than that of large ones. Thus, in any supercooled liquid, crystals smaller than a certain size are unstable, so that in order to form a stable nucleus one must first form crystallites having higher free energies than the same amount of liquid.

(2) The free energy barrier to crystal growth, on the other hand, is simply that which prevents the movement of a molecule at a crystal-liquid interface from a liquid-like position to crystal-like position.[16] According to Kauzmann, the ratio of the glass transition temperature (in degrees absolute) of a supercooled liquid is approximately two-third of the normal melting point. This ratio is identical for organic, inorganic, simple and polymeric materials. Beaman performed many systematic experiments with various materials like *n*-propyl alcohol, selenium, glycerol, glucose, linear polymers like polydimethylsiloxane, natural rubber etc.[17] He formulated a rule which is known as Boyer-Beaman Rule.

$$\frac{T_g[K]}{T_m[K]} \approx \frac{2}{3} \qquad 3.1$$

Where T_g[K] is glass transition temperature in Kelvin and T_m[K] is melting point in Kelvin. Here, it should be emphasized that the melting point is the equilibrium crystalline melting point and not the temperature at which the material appears molten.

3.4 Characterization of Organic Glasses

3.4.1 Decomposition Temperature

Vapour deposition is the most convenient way to fabricate organic electronic devices. In this process, the material is vaporized in vacuum. Therefore, it is important for the compounds to be highly thermally stable.

To determine the thermal stability of the materials, one uses the thermo gravimetric analysis (TGA). It is a process in which the loss of weight of a material is recorded as a function of temperature in nitrogen gas atmosphere whilst the compound is subjected to a controlled temperature program.[18] When the material starts decomposing, vaporization of the decomposed part takes place and thus causes the loss of weight.

3.4.2 Determination of Glass Transition Temperature

Any experiment, by means of which a material property is determined, has a characteristic time scale related to the time taken to probe the system and observe the result. This is of the order of seconds for a scanning calorimetry heat capacity determination, 10-12 seconds for a dielectric relaxation experiment. On the other hand, any material system when subjected to some influence which disturbs its state of equilibrium takes a certain time to recover the equilibrium state.[15]

The Differential Scanning Calorimetry (DSC) is a technique to examine thermal transitions of the spiro-linked glass materials synthesized in this work. DSC measures the rate of heat flow. It is a process in which the difference in energy inputs into a compound and a reference material is measured as a function of temperature whilst the compound and reference are subjected to a controlled temperature program.[18] This technique leads to the study of thermally induced phenomena like phase change, phase transition, melt temperature and reactions (exo- or endothermic) as well as temperature dependent properties like heat capacities and thermal stability.

Before using the instrument for the analysis of targeted properties of the materials, a temperature calibration of scanning calorimeters is done with respect to inert reference compounds[19] like cyclopentane, indium, lithium sulphate or gold. In thermal equilibrium, the oven, probe and the inert reference material have the same temperature, so the temperature of the probe and the reference can be determined independent of each other. A constant flow of inert gas like argon or nitrogen rinses the oven continuously. As reference, compounds are used which do not expose any change in the range of observed temperature. During the measurement, the oven is heated at a constant rate of a controlled temperature program. The different heat capacities of the probe and the reference cause different temperatures in the probe and the reference compound. This means a disturbance of the stationary state. The effect can be either endothermic or exothermic, leading to either upward or downward peaks, respectively (figure 3.2). The temperature range that can be measured by DSC-instrument is between –180-800 °C with a heating rate of 5-20 °C/min.

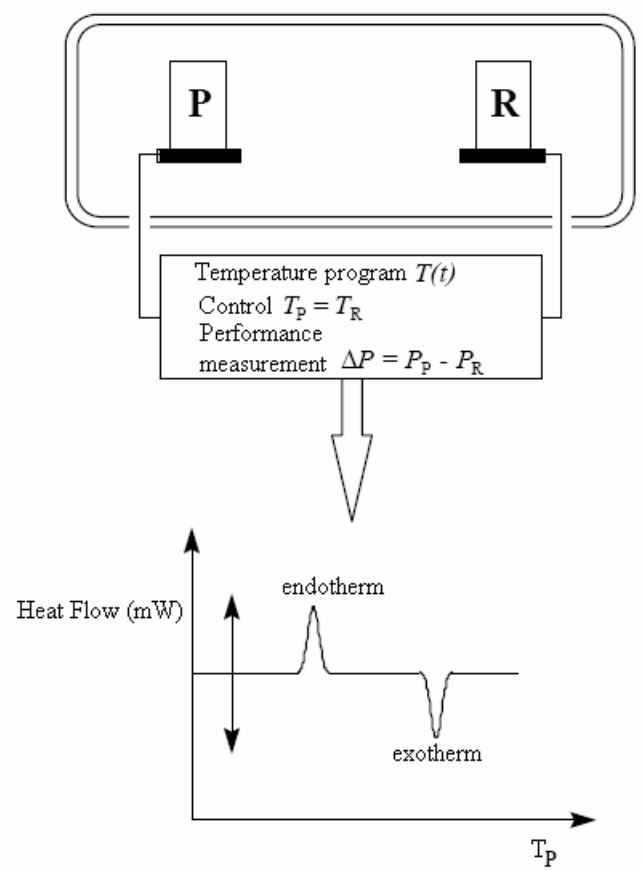

Figure 3.2 Schematic representation of experimental set-up of DSC. (P Probe, R Reference substance).

In a typical DSC experiment, about 10 mg of probe compound and reference substance are taken in two small pans and capsuled with their covers. In case of corrosive probe compounds, gold capsules are prepared. These capsules are heated in an oven just over the melting point of the probe compound as first heating step. This is necessary because the probe compounds do not possess well defined phase states but can be crystalline, partial crystalline or amorphous. Further, the melting point of the probe compound leads to maximum thermal contact between the probe and the capsule, which results in the better resolution.[20]

By rapid cooling of the probe after the first heating cycle, it remains in the amorphous state. Then in the second heating process, the glass transition temperature can be observed after subtracting the base line (obtained by heating two empty capsules at the same rate as that for the probe). Depending on the tendency of the probe to crystallize, the crystallization can be observed as an exothermic signal following the glass transition temperature of the probe. Further heating reveals the melting point of the probe, which is characterized as an endothermic signal. In case of a probe with low crystallization tendencies, the T_g becomes

observable only in the second heating cycle and the exo- or endothermic signals may be due to phase changes between two solid phases caused by chemical reactions or decomposition processes (figure 3.3).

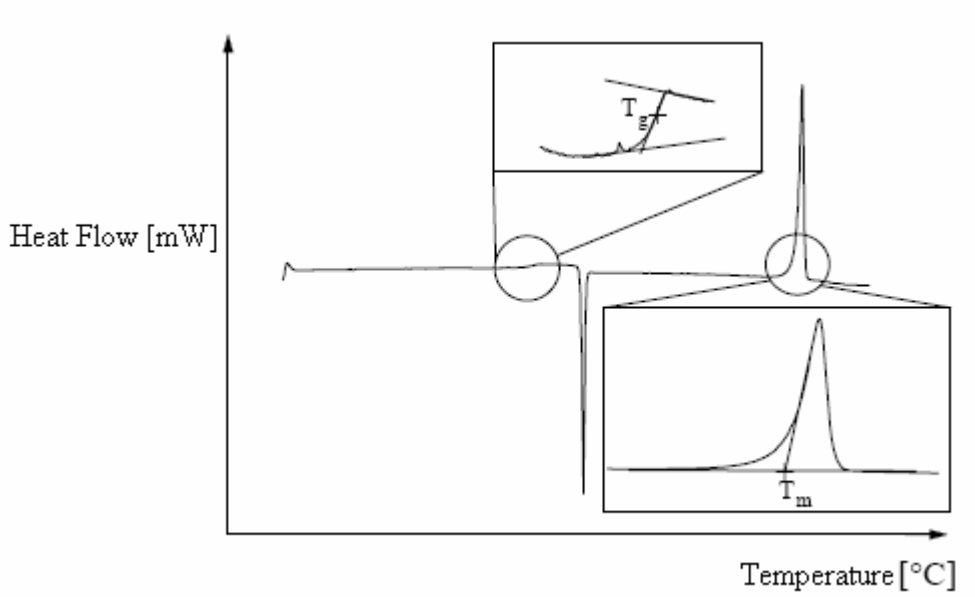

Figure 3.3 Typical DSC-measurement of an amorphous probe showing various parameters.

For an exact determination of the phase change temperatures like T_g, T_{crys} and T_m, an extrapolation of the peaks is needed. In general, the values of T_{crys} and T_m are considered as the peak-onset temperatures. The onset temperature is defined as the inflectional tangents of the auxiliary line that are drawn through the almost linear section of the two peak slopes.[19]

3.5 Examples of Organic Glasses

In past, a considerable amount of research was done to understand the relationship between the structure of a defined molecule and the stability of its glassy state.[21] Material **1** is 1,3,5-tri-α-naphthylbenzene, which was the first to be examined for its glass temperature by DSC method. The T_g was found to be 82 °C.[22]

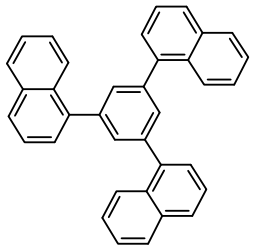

1

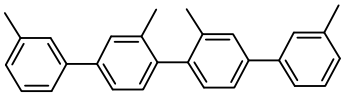

2

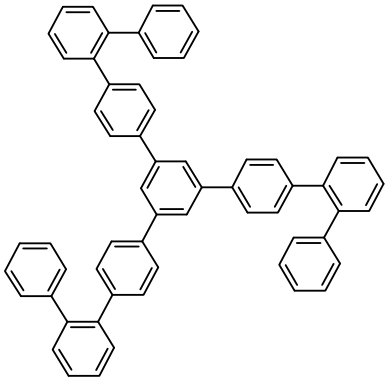

3

Kern and Wirth particularly synthesized molecules of oligophenyl compound class and examined their properties. The blue emitting *p*-quaterphenyl derivative **2** showed 7 °C as its T_g and 74 °C as melting point. The low T_g of this compound is due to the methyl side substituents which cause the higher solubility compared to the unsubstituted *p*-quaterphenyl parent compound. The melting point of the parent compound is 320 °C.[23] With this compound class, high T_g are reached through high molecular weight and rigidity of the compound.[22] The tendency of glass formation is influenced by molecular symmetry and possible internal mobility of the molecules. 1,3,5-tris(1,1',2'1'',4''-terphenyl)benzene **3** has a high T_g of 117 °C and T_m 278 °C with its molecular mass 762.9 g/mol.

3.5.1 New Class of Small Molecular Glass: 9,9'-spirobifluorene

According to Baeyer (1900), compounds with a quaternary carbon atom common to two rings are called spiro. The word spiro come from Greek word speira meaning torsion.[24] The spiro carbon atom is sp^3-hybridized and because of that the two rings remain perpendicular to one another. In a specialized form of spiro-compounds, it may possess dissymmetric isomers, which show optical activity. There are some naturally abundant spiro-compounds like terpens, sesquiterpens, alkaloids, stereoides and antibiotics.

Tour (1990) explained in his work that the substituted 9,9'-spirobifluorenes and spiro-linked polymers can be used for molecular electronics. This principle was also proposed by Aviram.[25] The *p*-sexiphenyl **4** as *p*-oligophenyl was firstly reported in 1924.

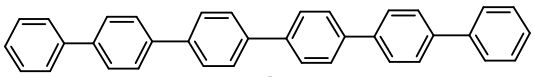

4

Then its various derivatives were synthesized and their physical properties were seriously explored. When the spiro-concept was introduced into the unsubstituted *p*-oligophenyl **4**, a new class of blue emitting molecules, zero generation of spiro-oligophenyls was formed. The resulting materials are electronically similar to their parent compounds up to their bridged biphenyl systems, but their morphology is dominated by high sterical restriction caused by the orthogonality of the two halves of the molecules. It influences the solubility of the spiro-linked compounds very positively compared to their parent compounds because an aggregation of the molecules become impossible.

3.6 Photoluminescence of Organic Molecules

"Light" in this work is used for electromagnetic radiation in the visible, near ultraviolet and near infrared spectral range. The interaction of light with a molecular system is generally an interaction between one molecule and one photon. When a molecule at ground state absorbs a photon, it becomes electronically excited with extra energy. The extra energy can be released as emission. This phenomenon is known as luminescence. An excited molecule is considered as a new species, which has its own chemical and physical properties, often quite different from the properties of the ground state molecule.

3.6.1 Absorption

A molecule can be promoted from the ground electronic state to an electronically excited state by the absorption of a quantum of light. During this process, an electron is promoted from the highest occupied molecular orbit (HOMO) to the lowest unoccupied molecular orbit (LUMO) (figure 3.4).

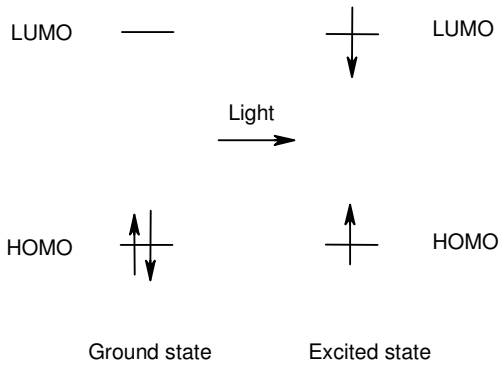

Figure 3.4 Electronic transition through photo excitation.

The necessary condition is that the photon energy, hν, matches the energy gap between the ground state and the excited state.

$$\Delta E = h\nu = E_2 - E_1 \qquad 3.1$$

This energy gap corresponds to light in the visible and near ultraviolet regions. When the condition is satisfied, the probability of transition of the electron from the ground state ψ_i to the excited state ψ_f is proportional to the square of the so called transition moment.

The ratio of the transmitted intensity I to the incident intensity I_0 at a given frequency is called the transmittance T of the sample at that frequency:

$$T = \frac{I}{I_0} \qquad 3.2$$

It is found empirically that the transmitted intensity varies with the length l of the sample and the molar concentration $[J]$ of the absorbing species J in accord with the Beer-Lambert law:

$$I = I_0 10^{-\varepsilon[J]l} \qquad 3.3$$

The quantity ε is called the molar absorption coefficient or extinction coefficient. It depends on the frequency of the incident radiation. It is greatest where the absorption is most intense. Its dimension is 1/(concentration*length).

To simplify eqn 3.3, a term called absorbance A of the sample at a given wave number is introduced.

$$A = \log\frac{I_0}{I} \qquad 3.4$$

Then the Beer-Lambert law becomes

$$A = \varepsilon[J]l \qquad 3.5$$

The product $\varepsilon[J]l$ is known as the extinction or optical density of the sample. It has no dimension. When the concentration is given in mol L^{-1}, the path length in cm, ε is expressed

in L mol^{-1} cm^{-1}. The Beer-Lambert law is an empirical result. The reduction in intensity, dI, that occurs when light passes through a layer of thickness dl containing an absorbing species J at a molar concentration $[J]$, is proportional to the thickness of the layer, the concentration of J, and the intensity, I, incident on the layer because the rate of absorption is proportional to the intensity. Hence it can be written as

$$dI = -\kappa[J]Idl \qquad 3.6$$

Where κ is the proportionality coefficient, or equivalently

$$\frac{dI}{I} = -\kappa[J]dl \qquad 3.7$$

This expression applies to each successive layer into which the sample can be regarded as being divided. Therefore, to obtain the intensity that emerges from a sample of thickness l when the intensity incident on one face of the sample is I_0, all the successive changes are integrated:

$$\int_{I_0}^{I} \frac{dI}{I} = -\kappa \int_{0}^{l} [J]dl \qquad 3.8$$

If the concentration is uniform, $[J]$ is independent of location, and the expression integrates to

$$\ln \frac{I}{I_0} = -\kappa[J]l \qquad 3.9$$

This expression gives the Beer-Lambert law when the logarithm is converted to base 10 and replacing κ by $\varepsilon \ln 10$.

$$\log \frac{I_0}{I} = A = \varepsilon[J]l \qquad 3.10$$

The molar extinction coefficient ε is valid for diluted solution of concentrations lower than 10^{-2} mol L^{-1}.[26]

Further, the absorbing molecules should not scatter the light or show interaction with it.

The maximum value of the molar absorption coefficient ε_{max} is an indication of the intensity of a transition. However, as absorption bands generally spread over a range of wave numbers, quoting the absorption coefficient at a single wave number might not give a true indication of the intensity of a transition. The integrated absorption coefficient is the sum of the absorption coefficient over the entire band and corresponds to the area under the plot of the molar absorption coefficient against wave number:

$$A = \int_{band} \varepsilon(\nu) d\nu \qquad 3.11$$

For the molecule to be able to interact with the electromagnetic field and absorb or create a photon of frequency ν, it must possess, at least transiently, a dipole oscillating at that frequency. This transient dipole moment is expressed quantum mechanically in terms of the transition dipole moment, μ_{fi}, between states ψ_i and ψ_f:

$$\mu_{fi} = \int \psi_f \mu \psi_i d\tau \qquad 3.12$$

Where μ is the electric dipole moment operator. ψ_f and ψ_i are wave functions of electrons at final and initial states. dτ is the change in life time of the electron at excited state. The size of the transition dipole can be regarded as a measure of the charge redistribution that accompanies a transition: a transition will be active (and generate or absorb photons) only if the accompanying charge redistribution is dipolar.

From the time-dependent perturbation theory, the coefficient of stimulated absorption (and emission), and therefore the intensity of the transition is also proportional to $\left|\mu_{fi}\right|^2$.

Only if the transition moment is non-zero $\mu_{fi} \neq 0$, does the transition contribute to the spectrum. Besides this, whether the value of μ_{fi} deviates from zero, or in other words: whether a transition is forbidden or allowed, is determined with the help of the so called selection rule, which states as follows:

(1) Overlap Requirement: Transitions are said to be overlap forbidden or space forbidden when the two orbitals involved in the transition do not simultaneously possess large amplitudes of their wave functions in the same region of space.

(2) Symmetry Requirement: According to Laporte's rule, in any molecule possessing one centre of inversion, only transitions between g (gerade parity) and u (ungerade peritaet) or vice versa are allowed (the electronic state is called gerade parity when its wave function does not change after passing a mirror plane through the centre of the inversion). For example, p-functions have u-parity, d-functions have g-parity. Hence, p-p and d-d transitions are forbidden but p-d transitions are allowed.

(3) Spin Requirement: If the spins remain paired during the transition, it is allowed, but if the spins become unpaired during the transition, it is forbidden. It means that the total s along with its multiplicity n=2s+1 is not allowed to change during transition. I.e., singulett-triplett transitions are forbidden.

However, singlet-triplet (spin-forbidden) transitions are observed. Therefore exceptions of this selection rule must be possible. A perturbation is required to "mix" pure singlet and pure triple states, thereby permitting transitions between the "impure" singlet and "impure" triplet. The classical operator, which corresponds this perturbation, is the spin-orbital operator. Spin-orbital coupling arises from magnetic interaction between the orbital motion of an electron (electron orbital angular-momentum) and the electron's spin magnetic moment (spin angular momentum). The spin-orbital coupling is more pronounced when the electron is in an orbital which has a high probability of being close to the nucleus, especially in an orbital which is close to a nucleus of high atomic number. The intensities of an electronic absorption are observed in a form of band as the electronic excitation is composed of the vibrational and rotational excitations too. It is rationalized by the Franck-Condon principle, which states: electronic transitions are so fast (10^{-15} sec) in comparison to nuclear motion (10^{-12} sec) that immediately after the transition, the nuclei have nearly the same relative position and velocities as they did just before the transition. This principle implies that the most probable transitions between different electronic and vibrational levels will be those transitions for which the momentum and position of the nuclei do not change very much. This principle essentially states that it is difficult to convert electronic energy rapidly into vibrational energy. This principle is best understood by reference to certain potential-energy curves. [27]

The vibrational structure of the spectrum depends on the relative horizontal position of the two potential energy curves, and a long vibrational progression is stimulated if the upper potential energy curve is appreciably displaced horizontally from the lower. The upper curve is usually displaced to greater equilibrium bond lengths because electronically excited states usually have more antibonding character than electronic ground states. In contrast to absorption, the displacement of the ground-state potential-energy curve minimum is to the left of the minimum of the excited state curve, so that the most probable emissions produce an elongated ground state, while absorption produces a compressed excited state immediately after transition.[27]

3.6.2 Fluorescence

All molecules absorb light. However, only a relatively low number of molecular species (usually rigid conjugated polyaromatic hydrocarbons or heterocycles) emit light as a result of

absorption of light from some other sources. If the emission is immediate or from the electronically excited singlet state, the phenomenon is called fluorescence.

Fluorescence is named after the mineral fluorite, composed of calcium fluoride, in which this phenomenon was observed. Fluorescent effects have been observed for thousands of years. In 1852 the true science of fluorescence was brought to light by Sir George Stokes.[28] He applied the scientific method to fluorescence and developed the "Stokes Law of Fluorescence", which dictates that the wavelength of fluorescence emission must be greater than that of the exciting radiation. Fluorescence is the emission of light from a molecule in which an electronically excited state has been populated. The emission of the light is usually in the ultraviolet to visible portion of the spectrum, sometimes in the near-infrared. The phenomenon can be illustrated by a simple electronic state diagram called Jablonski diagram (figure 3.5).

The electronic and vibrational energy levels of the fluorophore are represented by horizontal lines and grouped in bands. The lowest band is associated with the ground electronic state, S_o. The lowest energy level of the excited singlet state is represented by S_1, whereas T_1 is the lowest level of the excited triplet state.

Upon excitation, fluorophores in ground state absorb a photon and jump to higher vibrational energy levels of the electonically excited singlet state, shown as absorption of light, A. The photon of excitation is supplied by an external source, such as an *incandescent* lamp or a laser. The transition from S_o to higher excited levels of S_1 is responsible for the visible and ultraviolet absorption spectra observed for fluorophores. The absorption of photon is highly specific and it takes place in about 10^{-15} seconds.

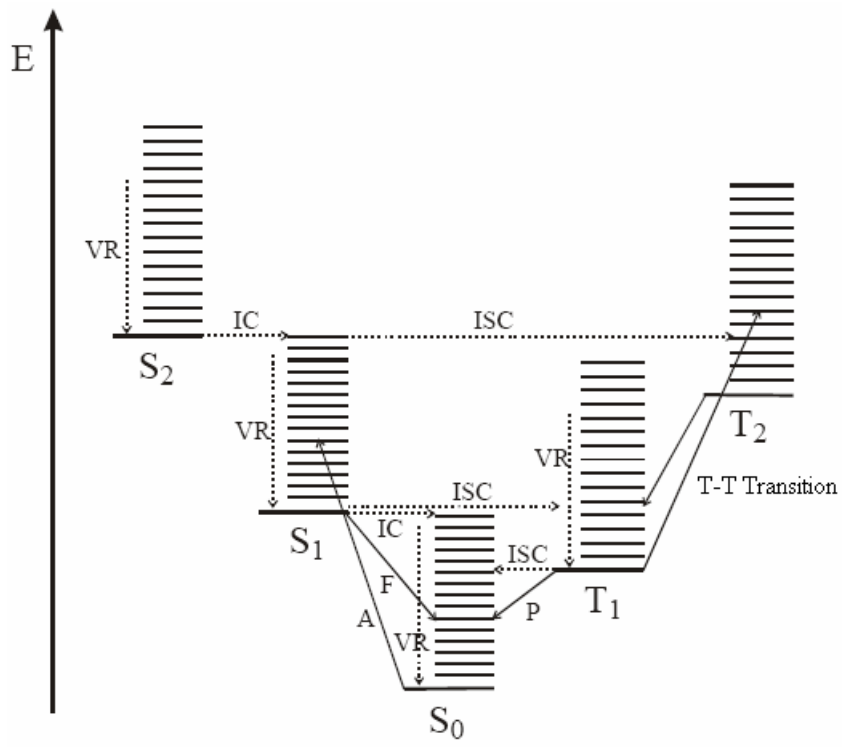

Figure 3.5 Jablonski-Diagramof of different monomolecular deactivation. (dotted line transtion: radiationless process, solid line transiton: radiating process; A = Absorption, F = Fluorescence, P = Phosphorescence, IC = Intercrossing, ISC = Intersystemcrossing, VR = Vibrational Relaxation[29].

Excitation is followed by a return to the lower vibrational levels of the electronically excited state. This relaxation occurs in about a picosecond. The excited state itself exists for a finite time. Typical values of excited-state lifetimes are in the range of nanoseconds.

From the singlet state, the fluorophore returns to the electronic ground state with the emission of the photon, shown as fluorescence F, but to higher vibrational levels of this state. In fluorescence emission, the spin multiplicities of the ground and excited states are the same. One can measure either a steady state spectrum of emitted light or the actual decay kinetics of emission.

Photoemission is unimolecular. It is a first order process in the concentration of the excited state. The energy of the photon that is emitted as the electron decays to the ground state depends on the energy difference between the excited and ground state at the time of emission. The rapid decay of excited vibrational states implies that the state from which the fluorophore decays is independent of the excitation wavelength. However, the state to which the fluorophore decays is not always the lowest vibrational state of the ground state, but it is

an equilibrium distribution of vibrational levels. Therefore, the emission spectra of fluorescent molecules show fine structure. The probablility of decay from the excited state to each vibrational level of the ground state is what determines the shape of the fluorescence spectrum.

Especially in rigid molecules like perylene, the fluorescence spectrum is more or less the mirror image of the absorption spectrum. The symmetry equilibrium is due to the vibrational frequency of the excited energy levels and the ground state that remain similar in fluorescence bands which actually determine the fine structure of the absorption bands. Further, the fluorescence and the absorption both exhibit comparable intensities.

An important term in fluorescence is quantum yield. The fluorescence quantum yield describes the efficiency of the fluorescence process. It is defined as the ratio of the number of photons emitted to the number of photons absorbed. The maximum fluorescence quantum yield is 1.0 (100%); every photon absorbed results in a photon emitted. Compounds with quantum yields of 0.10 are still considered quite fluorescent.

In rigid molecules, there are only small differences in the geometry equilibrium between the ground state and the excited state. This results in very small Franck-Condon-Factors for radiationless transition and so the inter conversion will be very slow. As a result, the total excitation energy will be emitted as fluorescence with high intensity so that the quantum yield will be increased. Thus the quantum yield is related with the intensity of the emission and partially related with the life time of the excited state too. The fluorescence lifetime refers to the average time the molecule stays in its excited state before emitting a photon. The fluorescence emitted will decay with time according to

$$F_{(t)} = F_0 e^{-t/\tau} \qquad 3.13$$

$$\frac{1}{\tau} = \sum_f \omega fik_i \qquad 3.14$$

In the equations 3.13 and 3.14 above, t is time, τ is the fluorescence lifetime, F_0 is the initial fluorescence at t = 0, and k_i are the rates for each decay pathway, at least one of which must be the fluorescence decay rate k_f. More importantly, the lifetime τ is independent of the initial intensity of the emitted light. This is an instance of exponential decay.

It is similar to a first-order chemical reaction. If the rate of spontaneous emission is fast, the lifetime is short. Generally, compounds emitting photons with energies from the UV to near infrared, typical excited state decay times are within the range of 0.5 to 20 nanoseconds. The fluorescence lifetime is an important parameter for practical applications such as fluorescence resonance energy transfer.

Through the intensity of the emission, the fluorescence quantum yield partially depends upon the lifetime of the excited state. When the lifetime of the excited state is very short, the most probable relaxation way is to release the excitation energy in form of emitted light. Other rates of excited state decay are caused by mechanisms other than photon emission and are therefore often called "non-radiative rates", which can include: dynamic collisional quenching, near-field dipole-dipole interaction (or resonance energy transfer), internal conversion and intersystem crossing. Thus, if the rate of any pathway changes, this will affect both the excited state lifetime and the fluorescence quantum yield.

When the spontaneous emission is the only probability for an excited state of a molecule to attain the relaxed position (ground state), the lifetime of the excited state of the molecule is given by τ_0. It is a reciprocal of velocity constant k_0, which can be obtained from the velocity law of the first order for the exponential fall of the intensity of the fluorescence. The natural lifetime in second is given by

$$\tau_0 = \frac{3.47 * 10^8}{\bar{\nu}^2{}_{\max}} \frac{1}{\int \varepsilon(\bar{\nu}) d\bar{\nu}} \approx \frac{1.5}{\bar{\nu}^2{}_{\max} . f} \qquad 3.15$$

where $\bar{\nu}_{\max}$ is the wave number of the absorption maximum (in cm^{-1}) and f is the strength of oscillator of the corresponding electronic transition.[30] This equation shows that shorter the lifetime of the excited state, more allowed is the electronic transition (greater f). According to this result, chromophores with higher numbers of phenyl rings or longer the *p*-oligophenyl chains, higher the extinction coefficients ε_{max} and shorter fluorescence life time with higher quantum yields.[31,32,33] This makes them interesting candidates for scintillator applications. To improve the spectroscopic characters of the *p*-oligophenyls, the spiro-concept is applied and the class of spiro-starburst-structures are developed which are stereochemically constrained and rigid.

The relation between ε_{max} and τ_0 is given as follows:[31]

$$\frac{1}{\tau_0} = A\bar{\nu}_0^{\,2}\int \varepsilon d\bar{\nu} \approx A\bar{\nu}_0^{\,2}\varepsilon_{max}\Delta\bar{\nu} \qquad 3.16$$

where A is a constant, $\bar{\nu}_0$ is wave number for the 0-0 transition and $\Delta\bar{\nu}$ is the half-width. According to this equation, the calculated life time is shorter as $\bar{\nu}_0$, ε_{max} and $\Delta\bar{\nu}$ are greater. Compared to other systems with a similar degree of conjugation, *p*-oligophenyls are found to be in advantage because their emission spectra are shifted more hypsochromically (greater $\bar{\nu}_0$) and their absorption spectra cover a greater range of wavelengths (greater $\Delta\bar{\nu}$). That is why the *p*-oligophenyls are found to be very good candidates of blue light emitters.

Due to the stereo constrains and rigidities of spiro-starburst-structures, they show advantages to *p*-oligophenyls possessing good spectroscopic characters and all other necessary criteria which should lead to high fluorescence quantum yields.

3.6.3 Phosphorescence

In some cases, the absorbed photon energy undergoes an unusual intersystem crossing into an energy state of higher spin multiplicity, usually a triplet state. As a result, the energy can become trapped in the triplet state with only quantum mechanically "forbidden" transitions available to return to the lower energy state. This causes a radiation called phosphorescence which has less intensity but lasts for longer time than fluorescence. This phenomenon is possible only with heavy atom containing molecules where the spin forbidden rule is excluded because of the spin-orbit coupling system.

During the lifetime of the excited state, it undergoes a variety of possible interactions with its molecular environment. Among these are processes such as partial dissipation to relaxed singlet excited states, called intercrossing, collisional quenching, fluorescence energy transfer and intersystem crossing. These may depopulate the excited singlet state and thus the energy is lost without fluorescence (figure 3.5). Some fluorophores may leave the electronically excited state via a process other than fluorescence, especially at high levels of excitation power. They can undergo intersystem crossing into the triplet state T_1, from which the fluorophore returns to the electronic ground state by emission of light as phosphorescence, shown as P (figure 3.5). Intersystem crossing occurs when a triplet state lies just below the

excited singlet electronic state, i. e. there is a near coincidence of two vibrational levels in the excited singlet state and triplet states. In triplet state, the spins of the excited and ground state electrons are no longer paired. This involves the flipping of one of the electron spins so that unpaired electron spin results. Thus, in phosphorescence emissions, the spin multiplicities of the ground and excited states are different. The decay from the triplet to ground state is very slow and occurs only if there are no other allowed energy paths open.

There are other mechanisms that can delay the fluorescence emission to very long periods. This can occur if the energy follows some circuitous path in the excited state before returning to the lower vibrational levels of the electronically excited state. Such a delayed fluorescence is different from true phosphorescence which is derived from the triplet state. Delayed fluorescence results from two intersystem crossings, first from the singlet to the triplet, then from the triplet back to the singlet.

3.6.4 Bimolecular Diactivation Process

The Jablonski diagram shows only the photophysical processes like fluorescence and phosphorescence of monomolecular system only. For the case of bimolecular systems, the deactivation process of the excited state is expressed in terms of quenching. Quenching is a shortening of the lifetime of an excited state.[34] Quenching may occur either in energy or electron transfer or in form of a side reaction that can decrease the quantum yield of a photo physical process.

Quenching effects may be studied by monitoring the emission from the excited state that is involved in a photochemical reaction. The addition of a quencher Q opens an additional channel to a lower excited state or the ground state B for deactivation of an excited state B*.

$$B^* \xrightarrow{Q} B$$

Depending on the quencher, the quenching can be either self-quenching (collisional quenching) due to concentration quenching or foreign quenching due to foreign molecules like impurities acting as quencher.

The increased intermolecular attraction in the excited state is due to an energy- or charge-transfer interaction between two partners. If the partners are alike molecules and do not

exhibit a large degree of charge transfer from one component to other, they form excimers [(BB)*]. If the partners are different and exhibit a large degree of charge transfer from one component to other, they form exciplexes [(BQ)*].

3.6.4.1 Excimers

The term excimer was introduced by Stevens and Hutton (1960) to describe $^1D^*$ and to distinguish it from the excited state of a stable dimer. The formation of excimers occurs on an excited potential energy surface by an encounter of an electronically excited molecule and one ground state molecule. Figure 3.6 shows a generation of pyrene excimer by an encounter of a ground state molecule with an excited neutral pyrene molecule.[35] Such condensed aromatic hydrocarbons are planar and their most stable excimer conformation is usually that of a sandwitch dimer. For more condensed aromatic hydrocarbons, formation of excimers causes the appearance of structureless broad bands in the fluorescence spectrum at lower energies, resulting in bathochromic shifts compared to the fluorescence spectrum of the monomolecular system.[36]

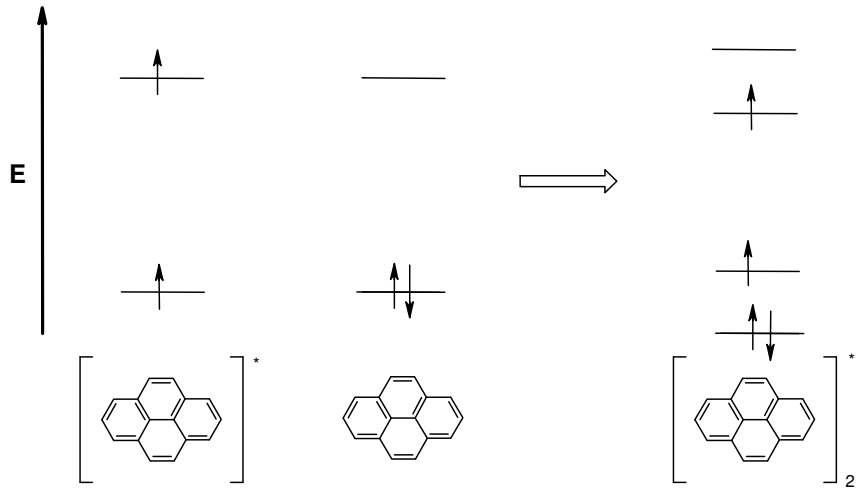

Figure 3.6 Generation of pyrene excimer.

3.6.4.2 Exciplex

An exciplex is defined as an electronically excited atomic or molecular complex of definite stoichiometry, which is dissociative or dissociated in its electronic ground state (Birks 1969, 1975). The stoichiometry is usually 1 : 1, but triple 2 : 1 exciplexes have also been observed (Beens and Weller 1968). The first aromatic molecular exciplex was discovered by Leonhardt

and Weller (1961, 1963), who observed exciplex formation between excited perylene and unexcited dimethylaniline (DMA) molecules in solution, yielding a structureless exciplex fluorescence band analogous to excimer fluorescence.

Exciplexes, in turn, are particular examples of stoichiometric atomic or molecular complexes. Molecular complexes are generally formed between electron-donor molecules (D) and electron-acceptor molecules (A), with the charge-transfer (CT) state (D^+ A^-) playing an important role in the interaction. The emission spectrum of the exciplex also consists of a structureless broad band in the fluorescence spectrum at lower energies, resulting in bathochromic shifts similar as in the case of excimers.

3.7 Electrochemistry

For the electrical injection of charges in organic semiconductors such as OLED, OFET and solar cells, the energy levels must be aligned carefully in order to allow the flow of electrical current without undesired energy barriers. The energy levels are governed by the redox properties of the materials. As the spiro-starburst-structures are used in OLEDs in the field of optoelectronic devices, their charge transfer character is important to be analysed.

The charge transfer character of a compound is analysed by a method called cyclic voltammetry (CV). With the help of this method, the number of electrons that are lost (oxidation) or received (reduction) by a compound can be determined during its electrolysis in solution.

In a typical CV experiment, a stationary working electrode (platinum disk) is used which is immersed into an electrolyte solution. In order to minimize the ohmic resistance, a three electrode arrangement is preferable. In this arrangement, the current passes between the working electrode and a counter electrode (glassy carbon). The potential of the working electrode is measured relative to a separate reference electrode (Ag/AgCl). In this experiment, the potential of the working electrode is varied linearly with time (figure 3.7 a) with sweep rates between 10 mV/s and 200 mV/s. The referring current is recorded as a function of potential (figure 3.7 b).

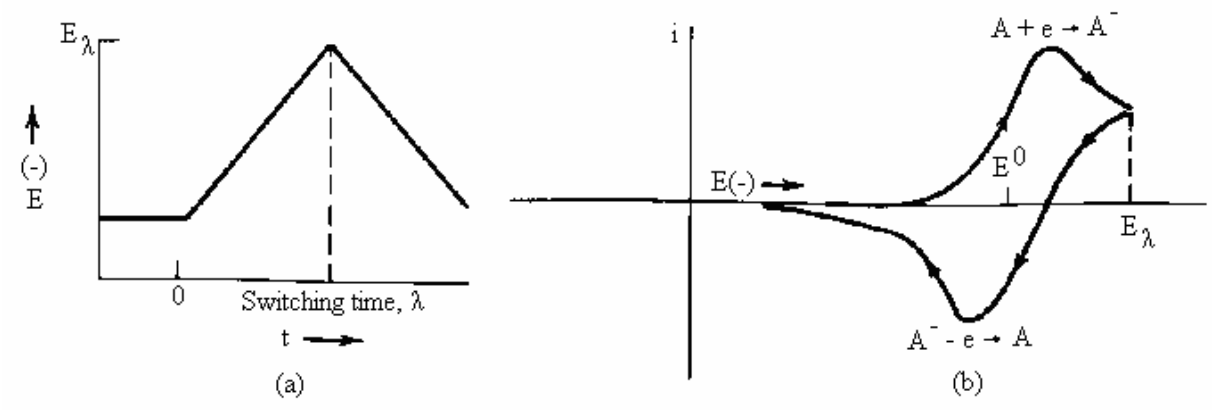

Figure 3.7 (a) Cyclic potential sweep (b) Resulting cyclic voltammogram

Provided the rate of electron transfer at the electrode surface is very fast (which corresponds to the absence of an inhibition), the concentration ratio of the oxidized and reduced species at the electrode surface is dictated by Nernst equation:

$$E = E^0 + (RT/nF)\ln C_0 / C_R \qquad 3.17$$

with

E = Electrode potential

E^0 = Standard electrode potential

R = Gas constant

T = Absolute temperature

n = Number of moles of electrons transferred

F = Faraday constant

C_O = Concentration of the oxidized species

C_R = Concentration of the reduced species

Under these circumstances the electrode reaction is said to be reversible. The Nernst equation relates the potential generated by an electrochemical cell to the concentrations of the chemical species involved in the cell reaction and to the standard potential, E^0.

During the electrolysis of the compound under experiment, the potential is determined versus the oxidation of ferrocene/ferrocenium.

The general features of a voltammogram are shown in figure 3.8. The peak potential E_P in the case of a reversible linear potential sweep is given by

$$E_p = E_{1/2} + /-1.109(RT/nF) \qquad 3.18$$

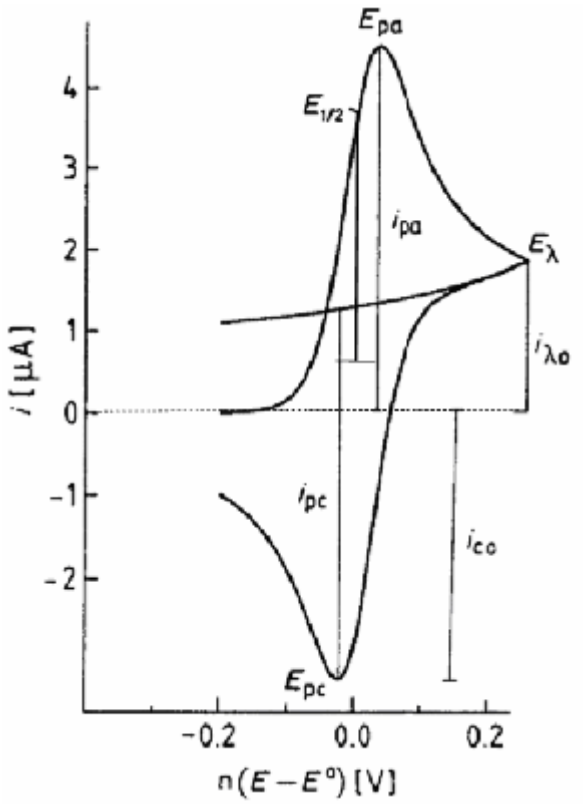

Figure 3.8 Linear potential sweep voltammogram in terms of current function

$E_{1/2}$ is the polarographic half-wave potential, which is very close to the standard potential E°. The positive sign in equation 3.19 corresponds to an anodic (E_{P+}) and the negative sign to a cathodic peak (E_{P-}). For the reversible case, the peak potential is independent of sweep rate and concentration. These characteristics can be used as a criterion of reversibility. Also the difference between E_{P+} and E_{P-} can be applied as diagnostic test of a reversible (Nernst) reaction. Although ΔE_P is slightly a function of the switching potential E_λ (figure 3.8), in general, it can be assumed that

$$\Delta E_p = \left|E_{P+} - E_{P-}\right| = 2.3(RT/nF) = 59/n mV\,(at\,25°C) \qquad 3.19$$

For repeated cycling, the cathodic peak current decreases and the anodic one increases until a steady-state pattern is attained where ΔE_P = 58/n mV (at 25°C). Also the current during the first cycle is quite different from that in the second cycle. After 5-10 cycles the system settles down and the voltammogram is independent of time.

Usually the peak in the voltammogram is rather broad, so the peak potential may be difficult to determine. That is why it is more convenient to report the potential at 0.5 i_P, called the half-peak potential $E_{P/2}$, which is

$$E_{P/2} = E_{1/2} + 1.09RT/nF \qquad 3.20$$

The difference between E_P and $E_{P/2}$ is

$$\left|E_P - E_{P/2}\right| = 2.2RT/nF = 56.5nmV\left(at 25°C\right) \qquad 3.21$$

The peak current i_P for a reversible linear potential sweep is given by the Randles-Sevčik equation

$$i_P = Pn^{3/2}AD^{1/2}c^{\infty}v^{1/2} \qquad 3.22$$

with

A – Area of Electrode

D – Diffusion coefficient

c^{∞} – Bulk concentration

n – number of exchanged electrons

v – Sweep rate

P - Randles-Sevčik-constant ($2.69*10^5$ As/V $^{1/2}$ mol)

The voltage-current curves are measured in a potentiostatic circuit. In a three-electrode arrangement, the potentiostat controls the potential difference between the working electrode (platinum) and the reference electrode (Ag/AgCl), which serves as the potential basis for the working electrode, to a predetermined value. In such experiment, the potential difference between the working electrode and the reference electrode is varied continuously from –500 mV to +300 mV. A current flows from the working electrode to the counter electrode (glassy carbon) when the redox species are converted to each other. This current (in Y-axis) is plotted against the potential difference (in X-axis).[37]

3.8 Zeolite

Zeolites are natural volcanic minerals with a number of unique characteristics. Zeolites were formed when volcanic ash was deposited in ancient alkaline lakes. The interaction of the volcanic ash with the salts in the lake water altered the ash into various zeolite materials. In 1756, the Swedish mineralogist Cronstedt discovered that stilbite, a natural mineral, visibly lost water when heated, and he named the class of materials “zeolites” from the classical

Greek words meaning “boiling stones”. Zeolites were considered an obscure group of minerals with unique properties for almost 200 years.

Zeolites have an unusual crystalline structure and a unique ability to exchange ions. A very large number of small channels are present in its structure. These channels have typical diameters of 0.5 to 0.7 nm, only slightly larger than the diameter of a water molecule. These channels are called micropores. Beside this, there are a number of larger pores, the so-called mesopores. Positive ions like sodium ions, protons, metal cations, and metal-oxo cations are present in the channels and can be exchanged for other cations.[38] This substitution of ions enables zeolites to selectively adsorb certain harmful or unwanted elements from soil, water and air. A classic example is the removal of calcium from hard water. Zeolites exchange sodium/calcium ions, which results in soft water. Zeolites also have a strong affinity for certain harmful heavy metals such as lead, chromium, nickel and zinc. In the mesopores of zeolites suspended and colloidal particles can be trapped. Organic molecules can also be adsorbed in these pores.[39]

Considering all of these properties and abilities, the commercial and environmental possibilities in zeolites seem to be unlimited. Some other examples are the application of zeolites in landfills and at industrial sites, which can help to prevent the release of a number of harmful or unwanted elements into the environment.

3.8.1 Chemical Structure

Zeolites are three-dimensional, microporous, inorganic crystalline solids with well-defined structures that contain aluminium, silicon, and oxygen in their regular framework; cations and water are located in the pores.

The silicon and aluminium atoms are tetrahedrally coordinated with each other through shared oxygen atoms. Compositionally, zeolites are similar to clay minerals. More specifically, both are alumino-silicates. They differ, however, in their crystalline structure. Zeolites have a rigid, 3-dimensional crystalline structure (similar to a honeycomb) consisting of a network of interconnected tunnels and cages. Water moves freely in and out of these pores but the zeolites framework remains rigid. Another special aspect of this structure is that the pore and channel sizes are nearly uniform, allowing the crystal to act as a molecular sieve.

The porous zeolite acts as host to water molecules and ions of potassium and calcium, as well as to a variety of other positively charged ions. However, only those of appropriate molecular size to fit into the pores are admitted, thus the zeolites act as “sieves”.

3.8.2 Types of Zeolite

There are different types of zeolites (clinoptilolite, chabazite, phillipsite, mordenite, etc.) with varying physical and chemical properties. Crystal structure and chemical composition account for the primary differences. Particle density, cation selectivity, molecular pore size and strength are only some of the properties that can differ depending on the zeolite in question.

In 1948, Barrer first produced a synthetic zeolite that did not have a natural counterpart. New synthetic zeolites are currently being invented in many laboratories around the world.

3.8.3 Zeolites Applications

There are three main uses of zeolites in industry: for catalysis, gas separation and ion exchange.

Catalysis: Zeolites are extremely useful as catalysts for several important reactions involving organic molecules. The most important are cracking, isomerisation and hydrocarbon synthesis. Zeolites can promote a diverse range of catalytic reactions including acid-base and metal induced reactions. Zeolites can also be acid catalysts and can be used as supports for active metals or reagents.

Zeolites can be shape-selective catalysts either by transition state selectivity or by exclusion of competing reactants on the basis of molecular diameter. They have also been used as oxidation catalysts. The reactions can take place within the pores of the zeolite, which allows a greater degree of product control.

The main industrial application areas are petroleum refining, synfuels production and petrochemical production. Synthetic zeolites are the most important catalysts in petrochemical refineries.

Adsorption: Zeolites are used to adsorb a variety of materials. This includes applications in drying, purification and separation. They can remove water to very low partial pressures and are very effective desiccants, with a capacity of up to more than 25% of their weight in water. They can remove volatile organic chemicals from air streams, separate isomers and mixtures of gases. A widely used property of zeolites is that of gas separation. The porous structure of zeolites can be used to “sieve” molecules having certain dimensions and allow them to enter the pores. This property can be fine tuned by varying the structure through changing the size and number of cations around the pores. Other applications that can take place within the pore include polymerisation of semi conducting materials and conducting polymers, producing materials with unusual physical and electrical attributes.

Ion exchange: Hydrated cations within the zeolite pores are bound loosely to the zeolite framework, and can readily exchange with other cations when in aqueous media. Applications of this can be seen in water softening devices, and the use of zeolites in detergents and soaps. The largest volume use for zeolites is in detergent formulations where phosphates have been replaced as water-softening agents by exchanging the sodium in the zeolite for the calcium and magnesium present in the water. It is even possible to remove radioactive ions from contaminated water.

4 Synthetic Section

4.1 Applied Reactions in Synthesis

4.1.1 Miyaura-Borylation Reaction[40]

The Miyaura borylation reaction enables the synthesis of boronates by cross-coupling of bis(pinacolato)diboron (B_2pin_2) with aryl halides and vinyl halides.

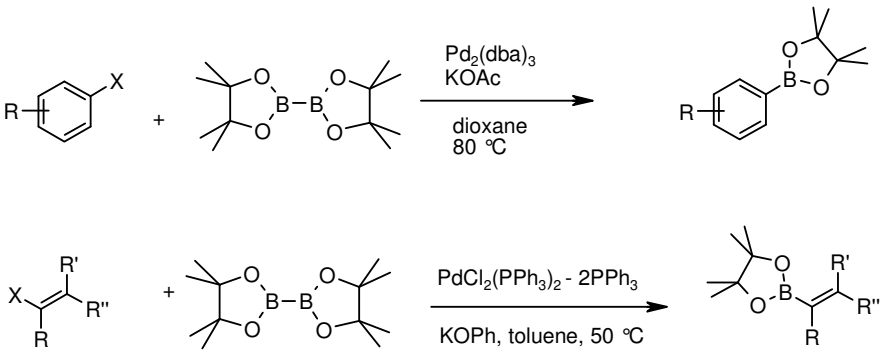

X = Br, I, OTf

Borylated products derived from B_2pin_2 allow normal work up including chromatographic purification and are stable towards air. Pinacol esters are difficult to hydrolyse but they may serve as coupling partners in the Suzuki cross-coupling and similar reactions without prior hydrolysis.

In this work, most of all borolated products (pinacol aryl borane) have been synthesized according to this reaction.

Crucial for the success of the borylation reaction is the choice of an appropriate base, as strong activation of the product enables the competing Suzuki cross-coupling reaction. The use of KOAc[40] and KOPh[41] is actually the result of a screening of different reaction conditions by the Miyaura group.

The starting material bis(pinacolato)diboron is poor Lewis acid and ^{11}B.NMR of KOAc and B_2pin_2 in DMSO-d_6[40] shows no evidence of the coordination of the acetoxy anion to a boron

atom leading to a tetrahedral activated species (compared to Suzuki coupling). However, the formation of an (acetato)palladium(II) complex after the oxidative addition of the halide influences the reaction rate of the transmetalation step. The Pd-O bond, which consist of a hard Lewis base with a soft Lewis acid, is more reactive than a Pd-X (X = Br, I) bond. In addition, the high oxophilicity of boron has to be considered as driving force for the transmetalation step, which involves an acetato ligand.

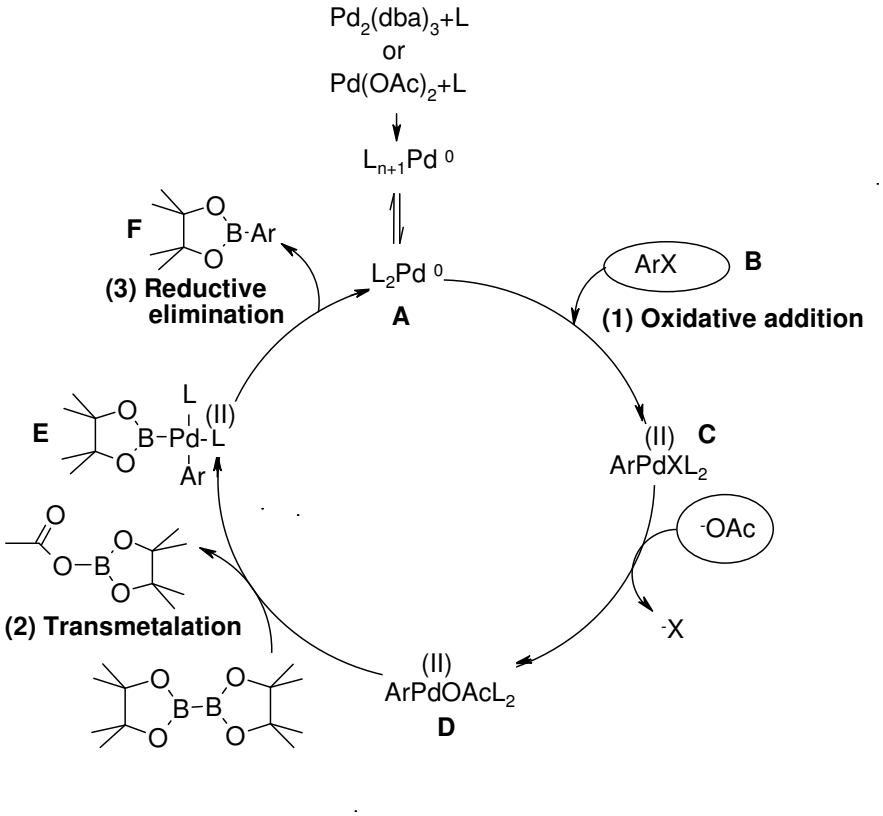

Figure 4.1 A general catalytic cycle for Miyaura-Borylation reaction.

The mild reaction conditions allow the preparation of boronates which are not accessible via lithium or Grignard inetermediates followed by borylation.

The mechanism of Pd-catalysed borylation is similar as the mechanism of C-C coupling reaction (Suzuki cross-coupling). Fingure 4.1 shows a general mechanism. The catalytic cycle begins with the an oxidative addition of aryl halides or triflates **B** on Pd(0)-complex **A**. Thus formed Pd(II)-complex **C** undergoes nucleophilic substitution reaction with acetate anion resulting acetoxide-complex **D**. Transmetalation of this complex with B_2pin_2 affords complex **E**. Reductive elimination leads to product **F** and regenerates the catalyst.

4.1.2 Suzuki Cross-Coupling Reaction (C-C bonding)[42]

Suzuki reaction is the palladium(0)-catalysed cross-coupling reaction between organoboronic acid and halides in the presence of a base. Similar to the Negishi, Kumada and Stille coupling reactions, Suzuki reaction is also one of the most important C-C cross-coupling reactions. The Negishi Coupling was the first reaction that allowed the versatile nickel- or palladium-catalyzed coupling of organozinc compounds with various halides (aryl, vinyl, benzyl, or allyl) preparing unsymmetrical biaryls in good yields.[43] In Kumada Coupling, unsymmetrical biaryls were synthesized by Pd- or Ni-catalyzed cross-coupling reaction of Grignard reagents with alkyl, vinyl or aryl halides.[44] The Stille Coupling is a Pd-catalyzed versatile C-C bond forming reaction between stannanes and halides.[45] Recent catalyst and methods developments have broadened the possible applications of Suzuki reaction enormously, so that the scope of the reaction partners is not restricted to aryls, but includes alkyls, alkenyls and alkynyls. Potassium trifluoroborates and organoboranes or boronate esters may be used in place of boronic acids. Some pseudohalides (for example triflates) may also be used as coupling partners.

Suzuki reaction takes place in mild condition with high yield with the tolerance for different functional groups.[46,47] The stability of the boron-reagents and the easy access to a broad variety of boronic-acids (figure 4.2) make the Suzuki reaction one of the most beloved reactions. The required boronic acids in this work have been derived from the corresponding lithiated aryl system or Grignard reagent with trimethyl borate, from aryltrimethylsilane and from $pd_2(dba)_3$ [tris(dibenzylideneacetone)dipalladium(0)] catalysed reaction of aryl halide with bis(pinacolatoborane) called Miyaura reaction The demanding purification can be done by esterification of the corresponding boronic acid with pinacol forming corresponding pinacol aryl boranes. Due to all these advantages, amongst the growing number of palladium-catalysed C-C-coupling reactions the Suzuki-Miyaura-reaction plays a leading role.[47]

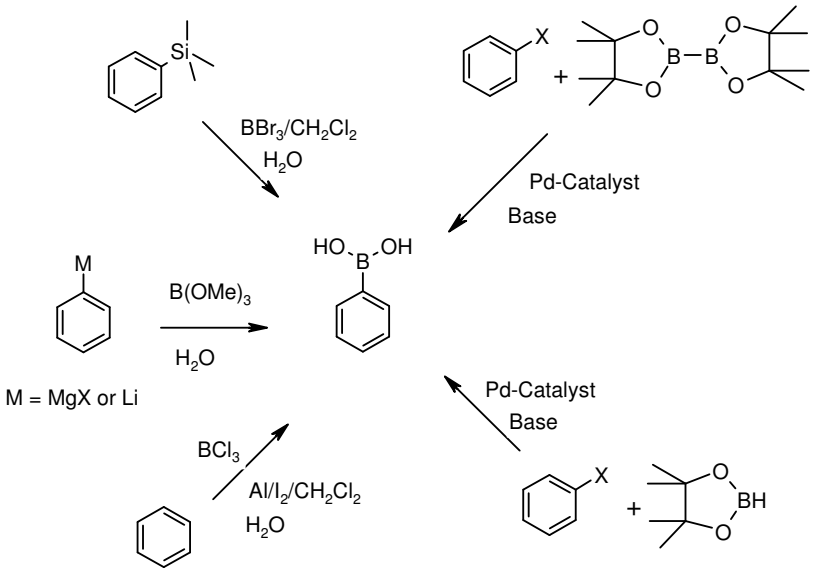

Figure 4.2 Various path to achieve boronic acid.

The catalysis system in the Suzuki reaction can be explained with the help of the following cycle (figure 4.3). In this mechanism, the boronic acid or the borane must be activated with a base.

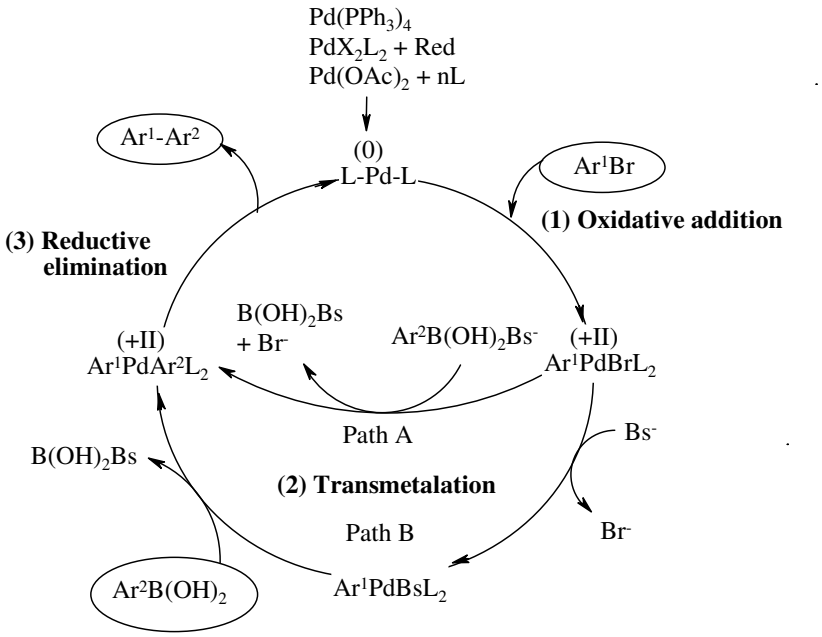

L = Ligand, Bs = Base, $Ar^1Br(X)$ (halide or triflate) = Arylbromide, $Ar^2B(OH)_2$ = Arylboronic acid

Figure 4.3 A general catalytic cycle for Suzuki cross-coupling reaction.

Analogous to other cross-coupling reactions, the catalysis takes place as follows:

1) **Oxidative Addition** of arylhalide to the Pd(0)-catalyst forming Pd(II) species.

2) **Transmetalation** to organopalladium(II)-species.

3) **Reductive Elimination** by the formation of coupling product Ar^1-Ar^2.

The oxidative addition is the rate-determining step in a catalytic cycle. The relative reactivity decreases in the order of I > OTf > Br >> C1.[Error! Bookmark not defined.] Aryl and 1-alkenyl halides activated by the proximity of electron-withdrawing groups are more reactive to the oxidative addition than those with donating groups, thus allowing the use of chlorides such as 3-chloroenone for the cross-coupling reaction. **A** very wide range of palladium(0) catalysts or precursors can be used for cross-coupling reaction. The catalyst tetrakis(triphenylphosphine)palladium is most common, but also other homogeneous catalysts as well as immobilized or heterogeneous[48] palladium-compounds have been used since they are stable to air and readily reduced to the active Pd(0) complexes with organometallics or phosphines used for the cross-coupling.[49] Palladium complexes that contain fewer than four phosphine ligands or bulky phosphines such as tris(2,4,6-trimethoxyphenyl)phosphine are, in general, highly reactive for the oxidative addition because of the formation of coordinate unsaturated palladium species.[50] Reductive elimination of organic partners from palladium(II) complex reproduces the palladium(0) complex.

Although the mechanism of oxidative addition and reductive elimination sequences are reasonably well understood and are presumably fundamentally common processes for all cross-coupling reactions of organometallics, less is known about the transmetalation step because the mechanism is highly dependent on organometallics or reaction conditions used for the couplings.

Organoboron compounds are quite unlikely to participate in the catalytic cycle of cross-coupling reaction since they are inert to the organopalladium(II) halides such as $PdC1_2$, $PdCl_2(PPh_3)_2$ &, or $PhPdI(PPh_3)_2$ [47] but the addition of sodium or potassium hydroxide bases exerts a remarkable effect on the transmetalation rate of organoboron reagents with metallic halides. Thus, the transmetalation with transition-metal complexes appears to proceed well indeed, but the choice of suitable bases and ligands on transition-metal complexes is essential.

Hence, cross-coupling reaction of organoboron compounds with organic halides or triflates selectively reacts in the presence of a negatively charged base, such as sodium or potassium carbonate, phosphate, hydroxide, and alkoxide. Since some bases are sparingly soluble in

organic solvents, Suzuki reaction is carried out in a mixture of aqueous, toluene and tetrahydrofurane solution. Suzuki cross-coupling reaction is widely applied in this work for the synthesis of various transition phases and end products.

4.1.3 Nitration

For the synthesis of triazenyl-spiro compound, which is required for Sandmayer reaction to convert into a halide species, spiro-amine reactant is prepared by the reduction of the corresponding nitro compound. The nitration of the aromatic systems is often carried out by a mixture of nitric acid/acetic acid or nitric acid/sulphuric acid. Further possible nitrating reagents for the nitration of aromatic compounds are fuming nitric acid, nitroniumtetrafluoroborate [$NO_2^+(BF_4)^-$] or acetylnitrate (CH_3COONO_2).[51] The nitration takes place as the electrophilic substitution reaction, where the nitronium ion (NO_2^+) acts as nitrating agent.[52] From the mixture of nitric acid and sulphuric acid, a protonated nitric acid as nitracidium ion ($H_2NO_3^+$) is formed, which is then followed by the dehydration forming nitronium ion (NO_2^+).

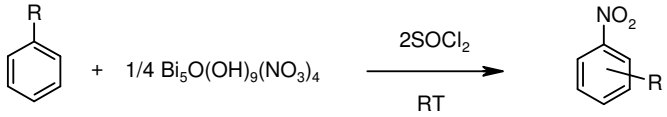

Bismuth subnitrate/thionyl chloride in dichloromethane has been found to be a new and an efficient combination of reagents for nitration of a wide range of aromatic compounds by controlling the stoichiometry.[53] The commercially available bismuth subnitrate, [$Bi_5O(OH)_9(NO_3)_4$] is inactive, on its own, towards aromatic nuclei in organic solvents but the use of thionyl chloride activates bismuth subnitrate to produce thionyl chloride nitrate [$ClSO(ONO_2)$]. When bismuth subnitrate is added to a solution of the aromatic substrate and thionyl chloride in dichloromethane at room temperature, formation of nitroniumchloride (NO_2Cl) as nitrating reagent enhances the nitration process. The advantage of this new nitrating reagent is that it is not toxic and the reaction takes place at room temperature. This method of nitration is applied for the nitration of the spiro-linked compound in this work.

During the nitration of an arylhalide, a nucleophilic substitution reaction, exchanging the halogen with the nitrite anion (NO_2^-) can appear,[51] where the decreasing tendency of the substitution of halogens may occur as following series:

$$I > Br >> Cl$$

The reduction of aromatic nitro compounds to primary amine can be carried out easily in an acidic solution in the presence of metal like Zn, Sn, Fe. As a transition state of the reduction process, the nitroso compound (R-N=O) and hydroxylamine (R-NH-OH) compound are formed. Reduction in neutral or weak acidic solution, the hydroxylamine state remains. In alkaline medium, hydrazo compound (R-NH-NH-R) is formed. The mechanism of the reduction of nitro compound in acidic solution is shown as follows where the first step is the transition of electron from metal to the nitrogen atom.[54]

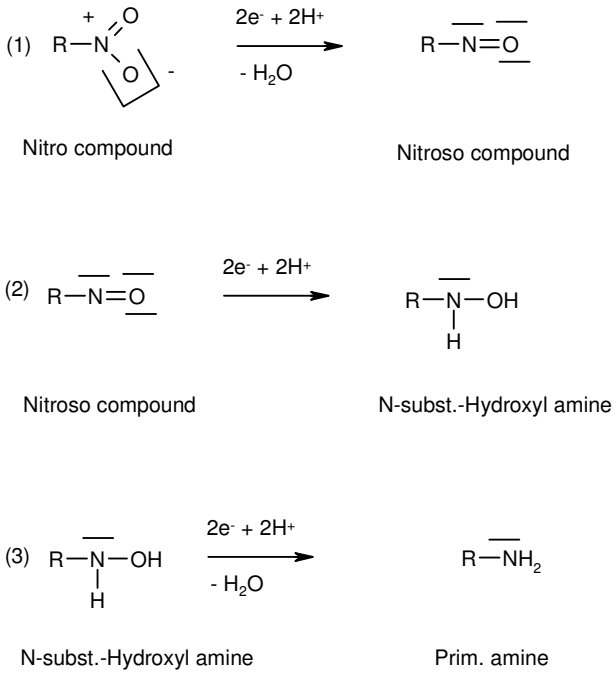

Figure 4.4 Mechanism of reduction of a nitro compound in acidic solution.

In the case of Pd/C catalysed hydrogenation of the nitro compound, at the first step, molecular hydrogen is formed by the electron transition. Palladium catalyses the electron transition from hydrogen to the nitrogen atom.[54]

A catalytic hydrogenation can be carried out also with hydrazinhydrate (NH_2-NH_2) instead of molecular hydrogen where the hydrogenation occurs from hydrazinhydrate to nitrogen atom.
In this work, the reduction process of spiro-linked compound has been carried out with Pd/C catalysed hydrogenation with hydrazinhydrate in ethanol solution with a high yield. To enhance the reaction towards high yield product and to overcome the weak solubility of the reactant, the reaction has been performed in an ultrasonic bath.

4.1.4 Sandmeyer Reaction[55]

The Sandmeyer reaction is used to synthesize aryl halides from aryl diazonium salts.

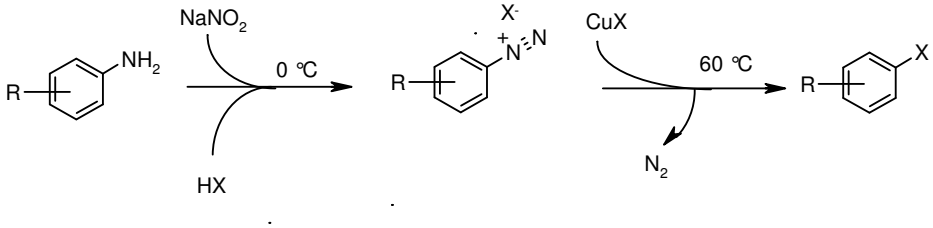

An aromatic (or heterocyclic) amine quickly reacts with a nitrite to form an aryl diazonium salt, which decomposes in the presence of copper(I) salts, such as copper(I) chloride, to form the desired aryl halide.[56] The reaction is a radical-nucleophilic aromatic substitution (figure 4.5). Several improvements have been made to the standard procedures.[57]

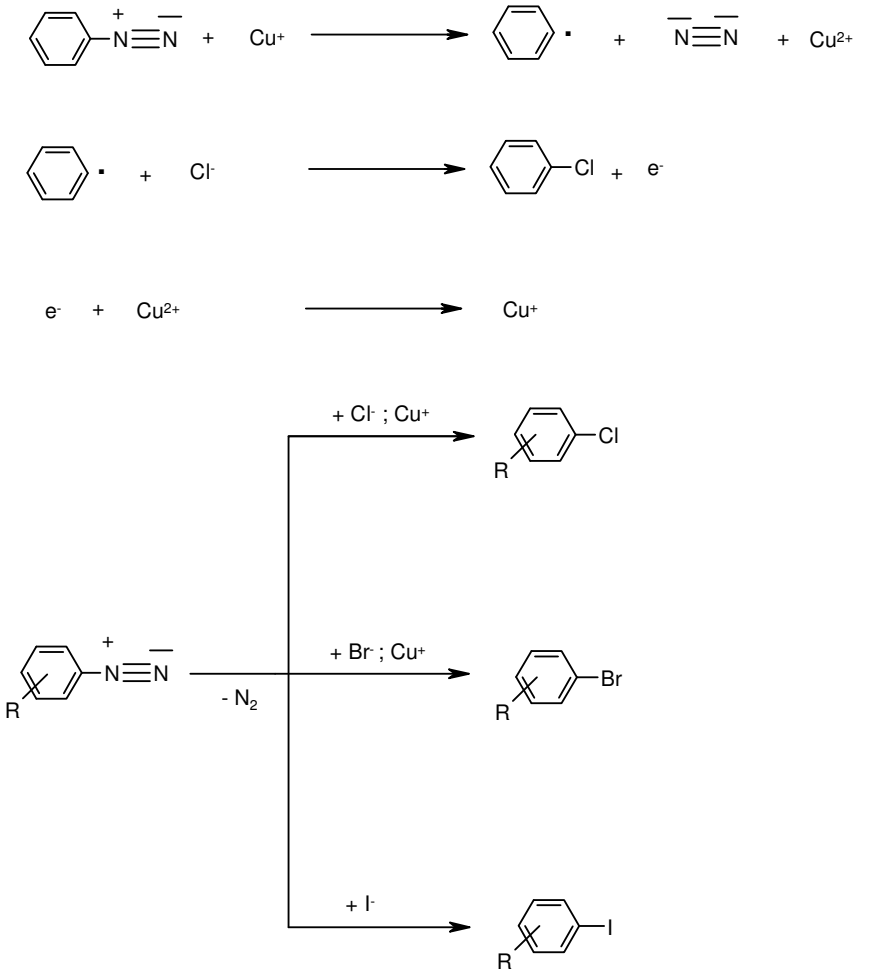

Figure 4.5 Mechanism of Sandmeyer Reaction.

In this work, the spiro-linked compound is subjected to Sandmeyer reaction, where the spiro-linked diazonium salt is decomposed in the presence of potassium iodide salt, to form the

spiro-linked iodide. Due to a heterogeneous reaction mixture, only very poor yield has been obtained. A trial to convert spiro-linked amine to spiro-linked bromide by Wei Huang's method[58] formed multi positioned halide. Hence, the spiro-linked amine has been converted into diethyltriazenyl derivative using Moore's methode.[59] The subsequent reaction of spiro-linked diethyltriazenyl compound with CH_3I in a sealed tube has afforded spiro-linked iodide compound[60] but also with unsatisfactory yield. An alternative method to obtain spiro-linked iodide compound in a good yield is a treatment of spiro-linked trimethylsilane with ICl in CH_2Cl_2 solution at room temperature, where iodine acts as an electrophile and cleaves the C-Si bond.[61]

4.1.5 Baeyer-Villiger Reaction

In Baeyer-Villiger-Oxidation reaction, a ketone is converted into ester using peroxy acid as oxidising agent. The nucleophilic addition of oxygen from peroxide to the carbonyl carbon species is enhanced in the presence of peracids such as metachlorobenzoeperacid (MCBPA) or hydrogen peroxide or Lewis acid. The mechanism of this reaction takes place as follows:

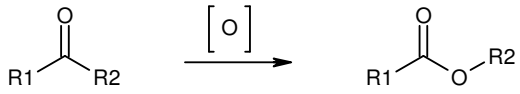

In first step, the carbonyl species is activated by protonation and the insertion of oxygen from peracid takes place.

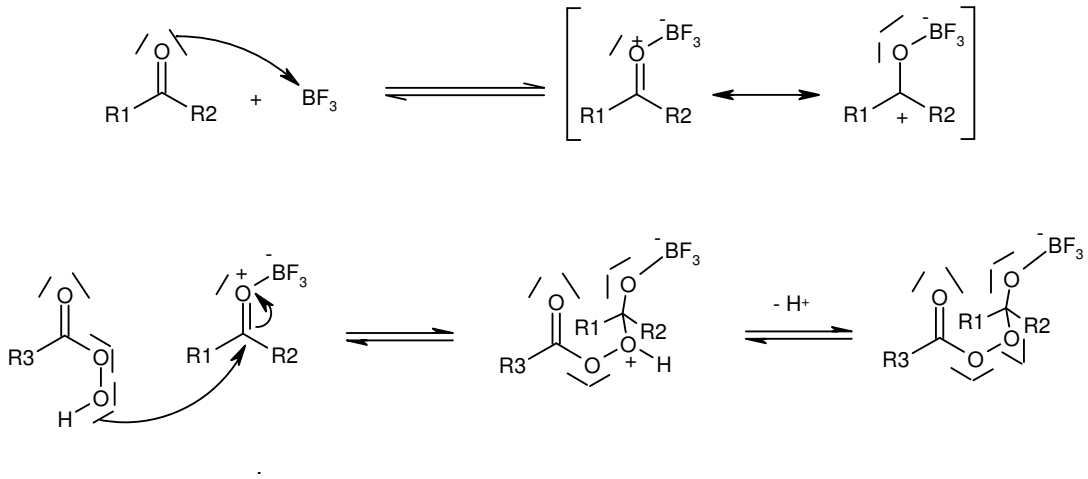

In second step, the rearrangement of the substituent takes place.

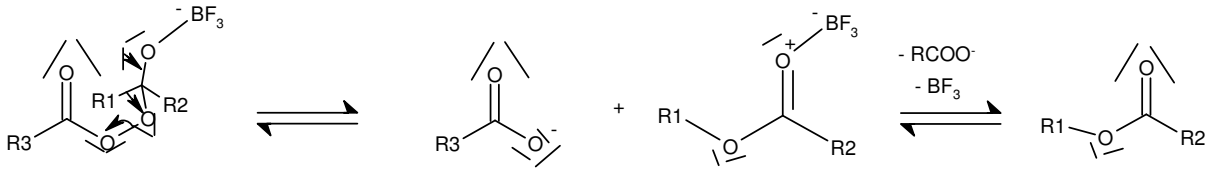

The regiospecificity of the reaction depends on the relative migratory abilities of the substituents attached to the carbonyl. Substituents which are able to stabilize a positive charge migrate more readily, so that the order of preference is:

tert. alkyl > cyclohexyl > sec. alkyl > phenyl > prim. alkyl > CH_3

In some cases, stereoelectronic or ring strain factors also affect the regiochemical outcome. The reaction of aldehydes preferably gives formates, but sometimes only the liberated alcohol may be isolated due to the solvolytic instability of the product formate under the reaction conditions.

In this work, halogenated acetyl spiro-linked compound has been subjected to the Baeyer-Williger- reaction to obtain the corresponding ester which is then further reduced to its corresponding alcohol form. A further reaction of the alcohol with triflate anhydrate adapting the J. D. Wuest's method[62] leads to the formation of its corresponding triflate compound.

4.2 Abbreviated Nomenclature of End Products

All end products synthesized in this work have been named in short form as follows:

- 2,2',7,7'-Tetrakis[1-(9,9'-spirobifluorene-2-yl)phenyl-4-yl]-9,9'-spirobifluorene **18** has been named in abbreviated form as 4SBFP-SBF since the 2,2',7,7'-positions of central core spirobifluorene are substituted by 1-(9,9'-spirobifluorene-2-yl)phenyl-4-yl moieties. 4SBFP represents 2,2',7,7'-tetrakis[1-(9,9'-spirobifluorene-2-yl)phenyl-4-yl]- and SBF represents the central core 9,9'-spirobifluorene.

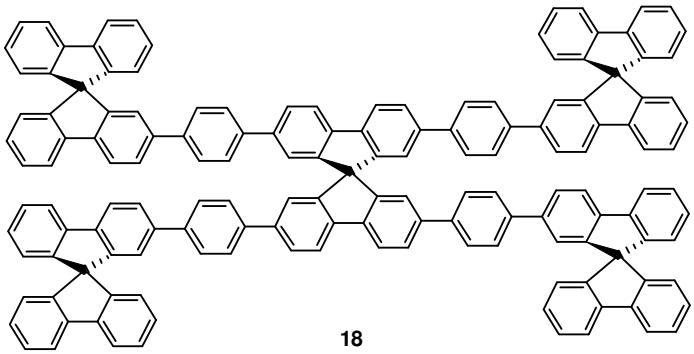

18

2,2',7,7'-Tetrakis[1-(9,9'-spirobifluorene-2-yl)phenyl-4-yl]-9,9'-spirobifluorene **18**
4SBFP-SBF

- 2,2',7,7'-Tetrakis[4-(9,9'-spirobifluorene-2-yl)-1,1'-biphenyl-4'-yl]-9,9'-spirobifluorene **21** has been named in abbreviated form as 4SBFBP-SBF **21** since the 2,2',7,7'-positions of central core spirobifluorene are substituted by 4-(9,9'-spirobifluorene-2-yl)-1,1'-biphenyl-4'-yl moieties. 4SBFBP represents 2,2',7,7'-tetrakis[4-(9,9'-spirobifluorene-2-yl)-1,1'-biphenyl-4'-yl]- and SBF represents the central core 9,9'-spirobifluorene.

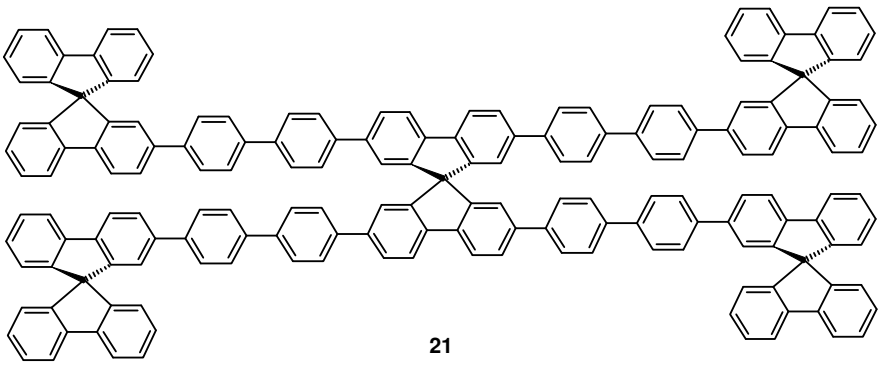

21

2,2',7,7'-Tetrakis[4-(9,9'-spirobifluorene-2-yl)-1,1'-biphenyl-4'-yl]-9,9'-spirobifluorene **21**
4SBFBP-SBF

- 2,2',7,7'-Tetrakis(2',7'-diphenyl-9,9'-spirobifluorene-2-yl)-9,9'-spirobifluorene **33** has been named in abbreviated form as 4DPSBF-SBF since the 2,2',7,7'-positions of central core spirobifluorene are substituted by 2',7'-diphenyl-9,9'-spirobifluorene-2-yl moieties. 4DPSBF represents 2,2',7,7'-tetrakis(2',7'-diphenyl-9,9'-spirobifluorene-2-yl)- and SBF represents the central core 9,9'-spirobifluorene.

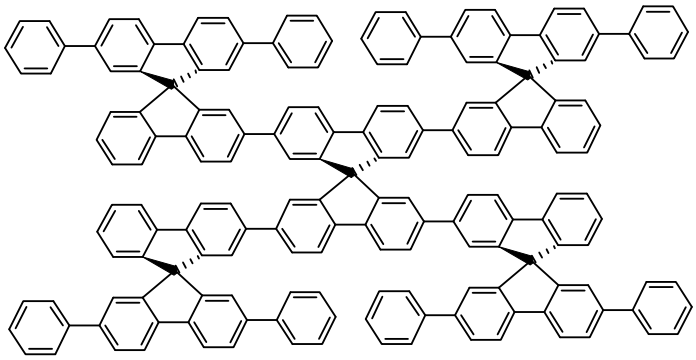

33

2,2’,7,7’-Tetrakis(2’,7’-diphenyl-9,9’-spirobifluorene-2-yl)-9,9’-spirobifluorene **33**

4DPSBF-SBF

- 2,2’,7,7’-Tetrakis[2’,7’-bis(1,1’-biphenyl-4-yl)-9,9’-spirobifluorene-2-yl]-9,9’-spirobifluorene **42** has been named in abbreviated form as 4B(BP)SBF-SBF since the 2,2’,7,7’-positions of central core spirobifluorene are substituted by 2’,7’-bis(1,1’-biphenyl-4-yl)-9,9’-spirobifluorene-2-yl moieties. 4B(BP)SBF represents 2,2’,7,7’-tetrakis[2’,7’-bis(1,1’-biphenyl-4-yl)-9,9’-spirobifluorene-2-yl]- and SBF represents the central core 9,9’-spirobifluorene.

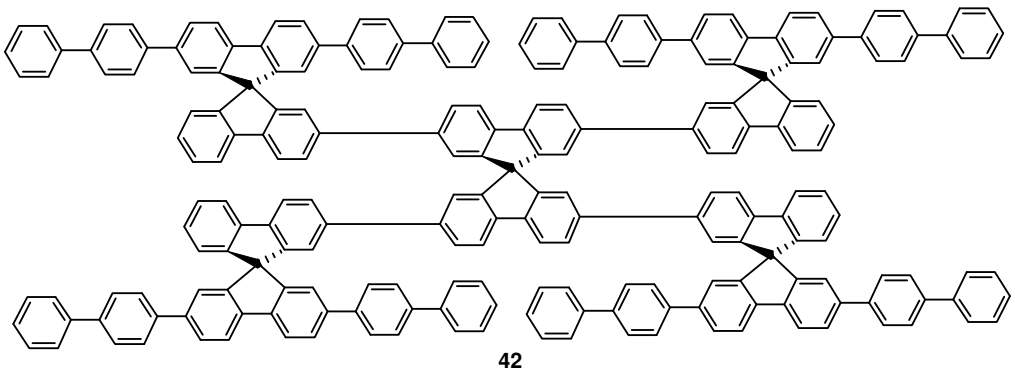

42

2,2’,7,7’-Tetrakis[2’,7’-bis(1,1’-biphenyl-4-yl)-9,9’-spirobifluorene-2-yl]-9,9’-spirobifluorene **42**

4B(BP)SBF-SBF

- 2,2’,7,7’-Tetrakis[2’,7’-bis(1,1’,4’,1’’-terphenyl-4-yl)-9,9’-spirobifluorene-2-yl]-9,9’-spirobifluorene **53** has been named in abbreviated form as since the 2,2’,7,7’-positions of central core spirobifluorene are substituted by 2’,7’-bis(1,1’,4’,1’’-terphenyl-4-yl)-9,9’-spirobifluorene-2-yl moieties. 4B(TP)SBF represents 2,2’,7,7’-

tetrakis[2',7'-bis(1,1',4',1''-terphenyl-4-yl)-9,9'-spirobifluorene-2-yl]- and SBF represents the central core 9,9'-spirobifluorene.

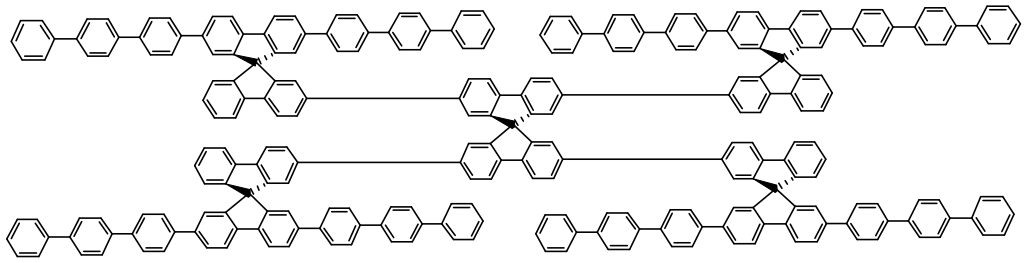

53

2,2',7,7'-Tetrakis[2',7'-bis(1,1',4',1''-terphenyl-4-yl)-9,9'-spirobifluorene-2-yl]-9,9'-spirobifluorene **53**

4B(TP)SBF

- 2,2',7,7'-Tetrakis[1-(2',7'-diphenyl-9,9'-spirobifluorene-2-yl)phenyl-4-yl]-9,9'-spirobifluorene **58** has been named in abbreviated form as 4DPSBFP-SBF since the 2,2',7,7'-positions of central core spirobifluorene are substituted by [1-(2',7'-diphenyl-9,9'-spirobifluorene-2-yl)phenyl-4-yl] moieties. 4DPSBFP represents 2,2',7,7'-tetrakis[1-(2',7'-diphenyl-9,9'-spirobifluorene-2-yl)phenyl-4-yl]- and SBF represents the central core 9,9'-spirobifluorene.

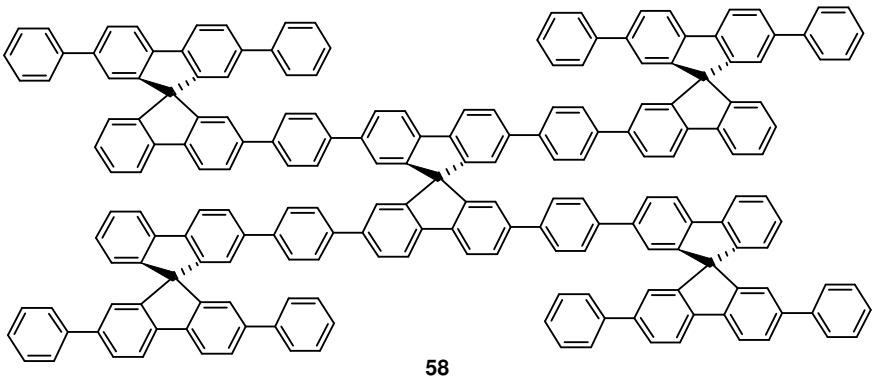

58

2,2',7,7'-Tetrakis[1-(2',7'-diphenyl-9,9'-spirobifluorene-2-yl)phenyl-4-yl]-9,9'-spirobifluorene **58**

4DPSBFP-SBF

- 2,2',7,7'-Tetrakis(2',7,7'-triphenyl-9,9'-spirobifluorene-2-yl)-9,9'-spirobifluorene **72** has been named in abbreviated form as 4TPSBF-SBF since the 2,2',7,7'-positions of

central core spirobifluorene are substituted by (2',7,7'-triphenyl-9,9'-spirobifluorene-2-yl) moieties. 4TPSBF represents 2,2',7,7'-tetrakis(2',7,7'-triphenyl-9,9'-spirobifluorene-2-yl)- and SBF represents the central core 9,9'-spirobifluorene.

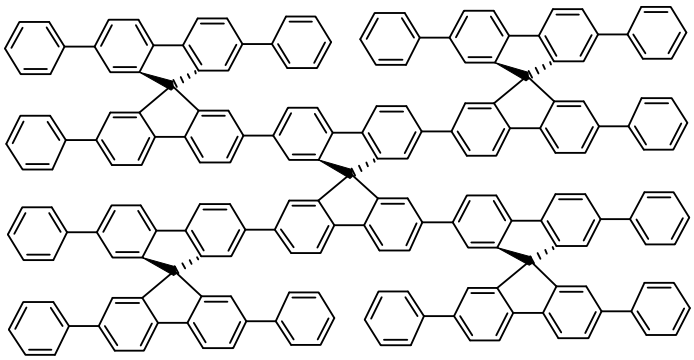

72

2,2',7,7'-Tetrakis(2',7,7'-triphenyl-9,9'-spirobifluorene-2-yl)-9,9'-spirobifluorene **72**
4TPSBF-SBF

- 2,2',7,7'-Tetrakis[2'-(9,9'-spirobifluorene-2-yl)-9,9'-spirobifluorene-2-yl]-9,9'-spirobifluorene **79** has been named in abbreviated form as 4SBFSBF-SBF since the 2,2',7,7'-positions of central core spirobifluorene are substituted by [2'-(9,9'-spirobifluorene-2-yl)-9,9'-spirobifluorene-2-yl] moieties. 4SBFSBF represents 2,2',7,7'-tetrakis[2'-(9,9'-spirobifluorene-2-yl)-9,9'-spirobifluorene-2-yl]- and SBF represents the central core 9,9'-spirobifluorene.

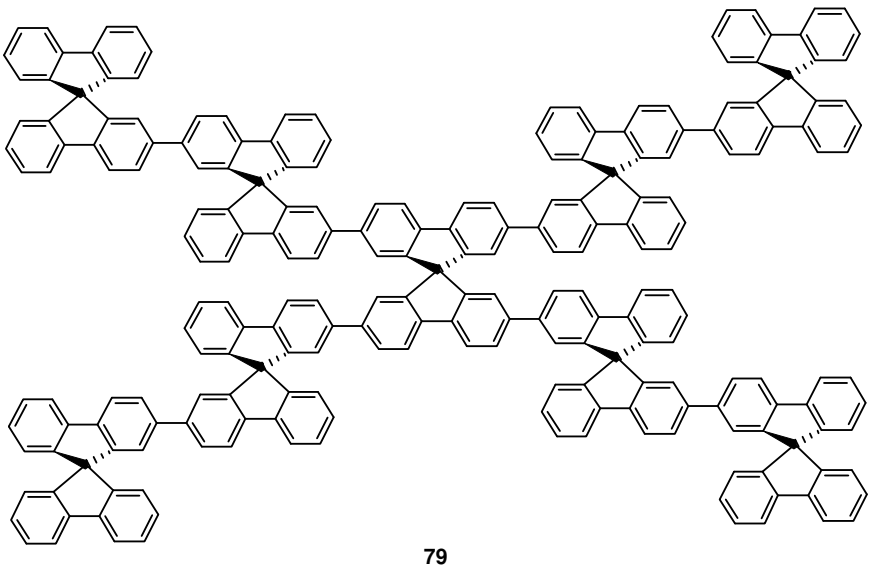

79

2,2',7,7'-Tetrakis[2'-(9,9'-spirobifluorene-2-yl)-9,9'-spirobifluorene-2-yl]-9,9'-spirobifluorene **79**

4SBFSBF-SBF

- 2,2',7,7'-Tetrakis[2',7'-bis(9,9'-spirobifluorene-2-yl)-9,9'-spirobifluorene-2-yl]-9,9'-spirobifluorene **84** has been named in abbreviated form as 4B(SBF)SBF-SBF since the 2,2',7,7'-positions of central core spirobifluorene are substituted by [2',7'-bis(9,9'-spirobifluorene-2-yl)-9,9'-spirobifluorene-2-yl] moieties. 4B(SBF)SBF represents 2,2',7,7'-tetrakis[2',7'-bis(9,9'-spirobifluorene-2-yl)-9,9'-spirobifluorene-2-yl]- and SBF represents the central core 9,9'-spirobifluorene.

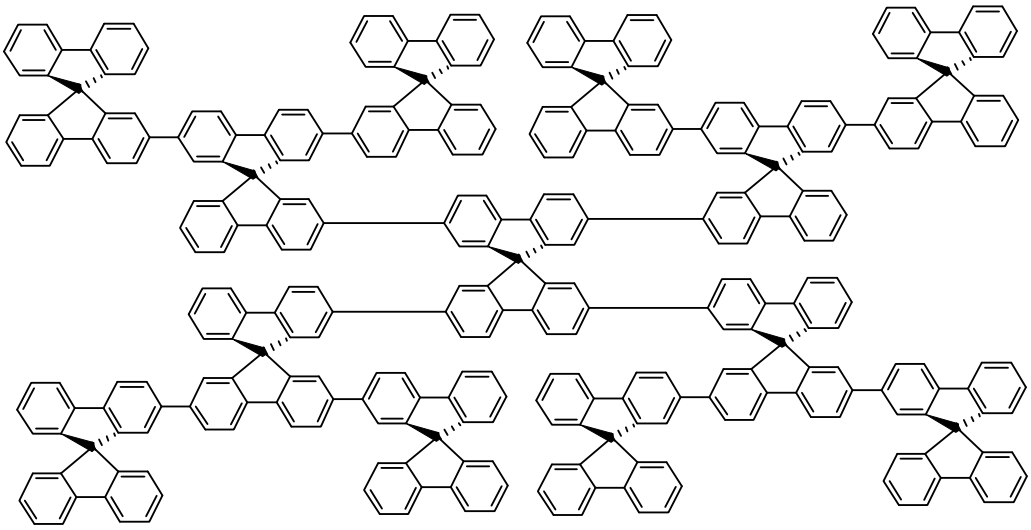

84

2,2',7,7'-Tetrakis[2',7'-bis(9,9'-spirobifluorene-2-yl)-9,9'-spirobifluorene-2-yl]-9,9'-spirobifluorene **84**

4B(SBF)SBF-SBF

4.3 General Synthetic Routes to Spiro-Starburst-Structures

Spiro-starburst-structures are derived from a fundamental central core spirobifluorene compound **4**. Spirobifluorene was firstly synthesized by Clarkson and Gomberg in 1930,[63] as shown in figure 4.6, starting with 2-iodobiphenyl **1**, which was obtained through Sandmeyer's reaction from 2-aminobiphenyl. The reaction of fluorenone with a Grignard reagent of 2-iodobiphenyl **2** leads to the formation of 9-(biphenyl-2-yl)-9-fluorenol **3**, a tertiary alcohol, as an intermediate product. To close the ring by the loss of a water molecule, a catalytic amount of concentrated hydrochloric acid is added to the boiling solution of the tertiary alcohol in acetic acid. It leads to a ring-closure reaction forming 9,9'-spirobifluorene **4** which

precipitates out on cooling the solution with a yield of 59%. Later on, several modifications in its synthetic procedure have been done.[64] The choice of the right pathway depends on the desired substitution pattern.

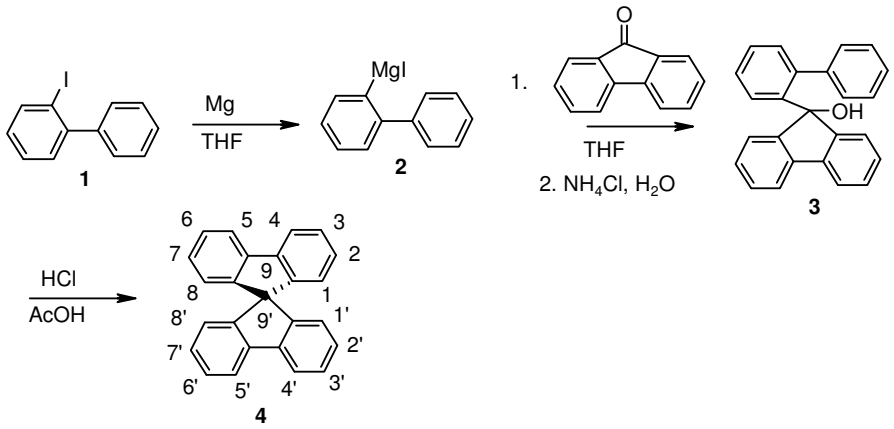

Figure 4.6 Synthesis of 9,9'-spirobifluorene

Not only to overcome obstacles like high tendency towards recrystallization and an extremely low solubility of oligophenyls but also to further enhance the morphological stability, optical properties with increasing the molecular weight, glass transition temperature and therefore the stability of the amorphous state along with the solubility of the compounds,[21, 22] new variants of spiro-starburst-structures have been synthesized. The rigidity of such compounds decreases the rotational freedom of the oligophenyl system and thus affects the fluorescence quantum yield positively.

Furthermore, these classes of materials seem to be promising for new zeolitic applications. Taking advantage of well-defined intercrystalline channels of the zeolitic materials, it is possible to introduce guest molecules into these channels. The resulting host-guest systems exhibit new physical and chemical properties as similar in the case of inorganic molecular sieve, which was reported by Ihlein,[65] offering versatile possible applications as luminophores,[66] pigments,[67] frequency doublers[68] or optical switches.[69] Such properties of molecular sieves suggest the construction of a new class of microlasers based on these materials, which could be considered as a hybrid between the solid-state and dye laser. Furthermore, the large variety of different laser active dyes that could be incorporated into the molecular sieve may yield a large number of different microlaser systems.

These spiro-starburst-structured compounds are classified into two categories, namely first generation and second generation of spiro-starburst-structures.

4.3.1 Spiro-Starburst-Structures of First Generation

In first generation spiro-starburst-structures, the central core spirobifluorene is substituted with equal substituents in the 2,2' and 7,7'-positions. The variations in end products from one to another are due to the addition of various numbers of phenyl ring to internal as well as external chromophores of the structures.

4.3.1.1 Synthesis of 2,2',7,7'-tetrakis[1-(9,9'-spirobifluorene-2-yl)phenyl-4-yl]-9,9'-spirobifluorene (4SBFP-SBF) (18)

4SBFP-SBF **18** (figure 4.10) represents a member of the first category (first generation). The compound 4SBFP-SBF **18** has been synthesized in a novel path although the same compound had been introduced in a previous work of our group.[70] In this compound, the 2,2',7,7'-postions of the central core spirobifluorene are substituted with terminal 2-phenyl-9,9'-spirobifluorene units. The phenyl ring present between the central core and terminal spirobifluorene unit undergoes rotation which reduces the rigidity of the compound compared to that of 4-spiro[2].[70]

4SBFP-SBF **18** (4-phspiro[2]) is synthesized by starting with 2-bromofluorene **5** as shown in figure 4.7. The 2-bromofluoren-9-one **6,**[71] obtained by the oxidation of 2-bromofluorene **5**, is treated with the Grignard reagent of 2-bromo-1,1'-biphenyl to prepare 2-bromo-9,9'-spirobifluorene **7**[72] analogous to the preparation of spirobifluorene **4**. It is then subjected to cross-coupling reaction with 4-trimethylsilylphenyl boronic acid **8** under Suzuki reaction condition leading to the formation of 2-(4-trimethylsilylphenyl)-9,9'-spirobifluorene **9** with 70% yield.[47] It is then subsequently converted into an intermediate product of 4-(9,9'-spirobifluorene-2-yl)dibromophenyl borate[73] and is followed by hydrolysis affording 4-(9,9'-spirobifluorene-2-yl)phenyl boronic acid **10** with 75% yield. Another trial to synthesize 2-[4-(9,9'-spirobifluorene-2-yl)phenyl]-4,4,5,5-tetramethyl-[1,3,2]dioxaborolane **12**, an alternative form of 4-(9,9'-spirobifluorene-2-yl)phenyl boronic acid **10**, leads to an unsuccessful Miyaura reaction[47] of 2-(4''-iodophenyl)-9,9'-spirobifluorene **11** whereas the

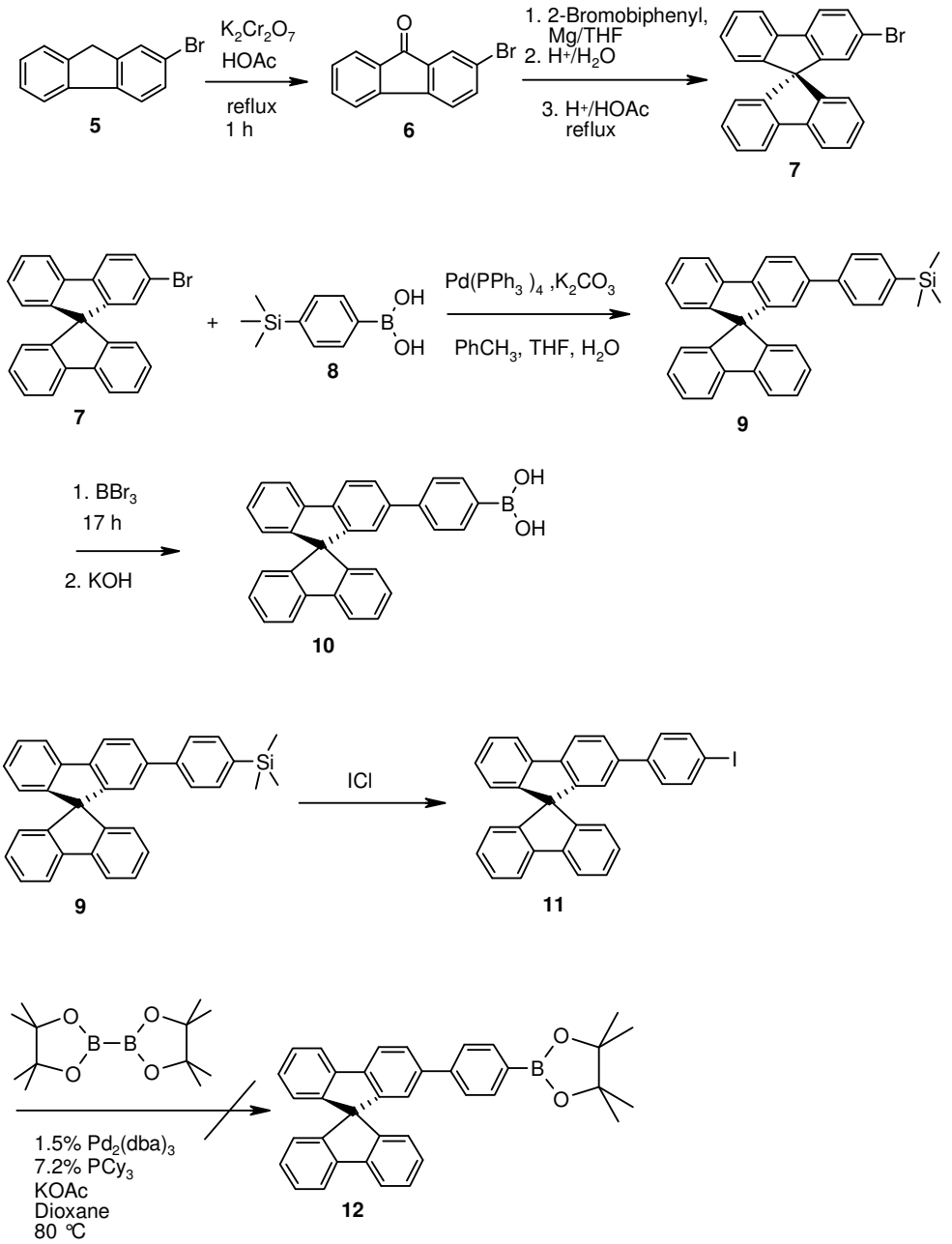

Figure 4.7 Synthesis of spiro phenyl boronic acid

conversion of trimethylsilyl group of 2-(4-trimethylsilylphenyl)-9,9'-spirobifluorene **9** to iodide runs smoothly with a good yield of 81%. The precursor compound 4-trimethylsilylphenyl boronic acid **8** is obtained with 70% yield as a derivative of the commercially available 1,4-dibromo benzene **13** after going through a series of reaction as shown in figure 4.8. Reaction of 1,4-dibromobenzene **13** with two equivalent of n-BuLi in Et_2O at -78 °C gives the dilithiated intermediate **14**, which further reacted with chlorotrimethylsilane affording the corresponding 1,4-bis(trimethylsilyl)benzene **15** in 90% yield.[74] 4-Trimethylsilylphenyl dibromoborane **16** is obtained in 80% yield by a treatment of 1,4-bis(trimethylsilyl)benzene **15** with tribromoborane at -78 °C. A treatment of 4-

trimethylsilylphenyl dibromoborane **16** with MeOH did not form the expected product but hydrolysis with KOH gave the expected product 4-trimethylsilylphenyl boronic acid **8**.

To obtain 2,2',7,7'-tetrasubstituted spiro compounds, tetrahalogenated derivative of spirobifluorene, 2,2',7,7'-tetrabromo-9,9'spirobifluorene is prepared. Halogenated compounds are versatile candidates for further substitution with cross-coupling reactions like Suzuki and Miyaura reactions. 2,2',7,7'-Tetrabromo-9,9'spirobifluorene can be synthesized according to the procedure proposed by Tour and co-workers, who reported a yield of 100% using stoichiometric amounts of bromine and ferric chloride as catalyst in chloroform at 0 °C.[75] In this work, the procedure which is developed by our group is followed where no cat-

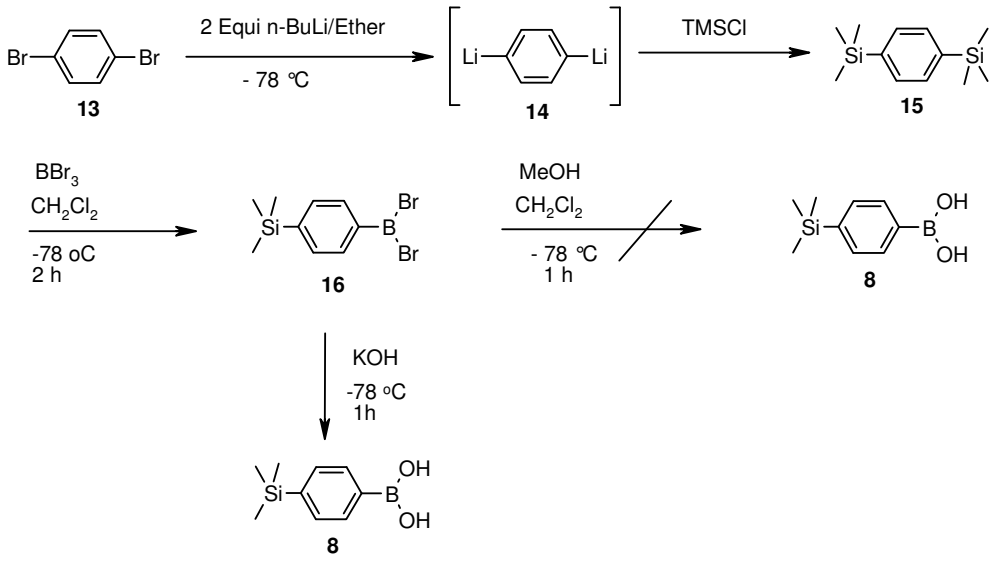

Figure 4.8 Synthesis of trimethylsilylphenyl boronic acid

alyst is used. It yields the product 2,2',7,7'-tetrabromo-9,9'-spirobifluorene with 91% (figure 4.9).[70]

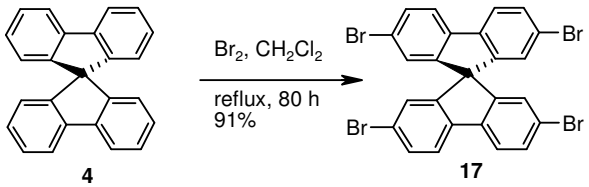

Figure 4.9 Synthesis of 2,2',7,7'-tetrabromo-9,9'-spirobifluorene

It has been found that an excess of bromine without the addition of a Lewis acid catalyst allows for the selective 4-fold bromination in 2,2',7,7'-positions of spirobifluorene, whereas the addition of ferric chloride combined with an excess of bromine results in 2,2',4,4',7,7'-

hexabromo-9,9'-spirobifluorene in good yield.[76] The final step for the synthesis of 4-phspiro[2] **18** involves Suzuki cross-coupling[47] of 4-(9,9'-spirobifluorene-2-yl)phenyl boronic acid **10** with tetrabromo compound **17** (figure 4.10).

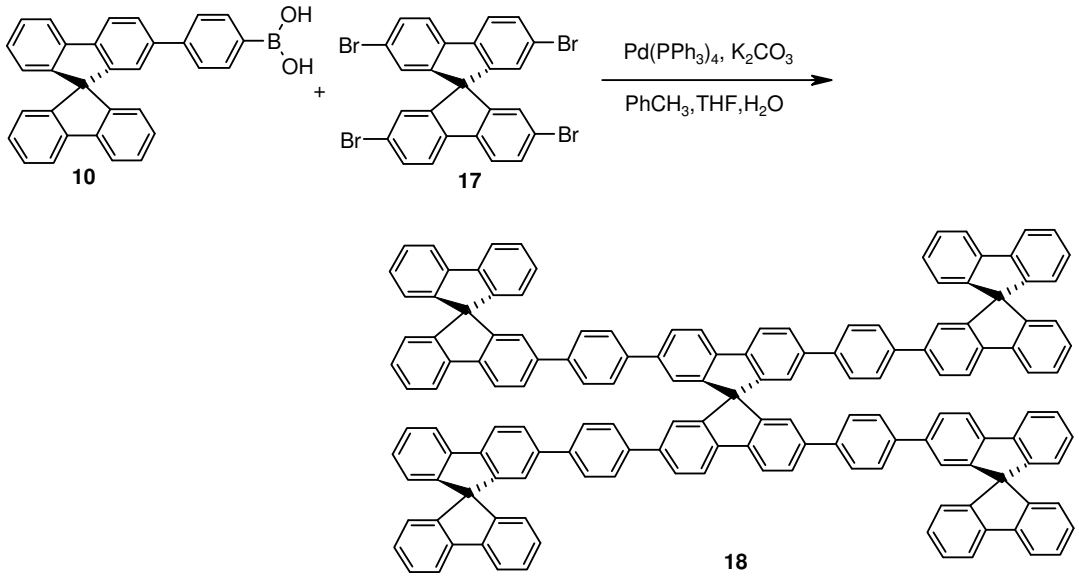

Figure 4.10 Synthesis of 4SBFP-SBF (18)

4.3.1.2 Synthesis of 2,2',7,7'-tetrakis[4-(9,9'-spirobifluorene-2-yl)-1,1'-biphenyl-4'-yl]-9,9'-spirobifluorene (4SBFBP-SBF) (21)

In 4SBFBP-SBF **21** compound (figure 4.12), the central core spirobifluorene is connected with four terminal spirobifluorenes through four biphenyl units. Out of total 28 phenyl rings of this molecule, 20 phenyl rings form two internal chromophores of deciphenyl chains and 8 phenyl rings form four external biphenyl units. The presence of the biphenyl units between the centre core and terminal spirobifluorene units, that can undergo rotation of certain degree, reduces the rigidity of the compound than that of 4-spiro[2] and 4-phspiro[2].[70] The motivation to synthesize this compound is to study the effect of restricted rotation of the compound in glass transition temperature and morphology of the compound in its thin film.

To synthesize 4SBFBP-SBF **21**, the necessary precursor 2,2',7,7'-tetrakis(4-iodophenyl)-9,9'-spirobifluorene **20** is prepared by treating 2,2',7,7'-tetrakis(4-trimethylsilylphenyl)-9,9'-spirobifluorene **19** with iodine monochloride at room temperature. The 2,2',7,7'-tetrakis(4-trimethylsilylphenyl)-9,9'-spirobifluorene **19** with 90% yield has been obtained as a Suzuki

reaction product of 2,2',7,7'-tetrabromo-9,9'-spirobifluorene **17** and 4-trimethylsilylphenyl boronic acid **8** (figure 4.11).

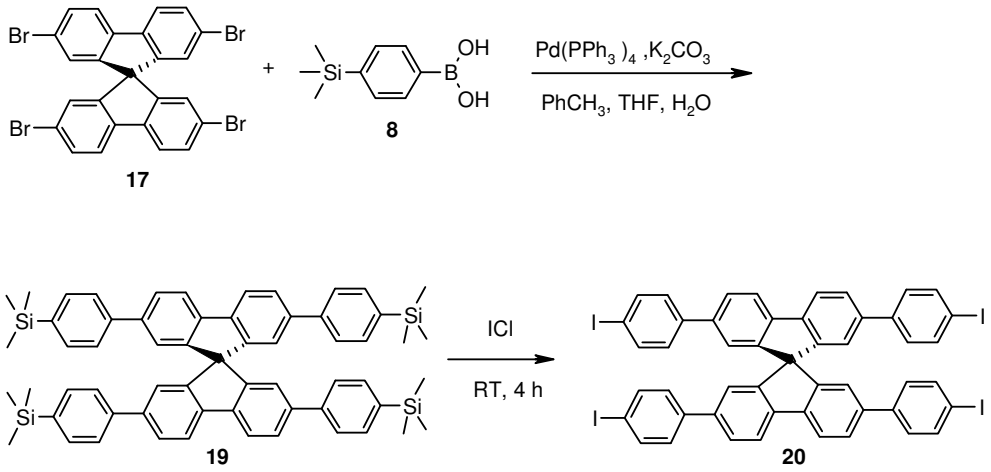

Figure 4.11 Synthesis of tetraiodo spiro quaterphenyl

Thus, the synthesis of the target compound 4SBFBP-SBF **21** completes successfully starting from 2,2',7,7'-tetrakis(4-iodophenyl)-9,9'-spirobifluorene **20** with subsequent Suzuki coupling employing 4-(9,9'-spirobifluorene-2-yl)phenyl boronic acid **10** with a yield of 35%. The poor yield of the product is due to the very inconvenient purification of the compound as it is only sparingly soluble in various solvents.

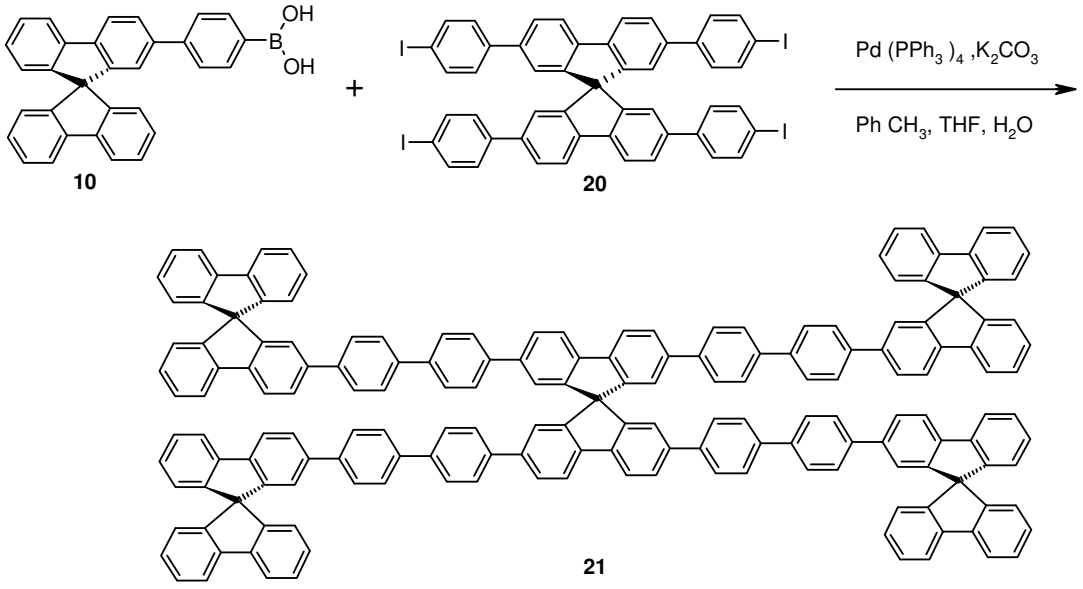

Figure 4.12 Synthesis of 4SBFBP-SBF 21

4.3.1.3 Synthesis of 2,2',7,7'-tetrakis(2',7'-diphenyl-9,9'-spirobifluorene-2-yl)-9,9'-spirobifluorene (4DPSBF-SBF) (33)

To examine an influence to the optical as well as thermal, electrochemical and morphological properties, due to the presence of free phenyl rings in external chromophores of spiro-starburst-structures, 4DPSBF-SBF **33** (figure 4.13) has been synthesized. In this compound, two free phenyl rings, one at the 2'- and the other at the 7'-positions of every terminal spirobifluorene, are added.

The synthesis of 4DPSBF-SBF **33** is outlined in figure 4.13 starting from fluorenone **22**. The bromination of fluorenone **22** with slight excess of bromine and a trace of surfactant in aqueous solution gives 2,7-dibromofluorenone **23**.[77] To obtain 2,7-dibromo-9,9'-spirobifluorene **24**, lithiated 2-bromobiphenyl is treated with 2,7-dibromofluorenone **23** and followed by refluxing the reaction mixture with concentrated acetic acid in the presence of catalytic amount of concentrated hydrochloric acid as analogous to the synthesis of 9,9'-spirobifluorene **4**. The nitration of 2,7-dibromo-9,9'-spirobifluorene **24** treating with bismuthsubnitrate ($Bi_5O(OH)_9(NO_3)_4$) and thionylchloride ($SOCl_2$) in dichloromethane leads to the formation of 2,7-dibromo-2'-nitro-9,9'-spirobifluorene **25** with a yield of 79%.[53] The nitration with bismuthsubnitrate is favoured in this case rather than the procedure of Weissburger et al. in which an equal ratio of nitric acid and concentrated acetic acid is used as a nitrating reagent.[78] The advantage of the nitration with bismuth salt is that the reaction mixture can be mixed in homogeneous phase. The Suzuki cross-coupling reaction between 2,7-dibromo-2'-nitro-9,9'-spirobifluorene **25** and phenyl boronic acid **26** forms 2,7-diphenyl-2'-nitro-9,9'-spirobifluorene **27** with a yield of 77%. The synthetic precursor phenyl boronic **26** acid is obtained by esterification of Grignard reagent of bromobenzene **28** followed by hydrolysis. The nitro group of 2,7-diphenyl-2'-nitro-9,9'-spirobifluorene **27** is then readily reduced by palladium catalysed hydrogenation to afford the 2-amino-2',7'-diphenyl-9,9'-spirobifluorene **29** with an isolated yield of 99%. Iron/hydrochloric acid is also a good candidate of reducing agents for the reduction of such nitro compounds.[78] Rather than following a modified Sandmeyer reaction approach,[54] the 2-amino-2',7'-diphenyl-9,9'-spirobifluorene **29** is converted into 3,3-diethyl-1-(2',7'-diphenyl-9,9'-spirobifluorene-2-yl)triazene **30** using Moore's method.[59, 79] In this step, the product is not isolated due to the heterogenous reaction mixture. The subsequent reaction of 3,3-diethyl-1-(2',7'-diphenyl-9,9'-spirobifluorene-2-yl)triazene **30** with iodomethane in a sealed tube at 100 °C affords 2,7-

diphenyl-2'-iodo-9,9'-spirobifluorene **31** in a very poor yield of 15%. The cross coupling reaction of pinacolborane with haloarenes in the presence of the palladium catalyst and triethylamine reported by Masuda and Murata is a convenient method and economical variant for the preparation of such pinacol arylboronates.[80] As shown in figure 4.13, the palladium-catalysed coupling reaction of 2,2',7,7'-tetrabromo-9,9'-spirobifluorene **17** with bis(pinacolato)diboron is carried out for the synthesis of 2,2',7,7'-tetrakis(pinacolato boron-2-yl)-9,9'-spirobifluorene **32**.

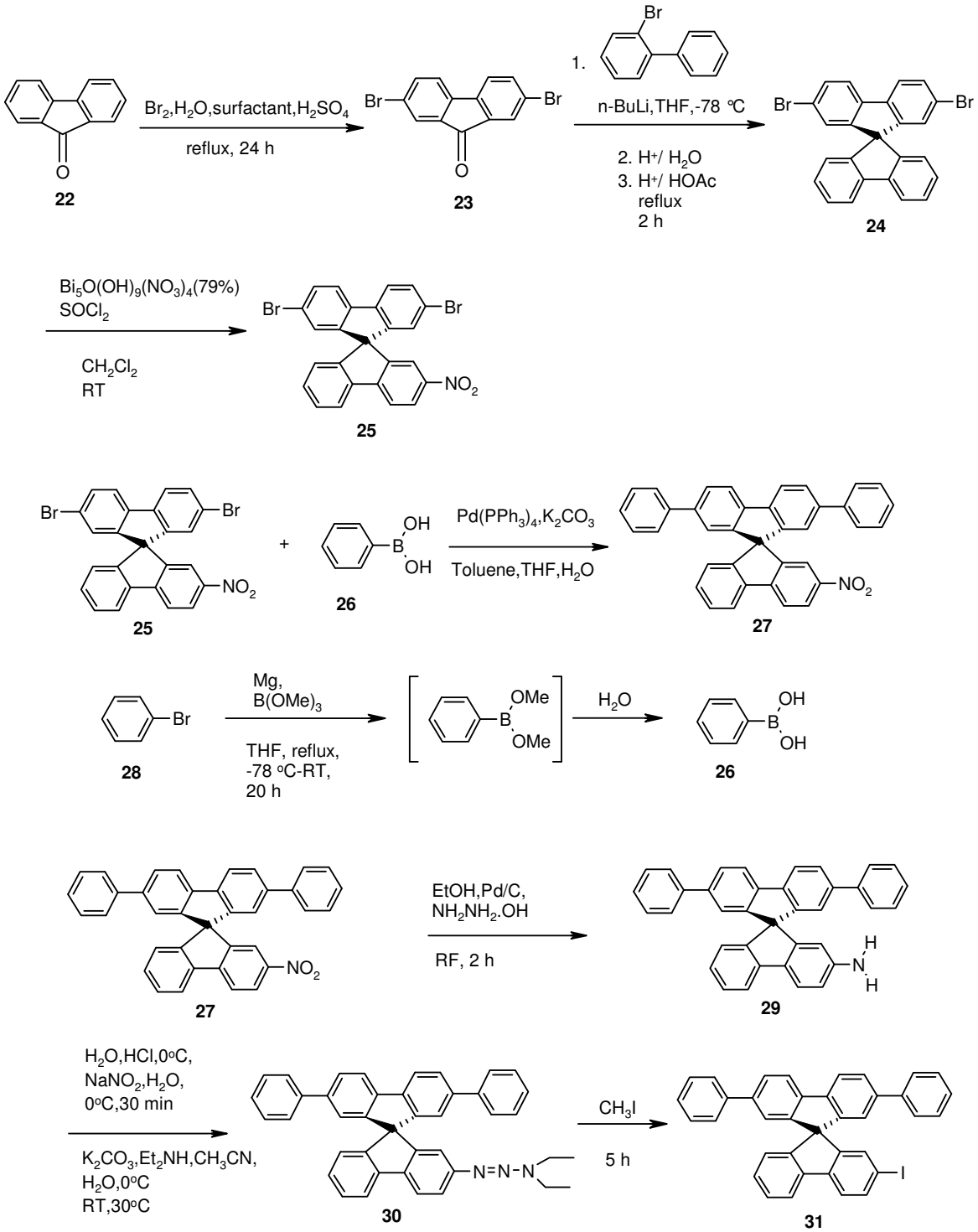

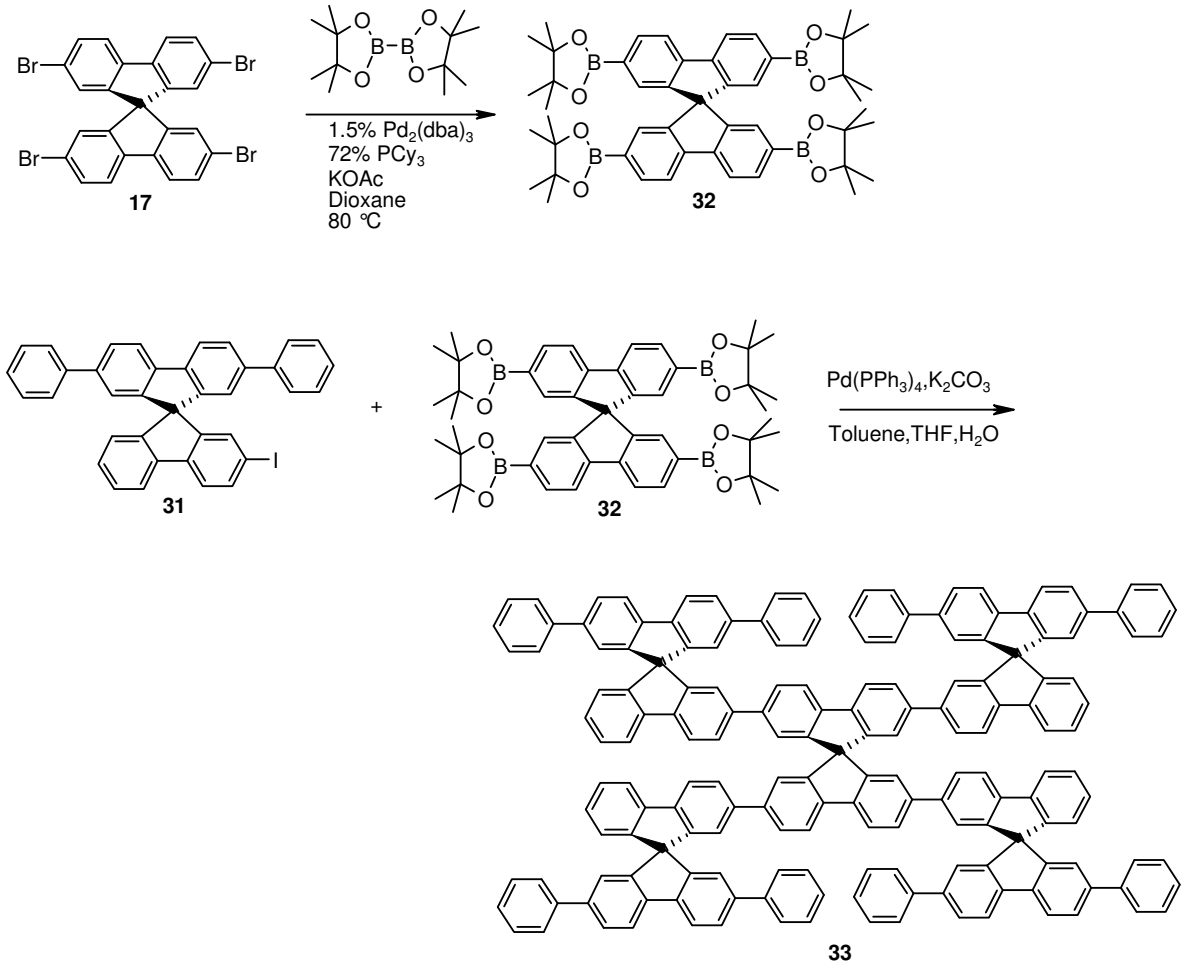

Figure 4.13 Synthesis of 4DPSBF-SBF 33

Although the oxidative addition of less active 2,2',7,7'-tetrabromo-9,9'-spirobifluorene **17** to palladium(0) complexes is very slow, a catalyst in situ generated from $Pd_2(dba)_3$ and PCy_3 efficiently catalyses the reaction at 80 °C.[81] The expected final product 2,2',7,7'-tetrakis(2',7'-diphenyl-9,9'-spirobifluorene-2-yl)-9,9'-spirobifluorene **33** is afforded with 58% yield by the Suzuki reaction of 2,2',7,7'-tetrabromo-9,9'-spirobifluorene **17** with 2,2',7,7'-tetrakis(pinacolato boron-2-yl)-9,9'-spirobifluorene **32**.

4.3.1.4 Synthesis of 2,2',7,7'-tetrakis[2',7'-bis(1,1'-biphenyl-4-yl)-9,9'-spirobifluorene-2-yl]-9,9'-spirobifluorene [4B(BP)SBF-SBF] (42)

Figure 4.14 shows the structure of 4B(BP)SBF-SBF **42**, in which all four external chromophores bear chains of the same number of phenyl rings as in two internal

chromophores, namely six phenyl rings. The aim to design this molecule is to watch the effect of the equally elongated external and internal chromophore chains in its characterization.

The synthesis of this compound begins with the acetylation of 2,7-dibromo-9,9'-spirobifluorene **24** (figure 4.14). The acetylation is carried out according to Hass and Prelog,[82] where the substitution of 2,7-dibromo-9,9'-spirobifluorene **24** takes place with acetylchloride in carbon disulfide solution affording 2-acetyl-2',7'-dibromo-9,9'-spirobifluorene **34**. A formylation of spirobifluorene with a system of dichloromethylmethylether/titanium(IV)chloride has been also reported.[83] Baeyer-Villiger oxidation of the acetyl group of 2-acetyl-2',7'-dibromo-9,9'-spirobifluorene **34** into 2',7'-dibromo-9,9'-spirobifluorene-2-ol acetate **35** with 51% yield is performed by treating 2-acetyl-2',7'-dibromo-9,9'-spirobifluorene **34** with an oxidising agent metachloroperbenzoic acid.[84]

A cross-coupling reaction of 2',7'-dibromo-9,9'-spirobifluorene-2-ol acetate **35** with biphenyl-4-yl boronic acid **36** under the Suzuki reaction condition affords 2-acetoxy-2',7'-bis(1,1'-biphenyl-4-yl)-9,9'-spirobifluorene **37** with 83% yield. The synthetic precursor biphenyl-4-yl boronic acid **36** is obtained by esterification of Grignard reagent of 4-bromobiphenyl **38** followed by reduction. Hydrolysis of 2',7'-bis(biphenyl-4-yl)-9,9'-spirobifluorene-2-ol acetate **37** affords 99% yield of an alcohol 2,7-bis(biphenyl-4-yl)-2'-hydroxy-9,9'-spirobifluorene **39**[84,85] which is subsequently converted into 2,7-bis(biphenyl-4-yl)-9,9'-spirobifluorene-2'-yl triflate **40** in 88% yield.[62] The palladium-catalysed coupling reaction of 2,7-bis(biphenyl-4-yl)-9,9'-spirobifluorene-2'-yl triflate **40** with bis(pinacolato)diboron is carried out for the synthesis of pinacol 2,7-bis(biphenyl-4-yl)-9,9'-spirobifluorene-2'-yl boronate **41** with a yield of 87%.

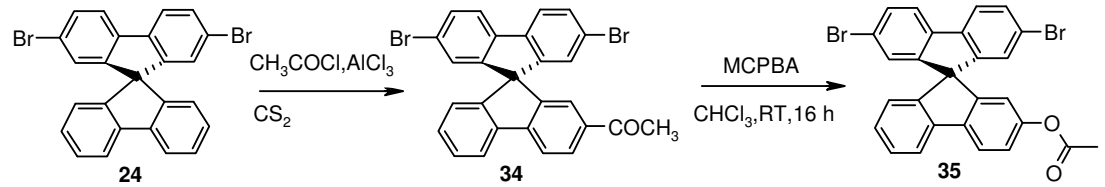

24 34 35

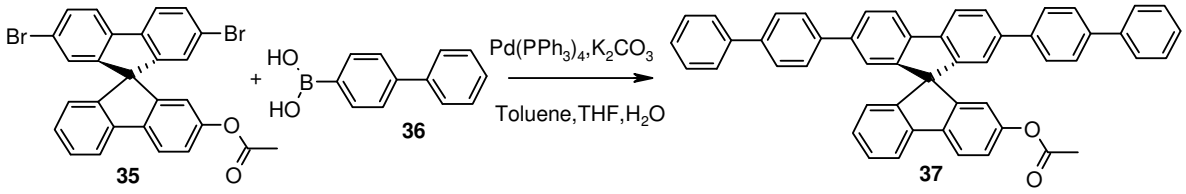

35 36 37

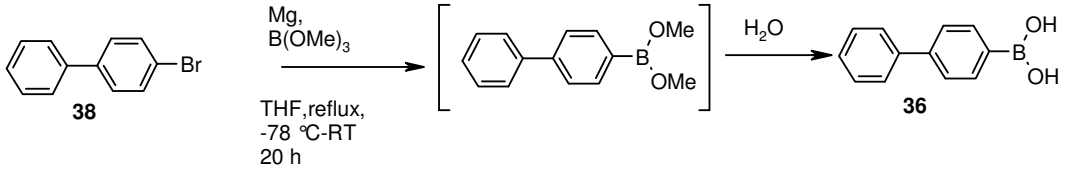

38 36

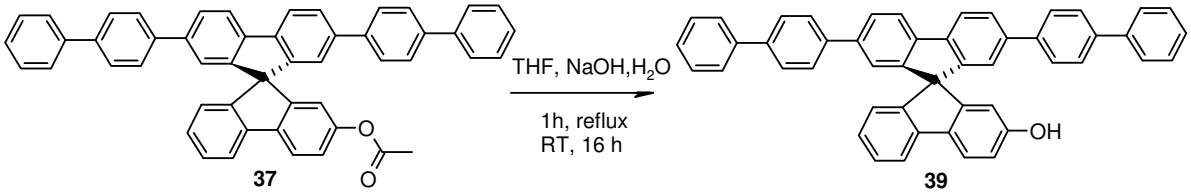

37 39

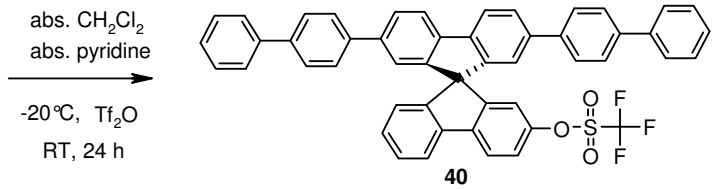

40

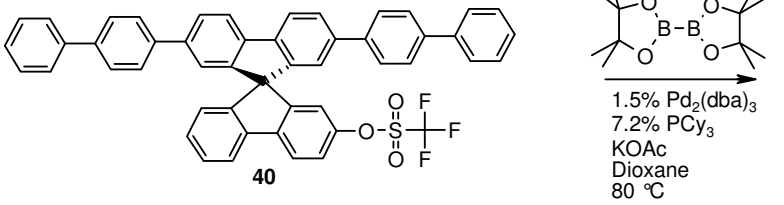

40

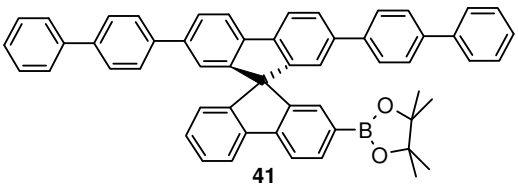

41

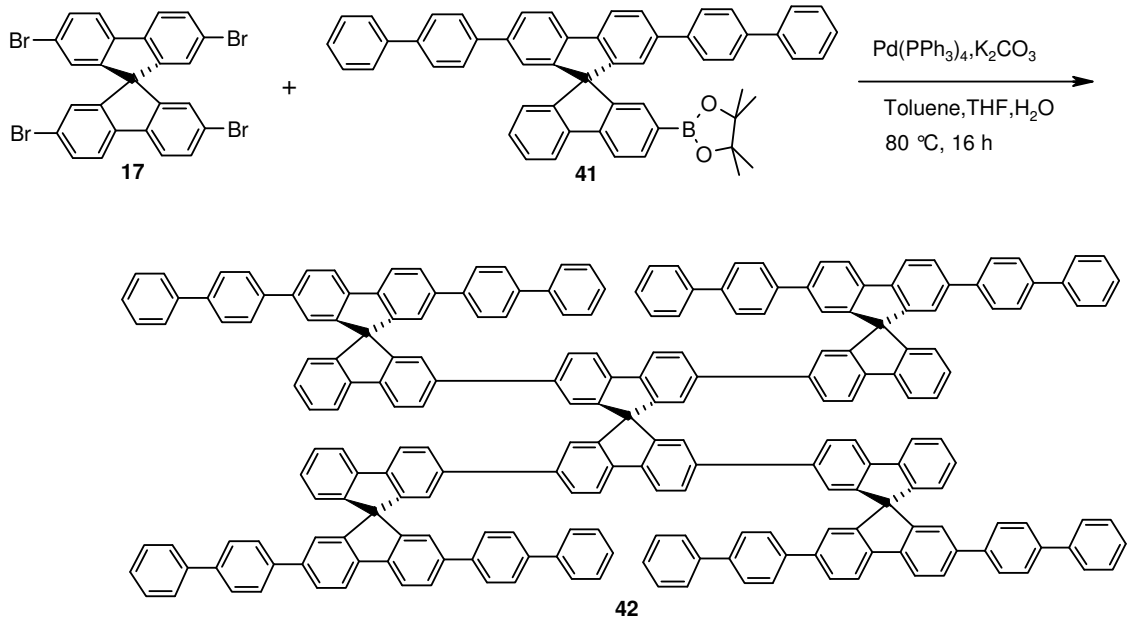

Figure 4.14 Synthesis of 4B(BP)SBF-SBF 42

A cross coupling reaction of pinacol 2,7-dibiphenyl-9,9'-spirobifluorene-2'-yl boronate **41** with 2,2',7,7'-tetrabromospirobifluorene **17** under the Suzuki coupling reaction condition leads to the formation of 2,2',7,7'-tetrakis[2',7'-bis(1,1'-biphenyl-4-yl)-9,9'-spirobifluorene-2-yl]-9,9'-spirobifluorene **42** (figure 4.14).

4.3.1.5 Synthesis of 2,2',7,7'-tetrakis[2',7'-bis(1,1',4',1''-terphenyl-4-yl)-9,9'-spirobifluorene-2-yl]-9,9'-spirobifluorene [4B(TP)SBF-SBF] (53)

Figure 4.15 shows a structure of 4B(TP)SBF-SBF **53**, in which the external chromophores bear longer chains of eight phenyl rings than the internal chromophores which is of six phenyl rings. This compound is synthesized to confirm the effect (positive or negative) of the elongation of the external chromophore on the characterization of this first generation class of compounds. The presence of free *p*-terphenyl chains on the terminal spirobifluorene reduces the rotational rigidity of this compound than that of previous structures. Figure 4.15 shows the synthetic route of this compound.

Starting from 2,7-dibromospirofluoren-9-one **23**, 2,7-dibromo-2'-methoxy-spirobifluorene **46** is obtained by a lithium-bromine exchange of 2-bromo-4'-methoxybiphenyl **45** followed by the treatment of 2,7-dibromospirobifluoren-9-one **23** analogous to the reaction of 2,7-dibromospirobifluoren-9-one **23** with 2-bromobiphenyl for the formation of 2,7-

dibromospirobifluorene **24**. 2-Bromo-4'-methoxybiphenyl **45** is afforded by Kumuda coupling of 1,2-dibromobenzene **43** with 4-methoxyphenylmagnesium bromide of 4-bromoanisole **46** catalysed by $Pd(PPh_3)_4$.[86] Suzuki cross-coupling reaction of 2,7-dibromo-2'-methoxyspirobifluorene **46** with 1,1',4',1''-terphenyl-4-yl boronic acid **47** affords 2,7-bis (1,1',4',1''-terphenyl-4-yl)-2'-methoxyspirobifluorene **48** with a yield of 75%. The 1,1',4',1''-terphenyl-4-yl boronic acid **47** is obtained by desilylation of 1,1',4',1''-terphenyl-4-yltrimethylsilane **50** using boron tribromide.[87] The Suzuki cross-coupling of 4-bromobiphenyl **49** with 4-trimethylsilylboronic acid **8** leads to the formation of 1,1',4',1''-terphenyl-4-yltrimethylsilane **50**. Cleaving of the methoxy group of 2,7-bis (1,1',4',1''-terphenyl-4-yl)-2'-methoxyspirobifluorene **48** with BBr_3 in CH_2Cl_2 affords the 2,7-bis (1,1',4',1''-terphenyl-4-yl)-2'-hydroxy-9,9'-spirobifluorene **49** in a 100% yield[88] which is subsequently converted into 2,7-bis(1,1'4',1''-terphenyl-4-yl)-9,9'-spirobifluorene-2'-yltriflate **52** in 85% yield.[Error! Bookmark not defined.] Suzuki cross-coupling reaction of 2,7-bis(1,1',4',1''-terphenyl-4-yl)-9,9'-spirobifluorene-2'-yltriflate **52** with 2,2',7,7'-tetrakis(pinacolato boron-2-yl)-9,9'-spirobifluorene **32** affords the target compound 2,2',7,7'-tetrakis[2',7'-bis[(1,1',4',1''-terphenyl-4-yl)-9,9'-spirobifluorene-2-yl)]-9,9'-spirobifluorene **53**.

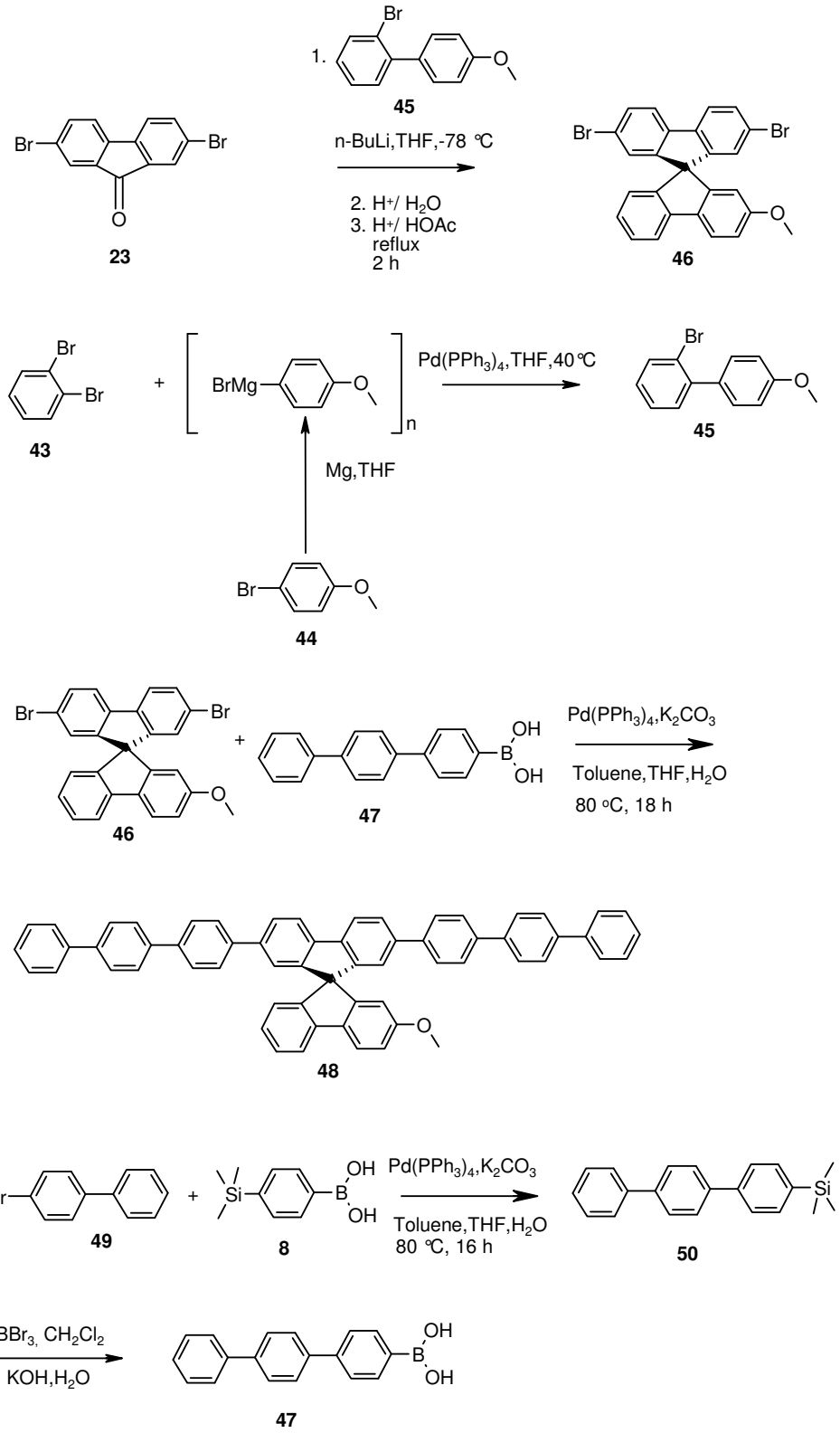
1.
45
n-BuLi,THF,-78 °C
2. H+/ H2O
3. H+/ HOAc
reflux
2 h
23
46
43
BrMg
n
Mg,THF
44
Pd(PPh3)4,THF,40°C
45
Pd(PPh3)4,K2CO3
Toluene,THF,H2O
80 °C, 18 h
47
48
49
8
Pd(PPh3)4,K2CO3
Toluene,THF,H2O
80 °C, 16 h
50
BBr3, CH2Cl2
KOH,H2O
47

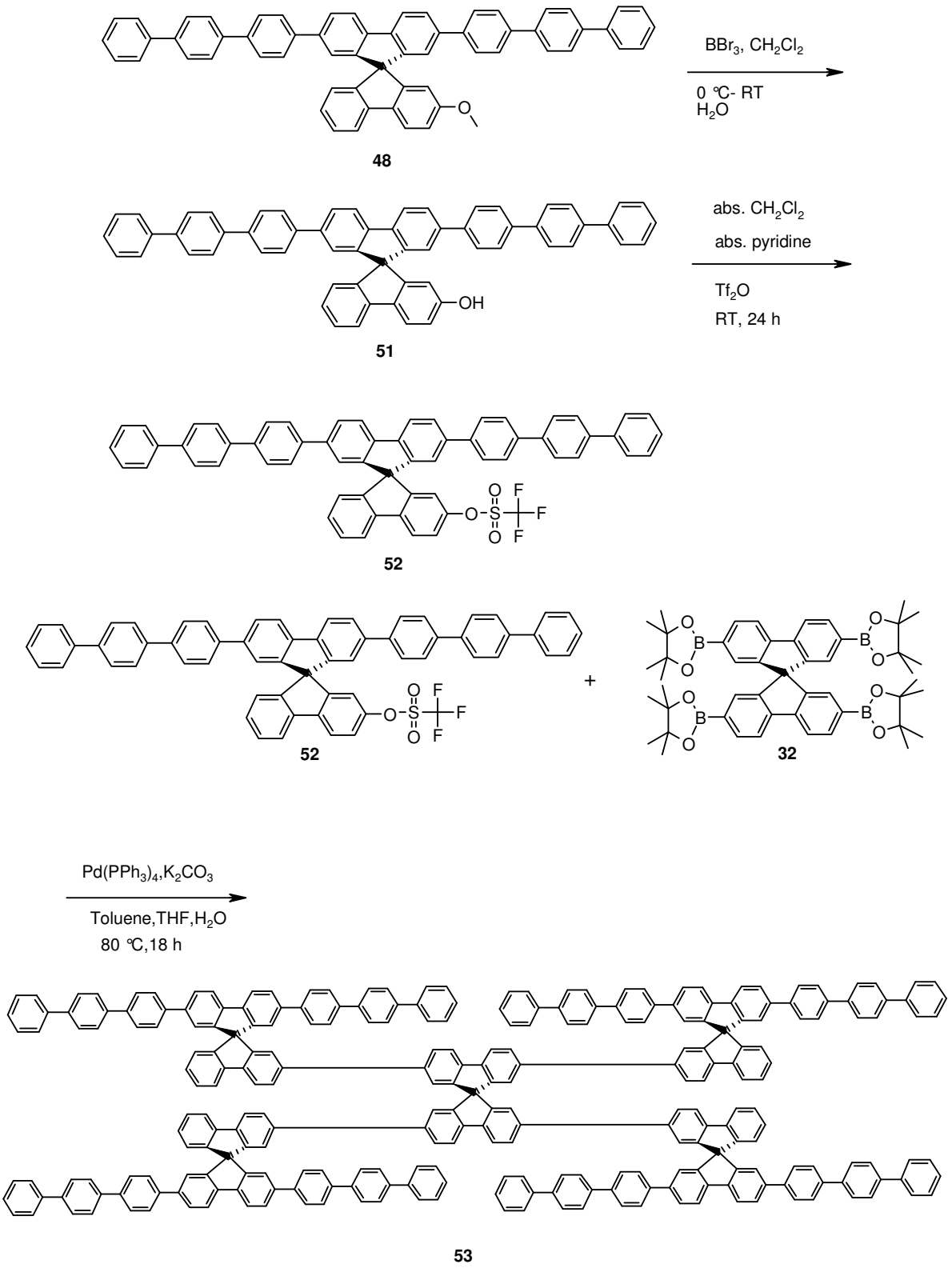

Figure 4.15 Synthesis of 4B(TP)SBF-SBF 53

4.3.1.6 Synthesis of 2,2',7,7'-Tetrakis[1-(2',7'-diphenyl-9,9'-spirobifluorene-2-yl)phenyl-4-yl]-9,9'-spirobifluorene (4DPSBFP-SBF) (58)

The 4DPSBFP-SBF **58** compound is designed to study the impact of the extension of the external as well as internal chromophores. In this compound, there are four times quaterphenyl rings chains as external chromophore and two times octiphenyl chains as internal chromophores. The central core spirobifluorene is connected to the terminal spiro units, formed with one half as biphenyl and the other half as quaterphenyl rings, through a phenyl ring. The rigidity of the compound is expected to be less than that of 4-spiro[2], 4-phspiro[2] and 4DPSBF-SBF **33**. The synthesis of this compound proceeds as shown in figure 4.16 below. Suzuki cross-coupling of 2,7-dibromo-2'-methoxy-9,9'-spirobifluorene **46** with phenylboronic acid **26** affords 2,7-diphenyl-2'-methoxy-9,9'-spirobifluorene **54**. Treatment of 2,7-diphenyl-2'-methoxy-9,9'-spirobifluorene **54** with borontribromide forms 2,7-diphenyl-2'-hydroxy-9,9'-spirobifluorene **55**. It is then converted into 2,7-diphenyl-9,9-spirobifluorene-2'-yltriflate **56** and then followed by the Miyaura reaction affording pinacol 2,7-diphenyl-9,9'-spirobifluorene-2'-yl boronate **57**. The Suzuki cross-coupling reaction of 2,2'7,7'-tetrakis-(4''-iodophenyl)-9,9'-spirobifluorene **20** with pinacol 2,7-diphenyl-9,9'-spirobifluorene-2'-yl boronate **57** affords the final product 2,2',7,7'-tetrakis[1-(2',7'-diphenyl-9,9'-spirobifluorene-2-yl)phenyl-4-yl)-9,9'-spirobifluorene **58**.

This end product is successfully synthesized with an another route too where a Suzuki cross-coupling reaction is carried out with 2,2',7,7'-tetrakis(pinacolato boron-2-yl)-9,9'-spirobifluorene **32** and 2',7'-diphenyl-2-(4-bromophenyl)-9,9-spirobifluorene **59**. A cross-coupling reaction of 2,7-diphenyl-2'-iodo-9,9'-spirobifluorene **31** with pinacol 4-bromo-phenyl borate **60** affords 2',7'-diphenyl-2-(4-bromophenyl)-9,9-spirobifluorene **59** (figure 4.17). Reaction of 1,4-dibromobenzene **13** with an equivalent of n-BuLi in Et_2O at –78 °C gives the mono-lithiated intermediate **61** which further reacts with trimethoxy borate affording 4-bromo-phenyl boronic acid **62**. As the purification of boronic ester is more convenient than that of boronic acid, it is treated with pinacol forming pinacol 4-bromophenyl borate **60**.

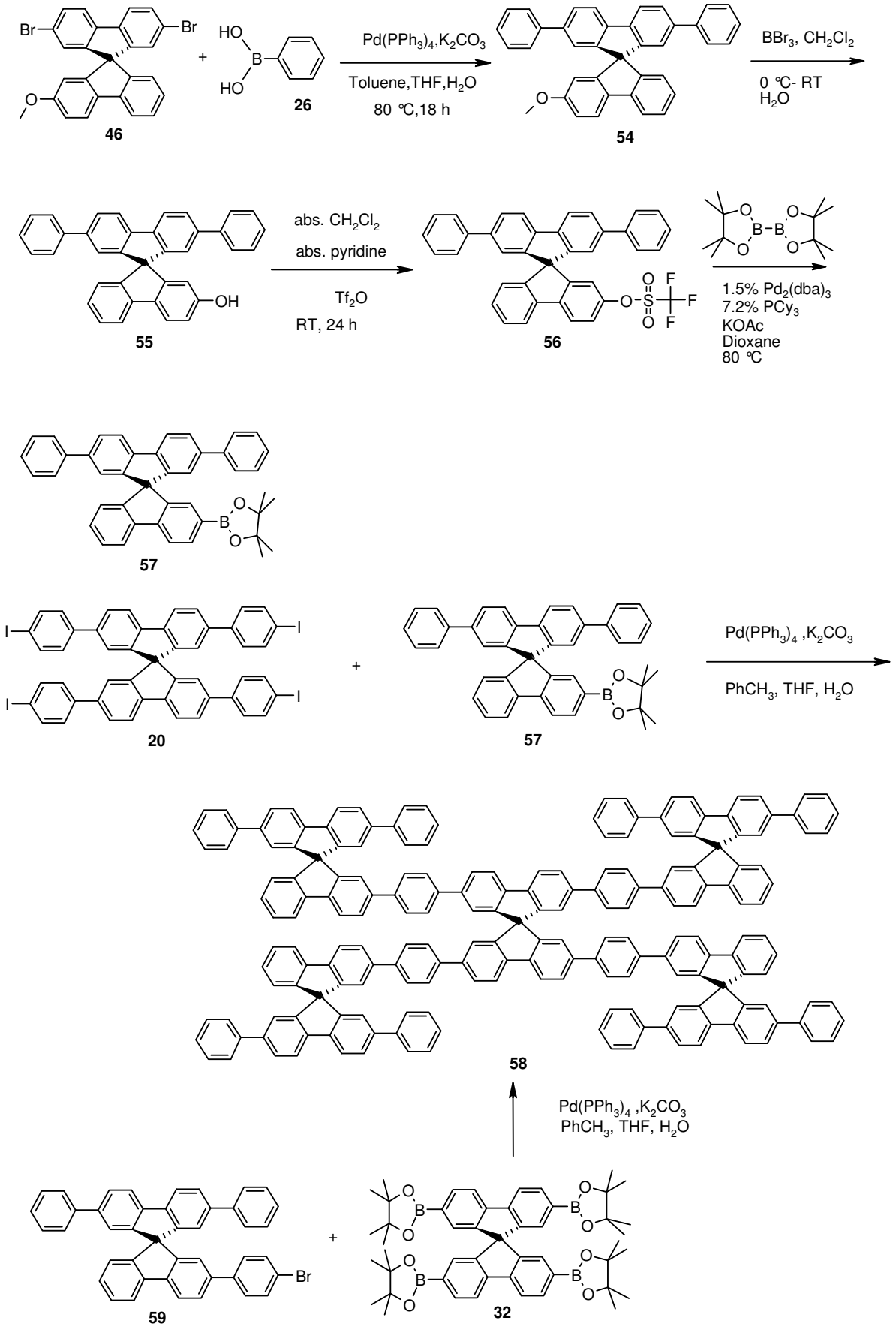

Figure 4.16 Synthesis of 4DPSBFP-SBF 58

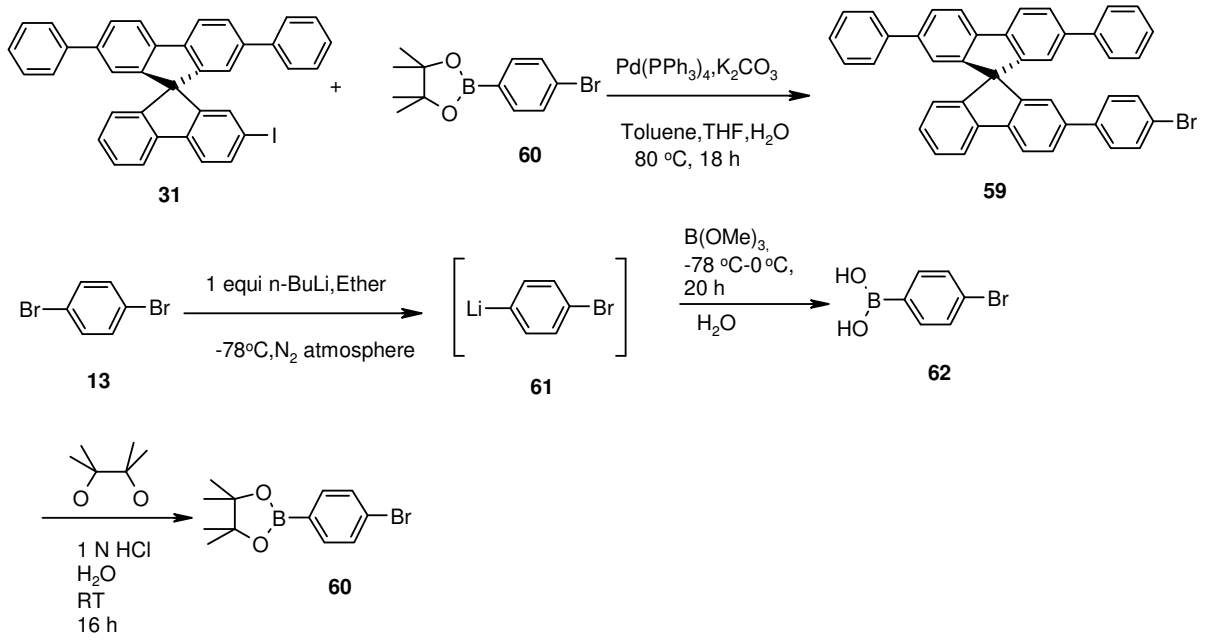

Figure 4.17 Synthesis of 2',7'-diphenyl-2-(4-bromophenyl)-9,9-spirobifluorene 59

A retrosynthetic analysis of the final product 2,2',7,7'-tetrakis[1-(2',7'-diphenyl-9,9'-spirobifluorene-2-yl)phenyl-4-yl]-9,9'-spirobifluorene **58** shows still an another route to synthesize it (figure 4.18). A cross-coupling reaction of 2,2',7,7'-tetrabromo-9,9'-spirobifluorene **17** with pinacol 1-(2',7'-diphenyl-9,9'-spirobifluorene-2-yl)phenyl-4-yl borate **63** affords **58**. As pinacol 1-(2',7'-diphenyl-9,9'-spirobifluorene-2-yl)phenyl-4-yl borate **63** is retrosynthetically analysed, it is confirmed that 2,7-dibromo-2'-(4-methoxyphenyl)-9,9'-spirobifluorene **64** is a necessary reactant for the further reactions. Hence, to synthesize 2,7-dibromo-2'-(4-methoxyphenyl)-9,9'-spirobifluorene **64**, a synthetic route is outlined in figure 4.18. A Suzuki cross-coupling of pinacol 4-bromophenyl boronate **60** with 4-bromoanisole affords 4-bromo-4'-methoxybiphenyl **65**. The Grignard reagent 2-bromophenyl magnesium bromide formed from 1,2-dibromobenzene **66** affords 2-bromophenylboronic acid **67** after esterification with trimethoxyborate. Reaction of 2-bromophenylboronic acid **67** with 4-bromo-4'-methoxybiphenyl **65** under Suzuki reaction condition affords 2-bromo-4'''-metho-

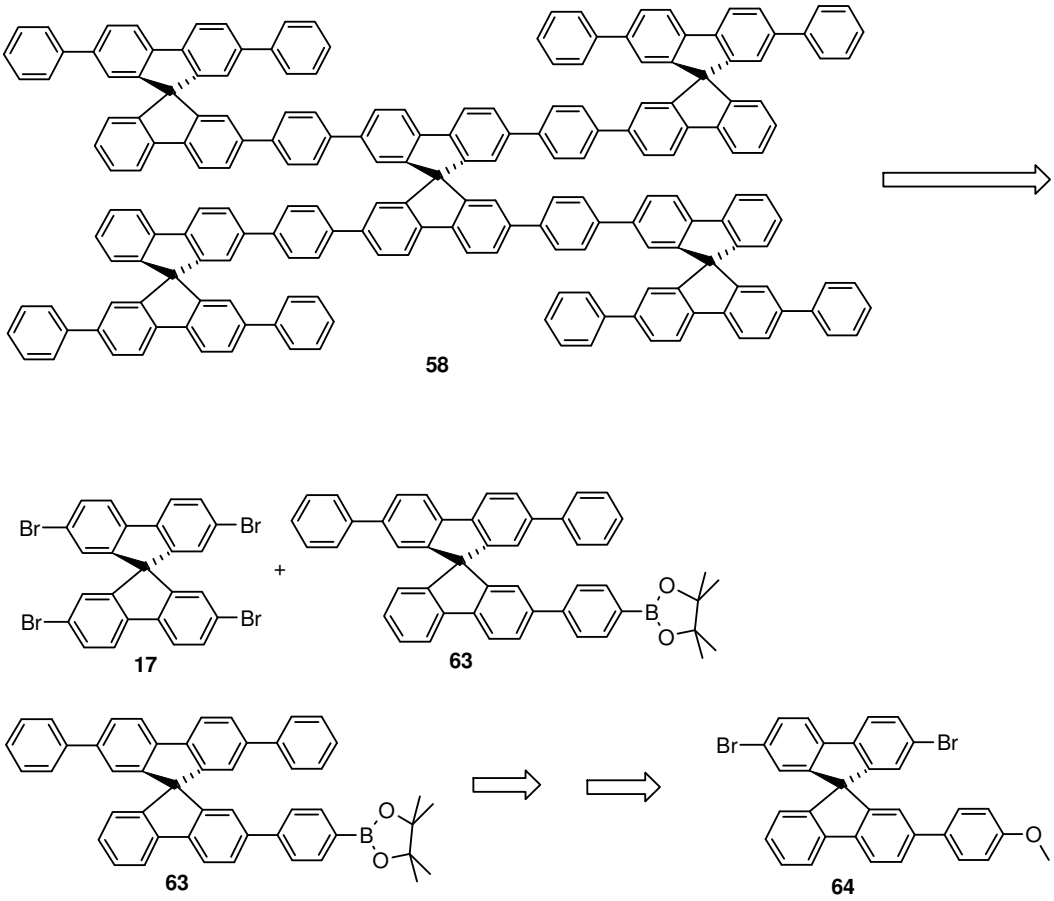

Figure 4.18 Retrosynthetic analysis of 4DPSBFP-SBF 58

xy-1',4',1''-terphenyl **68**. A next try to obtain 2-bromo-4'''-methoxy-1',4',1''-terphenyl **68** by the Suzuki reaction of in situ generated Grignard reagent of 4-bromo-4'-methoxybiphenyl **65** with 1,2-dibromobenzene **66** gives no expected product (figure 4.19).

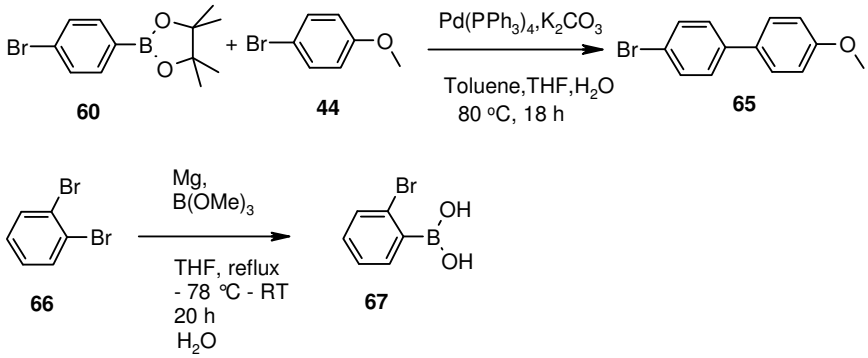

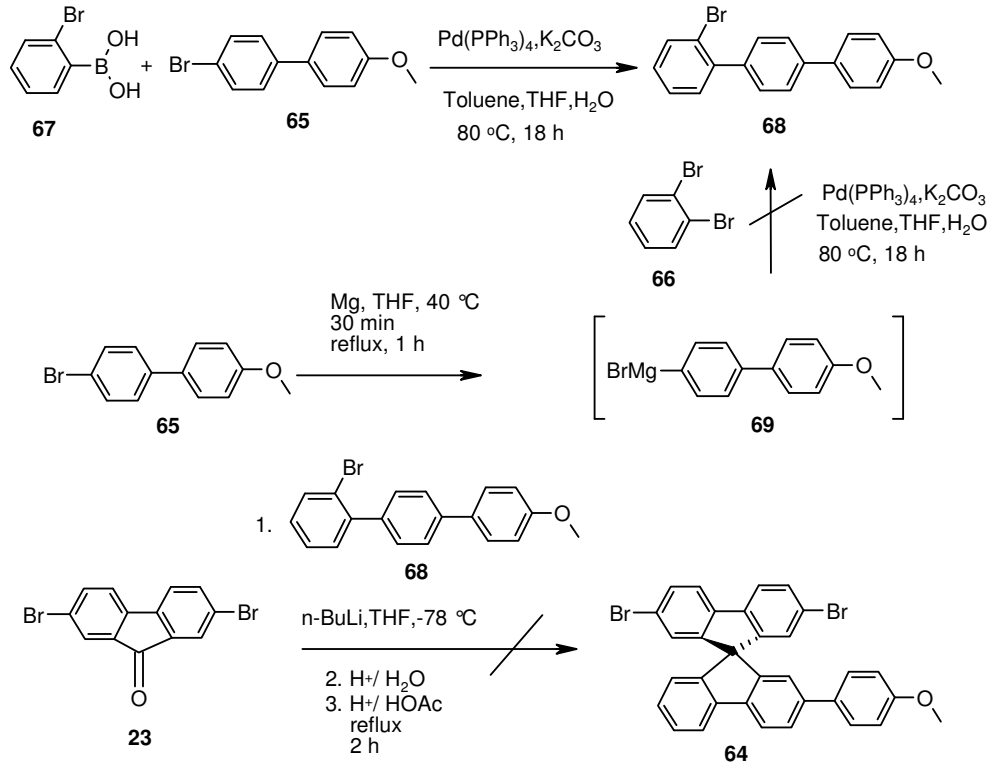

Figure 4.19 Synthetic strategy for 2',7'-dibromo-2-(4-methoxyphenyl)-9,9'-spirobifluorene 64

A trial to synthesize 2',7'-dibromo-2-(4-methoxyphenyl)-9,-9'-spirobifluorene **64** from 2,7-dibromofluoren-9-one **23** with the lithiated intermediate of 2-bromo-4'''-methoxy-1',4',1''-terphenyl **68** has not become successful too (figure 4.19).

4.3.1.7 Synthesis of 2,2',7,7'-tetrakis(2',7,7'-triphenyl-9,9'-spirobifluorene-2-yl)-9,9'-spirobifluorene (4TPSBF-SBF) (72)

In the case of 4TPSBF-SBF **72** (figure 4.20), the structure of the compound is modified in the internal chromophores although the number of phenyl rings in these chains are kept as same as in 2,2'7,7'-tetrakis(2',7'-diphenyl-9,9'-spirobifluorene-2-phenyl-4''-yl)-9,9'-spirobifluorene **58**. The modification is due to the location of the phenyl rings of the internal chromophore which are not more in between the central core and terminal spiro units but at the 7-position of the terminal spiro units. The rigidity of this compound is expected to be less than that of 2,2'7,7'-tetrakis(2',7'-diphenyl-9,9'-spirobifluorene-2-phenyl-4''-yl)-9,9'-spirobifuorene **58** as the phenyl rings of the 7-position of the terminal spiro units are bonded only at its 1-position and its 4-position is still free.

The synthesis of this compound is detailed as shown in figure 4.20. Starting with an iodination of 2-bromo-9,9'-spirobifluorene **7** using $I_2/PhI(O_2CCF_3)_2$, 2-bromo-2',7,7'-triiodo-9,9'-spirobifluorene **70** is obtained.[70] It is then subsequently subjected to a Suzuki reaction with phenylboronic acid **26** affording 2-bromo-2',7,7'-triphenyl-9,9'-spirobifluorene **71**. Here, an advantage of the different reactivity of halogene is utilized in Suzuki reaction. A cross-coupling reaction of 2-bromo-2',7,7'-triphenyl-9,9'-spirobifluorene **71** with 2,2',7,7'-tetrakis(pinacolato boron-2-yl)-9,9'-spirobifluorene **32** under the Suzuki reaction conditions leads to the formation of the target molecule 2,2',7,7'-tetrakis(2',7,7'-triphenyl-9,9'-spirobifluorene-2-yl)-9,9'-spirobifluorene **72**.

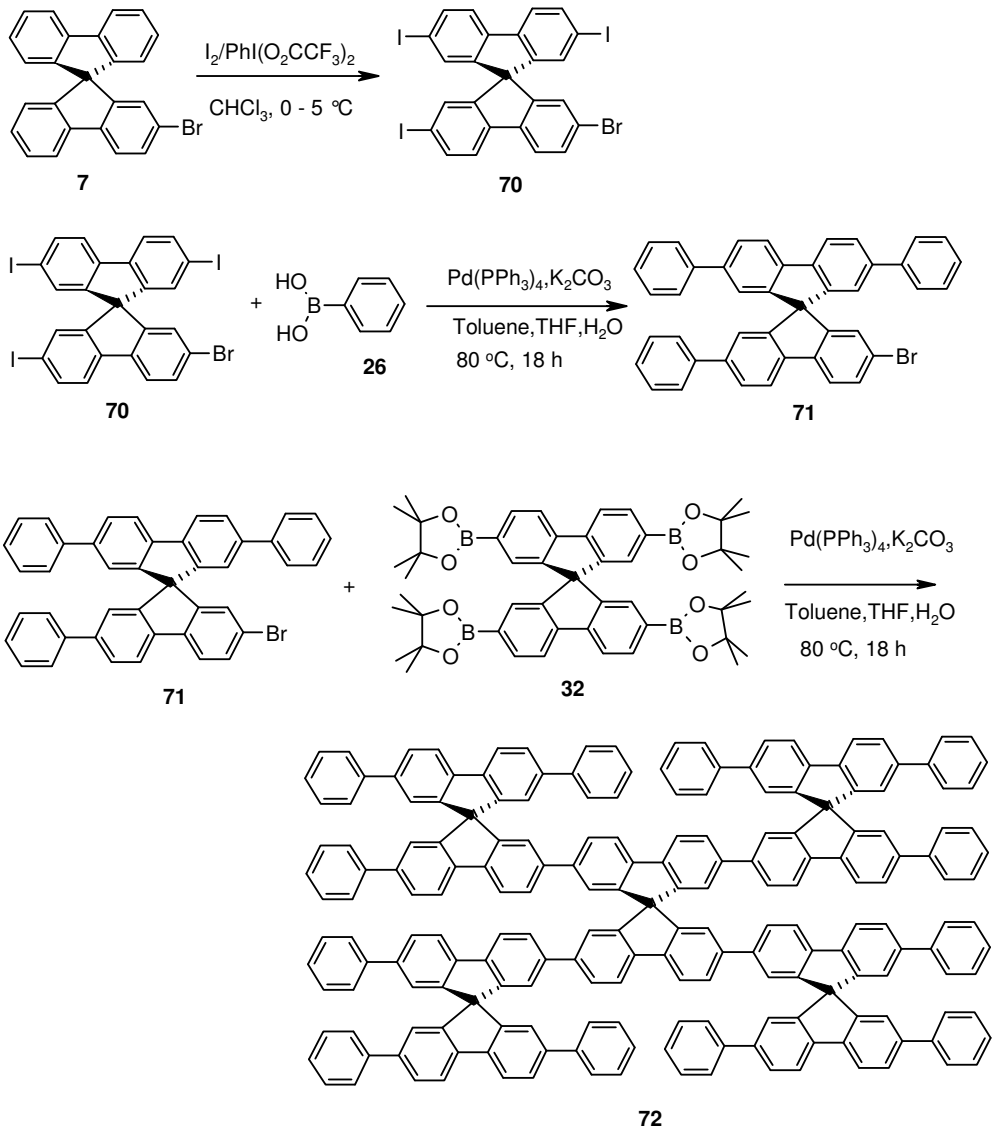

Figure 4.20 Synthesis of 4TPSBF-SBF 72

4.3.2 Spiro-Starburst-Structures of Second Generation

In all members of this class, the central spiro core (zero generation) is connected with first terminal spiro units at 2,2',7,7'-positions which are again connected with second terminal spiro units at various positions like 2'-only or 2',7'-only or 2',7,7'-positions of the first terminal spiro units. Although such compounds are with very high molecular weights, their dendrimer-like structures tend to exhibit a good solubility in organic solvents like CH_2Cl_2, $CHCl_3$. A further motivation for the synthesis of such second generation compounds is to scrutinize their morphological and spectroscopic characters as such starburst-dendrimer are well known as model of micelles.[89]

For the synthesis of starburst-dendrimer, two different synthetic strategies can be followed; divergent- and convergent-route. Divergent route, reported by Tomalia[90] and Newkome[91], begins with synthesis of a centre of a dendrimer as a nucleus initiator. A disadvantage of this route is loss of the valuable nucleus initiator as it has to be used in excess for every reaction required for addition of peripheral parts of the dendrimer. Hence, an alternative method is the convergent route. It begins with synthesis of parts which will be added later on to the nucleus as its periphery. The advantage of this route is that it lets to control the molecular weight as well as the positions of the materials. For the synthesis of the members of second generation category, the convergent route has been choosen.

Although a member of category, a highly branched 4-spiro[3], had been already synthesized in previous work of our group[70], new members of this category like 4SBFSBF-SBF **79** and 4BSBFSBF-SBF **84** are synthesized to observe the effect of the degree of its branching in their characterizations.

4.3.2.1 Synthesis of 2,2',7,7'-tetrakis[2'-(9,9'-spirobifluorene-2-yl)-9,9'-spirobifluorene-2-yl]-9,9'-spirobifluorene (4SBFSBF-SBF) (79)

Figure 4.21 represents a member of the second generation category of spiro-starburst-structures. A retrosynthetic analysis of this structure indicates that the final step succeeds with the cross-coupling reaction of 2,2',7,7'-tetrahalo-9,9'-spirobifluorene with corresponding boronic acid or ester.

Hence, the synthesis of corresponding boronic ester begins with the 2-bromo-7'-methoxy-9,9'-spirobifluorene **73** synthesized from the reaction of 2-bromofluoren-9-one **6** with 2-bromo-4'-methoxybiphenyl **44**. Suzuki cross-coupling of 2-bromo-7'-methoxy-9,9'-spirobifluorene **73** with pinacol 9,9'-spirobifluorene-2-yl-boronate **74** affords 2-(9,9'-spirobifluorene-2-yl)-7'-methoxy-9,9'-spirobifluorene **75**. The pinacol 9,9'-spirobifluorene-2-yl boronate **74** is obtained by the Miyaura reaction of 2-bromo-9,9'-spirobifluorene **7**. The 2-(9,9'-spirobifluorene-2-yl)-7'-methoxy-9,9'-spirobifluorene **75** is reduced to its alcohol 2-(9,9'-spirobifluorene-2-yl)-7'-hydroxy-9,9'-spirobifluorene **76** which is then converted to 2'-(9,9'-spirobifluorene-2-yl)-9,9'-spirobifluorene-2-yl triflate **77**. The Miyaura reaction of 2'-(9,9'-spirobifluorene-2-yl)-9,9'-spirobifluorene-2-yl triflate **77** affords pinacol 2'-(9,9'-spirobifluorene-2-yl)-9,9'-spirobifluorene-2-yl boronate **78**. Finally, the cross-coupling reaction of pinacol 2'-(9,9'-spirobifluorene-2-yl)-9,9'-spirobifluorene-2-yl boronate **78** with 2,2',7,7'-tetrabromo-9,9'-spirobifluorene **17** yields the target compound 2,2',7,7'-tetrakis[2'-(9,9'-spirobifluorene-2-yl)-9,9'-spirobifluorene-2-yl]-9,9'-spirobifluorene **79**.

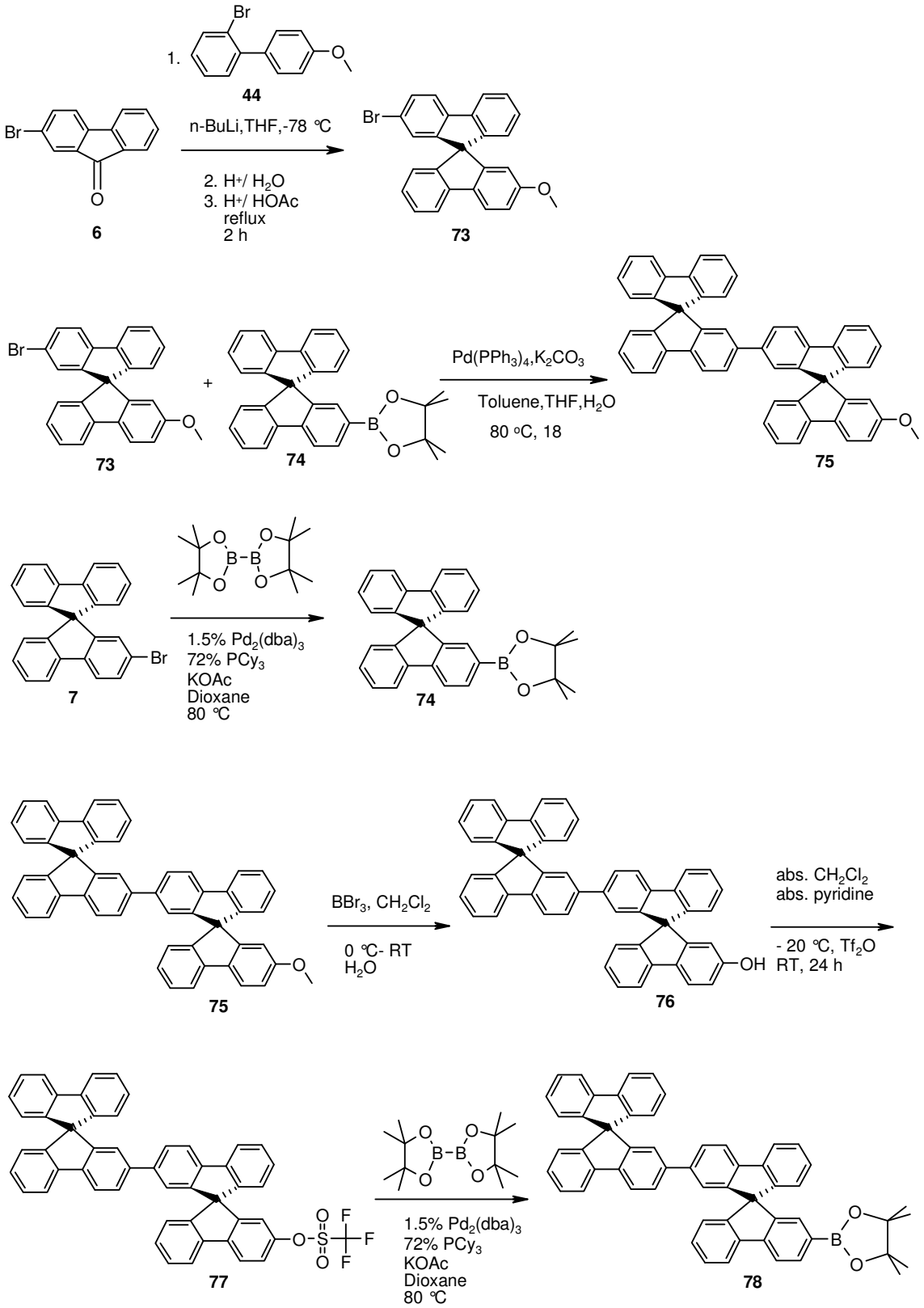
1.
44
n-BuLi,THF,-78 °C
2. H+/ H2O
3. H+/ HOAc
reflux
2 h
6
73
Pd(PPh3)4,K2CO3
Toluene,THF,H2O
80 °C, 18
74
75
1.5% Pd2(dba)3
72% PCy3
KOAc
Dioxane
80 °C
7
BBr3, CH2Cl2
0 °C- RT
H2O
abs. CH2Cl2
abs. pyridine
- 20 °C, Tf2O
RT, 24 h
76
77
78

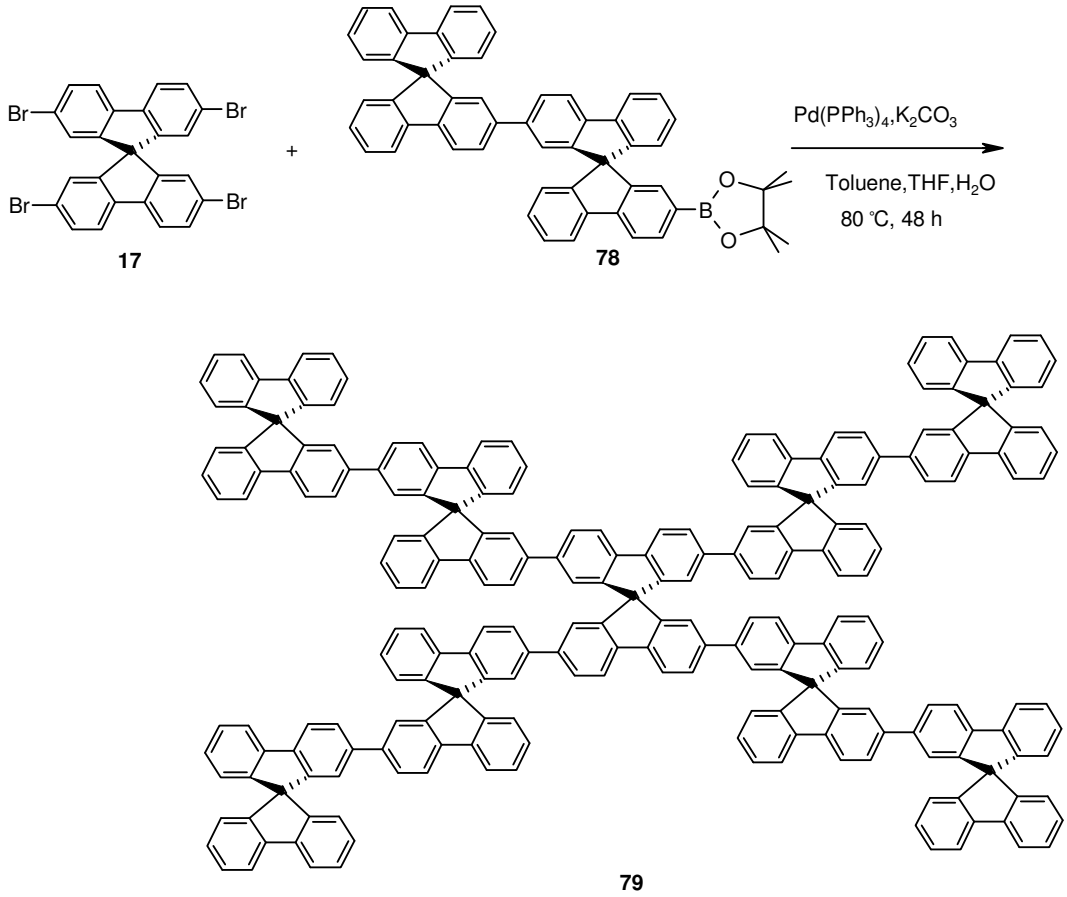

Figure 4.21 Synthesis of 4SBFSBF-SBF 79

4.3.2.2 Synthesis of 2,2',7,7'-tetrakis[2',7'-bis(9,9'-spirobifluorene-2-yl)-9,9'-spirobifluorene-2-yl]-9,9'-spirobifluorene [4B(SBF)SBF-SBF] (84)

4B(SBF)SBF-SBF **84** (figure 4.22) shows the structure of an another member of the second generation category. In this compound, the central spiro core is substituted at its 2,2',7,7'-positions with terminal spiro units whereas the 2',7'-positions of the terminal spiro units are again substituted with another two spiro units. Thus, this compound contains total thirteen spiro units. The structure of this compound is also assumed to be spheroidal as every chromophore is perpendicular to one another chromophore in every half of the molecule.

The synthesis of 2,2',7,7'-tetrakis[2',7'-bis(9,9'-spirobifluorene-2-yl)-9,9'-spirobifluorene-2-yl]-9,9'-spirobifluorene **84** is also started with a convergent route as shown in figure 4.22. The corresponding boronic ester, needed for the Suzuki cross-coupling with 2,2',7,7'-tetrabromo-9,9'-spirobifluorene **17** to yield the expected product 4B(SBF)SBF-SBF **84**, is synthesized starting from 2,7-dibromo-2'-methoxy-9,9'-spirobifluorene **46**. Suzuki cross-coupling of 2,7-

dibromo-2'-methoxy-9,9'-spirobifluorene **46** with pinacol 9,9'-spirobifluorene-2-yl boronate **74** affords 2',7'-bis(9,9'-spirobifluorene-2-yl)-2-methoxy-9,9'-spirobifluorene **80** which is then converted into 2,7-bis(9,9'-spirobifluorene-2-yl)-2'-hydroxy-9,9'-spirobifluorene **81**. Converting it into 2,7-bis-(9,9'-spirobifluorene-2-yl)-9,9'-spirobifluorene-2'-yl triflate **82** and followed by the Miyaura reaction affords pinacol 2,7-bis(9,9'-spirobifluorene-2-yl)-9,9'-spirobifluorene-2'-yl boronate **83**.

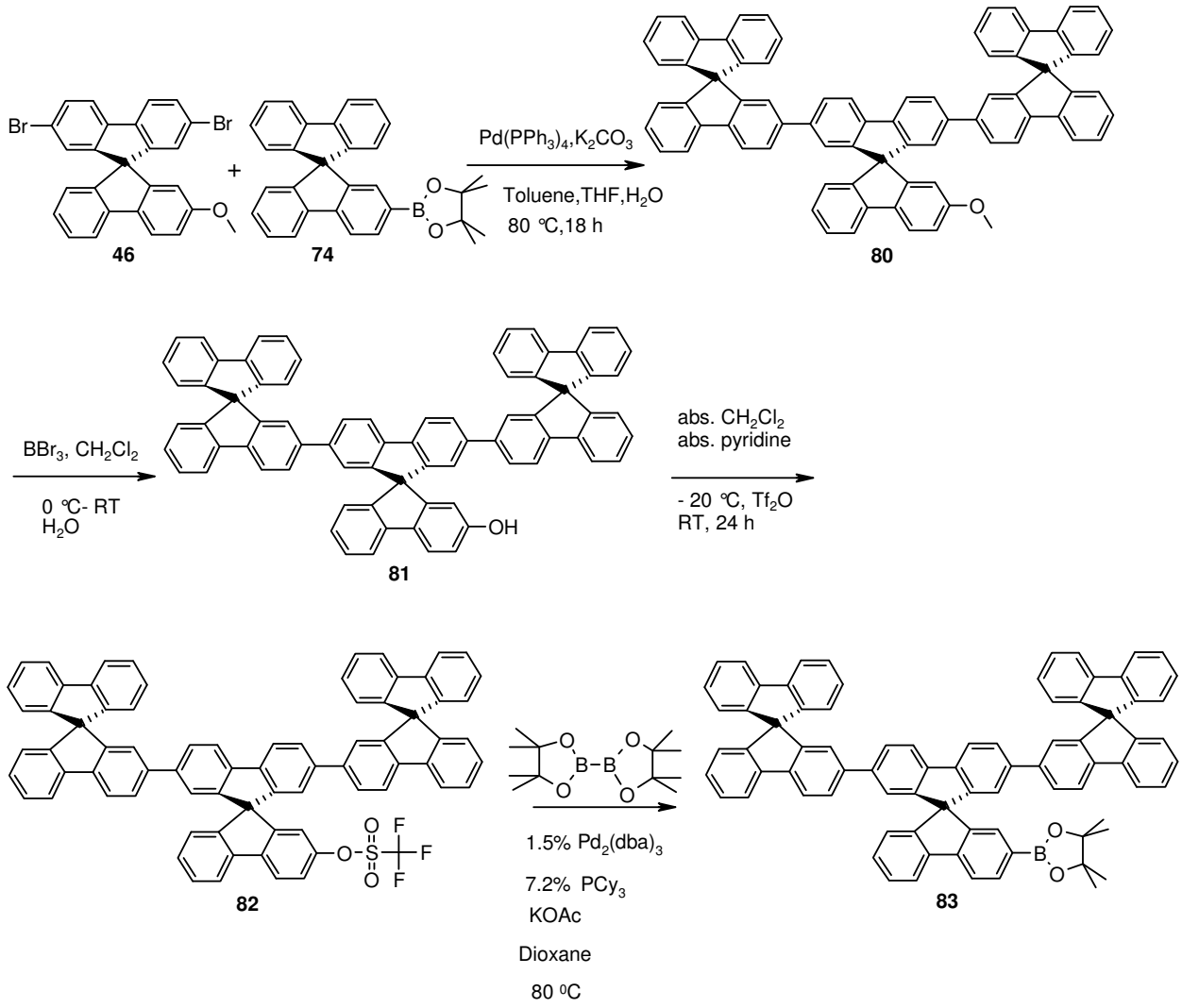

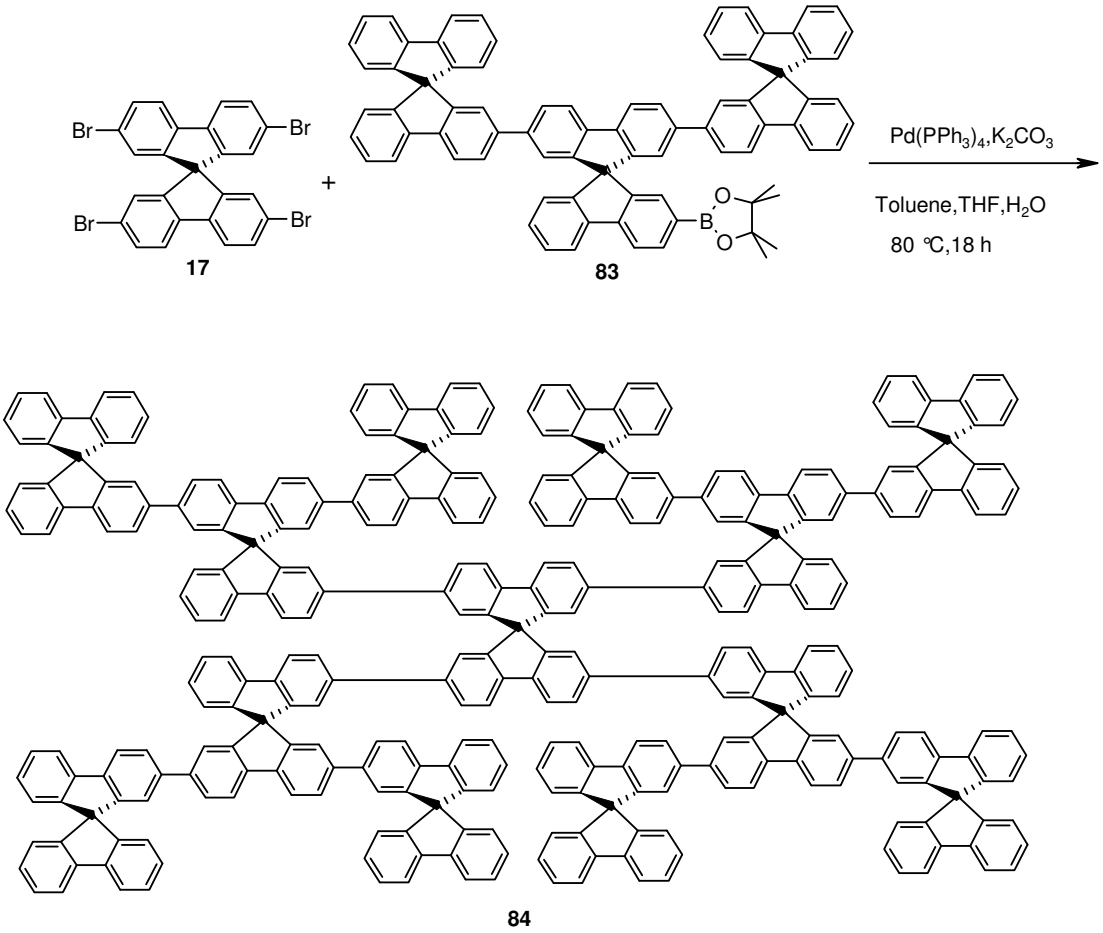

Figure 4.22 Synthesis of 4B(SBF)SBF-SBF 84

5 Results and Discussions

5.1 Spectroscopic Characterization of Spiro-Starburst-Structures

Optical spectra of all end products in certain concentrated solutions in dichloromethane (as mentioned below) as well as in thin film were measured. To prepare thin films of the compounds, solutions of the compounds were prepared in appropriate concentrations (~1 mg of the compound in 1 mL chloroform), then their films were prepared using the solutions by spin-coating (solution-based process) on quartz substrates (*665-QX 15*30*1.1 mm; the spinning speed was adjusted to 1500 rpm). The absorption spectra of the films were recorded with reference to the quartz substrate whereas the solvent was taken as reference recording the absorption spectra of solutions.

5.1.1 Spectra of 4SBFBP-SBF (21)

Absorption, fluorescence and excitation spectra of the $9.16*10^{-7}$ mol/L concentrated solution of 4SBFBP-SBF **21** in dichloromethane were measured (Figure 5.1). In the absorption spectrum, it shows a broad band with a peak maximum at 353 nm and a smaller peak at 310 nm with a shoulder at 299 nm. The extinction coefficient was determined to be 200000 L mol^{-1} cm^{-1} at the peak maximum. The peak at 310 nm with the shoulder at 299 nm resembles the absorption band of unsubstituted perpendicular fluorene units.[92] The broad band at 353 nm corresponds to the *p*-deciphenyl (10pp) chains. For 4SBFBP-SBF **21,** in comparison with spiro-10pp, the absorption maximum is shifted bathochromically by 9 nm. The higher wavelength maximum in 4SBFBP-SBF **21** is due to the spiro-link of each two terminal phenyl rings of the main conjugated chain. In spiro-10pp, the rotation of the terminal phenyl rings is not restricted.

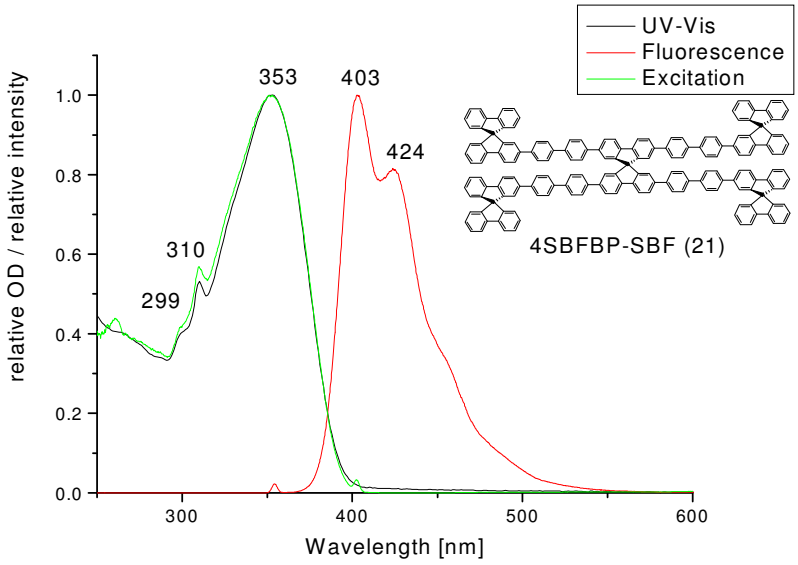

*Figure 5.1 Normalized absorption (black), fluorescence (red) and excitation (green) spectra of 4SBFBP-SBF 21 in dichloromethane (9.16*10^{-7} mol/L), each normalized to the maximum peak. The excitation spectrum was detected at 403 nm*

Spectra of 4SBFBP-SBF **21** were recorded in thin film. Figure 5.2 demonstrates the obvious difference between the absorption spectra of 4SBFBP-SBF in solution and in thin film. The absorption peak maximum in thin film is shifted bathochromically by 8 nm to 361 nm.

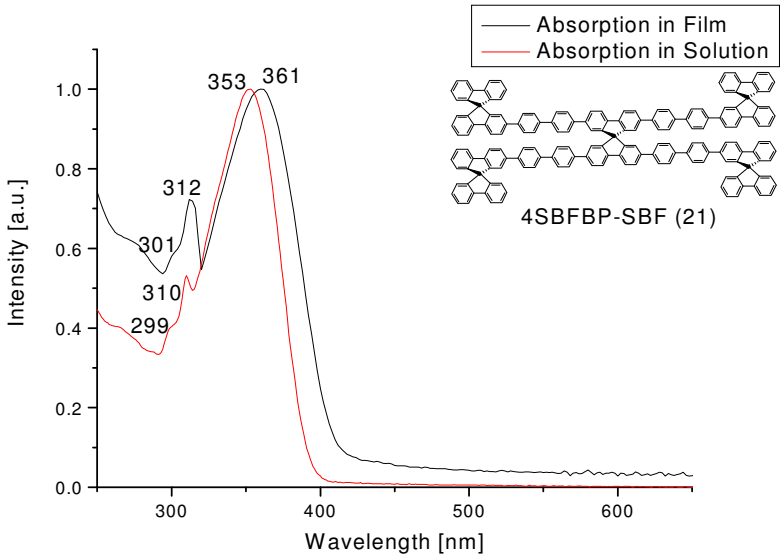

Figure 5.2 The absorption spectra of 4SBFBP-SBF 21 in solution (red) and in thin film (black)

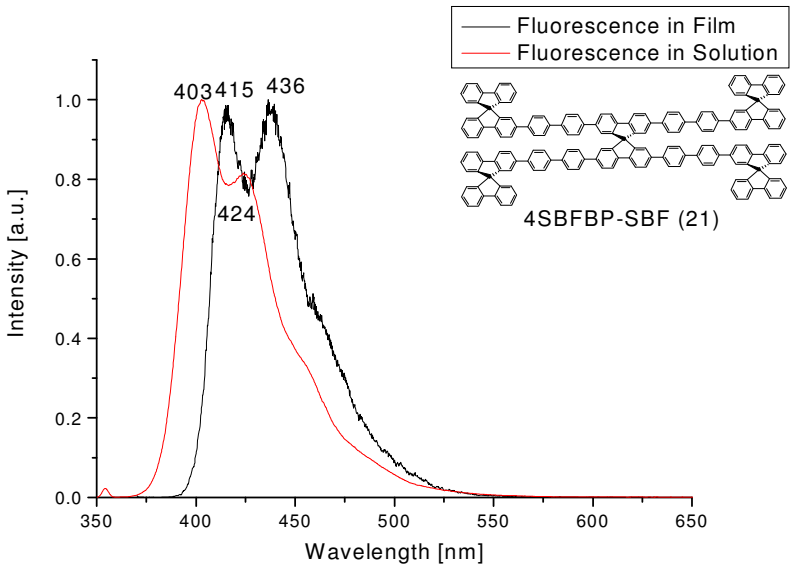

Figure 5.3 The emission spectra of 4SBFBP-SBF 21 in solution (red) and in thin film (black)

The emission spectrum of the compound in thin film is shifted bathochromically by 12 nm compared to the spectrum in solution (Figure 5.3).

The bathochromic shift of absorption and emission spectra in film of 4SBFBP-SBF can be due to the different dielectric constants of its environment. The linear relationship of dielectric constant with refractive index supports to interpret the increased dielectric constant of the material compared to its solution in dichloromethane. The refractive indices of similar class of material i. e. spiro-4pp and spiro-6pp in their thin film are found to be higher than that of dichloromethane (refractive index of dichloromethane 1.42); the refractive index of spiro-4pp varies from 1.6 - 2.5 and that of spiro-6pp varies from 1.5 - 2.5 in the range of 200 - 700 nm wavelengths. The values are obtained by variable angle spectroscopic ellipsometry (VASE).[93] The luminescence of 4SBFBP-SBF **21** in solid phase resembles to the luminescence of its isolated molecule in very dilute solution.[94] The steric conformation of the molecule prevents it to aggregate, so, no excimer band is found in long wave length region.

The emission spectra of 4SBFBP-SBF show fine structure unlike to its absorption spectra. As in the case of 4-spiro[2],[70] the vibrational splitting of the emission spectrum of 4SBFBP-SBF **21** is due to the fact that its excited state is more planar than its ground state. Unsubstituted *p*-oligophenylene (e.g., *p*-terphenyl) and some of its substituted derivatives (e.g., 3,3'-dimethyl-*p*-terphenyl) also show absorption spectra with no fine structure because at their ground

states, the steric hindrance dominates their planar configuration. Suzuki reported that the terminal phenyl rings of *p*-terphenyl in solution remain in 10° angle to the middle phenyl ring.[95] At the excited state, a higher resonance occurs between the rings, which results in a double bond character between the rings leading to more planar configuration of the species. Hence, their emission spectra also show the fine vibration structures[96,97] similar to the 4-spiro[2]. Thus, it can be concluded that the excited state of 4SBFBP-SBF **21** is more planar than its ground state. Further, for a rigid and torsion constraint molecule like 4SBFBP-SBF **21**, the fluorescence quantum yield remains higher and the velocity constant of the inter system crossing to T_1-state will be lower. A similar result was observed when the influence of the polarity and rigidity of more than 20 aromatic compounds were analysed for their spectroscopic characters. The lower velocity constant of the intersystemcrossing to T_1-state can be well explained with the help of the very short lifetime of the excited state. As the excited state has very short lifetime to undergo the inter system crossing phenomenon, it prefers to lose its energy via fluorescence emission. The rigidity of the molecule 4SBFBP-SBF **21** is caused by the spiro-linkages of terminal and the central biphenyl rings, connecting them with another perpendicular bifluorene unit through the bridged carbon atom. Although it causes the molecule torsion constraint, the remaining degrees of freedom (rotation, vibration) of the molecule are enough to demonstrate the Stokes shift. Hence, it prevents self-absorption. This is actually proved by the broad and structureless absorption band and the fine structured emission band as shown in figure 5.1. Because of this reason, such a rigid and torsion constraint molecule exposes good spectroscopic characters. Hence, such molecules can be used as emitters in optoelectronic devices. The theoretical explanation of the spectroscopic properties of *p*-oligophenylene is well described in the publication of Dewar[98] as well as Murrell and Longuet-Higgins.[99]

In comparison to the emission spectrum of 4-spiro[2] where the maximum was found to be at 396 nm with a shoulder at 418 nm, the wavelength maximum of 4SBFBP-SBF **21** is found at higher wavelength. It is found to be similar with the emission maximum of 4SBFBP-SBF **21**. The difference to 4-spiro[2] and the similarity with 4-phspiro[2] are due to the extended chain of phenyl rings between the terminal spirobifluorenes and the central core spirobifluorene. In general, increasing number of phenyl rings upto certain length (i. e., up to eight phenyl rings) in the main conjugation chain of spirobifluorene results in bathochromic shift. It is found to be maintained in the first generation spirobifluorenes too. The fluorescence quantum yield of

4SBFBP-SBF **21** in dichloromethane solution is determined to be 93% (with the spiro-6pp solution in dichloromethane as reference).

Along with the application of 4SBFBP-SBF **21** as emitter, it can also be applied as a species of intramolecular energy transfer. When one observes the upper half of the 4SBFBP-SBF, both of the terminal spirobifluorene units remain perpendicular to the deciphenyl chain but parallel to the deciphenyl chain of the lower half of the molecule. This means that the optical transition moment for both of these structural units are parallel and there is the possibility of an energy transfer from the biphenyl unit which shows the absorption at lower wavelength to the higher wavelength absorbing deciphenyl unit. An evidence for this phenomenon is observed in its excitation spectrum. As shown in figure 5.1 above, the excitation spectrum was measured by using the emission maximum wavelength that is 403 nm and the maximum of the excitation spectrum is found to be at 353 nm and 310 nm as shoulder, same as in case of the absorption spectrum. It exhibits an effective energy transfer from the biphenyl unit to the parallel deciphenyl unit. This phenomenon is well supported by the key word "optical funnel" which was explored for many other compounds too. As shown in figure 5.1 above, the excitation spectrum is almost identical to the absorption spectrum. Hence, it indicates almost complete energy transfer between the biphenyl and the parallel lying deciphenyl chain at the core.

5.1.2 Spectra of 4DPSBF-SBF (33)

Absorption, fluorescence and excitation spectra of the $1.25*10^{-6}$ mol/L concentrated solution of 4DPSBF-SBF **33** in dichloromethane were measured (Figure 5.4). In absorption spectrum, it shows a broad band with a peak maximum at 337 nm and a shoulder at 317 nm. The extinction coefficient was determined to be 230000 L mol^{-1} cm^{-1} at the peak maximum. The shoulder resembles the absorption band of diphenyl substituted perpendicular fluorene units which is comparable to one half of a spiroquaterphenyl.[76] In contrast to the unsubstituted spiro-6pp which shows the absorption peak maximum at 342 nm,[76] the absorption peak maximum which corresponds to the sexiphenyl ring as a main conjugated chain of 4DPSBF-SBF **33** is shifted hypsochromically by 5 nm. The lower wavelength maximum compared to that of 4-spiro[2] can be explained considering the less restricted rotation of the free phenyl rings at one half of every terminal spirobifluorene.

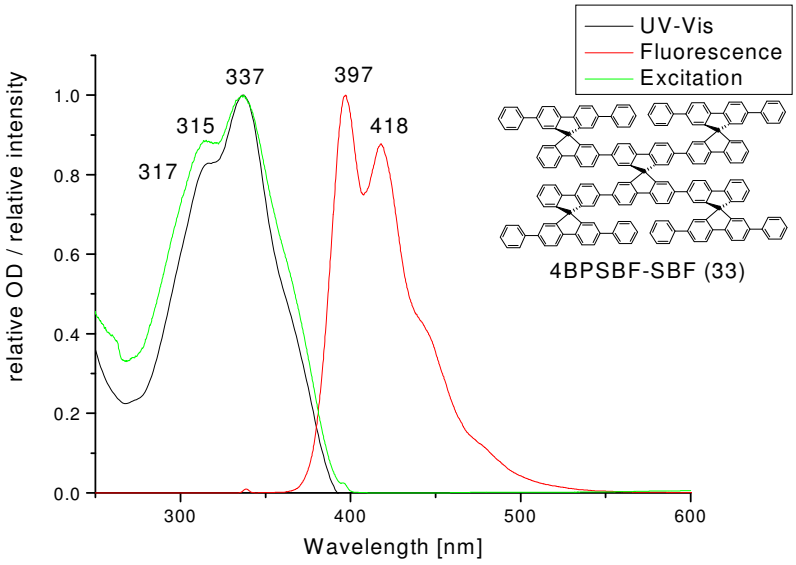

*Figure 5.4 Normalized absorption (black), fluorescence (red) and excitation (green) spectra of 4DPSBF-SBF 33 in dichloromethane (1.25*10^{-6} mol/L), each normalized to the maximum peak. The excitation spectrum was detected at 397 nm*

The absorption spectrum in thin film has a maximum peak at 342 nm which is bathochromically shifted by 5 nm compared to that in solution.

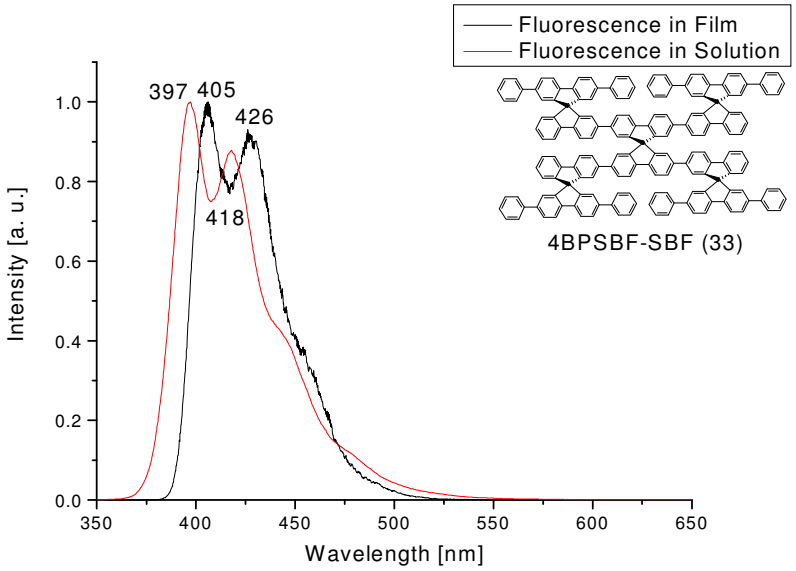

Figure 5.5 The emission spectra of 4DPSBF-SBF 33 in solution (red) and in thin film (black)

The emission band of the thin film is bathochromically shifted by 8 nm compared to the spectrum in solution (Figure 5.5). The emission spectra show fine structure which resemble

the 4-phspiro[2]. The fluorescence quantum yield of 4DPSBF-SBF **33** in dichloromethane solution is determined to be 87%.

The higher extinction coefficient of 4DPSBF-SBF **33** compared to that of 4SBFBP-SBF **21** is due to the extended biphenyl unit with phenyl rings on one half of every terminal spirobifluorene which causes the additional absorption.

As shown in figure 5.4 above, the excitation spectrum was detected at 397 nm and showed its maximum at 337 nm with a shoulder at 315 nm, similar as in the case of its absorption spectrum. It evidences an effective energy transfer from the diphenyl substituted fluorene unit to the sexiphenyl unit.

5.1.3 Spectra of 4DPSBFP-SBF (58)

Absorption, fluorescence and excitation spectra of the $9.65*10^{-7}$ mol/L concentrated solution of 4DPSBFP-SBF **58** in dichloromethane were measured (Figure 5.6). In absorption spectrum, it shows a peak maximum at 338 nm with a shoulder at 319 nm. The extinction coefficient was determined to be 280000 L mol^{-1} cm^{-1} at the peak maximum. The shoulder resembles the absorption band of quaterphenyl unit perpendicular to fluorene units. As the molar extinction coefficient increases with molecular size,[31] the extinction coefficient of 4DPSBFP-SBF **58** is higher than that of 4DPSBF-SBF **33** and 4-phspiro[2] (220000 L mol^{-1} cm^{-1}). The absorption peak maximum at 338 nm corresponds to the conjugation of the octiphenyl chain at the centre of the molecule. It consists of spiro-linked quaterphenyl units at each end of the the central chains and, a phenyl ring between the central spiro core and terminal spiro units. In contrast to 4-phspiro[2], the absorption peak maximum of 4DPSBFP-SBF **58** at 338 nm is shifted hypsochromically by 15 nm. The absorption band maximum of spiro-8pp is found to be at 344 nm.[76] Compared to spiro-8pp, the slightly hypsochromic shift of 4DPSBFP-SBF **58** by 6 nm is observed. Obviously, the four terminal substituted spirobifluorene units are not rigid enough to prevent the possible rotation, which actually should lead to the absorption at higher wavelength regarding to its rigidity as in the case of 4-phspiro[2].

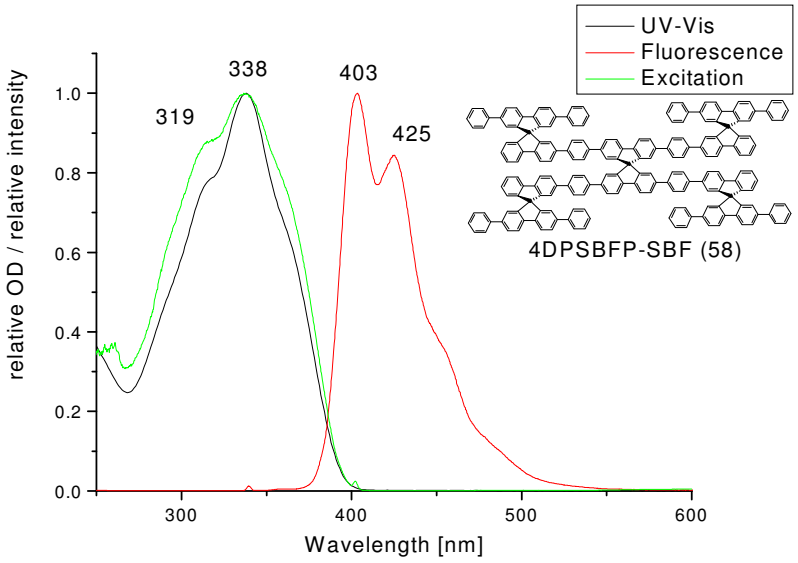

*Figure 5.6 Normalized absorption (black), fluorescence (red) and excitation (green) spectra of 4DPSBF-SBF 33 in dichloromethane (9.65*10^{-7} mol/L), each normalized to the maximum peak. The excitation spectrum was detected at 403 nm*

The absorption spectrum in thin film has a maximum peak at 344 nm which is found to be shifted bathochromically by 6 nm compared to in solution.

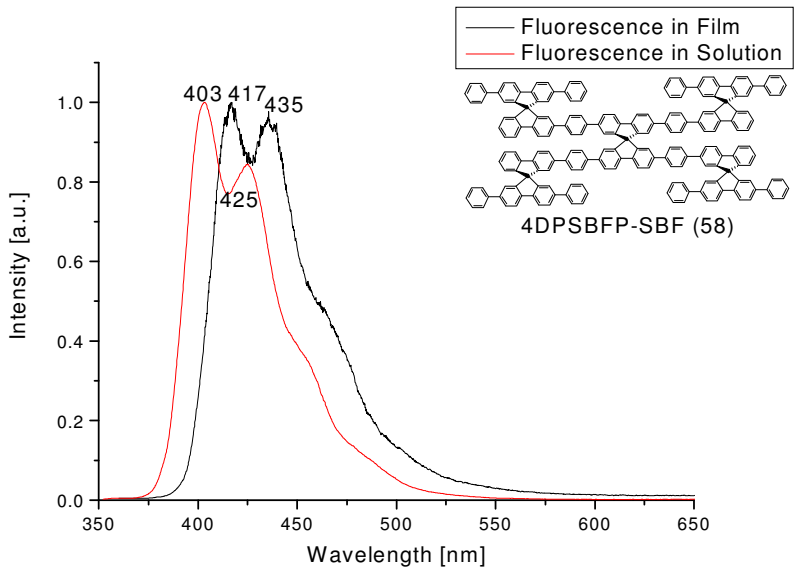

Figure 5.7 The emission spectra of 4DPSBFP-SBF 58 in solution (red) and in thin film (black)

The emission band of the thin film is shifted bathochromically by 14 nm compared to the spectrum in solution (figure 5.7).

The emission band appears quite similar to the emission spectrum of 4SBFBP-SBF **21**, but when compared to 4DPSBF-SBF **33**, it is found to be bathochromically shifted by 6 nm. The absorption peak maximum, however, remains almost the same. The bathochromic shift is due to the extension of the conjugated chromophore by additional phenyl ring between terminal and central spirobifluorene units. The greater Stokes shift is due to the considerable difference in equilibrium geometries of its ground state and the excited state. The fluorescence quantum yield of 4DPSBFP-SBF **58** in dichloromethane solution is determined to be 85%.

A possibility of energy transfer occurs from the diphenyl substituted fluorene unit to higher wavelength absorbing octiphenyl unit. As shown in figure 5.6 above, the excitation spectrum was measured by using the emission maximum wavelength that is 403 nm and the maximum of the excitation spectrum is found to be at 338 nm and 319 nm as shoulder, similar as in the case of its absorption spectrum.

5.1.4 Spectra of 4TPSBF-SBF (72)

Absorption, fluorescence and excitation spectra of the $9.65*10^{-7}$ mol/L concentrated solution of 4TPSBF-SBF **72** in dichloromethane were measured (Figure 5.8). In absorption spectrum, it shows a peak maximum at 340 nm with shoulders at 320 nm and 360 nm. The extinction coefficient was determined to be 240000 L mol^{-1} cm^{-1} at the peak maximum. The shoulder at 320 nm resembles the absorption band of the quaterphenyl units. The pronounced shoulder at 360 nm is most probably due to the changed position of both of the phenyl rings compared to 4DPSBFP-SBF **58**, one at every end of octiphenyl chain at one half of the molecule. For 4TPSBF-SBF **72**, in comparison with 4DPSBFP-SBF **58**, absorption and emission maxima are shifted bathochromically by approximately 3 nm while maintaining the Stokes shift. The presence of phenyl rings at the terminals of the octiphenyl conjugation chain causes an even more pronounced torsional constraint in this molecule, thus, leading to the finer structured absorption spectrum.

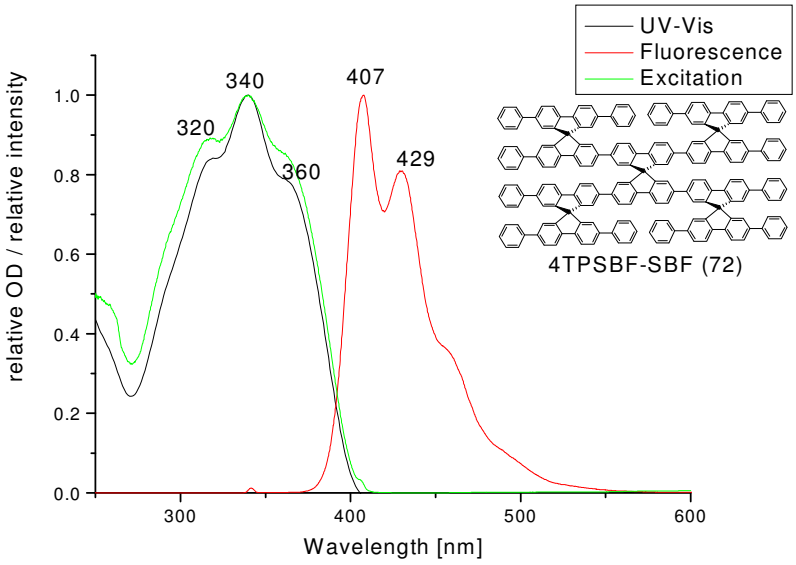

*Figure 5.8 Normalized absorption (black), fluorescence (red) and excitation (green) spectra of 4TPSBF-SBF 72 in dichloromethane (9.65*10^{-7} mol/L), each normalized to the maximum peak. The excitation spectrum was detected at 407 nm*

The absorption spectrum in thin film has a maximum peak at 345 nm which is found to be bathochromically shifted by 5 nm compared to that in solution.

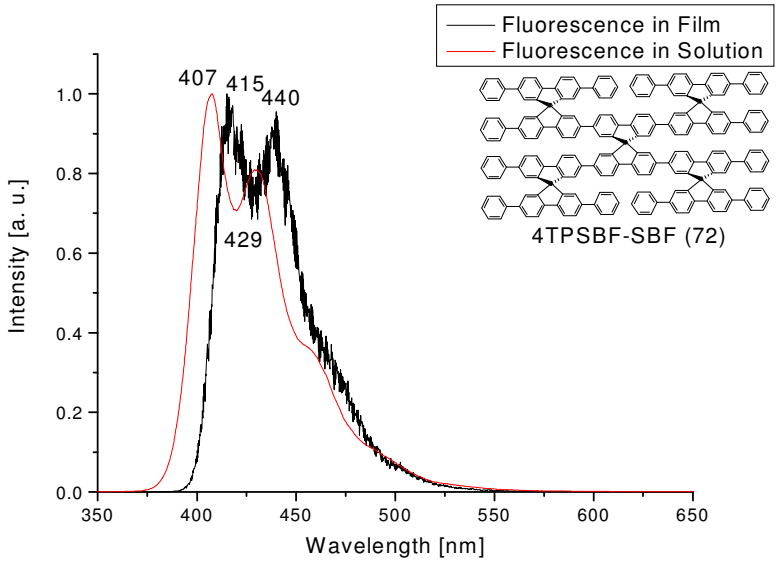

Figure 5.9 The emission spectra of 4TPSBF-SBF 72 in the solution (red) and in thin film (black)

The emission band of the thin film is bathochromically shifted by 8 nm and 11 nm compared to the spectrum in solution (Figure 5.9).

The fluorescence quantum yield of 4TPSBF-SBF **72** in dichloromethane solution is determined to be 95%.

As shown in figure 5.8 above, the excitation spectrum was measured by using the emission maximum wavelength that is 407 nm, the maximum of the excitation spectrum is found at 340 nm with shoulders at 320 nm and 360 nm, as is the case in its absorption spectrum. Hence, it shows that the energy transfer occurs from the quaterphenyl units of one half of the molecule to the octiphenyl unit of the other half of the molecule.

5.1.5 Spectra of 4B(BP)SBF-SBF (42)

Absorption, fluorescence and excitation spectra of the $9.67*10^{-7}$ mol/L concentrated solution of 4B(BP)SBF-SBF **42** in dichloromethane were measured (figure 5.10). In absorption spectrum, it shows a peak maximum at 345 nm with a shoulder at 322 nm. The extinction coefficient was determined to be 360000 L mol^{-1} cm^{-1} at the peak maximum. The shoulder at 322 nm, which is not so pronounced as in the case of 4DPSBF-SBF **33**, resembles the absorption band of the biphenyl substituted fluorene units, which are perpendicular to the plane of the core sexiphenyl chain. For 4B(BP)SBF-SBF **42**, in comparison with 4DPSBF-SBF **33** and spiro-6pp, the absorption maximum is shifted bathochromically by 8 nm and 3 nm respectively. The higher value of the extinction coefficient compared to that of 4DPSBF-SBF **33** is due to the presence of the additional terminal phenyl rings, which leads to increased molecular size.

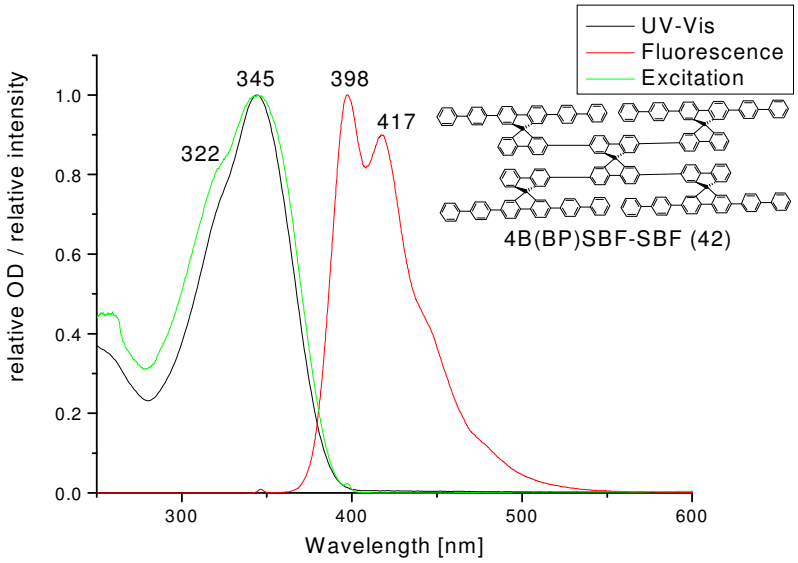

*Figure 5.10 Normalized absorption (black), fluorescence (red) and excitation (green) spectra of 4B(BP)SBF-SBF 42 in dichloromethane (9.67*10^{-7} mol/L), each normalized to the maximum peak. The excitation spectrum was detected at 398 nm*

The absorption spectrum in thin film has a maximum peak at 349 nm which is found to be bathochromically shifted by 4 nm compared to that in solution.

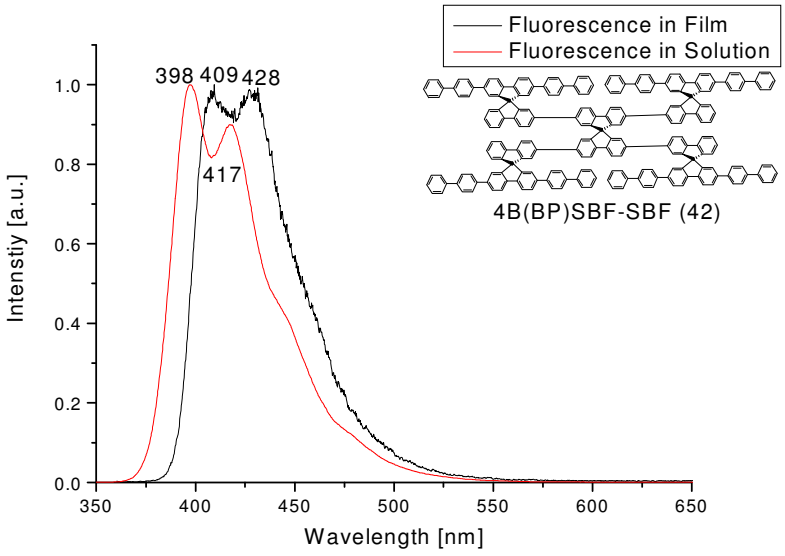

Figure 5.11 The emission spectra of 4B(BP)SBF-SBF 42 in the solution (red) and in thin film (black)

The emission band of the thin film is shifted bathochromically by 11 nm compared to the spectrum in solution (figure 5.11).The fine structured emission band in solution with its peak maximum at 398 nm appears to be bathochromically shifted by just 1 nm compared to 4DPSBF-SBF **33**. The fluorescence quantum yield of 4B(BP)SBF-SBF **42** has been determined in dichloromethane solution to be 96%.

Energy transfer occurs from the outer sexiphenyl units to the core sexiphenyl chain standing parallel. As shown in figure 5.10 above, the excitation spectrum was detected by using the emission maximum wavelength that is 398 nm and the maximum of the excitation spectrum is found at 345 nm, as is the case in its absorption spectrum.

5.1.6 Spectra of 4B(TP)SBF-SBF (53)

Absorption, fluorescence and excitation spectra of the $8.79*10^{-7}$ mol/L concentrated solution of 4B(TP)SBF-SBF **53** in dichloromethane were measured (figure 5.12). In absorption spectrum, it shows a peak maximum at 347 nm with a very distinguished shorter peak at 280 nm and a shoulder at 325 nm. The extinction coefficient was determined to be 430000 L mol^{-1} cm^{-1} at the peak maximum. For 4B(TP)SBF-SBF **53** in comparison with 4B(BP)SBF-SBF **42**, absorption and emission maxima are shifted bathochromically by 2 nm. The presence of the additional terminal phenyl rings causes the greater molecular size compared to 4B(BP)SBF-SBF **42**, which results in the higher value of extinction coefficient.

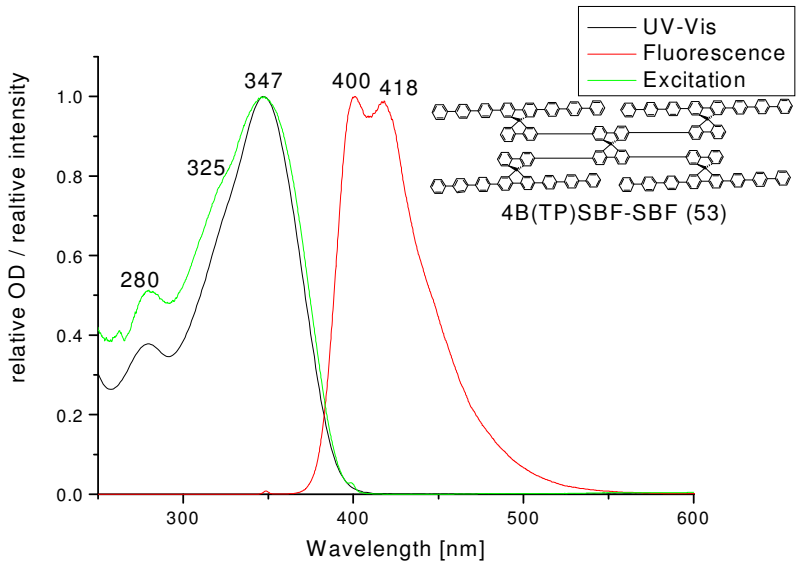

*Figure 5.12 Normalized absorption (black), fluorescence (red) and excitation (green) spectra of 4B(TP)SBF-SBF 53 in dichloromethane (8.79*10^{-7} mol/L), each normalized to the maximum peak. The excitation spectrum was detected at 400 nm*

The absorption spectrum of the thin film is shifted bathochromically by 6 nm compared to the spectrum in solution.

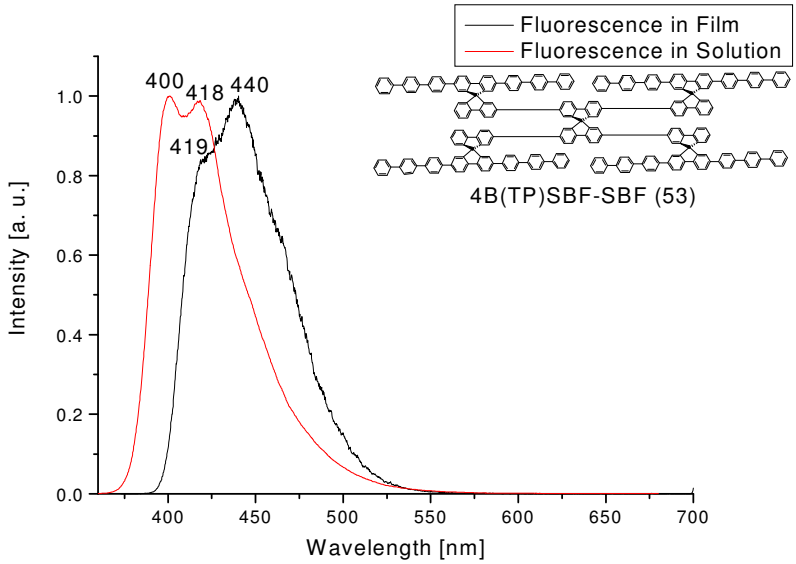

Figure 5.13 The emission spectra of 4B(TP)SBF-SBF 53 in the solution (red) and in the film (black).

The emission band of the thin film is bathochromically shifted by 18 nm and 21 nm compared to the spectrum in solution (figure 5.13). The fluorescence quantum yield of 4B(TP)SBF-SBF **53** has been determined in dichloromethane solution to be 89%.

As shown in figure 5.12 above, the excitation spectrum was detected by using the emission maximum wavelength that is 400 nm, the peak maximum of the excitation spectrum is monitored to be at 347 nm, as is the case in its absorption spectrum. Therefore, the energy transfer occurs from the central sexiphenyl chains to the parallel standing terminal octiphenyl chain of the molecule.

5.1.7 Spectra of 4SBFSBF-SBF (79)

Absorption, fluorescence and excitation spectra of the $1.04*10^{-6}$ mol/L concentrated solution of 4SBFSBF-SBF **79** in dichloromethane were measured (figure 5.14). In absorption spectrum, it shows a peak maximum at 325 nm and another peak at 312 nm with a shoulder at 299 nm. The extinction coefficient was determined to be 240000 L mol^{-1} cm^{-1} at the peak maximum. The peak at 312 nm possesses intensity almost similar to that of the peak with the maximum wavelength. It can be concluded that the four chromophores with quaterphenyl chain play an important role during the absorption as well as the two main sexiphenyl chains. The unsubstituted fluorene units perpendicular to the plane of the quaterphenyl chain show an additional characteristic absorption band at 299 nm.

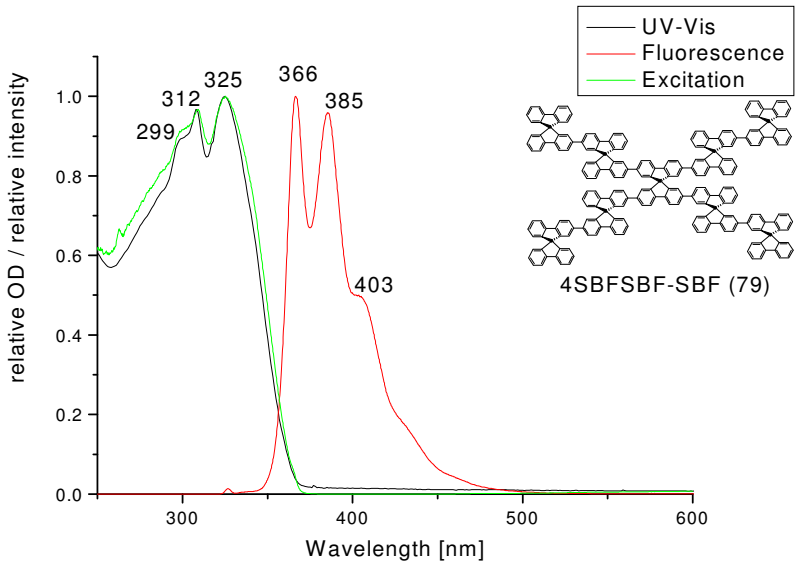

Figure 5.14 Normalized absorption (black), fluorescence (red) and excitation (green) spectra of 4SBFSBF-SBF 79 in dichloromethane ($1.04*10^{-7}$ mol/L), each normalized to the maximum peak. The excitation spectrum was detected at 366 nm

The absorption spectrum in thin film is bathochromically shifted by 41 nm compared to the spectrum in solution.

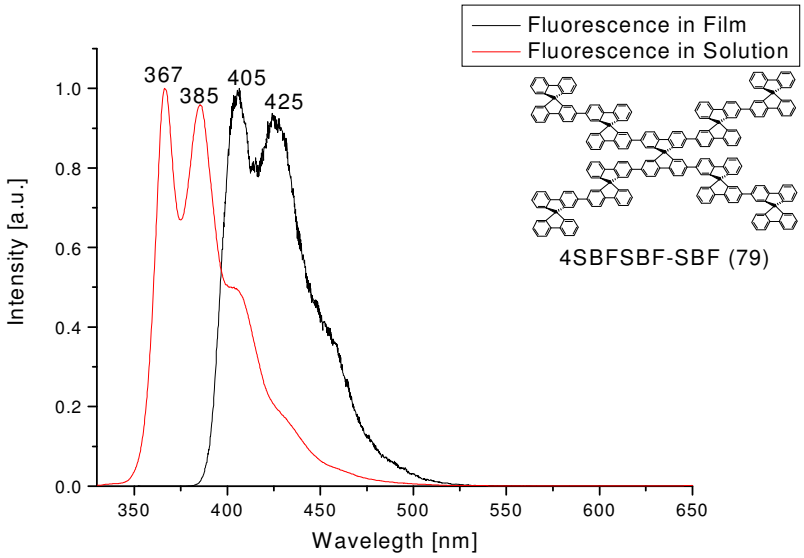

Figure 5.15 The emission spectra of 4SBFSBF-SBF 79 in the solution (red) and in thin film (black)

The emission band of the thin film is bathochromically shifted by 38 nm and 40 nm compared to the spectrum in solution (figure 5.15).

The emission band with its peak maximum at 366 nm shows a very peculiar fine structure. The fluorescence quantum yield of 4SBFSBF-SBF **79** in dichloromethane as very dilute solution has been determined to be 94%.

Intramolecular energy transfer occurs from the shorter chains to longer chains which are parallel to each other. Thus, the energy transfer takes place in cascade form. As shown in figure above, the excitation spectrum was detected by using the emission maximum wavelength that is 366 nm and the maximum of the excitation spectrum is monitored to be 325 nm, similar as in the case of its absorption spectrum.

5.1.8 Spectra of 4B(SBF)SBF-SBF (84)

Absorption, fluorescence and excitation spectra of the $5.33*10^{-7}$ mol/L concentrated solution of 4B(SBF)SBF-SBF **84** in dichloromethane were measured (figure 5.16). In absorption spectrum, it shows a peak maximum at 351 nm with an another peak at 310 nm and a shoulder at 299 nm. The extinction coefficient was determined to be 440000 L mol^{-1} cm^{-1} at the peak

maximum. The higher value of the extinction coefficient compared to that of 4SBFSBF-SBF **79** is an evidence of the bigger size of the molecule. Extra four bridged fluorene units present in 4B(SBF)SBF-SBF **84** play a role of more photon absorbing groups leading to the greater value of the extinction coefficient. The shoulder at 310 nm resembles the unsubstituted fluorene units, which is the most abundant in the molecule. The broad band at 351 nm resembles the sexiphenyl chains located as a part of central core and four times as terminal chromophores.

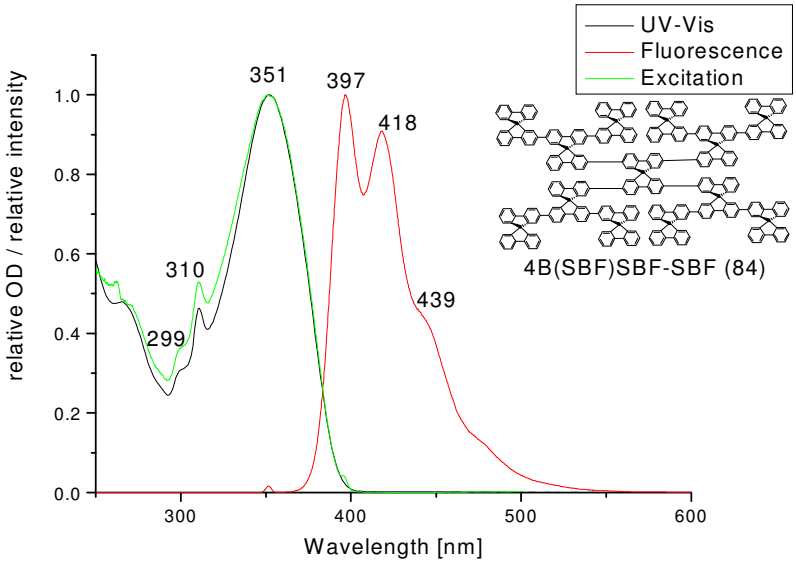

Figure 5.16 Normalized absorption (black), fluorescence (red) and excitation (green) spectra of 4B(SBF)SBF-SBF 84 in dichloromethane ($5.33*10^{-7}$ mol/L), each normalized to the maximum peak. The excitation spectrum was detected at 397 nm.

The absorption spectrum in thin film has a peak mximum at 358 nm which is bathochromically shifted by 7 nm compared to the spectrum in solution.

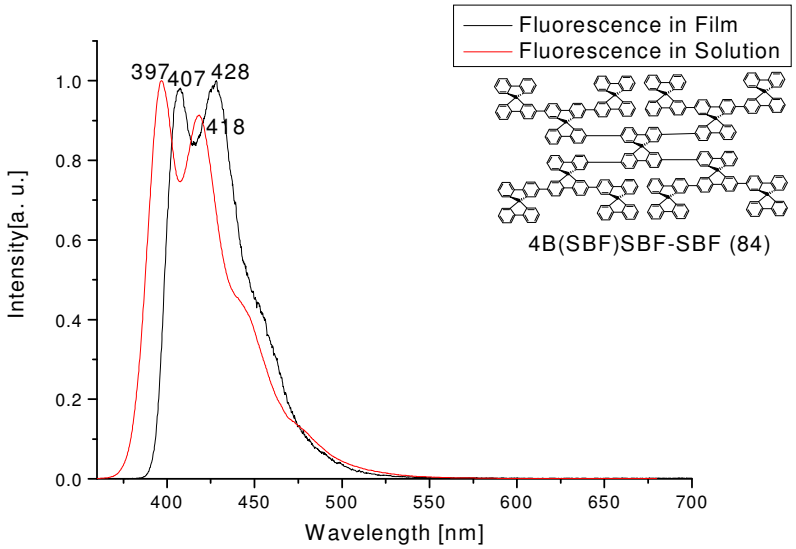

Figure 5.17 The emission spectra of 4B(SBF)SBF-SBF 84 in solution (red) and in thin film (black)

The emission band of the thin film is bathochromically shifted by 10 nm compared to the spectrum in solution (figure 5.17).

The emission band is fine structured. The absorption and the emission band peak maxima are found to be hypsochromically shifted compared to 4-spiro[3] by 7 nm and 16 nm respectively. In 4-spiro[3], the presence of the deciphenyl chromophore leads to the absorption at higher wavelength. The fluorescence quantum yield of a very dilute solution of 4B(SBF)SBF-SBF **84** has been determined in dichloromethane and is found to be 72%.

As mentioned above, the intramolecular energy transfer takes place according to the optical funnel phenomenon in the case of 4B(SBF)SBF-SBF **84** too. As shown in figure 5.16 above, the excitation spectrum was detected by using the emission maximum wavelength (397 nm) and the peak maximum of the excitation spectrum is monitored to be at 351 nm, similar as in the case of its absorption spectrum.

5.1.9 Conclusion of the Spectroscopic Characterization

Spiro starburst structures of first and second generation emit radiation in the blue region of the visible spectrum (table 5.1). The overlaps between absorption and emission spectra do not appear to be large. This fact prevents self absorption of the molecules. The peak maxima of

absorption and emission spectra are observed to be at higher wavelength in the molecules with longer chromophore chains than in the molecules with shorter chromophore chains. In contrast to the absorption spectra, emission spectra are observed with fine structure. Excitation spectra are monitored with their emission peak maxima. The peak maxima of excitation spectra resemble their absorption peak maxima.

Increasing absorbing species in molecule lead to increasing molar extinction coefficients. In case of 4B(TP)SBF-SBF **53** and 4B(SBF)SBF-SBF **84**, the greater values of the molar extinction coefficients are evidence of the presence of four times octiphenyl conjugation chains and eight times terminal fluorene units respectively.

Although the regions of emission spectra of the shorter chains and their corresponding longer chains of the compounds do not distinguish in large extent, the excitation spectra are almost similar to their corresponding absorption spectra. Hence, it indicates almost complete intramolecular energy transfer. In the case of 4B(TP)SBF-SBF **53**, the terminal chains of phenyl rings are longer than that of the central core. Hence, the optical funnel to energy transfer phenomenon is observed in inverse position.

Various lengths of the terminal and central chain of phenyl rings independent to one another reveal characteristic spectra which is distinct in the cases of 4DPSBFP-SBF **58** and 4TPSBF-SBF **72**.

Since these compounds are used as solid thin films for the practical applications, molecular design that controls not only electronic but also solid state structures of the materials is of great significance. Hence, the optical properties of solid states in the form of thin film were studied. The result indicates that the intermolecular interaction and aggregation of individual molecules in neat amorphous films are effectively hindered by their sterically demanding structures. Accordingly, they behave like isolated molecules in highly dilute solution.

Due to the peculiar structures of these molecules, the phenomenon of optical funnel to exhibit the energy transfer become possible. The observations conclude that the efficiency of energy transfer decreases with increasing generation.

Table 5.1 Absorption Maxima [$\lambda_{max}(abs)$], Extinction Coefficients(ε), Emission Maxima [$\lambda_{max}(flu)$] , and Fluorescence Quantum Yields[$\Phi_{(flu)}$] of Spiro-Starburst-Structures [a]

Compounds	λ_{max}(abs), nm	ε, L mol^{-1} cm^{-1}	λ_{max}(flu), nm	$\Phi_{(flu)}$
4SBFBP-SBF **21**	353	$16*10^4$	403	93%
4DPSBF-SBF **33**	337	$20*10^4$	397	87%
4DPSBFP-SBF **58**	338	$30*10^4$	403	85%
4TPSBF-SBF **72**	340	$20*10^4$	407	95%
4B(BP)SBF-SBF **42**	345	$36*10^4$	398	96%
4B(TP)SBF-SBF **53**	347	$43*10^4$	400	89%
4SBFSBF-SBF **79**	325	$24*10^4$	366	94%
4B(SBF)SBF-SBF **84**	351	$44*10^4$	397	72%

[a] All spectra were recorded in dichloromethane solution at room temperature and the spiro-6pp in dichloromethane solution ($\Phi_{(Ref)}$ = 95%) was considered as reference for fluorescence quantum yield determination.

5.2 Electrochemical Characterization of Spiro-Starburst-Structures

All end products along with a reference compound spiro-8pp are electrochemically characterized by Mrs. Schaefler. A detailed characterization with spectro electrochemistry is planned in her Ph. D. thesis.

Among all the end products, one compound (4DPSBF-SBF **33**) has been selected to explain its electrochemical characterization. For the rest of all other end products, only their oxidation and reduction half wave potential values are tabulated in conclusion. CV curves of oxidation and reduction of all compounds have been measured in DCM and THF solutions respectively with sweep rates 100 mV/s.

CV curve of 4DPSBF-SBF **33** (figure 5.18) shows two oxidation signals with half wave potential values 0.83 V and 1.03 V. Out of two chromophores (sexiphenyl chains as central chromophores and quaterphenyl chains as peripheral chromophores of the compound 4DPSBF-SBF **33**), to interpret which chromophore undergoes firstly to redox reaction, its CV is compared with CVs of spiro-4pp and spiro-6pp separately. Spiro-4pp shows a reversible oxidation signal with a half wave potential value 0.99 V [100] which is found to be higher by 0.6 V than that of 4DPSBF-SBF **33**. It shows that 4DPSBF-SBF **33** is easier to oxidise than spiro-4pp which is due to the presence of the internal sexi phenyl chains.as its half wave potential values are comparable with that of a CV oxidation curve spiro-6pp. The CV curve of spiro-6pp shows two reversible oxidation signals with half wave potential values 0.94 V and 1.10 V.[101] The amount of current shown by these first and second signals of the compound 4DPSBF-SBF **33** is found to be in a ratio of 1:2. It means the second signal corresponds to a transition of double amount of electrons than that of the first signal.

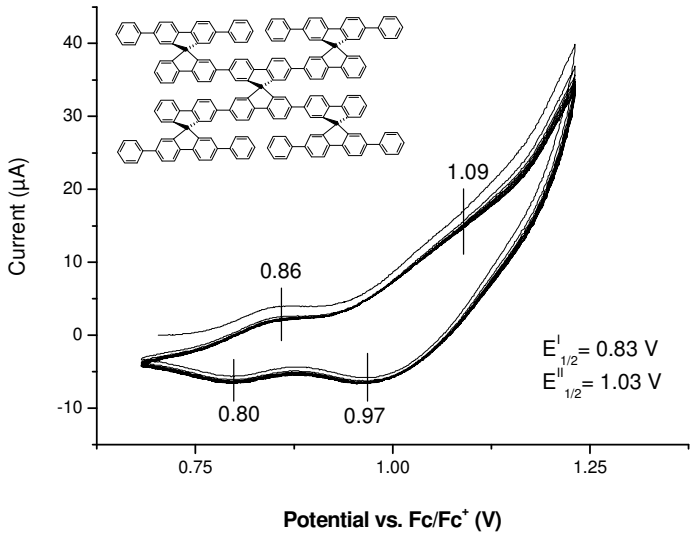

*Figure 5.18 CV of 4DPSBF-SBF **33** in DCM (oxidation)*

The reduction CV curve of the 4DPSBF-SBF **33** (figure 5.19) shows two signals with half wave potential values –2.66 V and –2.75 V representing transitions of equal number of electrons in each signal.

In spiro-4pp, the reversible reduction signals are recorded with half wave potential values -2.86 V, -3.07 V and -3.22 V.[100] Compared to this reference compound, 4DPSBF-SBF **33** easily undergoes reduction reaction. The reversible reduction signals of spiro-6pp are recorded with half wave potential values -2.63 V, and -2.75 V[101] which are more or less

comparable with that of the compound 4DPSBF-SBF **33**. Hence, the reduction signals represent the formation of anion radical of internal sexi phenyl chromophores.

Repeated cyclic measurements of redox potentials of the compound 4DPSBF-SBF **33** show that it is electrochemically reversible and stable.

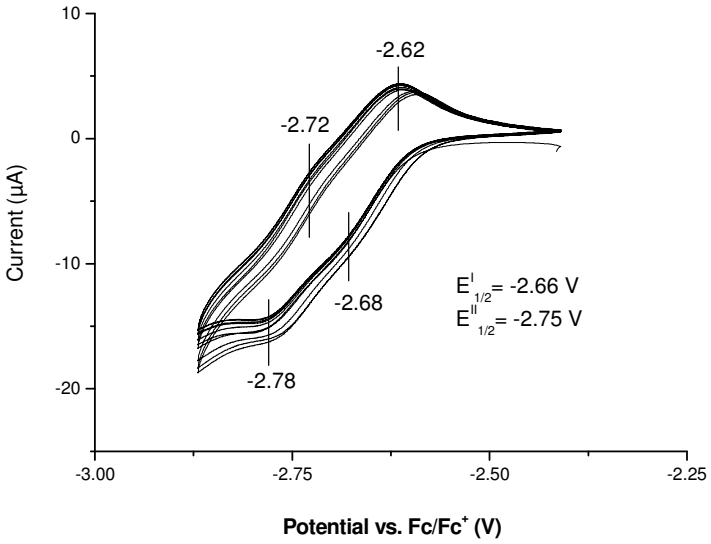

*Figure 5.19 CV of 4DPSBF-SBF **33** in THF (reduction)*

5.2.1 Conclusion of the Electrochemical Characterization

Spiro-starburst-structures act as electron acceptors and donors. Indeed, reversible reduction and also oxidation steps are detected in compounds of various conjugation lengths (Table 5.2).

Table 5.2 Electrochemical characterization of starburst-spiro oligophenyl compounds with half wave oxidation and reduction potentials.

Compounds	$E_{1/2}$ Oxidation [V vs. Fc/Fc^+][(a)]	$E_{1/2}$ Reduction [V vs. Fc/Fc^+][(b)]	Result
4SBFBP-SBF **21**	0.89 1.00	-2.55	Reversible
4DPSBF-SBF **33**	0.83 1.03	-2.66 -2.75	Reversible
4B(BP)SBF-SBF **42**	0.85 0.99	-2.61	Reversible
4B(TP)SBF-SBF **53**	0.93	-2.58 -2.67	Reversible

4DPSBFP-SBF **58**	0.86	1.01	1.14	-2.54	-2.81	-3.00	-3.17	Reversible
4TPSBF-SBF **72**	0.82	0.95	1.02	-2.55	-2.71	-2.76		Reversible
4SBFSBF-SBF **79**	0.86	1.01	1.16	-2.63	-2.72	-2.93	-3.15	Reversible
4B(SBF)SBF-SBF **84**	0.91	1.10	1.14	-2.58	-2.74			Reversible

(a) measured in DCM solution, (b) measured in THF solution

The compound 4TPSBF-SBF **72** shows the first oxidation signal at 0.82 V, the most positively shifted half wave potential value. It means that this compound is the most easily oxidable among all other compounds synthesized in this work. Most probably, the formation of radical cation of this compound takes place by the loss of one electron from a phenyl ring adjacent to the terminal spirobifluorene units firstly. The most easily reducible compound is found to be 4DPSBFP-SBF **58** with the reduction half wave potential value -2.54 V.

The electrochemically reversible and stable character of these compounds makes them very promising candidates for optoelectronic materials.

5.3 Thermoanalytic Characterization of Spiro-Starburst-Structures

The class of *p*-oligophenyl compounds exhibits very high thermal stability. The solubility of *p*-oligophenyls decreases rapidly and the melting point increases with increasing degree of condensation (number of phenyl rings). In the case of poly-*p*-phenyl, no melting point could be detected even at 800 °C to 900 °C.[102] Many species of *p*-oligophenyl, like poly-*p*-phenyl, were characterized with their higher thermal stabilities.[103] Analogous to the *p*-oligophenyl, spiro-starburst-structures also possess very high thermal stability. The decomposition of the poly-*p*-phenyl undergoes carbonation in its vacuum-pyrolysis and leads to the formation of benzene, biphenyl and small oligophenyl.[104] As explained above in general parts, spiro compounds are generally characterized by a high glass transition temperature T_g due to their bulky shape. The crystallization kinetics above T_g can vary substantially, depending on the substitution pattern and is independent of the value of T_g.[76] This means, in the typical time scale of calorimetric experiment, recrystallization can be observed for some spiro linked compounds, whereas other compounds do not recrystallize.

5.3.1 Thermal Properties of 4SBFBP-SBF (21)

Figure 5.20 shows a thermogravimetric analysis (TGA) curve of 4SBFBP-SBF **21** as an example of very high thermal stability. The decomposition temperature of a compound, T_d, is defined as the temperature at which a 5% weight loss of the compound occurs during heating. For 4SBFBP-SBF **21**, this is the case at 557 °C, which is 23 °C lower than that of 4-phspiro[2] (T_d of 4-phspiro[2] is 580 °C[70]) The decrease in T_d is due to the presence of an extra phenyl ring between the terminal and central spiro-bifluorene, which decreases the rigidity and the steric hindrance of the molecule compared to 4-phspiro[2].

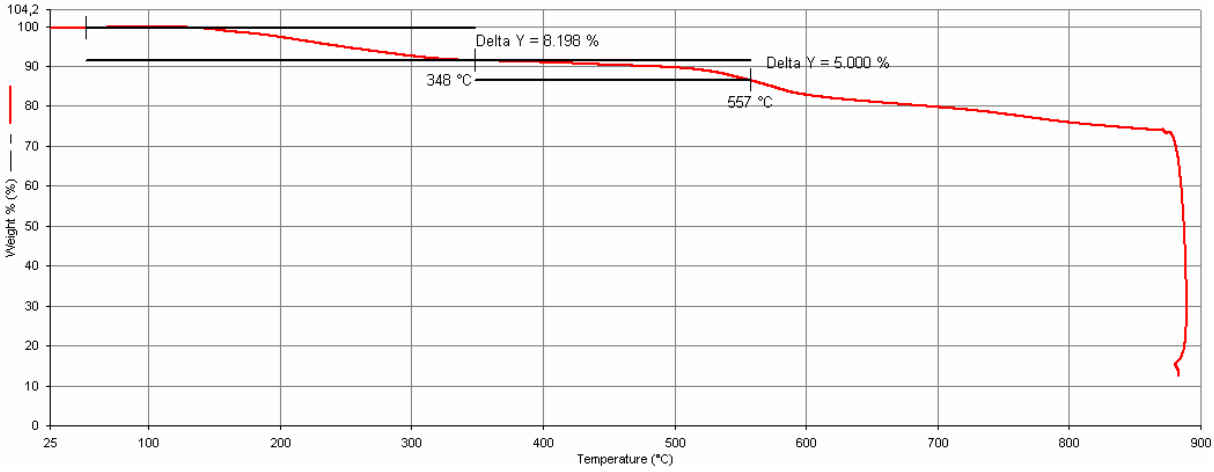

*Figure 5.20 TGA curve of 4SBFBP-SBF **21** measured at rate of 5 K/min under N_2 purging (200 mL/min)*

Spiro-starburst-structures show zeolite-like character enclosing channels in the intercrystalline systems. The presence of the channels can be monitored by firstly trapping some solvents in the channels and later observing the loss of the solvents from the channels during TGA of the material.

The material purified through a column chromatography (dichloromethane and *n*-hexane eluant) is dried in vacuum at 80 °C (above the boiling point of solvents like dichloromethane and *n*-hexane) and subjected to TGA. With increasing temperature, the TGA curve (figure 5.20) first shows a short straight line without loss in weight but just after 348 °C, it shows the loss in weight up to about 8% and further it goes as a straight line up to about 400 °C and then leads to the slow thermal decomposition of the material. The first step of about 8% loss of weight is due to the loss of the solvent molecules trapped in the channels of the

intercrystalline system of the material. This assumption is continued by the fact that solvents can be detected in ^{1}H-nuclear magnetic resonance spectrum even after drying in vacuum at 80 °C. Since the drying temperature exceeded the boiling temperature of the used solvents like dichloromethane and *n*-hexane, it stands to reason that the remaining solvent molecules are trapped in the intercrystalline channel of the material.

A typical calorimetric experiment was carried out with 4SBFBP-SBF **21** (Figure 5.21), which shows the melting point at 326 °C onset.

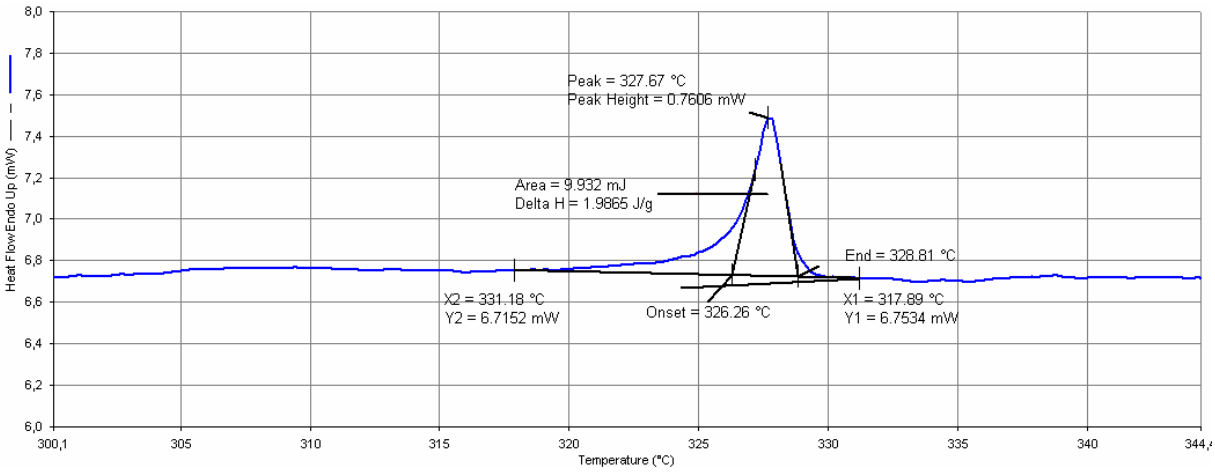

Figure 5.21 Differential scanning calorimetric (DSC) curve of 4SBFBP-SBF 21 (fourth heating curve). The melting point is indicated by an endothermic peak. All measurements were carried out under N_2 purging (20 mL/min) and at a rate of 10 K/min

No T_g and crystallization temperature (T_{cry}) were recorded as the compound was heated from room temperature to 400 °C under nitrogen purging at a rate of 10 K/min. In first to fourth heating cycle, only the melting point was distinct. Obviously, the compound could not be frozen in a glassy solid state but crystallized when cooling.

5.3.2 Thermal Properties of 4DPSBF-SBF (33)

The T_d of 4DPSBF-SBF **33** was determined at 574 °C. This valued is 46 °C lower than that of 4-spiro[2]. The diminished T_d is due to the extra phenyl rings of 4DPSBF-SBF **33**, which are placed at the 2'- and 7'- positions of each terminal spirobifluorene units. The extra rings can

rotate around the bond axis and thus cause the lower T_d. As T_d of 4DPSBF-SBF-**33** is compared with spiro-6pp, it is found to be increased by 24 °C, which is due to the steric demand governed by the bridged terminal biphenyl units to fluorene units.

The first step of losing weight (about 10%), which ends at about 353 °C, appears to be due to solvent molecules trapped inside the intercrystalline channels.

Calorimetric experiment carried out with 4DPSBF-SBF **33** shows the T_g at 276 °C onset.

The T_g of 4DPSBF-SBF **33** is found to be at 276 °C, which is higher by 3 °C than that of 4-spiro[2]. This fits well into the theory of increasing T_g with increasing chain length.[5,105] No T_{cry} and melting point were detected as the compound was heated from room temperature to 400 °C under nitrogen purging at a rate of 10 K/min from first to fourth heating cycles. Obviously, the compound is amorphous and does not crystallize due to the steric hindrance of the molecule.

5.3.3 Thermal Properties of 4DPSBFP-SBF (58)

The T_d of 4DPSBFP-SBF **58** is determined at 564 °C, which is 10 °C lower than that of 4DPSBF-SBF **33**. This is because of the presence of a phenyl ring between the terminal substituted and central spirobifuorene units, which decreases the steric rotational hindrance.

The loss of mass of the compound by about 2% at 104 °C indicates the evaporation of trapped solvent molecules in the intercrystalline channels of the compound.

The DSC of 4DPSBFP-SBF **58** determines the T_g at 307 °C onset. Crystallization temperature (T_{cry}) and melting point cannot be detected. Due to the steric hindrance of the molecule, it obviously does not crystallize just as 4DPSBF-SBF **33**.

Compared to 4DPSBF-SBF **33**, the T_g is about 29 °C higher. This is due to the longer central chain of the molecule which leads to the higher molecular weight than that of 4DPSBF-SBF **33**.

5.3.4 Thermal Properties of 4TPSBF-SBF (72)

The T_d of 4TPSBF-SBF **72** is determined at 576 °C. The position of the phenyl ring in the main conjugation chain of the molecule influences the thermal stability of the molecule positively.

The DSC of 4TPSBF-SBF **72** determines the T_g at 292 °C onset which is 15 °C lower than that of 4DPSBFP-SBF **58**.

T_{cry} and melting points are not observed.

5.3.5 Thermal Properties of 4B(BP)SBF-SBF (42)

The T_d of 4B(BP)SBF-SBF **42** is determined at 573 °C, which is 1 °C lower than that of 4DPSBF-SBF **33**. The small difference is clearly due to the minimum structural change in these molecules. The presence of one extra phenyl ring in *p*-position of every terminal of quarter phenyl chain does not affect so drastic in rotation of a single ring through the single bond and steric conformation of the compounds.

The loss of mass of the compound by about 2% at 180 °C indicates the loss of the trapped solvent molecules in the intercrystalline system of the compound.

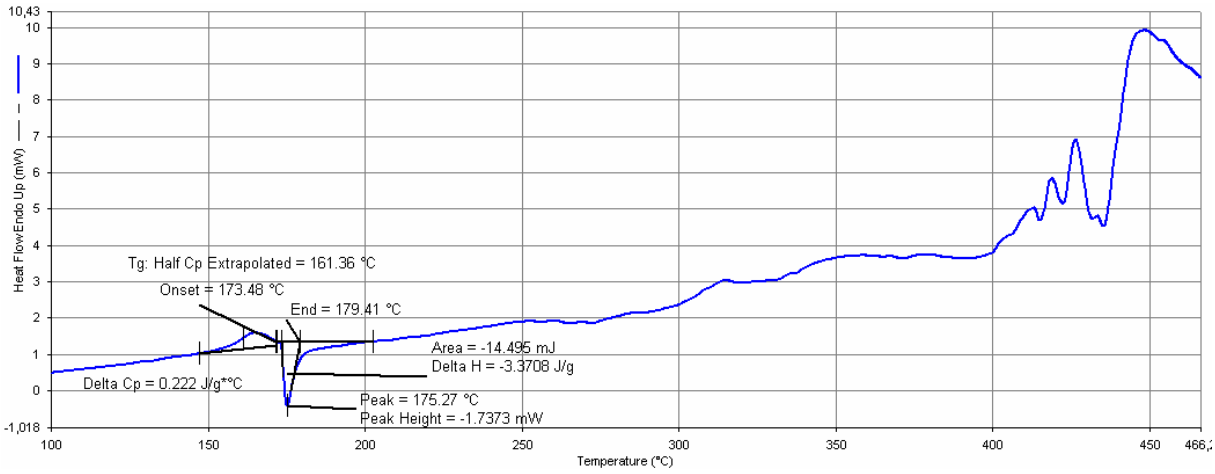

Figure 5.22 DSC curve of 4B(BP)SBF-SBF 42 (fourth heating curve). The T_g is indicated by a characteristic step. All measurements were carried out under N_2 purging (20 mL/min) and at a rate of 10 K/min.

The DSC measurement of 4B(BP)SBF-SBF **42** shows the T_g at 173 °C onset (figure 5.22) which is 105 °C lower than that of 4DPSBF-SBF **33**. Although the presence of extra phenyl rings on the terminal chains does not influence T_d in large extent, the T_g is found to be negatively affected.

T_{cry} is observed at 175 °C and the melting points are found to be at various temperatures like 412, 418, and 425 °C. More than one melting point indicates that modifications of the compound take place in various forms as the compound is heated further after its crystallization point.

5.3.6 Thermal Properties of 4B(TP)SBF-SBF (53)

The T_d of 4B(TP)SBF-SBF **53** is found to be recorded at 571 °C, which is 2 °C lower than that of 4B(BP)SBF-SBF **42**. As mentioned above too, the small difference in T_d between these two compounds is clearly due to the minimum structural change in these molecules. The presence of one extra phenyl ring in every terminal phenyl ring chain does not affect so drastic in rotation of a single ring through the single bond and steric conformation of the compounds.

No T_g, T_{cry} and the T_m points are detected in its calorimetric scanning.

5.3.7 Thermal Properties of 4SBFSBF-SBF (79)

The T_d of 4SBFSBF-SBF **79** is found to be recorded at 576 °C which is found to be higher by 26 °C than that of spiro-6pp. Although the central phenyl ring chains of 4SBFSBF-SBF **79** are comparable with spiro-6pp, its terminal biphenyl rings are bridged to a quaterphenyl chain of sub terminal spiro units causing a higher T_d.

The loss of mass of the compound by about 3% at 296 °C indicates the loss of the trapped solvent molecules in the intercrystalline system of the compound.

The DSC measurement of 4SBFSBF-SBF **79** shows the T_g at 307 °C onset which is less by 23 °C than that of 4-spiro^3 [76]. The absence of two spirobifluorene units branching at 2'- and 7-positions of the first generation spirobifluorene unit leads to the fall of T_g.

No recrystallization and melting points are detected in the calorimetric scan after vitrification[106].

5.3.8 Thermal Properties of 4B(SBF)SBF-SBF (84)

The T_d of 4B(SBF)SBF-SBF **84** is found to be recorded at 572 °C, which is less by 5 °C than that of 4SBFSBF-SBF **79**.

The loss of mass of the compound by about 3% at 231 °C indicates the loss of the trapped solvent molecules in the intercrystalline system of the compound.

The DSC measurement of 4B(SBF)SBF-SBF **84** shows the T_g at 318 °C onset which is increased by 11 °C than that of 4SBFSBF-SBF **79**. It is due to the presence of one more spirobifluorene unit at 2' position of spirobifluorene unit of the first generation. As the T_g of 4B(SBF)SBF-SBF **84** is compared to that of 4-spiro^3, then it is found to be decreased by 12 °C than that of 4-spiro^3 [76]. In the case of 4-spiro^3, all 2',7,7'-positions of the second generation spirobifluorene are occupied by terminal spirobifluorene units. It makes an obvious explanation that the absence of every terminal unit of spirobifluorene leads to the fall of T_g by 11 or 12 °C.

No recrystallization and melting points are detected in the calorimetric scanning.

5.3.9 Conclusion of the Thermoanalytic Analysis of Spiro-Staburst-Structures

All the spiro-starburst-structures, both of the first and second generations, are highly thermo stable (table 5.3). Furthermore, most of the compounds retain more than 80% of their original weight even after heating beyond 800 °C. Most of the compounds show the evidence of the trapping of the solvent molecule in the intramolecular system exhibiting the zeolite character, which is characterized by the first step of the loss of the mass of the compound. As shown in

table 5.3, the T_g of the spiro-starburst-structures increases with a higher degree of branching and molecular rigidity. Within the species of second generation compounds, for example, 4-spiro[3] shows the highest T_g (330 °C) and the highest branching degree. When one [4B(SBF)SBF-SBF **84**] or two [4SBFSBF-SBF **79**] terminal spirobifluorene units are removed, the T_g decreases to 318 °C and 307 °C respectively.

Table 5.3 Thermoanalytic Data of Spiro-Starburst-Structures

Compounds	T_d (°C)	T_g (Onset °C)	T_{cry} (Peak °C)	T_{mel} (Peak °C)
4SBFBP-SBF **21**	557	-	-	326
4DPSBF-SBF **33**	574	278	-	-
4DPSBFP-SBF **58**	564	307	-	-
4TPSBF-SBF **72**	576	292	-	-
4B(BP)SBF-SBF **42**	573	173	175	412
4B(TP)SBF-SBF **53**	571	-	-	-
4SBFSBF-SBF **79**	576	307	-	-
4B(SBF)SBF-SBF **84**	572	318	-	-

5.4 Zeolite Character of Organic Molecules

In last years, many efforts have been made to develop new organic zeolites. [107] Compared to inorganic zeolites, the organic porous structures feature advantages such as diversity on the molecular level (supramolecular synthons) and variability on the supramolecular level (properties of pores). However, these materials generally show a rather low thermal stability. Only a few compounds based on weak intermolecular interactions are known to form channel structures with a persistent porosity. These new organic zeolite gives rise to a number of inclusions with varying guest molecules.[108]

Spiro-starburst-structures also exhibit channels among the aggregated tectons. These channels have a tendency of tectonic association to favour the trapping of suitable solvent molecules forming host-guest systems. Thus, the spiro-starburst-structures act as organic zeolites with very high thermal stability, which is a striking phenomenon of substantial fundamental interest and potential utility.

Spiro-starburst-structure can also be designed as a new class of micro lasers based on nanoporous molecular sieve host-guest systems. Organic dye guest molecules can be inserted into the intercrystalline channels of spiro-starburst-structures host as similar in the case of inorganic zeolites reported by F. Laeri and his coworkers.[109]

5.4.1 Experiment, Result and Discussion

Although it is not always possible to crystallize the spiro-linked compounds, in a previous work of our group, x-ray diffraction structure analysis of one such spiro-starburst-structure exhibited channels among the aggregated tectons.[70] In this work, various spiro-starbust-structures with increasing molecular sizes have been synthesized. Unfortunately, the larger size of the molecules seems to be counter acting their crystallization abilities. Hence, the investigation of the zeolite-like property of the compound by x-ray diffraction method is substituted by thermo analysis of solvent trapping and exclusion method.

First of all, the sample is dried in vacuum above the boiling temperature of the respective solvents. Then, the compound is subjected to TGA, which shows a straight line up to the temperature where thermal decomposition of the compound starts. It actually ensures that the compound is free of any solvent molecule in it. In second phase, the compound is kept in a solvent vapour chamber for about 16 hours and then again subjected to TGA. TGA is programmed in such a way that the sample is heated from room temperature to 116 °C with a rate of 5 °C per minute. It is then halted at 116 °C for 1 hour to allow evaporating the trapped solvent molecules through the channels and then again heated up to 205 °C with the same rate. Again, it is allowed to hold for 1 hour at this temperature to be sure that no more solvent molecules are available in those channels. The sample is further heated with the same rate up to 350 °C expecting with no loss of the weight of the sample.

The results of 4B(BP)SBF-SBF **42** with *n*-hexane, *n*-propanol and toluene, separately, are shown in figure 5.23. The curves show very distinguished steps before the beginning of the thermal decomposition (T_d at 573 °C) of the compound. The prompt fall of the curve from the room temperature up to about 120 °C is due to the loss of the solvent remained adsorbed on the surface of the compound. The following steps, starting from about 120 °C (in the case of *n*-hexane and *n*-propanol) and 140 °C (in the case of toluene) up to the temperature where the decomposition of the compound begins, exhibit the evaporation of the trapped solvent from

the channels of the intercrystalline system of the molecule. These experiments are repeated for many times and lead to the same results.

The experiment has been carried out with another solvent vapour like DCM too but in this case, the compound has been found to be dissolved after exposing for 16 hours in a DCM vapour chamber. Hence, no TGA measurement has been carried out as the compound remained dissolved in the solution, the structure of the compound which is needed to trap the solvent was no more available.

In the case of *n*-hexane, the structure and size of the solvent seems to fit neatly into the channels. The insertion and the exclusion of the solvent actually does not disturb the tectonic networks. The tectons are robust enough to allow the *n*-hexane as guest to be trapped in channels and to exclude it through the channels without a loss of materials framework.

In the case of *n*-propanol too, the insertion of the solvent seems to be with no disturbance to the tectonic networks. During TGA, after a prompt fall of the TGA curve, it shows a very distinct step with 1.37% weight loss of the sample and then is followed by a next parabolic slow fall. The parabolic curve might be either due to the loss of the remaining solvent molecules which was not completely evaporated at the first halt duration at 116 °C or due to the new physical property possessed due to the most possible hydrogen bonding of the sample with the oxygen atom of the solvent.

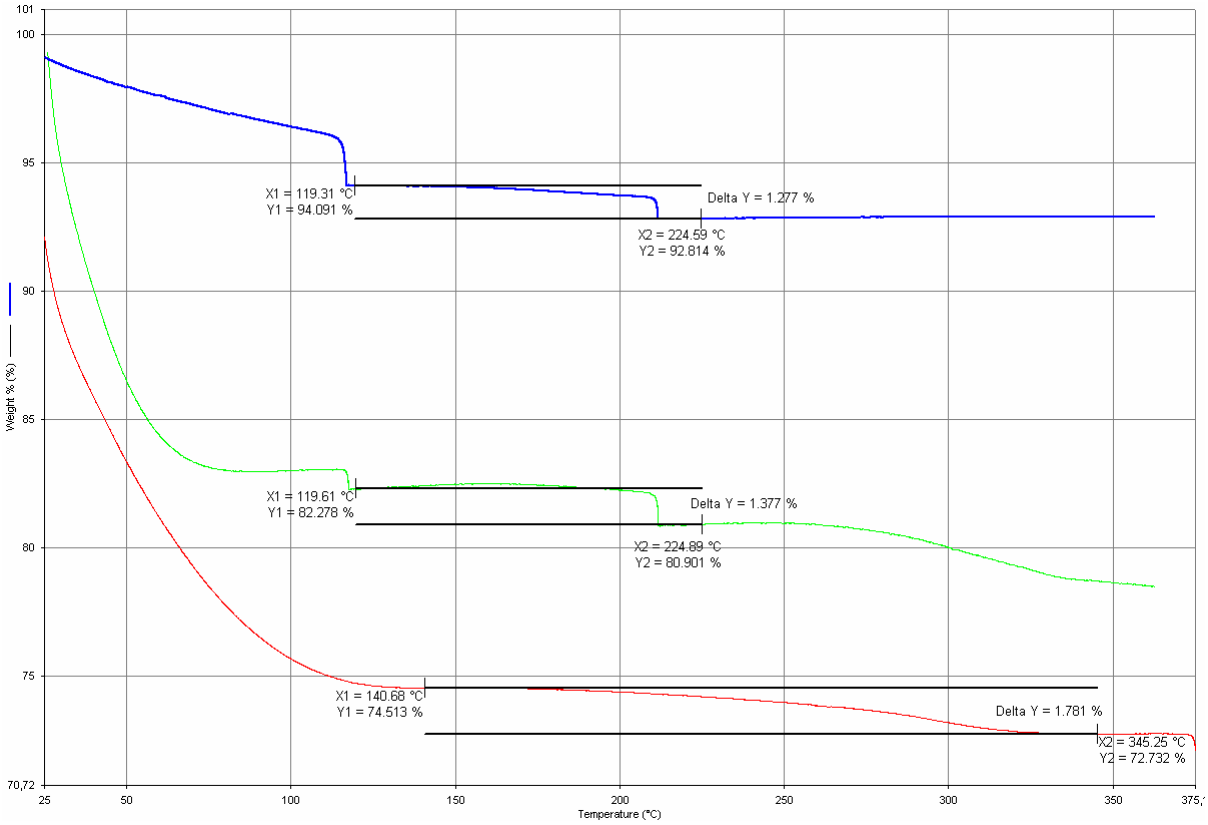

*Figure 5.23 Blue TGA curve shows the weight loss of 1.3% indicating the evaporation of n-hexane, green TGA curve shows the weight loss of 1.4% indicating the evaporation of n-propanol and red TGA curve shows the weight loss of 1.8% indicating the evaporation of toluene from the sample 4B(BP)SBF-SBF **42**.*

(TGA is programmed to heat upto 350 °C with a heating rate of 5 °C per minute and one hour halt at 116 °C and 205 °C.)

In the case of toluene solvent, the flow of the TGA curve shows no distinct steps for a loss of superficially adsorbed solvent and the evaporation of the trapped solvent molecules. The only one step at 345 °C is a united step of these two steps. The size and shape of the solvent molecule is most probably not easy to exclude through the channels as the complete exclusion of the solvent seems to take place only at 345 °C but the exact percentage of the weight loss of the compound as the loss of trapped solvent molecules can not be predicted.

Similar experiments have been carried out with another sample 4TPSBF-SBF **72** (T_d at 576 °C) too. The sample has been exposed in *n*-hexane vapour chamber and subjected to the TGA programmed as in above case too. It has been repeated twice which lead to the almost same result (figure 5.24). Green TGA curve shows the weight loss of 0.98% indicating the

evaporation of *n*-hexane. Blue TGA curve represents the second heating phase which also shows the weight loss of 1.2% more or less equal as in the first phase heating of the sample.

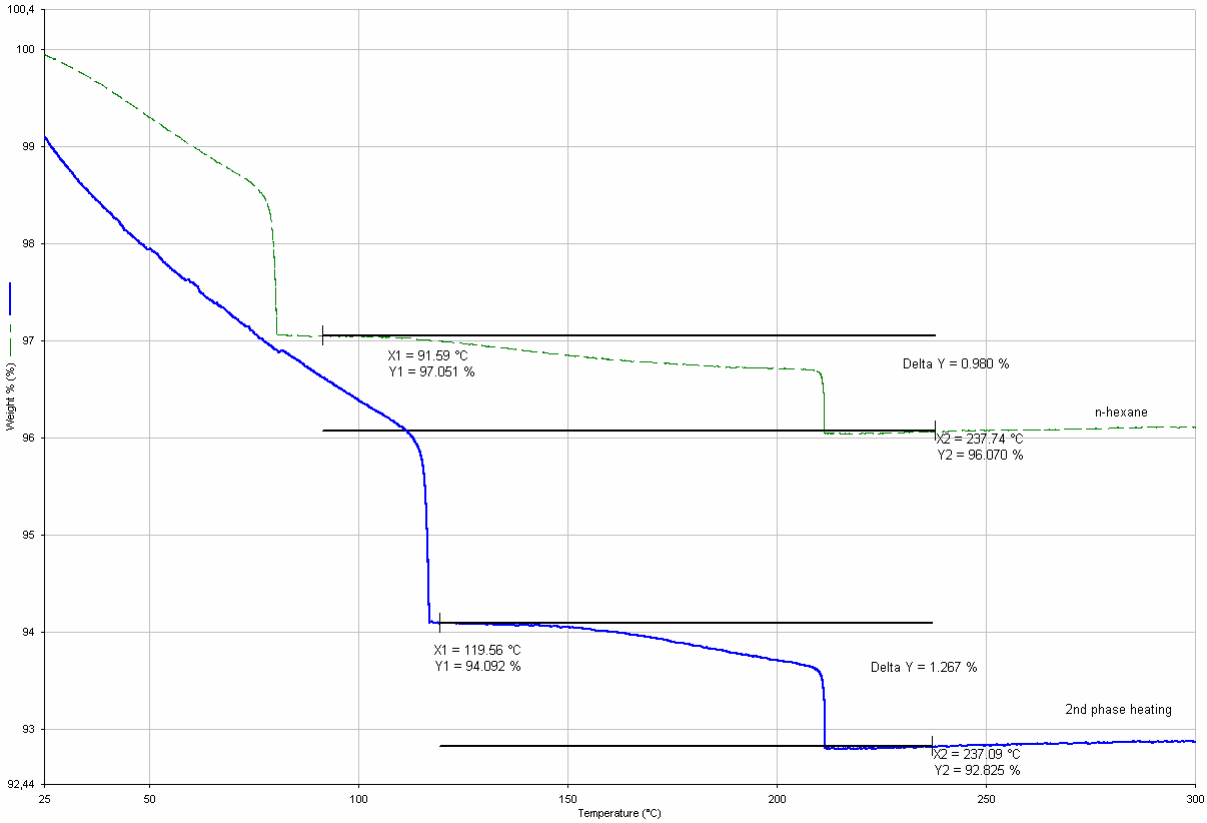

Figure 5.24 Green TGA curve shows the weight loss of 0.98% indicating the evaporation of n-hexane, blue TGA curve represents the second heating phase which also shows the weight loss of 1.2% more or less equal as in the first phase heating of the sample 4TPSBF-SBF ***72****.*

The TGA curve taken after exposing the sample 4TPSBF-SBF **72** to the *n*-propanol vapour chamber shows undistinguished second step (figure 5.25). Just over 100 °C, the curve shows the continuous loss of the weight. As explained above in the case 4B(BP)SBF-SBF **42**, it indicates that the oxygen atom of *n*-propanol is involved in the hydrogen bonding with the compound itself and with the increasing temperature, the breaking of the hydrogen bond occurs and causes the breaking of the tectonic arrangements of the compounds exposing a new physical property.

In the case of toluene solvent, the flow of the TGA curve shows no step at all (figure 5.26). The loss of superficially adsorbed solvent and the evaporation of the trapped solvent molecules.is represented in the continuous fall of the curve up to 260 °C. Similarly as in the

case of 4B(BP)SBF-SBF **42**, the size and shape of the solvent molecule is most probably not easy to exclude through the channels as the complete exclusion of the solvent seems to take place only at 260 °C and hence, the exact percentage of the weight loss of the compound as the loss of trapped solvent molecules can not be predicted.

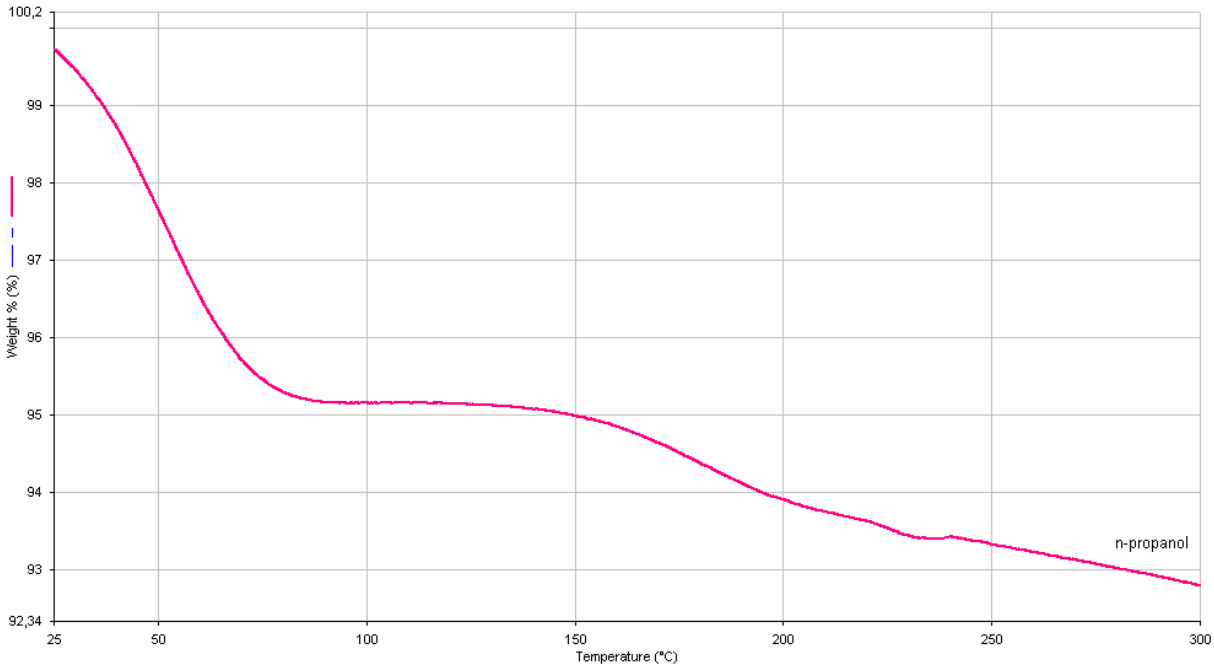

*Figure 5.25 TGA curve taken after exposing the sample 4TPSBF-SBF **72** in n-propanol vapour for 16 h*

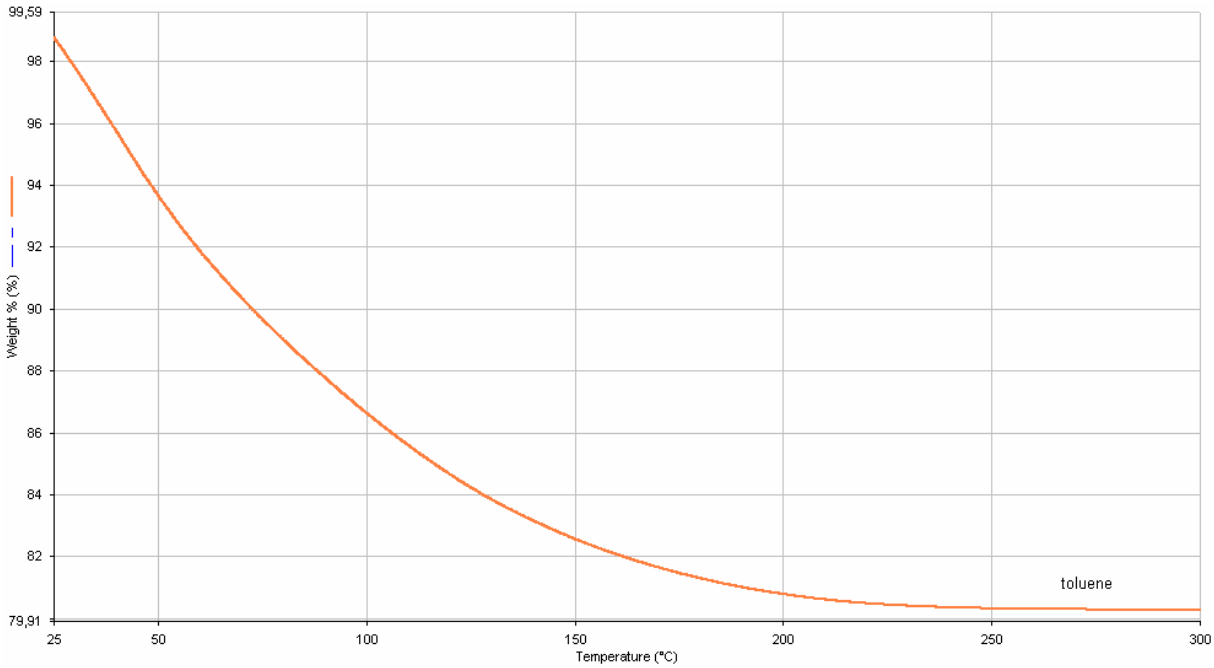

*Figure 5.26 TGA curve taken after exposing the sample 4TPSBF-SBF **72** in toluene vapour for 16 h*

5.4.2 Conclusion of Zeolite Character

The channels present among the tectonic networks of the compound are big enough to enclose solvent molecules like *n*-hexane and *n*-propanol whereas toluene does not seem to fit into the channels or strongly retained in the channels as it is almost impossible to distinguish the amount of solvent molecule that is superficially adsorbed and trapped in intercrystalline channels. It is concluded that the tectonic networks are robust enough to allow the selected types of guest to be trapped in and excluded through the channels without loss of materials framework. Such crystals, therefore, behave as sensitive microporous molecular solids analogous to specialized zeolites, and similar applications in separation, sensing, and other areas are also opened to be explored.

6 Summary and Further Work

6.1 Summary

All the optronic devices involve charge transport as an essential operation process and hence, require charge-transporting materials. Spiro-starburst-structures are the best examples of charge transporting materials as these structures are based on π-electron systems, which are characterized by properties such as light absorption and emission in ultraviolet- to visible-wavelength region of a spectrum. Such structures mostly form stable amorphous glasses, namely amorphous molecular materials, which have enabled the fabrication of blue light emitting diods.

These spiro compounds are formed from two individual π-systems, which are connected to one another through a common sp^3-hybridized spiro carbon atom.

Spiro linked *p*-oligophenyl species in form of first and second generations emit radiation in the blue region of the visible spectrum. The overlap between absorption and emission spectra do not appear to be large extent. This fact evidences for no self absorption in the molecules. The peak maxima of absorption and emission spectra are observed to be at higher wavelength in the molecules with longer chromophore chains than in the molecules with shorter chromophore chains. In contrast to the absorption spectra, emission spectra are observed with fine structure. Excitation spectra are monitored with their emission peak maxima. The excitation spectra resemble to their absorption spectra indicating almost complete intramolecular energy transfer from the peripheral chromophores to the chromophores lying parallel to them.

The increasing absorbing species in molecule leads to increasing molar extinction coefficient. In the case of 4B(TP)SBF-SBF **53** and 4B(SBF)SBF-SBF **84**, the greater values of the molar extinction coefficients ($43*10^4$ and $44*10^4$ L mol^{-1} cm^{-1} respectively) are the evidences of the presence of four times octiphenyl conjugation rings and eight times terminal fluorene units respectively.

Since these compounds are used as solid thin films for the practical applications, molecular design that controls not only electronic but also solid state structures of the materials is of great significance. Hence, the optical properties of solid states in the form of thin film were studied. The result indicates that the intermolecular interaction and aggregation of individual molecule in neat amorphous films are effectively hindered by their sterically demanding structures. Accordingly, in solid state, they behave like isolated molecules in highly dilute solution.

Spiro-starburst-structures act as electron acceptors and donors. Indeed, reversible reduction and also oxidation steps are detected in compounds of various conjugation lengths.

The electrochemically reversible and chemically stable character of these compounds make them very promising candidates for optronic materials.

All the spiro-starburst-structures, both of the first and second generation, are highly thermo stable. Furthermore, most of the compounds retain more than 80% of their original weight even heating beyond 700 °C. As the structures of the compounds play a counter role to achieve their crystal structures, amorphous state of most of the compounds show the evidence of the trapping of the solvent molecule exhibiting the zeolite-like character, which is characterized by the first step of the loss of weight of the compound. T_g of spiro-starburst-structures increases with a higher degree of branching and molecular rigidity. Within the species of second generation compounds, for example, 4-spiro[3] shows the highest T_g (330 °C) and the highest branching degree. When one [4B(SBF)SBF-SBF **84**] or two [4SBFSBF-SBF **79**] terminal spirobifluorene units are removed, the T_g decreases to 318 °C and 307 °C respectively.

T_g, which is one of the most important parameter indicating the thermal stability of the amorphous state of the material for optronic devices, should be high. The derivatives of spiro-starburst-structures synthesized in this work meet this requirement promising to prevent the degradation of devices in application.

The channels present among the tectonic networks of the compound are big enough to enclose certain solvent molecules. It is concluded that the tectonic networks are robust enough to allow some selected types of guest solvents to be trapped in and excluded through the

channels without loss of materials network. Such crystals, therefore, behave as sensitive microporous molecular solids analogous to specialized zeolites, and similar applications in separation, sensing, and other areas.

6.2 Further Work

As the compounds that have been synthesized in this work possess tendencies to the applications like that of Metal-Organic Frameworks (MOFs), further work can be directed towards synthesizing MOFs referring spiro-starburst-structures as ligands.

MOFs are crystalline compounds consisting of metal ions or clusters coordinated to often rigid organic molecules to form one-, two-, or three-dimensional structures that can be porous. In some cases, the pores are stable to elimination of the guest molecules (often solvents) and can be used for the storage of gases such as hydrogen and carbon dioxide. Other possible applications of MOFs are gas purification, gas separation, catalysis and sensors.

Due to the porousity in MOFs, it shows great promise as a practical method of storing large volumes of hydrogen. This brings fuel-cell powered cars a step closer to being realised.[110]

Furthermore, triphenyl amine derivatives are frequently used in optronic devices as hole transporting material. Generally, the T_g of such compounds are under 100 °C with low thermal stability of the amorphous state. By introducing the spiro-concept in such materials, the thermal stability was increased but not satisfactorily. Hence, by applying the spiro-starburst-structures, a novel category of hole transporting material with optimal thermal stability can be prepared. A Suzuki cross-coupling reaction between a boron ester of a 9,9'-spirobifluorene-linked aryl amine and 2,2',7,7'-tetrahalogenated 9,9'-spirobifluorene affords spiro-starburst-structured aryl amine derivative (figure 6.1).

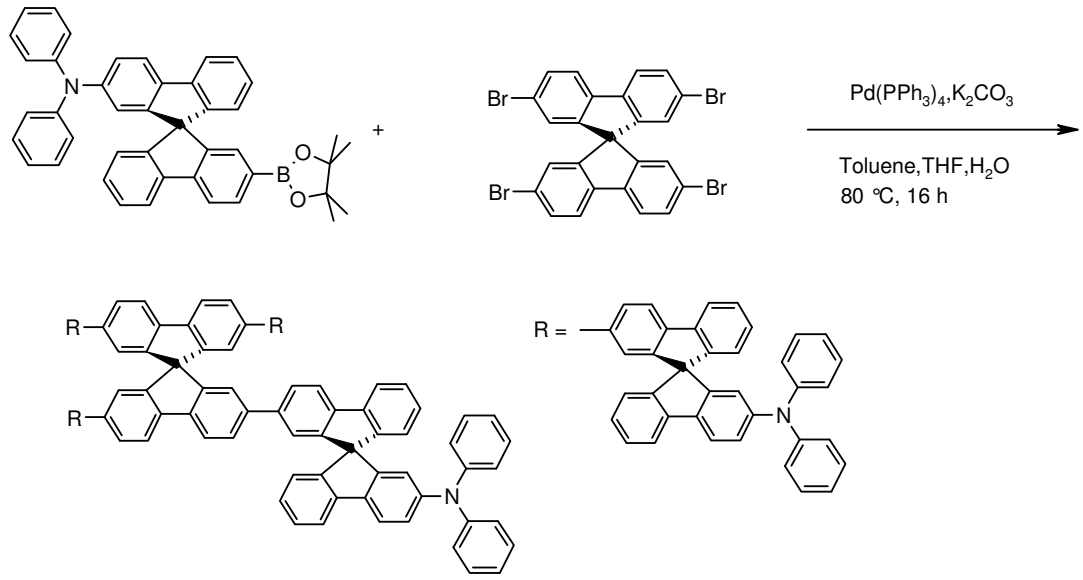

Figure 6.1 Hole transporting spiro-starburst-structure as derivative of aryl amine.

The required reactants can be prepared as follows:
2,7'-Dibromo-9,9'-spirobifluorene can be prepared by regioselective, chemoselective bromination of 9,9'-spirobifluorene by treating with 2.1 equivalent Br_2 in the presence of $FeCl_3$ catalyst (figure 6.2).[111]

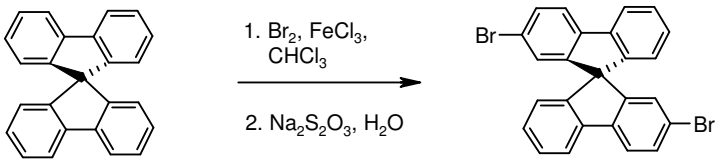

Figure 6.2 Regioselective and chemoselective bromination of 9,9'-spirobifluorene

2,7'-dibromo-9,9'-spirobifluorene is subjected to Hartwig-Buchwald coupling reaction with diphenylamine affording 7'-bromo-9,9'-spirobifluorene-2-amine (figure 6.3).

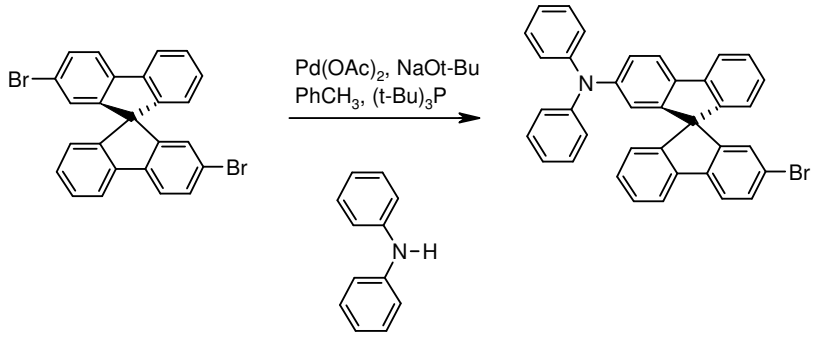

Figure 6.3 Hartwig-Buchwald coupling reaction

7'-Bromo-9,9'-spirobifluorene-2-amine is subjected to Miyaura reaction converting it into corresponding boron ester (figure 6.4).

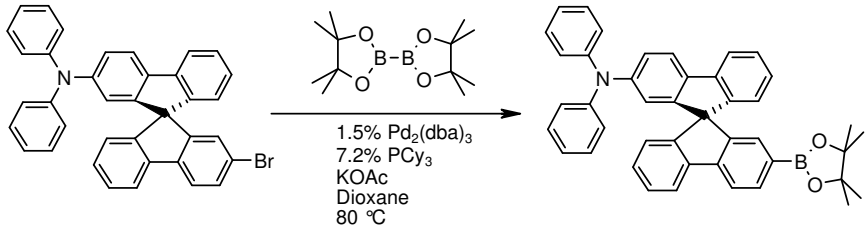

Figure 6.4 Miyaura reaction.of 7'-bromo-9,9'-spirobifluorene-2-amine

This new category of material can be used as hole transporting material in dye sensitized solid-state solar cell. Furthermore, spiro-starburst-structure of MeO-TTB (figure 6.5) is an example of this category.

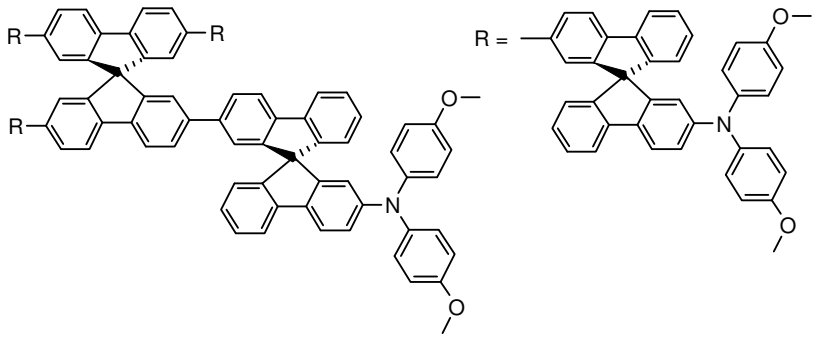

Figure 6.5 Spiro-starburst structure of MeO-TTB

In this way, spiro-starburst-structures with hetero atoms can be subjected to crystallization expecting suitable sized crystals for x-ray diffraction analysis too.

7 Experimental Section

7.1 Methods and Instruments

7.1.1 High Performance Liquid Chromatography (HPLC)

High Performance Liquid Chromatography (HPLC) analysis was performed by using a HPLC instrument of Knauer firm.
Pump: Well Chrom K-1800 with 100 mL pump head.
Detector: Fast scanning UV/Vis-photometer K-2600.
Column: Vertex-column (Ø = 20 mm, h = 25 cm) with spherical Eurospher-100 silica gel.

7.1.2 NMR-Spectroscopy

NMR probes were prepared in mentioned deuteriated solvent or in a mixture of deuteriated solvent and NMP. NMR-spectra were measured in an instrument of model INOVA 500 of Varian firm. The measuring frequencies were 500 MHz (^{1}H-NMR) and 125.7 MHz (^{13}C-NMR). The chemical shifts (δ) are expressed in ppm relative to the used deuteriated solvents and tetramethylsilane as internal standard. The multiplicity of the ^{1}H spectra is expressed as follows:
s = singlet; d = doublet; pd = pseudo doublet, dd = doublet of doublet; t = triplet; m = multiplet.
The mode of ^{1}H spectra is given as: (measuring frequency, solvent): δ-value (number of proton, multiplicity, coupling constant).

The mode of ^{13}C is given as: (measuring frequency, solvent): δ-value.

7.1.3 Mass Spectrometry (MS)

MALDI-mass spectra were measured in an instrument BiFlex IV of Bruker Daltonics.

7.1.4 IR-Spectroscopy

IR-spectra were measured in an instrument of model FTS 40A of Biorad firm. The measurements were carried out with the Biorad Win-IR software in ATR-modus. The absorption bands are expressed in wave number (1/cm).

7.1.5 Thermo Gravimetry Analysis (TGA)

The decomposition temperatures of samples were determined in an instrument of model Diamond TG/TA with a heating rate of 5 °C/min and N_2 flow rate of 200 mL/min.

7.1.6 Differential Scanning Calorimetry (DSC)

The samples for the DSC analysis were prepared in capsules and subjected to an instrument of model Perkin-Elmer DSC 7X Thermal Analysis System. The heating rate was adjusted at 10 °C/min with N_2 flow rate 20 mL/min. The melting points are expressed as the peak onset value. The T_g values are determined from the second to fourth heating cycles.

7.1.7 UV/Vis-Spectroscopy

Samples for UV/Vis-spectra were prepared as dilute solutions in 1 cm standard quartz cuvettes (Hellma firm). Required solvents (UVASOL 99.9%) from Merck and Sigma-Aldrich firms were used for the samples' preparation. UV/Vis-spectra were taken in an instrument of model Lambda 900 UV/Vis/NIR-specrtrometer of Perkin-Elmer firm.

7.1.8 Fluorescence Spectroscopy

The same samples that have been used for the UV/Vis-spectra measurements were used for fluorescence spectra measurements, too. Fluorescence spectra were measured in an instrument of Hitachi F-4500 Fluorescence Spectrophotometer. The quantum yields in solutions were determined relative to solution of a reference compound with the help of the following equation:

$$\Phi_{sample} = \frac{\Phi_{reference} * S_{sample} * A_{reference}}{S_{reference} * A_{sample}}$$

Φ = Quantum yield of the sample as well as of the reference substance.

A = Absorption of the sample as well as of the reference substance at the excitation wave length.

S = Surface area under the fluorescence band of sample as well as of the reference substance. As reference substance, 2,2',7,7'-tetrakis(4,1'-biphenyl)-9,9'-spirobifluorene was used with its quantum yield 95% in DCM.[105(b)]

7.1.9 Cyclic voltammetry (CV)

The measurements were performed with an instrument of model Potentiostate/Galvanostate 273 of EG & G Princeton. Absolute DCM as well as THF was used as solvents, with a continuous flow of N_2 stream. *n*-Bu_4NPF_6 conducting salt was dissolved in the solvent with 0.1 M concentration. The concentration of the sample in the solution was attempted to be $5x10^{-4}$ M. Following electrodes were used:
Pt-electrode as working electrode, glassy-carbon electrode as counter electrode and silver chloride electrode as reference electrode

The scan was maintained at 50 mV/s (when not specified differently). The measurements were performed versus ferrocene/ferrocenium (Fc/Fc^+) as internal standard reference.

7.1.10 X-ray Structure Analysis

An instrument STOE IPDS served for the x-ray structure analysis.

7.1.11 Elemental Analysis

The elemental analysis was performed externally in Regensburg University in the department of central analysis.

7.2 Synthesis

For the reaction monitoring, thin-layer chromatography (TLC) was performed on TLC aluminium sheets of Machery-Nagel Alugram SIL G/UV_{254} (40 x 80 mm) pre-coated with silica gel (0.2 mm layer) with fluorescent indicator. The substances were visualized by quenching of ultraviolet fluorescence (λ = 254 – 366 nm).

For the purification of the reaction products, column chromatography was performed under ambient pressure using silica gel (0.036 – 0.200 mm) of Merck firm.Only distilled solvents were used as eluents.

Reagents were used as obtained from commercial sources or purified according to known procedures.

All reaction solvents were distilled before use and stored over activated 4 Å molecular sieves, unless otherwise indicated. Anhydrous CH_2Cl_2 was obtained by refluxing over calcium hydride. Anhydrous THF and Et_2O were obtained by distillation, immediately before use, from sodium/benzophenone ketyl under an atmosphere of nitrogen.

7.2.1 2-Bromofluoren-9-one (6)

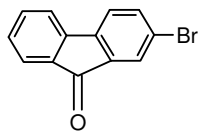

In a 500 mL r. b. flask, a solution of 25 g of 2-bromofluorene (100 mmol), 95 g of potassiumdichromate (322 mmol) and 250 ml of conc. acetic acid was refluxed for one hour. Then, it formed a dark green paste like crystals which was dissolved in chloroform and extracted with water. The organic phase was dried over sodium sulphate. The solvent was removed by rotary evaporator and the remaining yellow crystals were dissolved in acetic acid to recrystallise the product 2-bromofluoren-9-one. It was then washed with water and dried. More crystals could be obtained from the mother liquor after addition of water. [71]

$C_{13}H_7BrO$ (259.10 g/mol)

Yield: 21 g (81 mmol, 81 %), yellow crystal.

^{1}H-NMR (500 MHz; $CDCl_3$) (δ [ppm])

7.72 (d, 1H, *J* = 1.46 Hz), 7.62 (d, 1H, *J* = 7.32 Hz), 7.57 (dd, 1H, *J* = 7.81 Hz), 7.47 (m, 2H), 7.36 (d, 1H, *J* = 7.81 Hz), 7.29 (m, 1H).

^{13}C-NMR (125.7 MHz; $CDCl_3$) (δ [ppm])

192.66, 143.92, 143.24, 137.35, 136.00, 135.29, 133.93, 129.68, 127.81, 124.86, 123.17, 121.97, 120.69.

7.2.2 2-Bromo-9,9'-spirobifluorene (7)

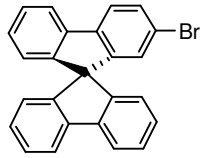

In a pre-heated (in a drying cupboard about 150 °C) three necked r. b. flask, 1.17 g of magnesium (48.7 mmol) was taken. The flask was connected with a pre-heated reflux condenser in a nitrogen gas environment. Then, 10 mL of dried THF were added to it. The mixture was stirred for a while and about 2.5 mL of 11.2 g (48.2 mmol) of 2-bromobiphenyl were added to it. Then again 90 mL of THF were added and the rest of the 2-bromobiphenyl was also added at the end. The solution became hot but not up to refluxing phase. So, it was heated and refluxed for about 2 hours and left stirring overnight. The solution was left to sediment, then decanted to another three necked 500 mL r. b. flask and cooled up to 0 °C. Afterwards a solution of 12.5 g (48.2 mmol) of 2-bromofluoren-9-one in 145 mL of THF was dropped to it within 20 minutes. The mixture was left to stir for an hour at room temperature and then refluxed for 2 hours. After the solution cooled down, the white precipitate was filtered and washed quickly with THF. The precipitate was hydrolyzed with a mixture of ice water (90 mL) and 2.5 mL conc. HCl. The mixture was then extracted with 150 mL chloroform. After uniting the organic phases, they were washed with aqueous $NaHCO_3$ solution and at the end with water. Then the solution was dried over Na_2SO_4 and the organic solvent was removed by rotary evaporator and the residue was dissolved in warm ca. 100 mL CH_2Cl_2. 200 mL hexane were added to it, the mixture was filtered, the precipitate was washed with hexane and a colourless crystalline powder was obtained. It was then dried and then treated with 90 mL conc. acetic acid and 0.5 mL HCl and then refluxed for two hours. It was left to cool and colorless crystalline needles were formed. These were filtered off, slowly stirred with water and then dried.

$C_{25}H_{15}Br$ (395.30 g/mol)

Yield: 13 g (32.29 mmol, 67 %), colourless crystal.

^{1}H-NMR (500 MHz; $CDCl_3$) (δ [ppm])

7.83 (d, *J* = 7.65 Hz, 2H), 7.80 (d, *J* = 7.67 Hz, 1H), 7.69 (d, *J* = 8.14 Hz, 1H), 7.47 (dd, *J* = 8.15, 1.65 Hz, 1H), 7.37 (m, 3H), 7.11 (t, 3H), 6.84 (pd, *J* = 1.72 Hz, 1H), 6.71 (m, 3H).

^{13}C-NMR (125.7 MHz; $CDCl_3$) (δ [ppm])

150.77, 148.50, 147.87, 141.70, 140.72, 140.61, 130.86, 128.22, 127.96, 127.91, 127.87, 127.24, 124.06, 124.01, 121.36, 121.29, 120.10, 120.02, 65.76.

7.2.3 1,4-Bis(trimethylsilyl)benzene (15)

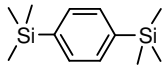

In a preheated 2 L three necked r.b. flask, a magnet stirrer, 94.36 g (0.40 mol) of *p*- dibromobenzene and 400 mL diethyl ether were taken. The flask was connected with a reflux condenser, a dropping funnel, a minus degree thermometer and with the nitrogen storm. First of all, the compound was dissolved and then the flask was cooled to –78 °C. Two equivalent amount of *n*-butyllithium (320 mL) was added dropwise into the mixture. After about three hours, two equivalent amount of trimethylsilylchloride (112 mL) was added dropwise into the mixture at -78 °C. The reaction mixture was left to warm up to room temperature and left stirring overnight. 200 mL water was added to it and the phases were separated. The organic phase was washed with 2x150 mL water and dried over sodium sulphate. The solution was concentrated by rotary evaporator and then left to crystallize.

$C_{12}H_{22}Si_2$ (222.48 g/mol)
Yield: 49 g (0.22 mol, 55 %), colourless crystal.
^{1}H-NMR (500 MHz; $CDCl_3$) (δ [ppm])
7.514 (d, 4H), 0.259 (s, 18H).

7.2.4 4-(Dibromoboryl)phenyltrimethylsilane (16)

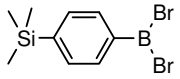

To the –78 °C cooled solution of 40 g (0.18 mol) 1,4-bis(trimethylsilyl)benzene in 90 mL dried dichloromethane, provided with a magnetic stirrer, 47.35 g (0.189 mol) (18 mL; ρ = 2.650) tribromoborane was added dropwise within 15 minutes. The reaction mixture was left stirring at the same temperature for two hours (it seemed to be like paste) and then let to warm up to room temperature (became dark brown solution). The solvent was removed by rotary evaporator (till 20 mbar). The remaining solution was subjected to the vacuum distillation.

$C_9H_{13}BBr_2Si$ (319.91 g/mol).
Yield : 46.15 g (0.14 mol, 80%), colourless oil, (became pale yellow after exposure to air).
^{1}H-NMR (500 MHz; $CDCl_3$) (δ [ppm])

8.21 (d, *J* = 7.81 Hz, 2H), 7.67 (d, *J* = 7.86 Hz, 2H), 0.35 (s, 9H).

7.2.5 4-Trimethylsilylphenyl boronic acid (8)

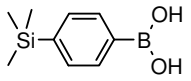

To a –78 °C cooled solution of 43.3 g of 4-(dibromoboryl)phenyltrimethylsilane (0.13 mol) in 100 mL dichloromethane, 200 mL of 5 M solution of potassium hydroxide was added dropwise and stirred for 1 hour. It was allowed to warm to room temperature and the two-phase solution was filtered to remove the potassium salt of 4-trimethylsilylphenyl boronic acid. The wet salt was suspended in a mixture of diethyl ether and 2 M HCl (200 mL of each) and stirred vigorously for 2 h. After this period, two clear layers had formed. The aqueous layer was discarded, and the organic layer was washed with 150 mL of 2 M HCl, followed by distilled water (2 volumes of 200 mL each), and finally washed with brine (200 mL). The ethereal solution was dried over $MgSO_4$, and the solvent was removed to yield a white solid.

$C_9H_{15}BO_2Si$ (194.12 g/mol).

Yield: 17.66 g (0.09 mol, 70 %), colourless amorph.

^{1}H-NMR (500 MHz; $CDCl_3$) (δ [ppm])

8.19 (d, *J* = 7.49 Hz, 2H), 7.66 (d, *J* = 7.50 Hz, 2H), 0.30 (s, 9H).

^{13}C-NMR (125.7 MHz; $CDCl_3$) (δ [ppm])

146.07, 134.60, 132.83, -1.255.

7.2.6 2-(4-Trimethylsilylphenyl)-9,9'-spirobifluorene (9)

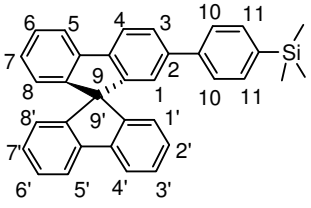

6.44 g (16.29 mmol) 2-bromo-9,9'-spirobifluorene, 3.5 g (18 mmol) 4-trimethysilyl boronic acid, 5 g (2x18 mmol) K_2CO_3 were taken in a pre-heated three necked r.b. flask containing a magnetic stirrer and connected with a pre-heated reflux condenser and a pipette to blow nitrogen gas into the solution for an hour. Then, 50 mL toluene, 150 mL THF and 75 mL

water were added to it (and refluxed stirring at about 70 °C for about an hour). After that, 0.9 g (1.25 mol%) palladium(0)tetrakis(triphenylphosphine) was added in nitrogen gas atmosphere and refluxed at about 68 °C for about 17 hours. The reaction mixture became dark brown. For reaction monitoring, a TLC was done. For complexation and separation of the catalyst metal, about 1 g of KCN was added to the reaction, which was again refluxed for about 2 hours. The mixture became light yellow colour. After letting the mixture cool down, the phases were separated and the aqueous phase was washed with dichloromethane (2 times 50 mL) and all the organic phases were united. They were dried over sodium sulphate and subjected to the rotary evaporator to remove the solvent. The crystals were filtered and washed with *n*-hexane. The mother liquor contained some crystals too, therefore it was transferred into an r.b. flask and the solvent was removed by rotary evaporator.

$C_{34}H_{28}Si$ (464.69 g/mol)

Yield : 5.19 g (11 mmol, 70%), colourless crystal. TLC (CH_2Cl_2:*n*-Hexane;1:2) showed the non fluorescent spot.

^{1}H-NMR (500 MHz; $CDCl_3$) (δ [ppm])

7.90 (d, *J* = 7.96 Hz, 1H, H4), 7.85 (m, 3H, H5, H5', H4'), 7.62 (dd, *J* = 7.95, 1.67 Hz, 1H, H3), 7.49 (m, 2H, H11), 7.43 (m, 5H, H6, H6', H3',H10), 7.10 (m, 3H, H2', H7, H7'), 6.92 (pd, *J* = 1.54 Hz, 1H, H1), 6.76 (dd, *J* = 7.58, 0.66 Hz, 2H, H1', H8'), 6.73 (dd, *J* = 7.48, 0.57 Hz, 1H, H8), 0.22 (s, 9H, -CH_3).

^{13}C-NMR (125.7 MHz; $CDCl_3$) (δ [ppm])

149.47, 149.06, 148.65, 141.74, 141.38, 141.33, 141.04, 140.82, 139.11, 133.59, 127.80, 127.73, 127.69, 126.74, 126.34, 124.11, 124.02, 122.85, 120.22, 120.02 119.95, 65.97, -1.17.

7.2.7 4-(9,9'-Spirobifluorene-2-yl)-phenyl boronic acid (10)

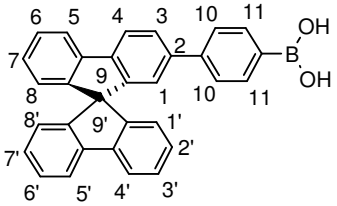

To the -78 °C cooled solution of 2 g (4 mmol) of 2-(4-trimethylsilylphenyl)-9,9'-spirobifluorene in 50 mL dried dichloromethane, provided with a magnetic stirrer, (0.5 mL; 5 mmol; ρ = 2.650) tribromoborane was added dropwise within 15 minutes. The reaction mixture was left stirring at the same temperature for two hours (it seemed to be like paste) and

then let to warm up to room temperature (became dark brown solution) over a period of approximately 3 h, and finally heated to 40 °C for 18 h. The solution was cooled to -78 °C and a solution of KOH in water (10 mL of a ca. 5 M solution) was added in excess. The solution was allowed to warm up to room temperature and the two-phase solution was filtered to remove the potassium salt of 4-trimethylsilylphenyl boronic acid. The wet salt was suspended in a mixture of diethyl ether and 2 M HCl (40 mL of each) and stirred vigorously for 2 h. After this period, two clear layers had formed. The aqueous layer was discarded, and the organic layer was washed with 50 mL of 2 M HCl, followed by distilled water (2 volumes of 40 mL each), and finally washed with brine(sodiumchloride solution) (200 mL). The ethereal solution was dried over $MgSO_4$, and the solvent was removed. An analogous synthesis is explained in Bair et. al. [112]

The product was at first oily and later foam-like solid.

$C_{31}H_{21}BO_2$ (436.32 g/mol)

Yield: 1.22 g (2.79 mmol, 75 %), colourless amorph.

^{1}H-NMR (500 MHz; $CDCl_3$) (δ [ppm])

8.11 (d, *J* = 8.00 Hz, 1H, H4), 8.07-7.99 (m, 3H, H5, H4', H5'), 7.80-7.72 (m, 3H, H3, H10), 7.40 (m, 5H, H6, H3', H6', H11), 7.12 (t, *J* = 7.36, 7.36 Hz, 3H, H7, H2', H7'), 6.83 (pd, *J* = 1.23 Hz, 1H, H1), 6.65 (d, *J* = 7.59 Hz, 2H, H1', H8'), 6.58 (d, *J* = 7.60 Hz, 1H, H8).

^{13}C-NMR (125.7 MHz; $CDCl_3$) (δ [ppm])

149.59, 149.11, 148.53, 141.74, 141.40, 14.12, 139.77, 139.57, 131.60, 128.60, 127.97, 127.861, 127.78, 126.65, 124.08, 124.01, 122.39, 121.31, 120.36, 120.08, 120.02, 65.97.

7.2.8 2-(4-Iodophenyl)-9,9'-spirobifluorene (11)

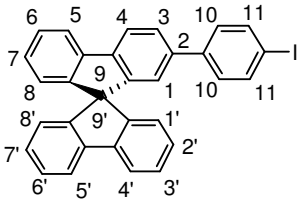

To a solution of 2 g (4 mmol) of 2-(4-trimethylsilylphenyl)-9,9'-spirobifluorene in 50 mL dichloromethane, provided with a magnetic stirrer, one equivalent of iodine monochloride was added dropwise at room temperature. The reaction mixture was left stirring at the same temperature for two hours. The reaction was monitored by TLC. As no trace of reactant was detected any longer, the reaction mixture was washed with aqueous solution of $Na_2S_2O_3$. The

organic phase was separated and dried over Na_2SO_4, then the solvent was removed by rotary evaporator. White amorphous product was obtained which was subjected to recrystallization in chloroform for purification.

$C_{31}H_{19}I$ (518.40 g/mol)

Yield: 1.67 g (3.24 mmol, 81 %), colourless amorph.

^{1}H-NMR (500 MHz; $CDCl_3$) (δ [ppm])

7.87 (d, *J* = 7.98 Hz, 1H, H4), 7.84 (d, *J* = 7.68 Hz, 3H, H5, H4', H5'), 7.60 (m, 2H, H10), 7.55 (dd, *J* = 7.92, 1.61 Hz, 1H, H3), 7.36 (t, *J* = 7.36, 7.36 Hz, 3H, H6, H3', H6'), 7.13 (m, 2H, H11), 7.10 (t, *J* = 7.48, 7.48 Hz, 3H, H2', H7, H7'), 6.87 (d, *J* = 1.57 Hz, 1H, H1), 6.75 (d, *J* = 7.61 Hz, 2H, H1', H8'), 6.71 (d, *J* = 7.64 Hz, 1H, H8).

^{13}C-NMR (125.7 MHz; $CDCl_3$) (δ [ppm])

149.60, 149.12, 148.52, 141.75, 141.47, 141.13, 140.38, 139.63, 137.58, 128.87, 127.98, 127.86, 127.78, 126.60, 124.08, 124.02, 122.36, 120.36, 120.09, 120.02, 92.79, 65.97.

7.2.9 9-(Biphenyl-2-yl)-fluorene-9-ol

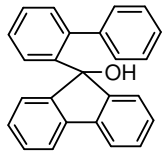

In a 500 mL three necked r. b. flask provided with reflux condenser, N_2 gas storm, dropping funnel and a magnet stirrer, 1.7 g (70.0 mmol) magnesium (activated by adding some crystals of iodine overnight), were dissolved in 20 mL absolute THF. 16.0 g (69.0 mmol) 2-bromobiphenyl was added dropwise from the dropping funnel in such a way that the solution boiled itself. Then, to complete the reaction, the mixture was refluxed for 2 h and 180 mL THF were added to dissolve the formed Grignard reagent into the solution. The clear hot Grignard-solution was decanted into a 1 L three necked r. b. flask provided with reflux condenser and magnet stirrer to separate from the unsubstituted magnesium. To the cooled Grignard-solution, a solution of 12.3 g (68.0 mmol) fluorenone in 100 mL THF was added dropwise within 30 minutes. Finally, the mixture was refluxed for 2 h and left stirring at room temperature overnight. From the yellow solution, white solid product was formed which was filtered off and washed with THF (2 x 60 mL). The white solid was treated with 200 mL ice cooled ammoniumchloride solution. The aqueous phase was extracted firstly with 100 mL and then 4 times with 50 mL chloroform. The organic phases were united and washed with 100

mL destilled water. It was then dried over Na_2SO_4 and then the solvent was removed by rotary evaporator. The paste-like white solid was treated with 100 mL *n*-hexane, filtered and dried in vacuum at 60 °C.

$C_{25}H_{18}O$ (334.42 g/mmol)

Yield: 15.5 g (46.4 mmol, 68 %), white powder.

^{1}H-NMR (500 MHz; $CDCl_3$) (δ [ppm])

8.45 (d, *J* = 7.99 Hz, 1H), 7.53 (dt, *J* = 7.63, 1.27 Hz, 1H), 7.30 (dt, *J* = 7.08, 1.27 Hz, 1H), 7.15 (m, 8H), 6.90 (dd, *J* = 7.45, 1.45 Hz, 1H), 6.80 (tt, *J* = 7.45, 1.27 Hz, 1H), 6.60 (tt, *J* = 7.90, 1.27 Hz, 2H), 6.0 (d, *J* = 8.36 Hz, 2H).

^{13}C-NMR (125.7 MHz; $CDCl_3$) (δ [ppm])

151.30, 141.73, 141.08, 140.93, 140.37, 132.02, 129.59, 129.40, 128.63, 127.87, 127.61, 126.98, 126.83, 125.82, 125.07, 120.81, 83.19.

7.2.10 9,9'-Spirobifluorene (4)

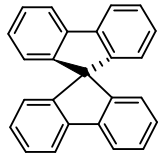

In a 100 mL r. b. flask, 12.0 g (36 mmol) 9-(biphenyl-2-yl)-fluorene-9-ol was dissolved in 30 mL 98% acetic acid and refluxed by stirring. The clear solution was treated with 0.5 mL conc. HCl, whereafter white solid product was formed. After refluxing for 10 minutes, the solution was allowed to cool to room temperature. It was then filtered and treated with distilled water which resulted some more product precipitating. The united solids were dried in vacuum.

$C_{25}H_{16}$ (316.41 g/mol)

Yield: 11.2 g (35.0 mmol, 98 %), white powder.

^{1}H-NMR (500 MHz; $CDCl_3$) (δ [ppm])

7.86 (dd, *J* = 7.62, 1.08, 0.77 Hz, 4H), 7.38 (dt, *J* = 7.51, 1.09 Hz, 4H), 7.11 (dt, *J* =7.51, 1.15 Hz, 4H), 6.75 (ddd, *J* = 7.59, 1.01, 0.76 Hz, 4H).

^{13}C-NMR (125.7 MHz; $CDCl_3$) (δ [ppm])

148.78, 141.77, 127.80, 127.68, 124.03, 119.95, 65.97.

7.2.11 2,2',7,7'-Tetrabromo-9,9'-spirobifluorene (17)

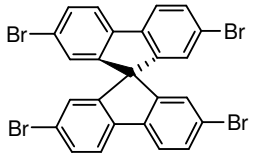

To a solution of 500 mg (1.58 mmol) 9,9'-spirobifluorene in 10 mL DCM in a 50 mL two necked r. b. flask connected with a reflux condenser, dropping funnel and magnet stirrer, 1.55 g (9.69 mmol) bromine was added dropwise. After refluxing for 80 h, about 20 mL DCM were added to dissolve the formed solid product. Finally, the solution was extracted with saturated solutions of Na_2SO_3, $NaHCO_3$ and water, then the organic phase was dried over Na_2SO_4 and then the solvent was removed by rotary evaporator. The product was dissolved in THF and precipitated by adding MeOH.

$C_{25}H_{12}Br_4$ (631.99 g/mol)

Yield: 0.902 g (1.43 mmol, 91 %), white amorph.

^{1}H-NMR (500 MHz; $CDCl_3$) (δ [ppm])

7.68 (d, *J* = 8.28 Hz, 4x1H), 7.53 (dd, *J* = 8.04, 1.76 Hz, 4x1H), 6.83 (d, *J* = 1.76 Hz, 4x1H).

7.2.12 2,2',7,7'-Tetrakis[4-(9,9'-spirobifluorene-2-yl)-phenyl]-9,9'-spirobifluorene (18)

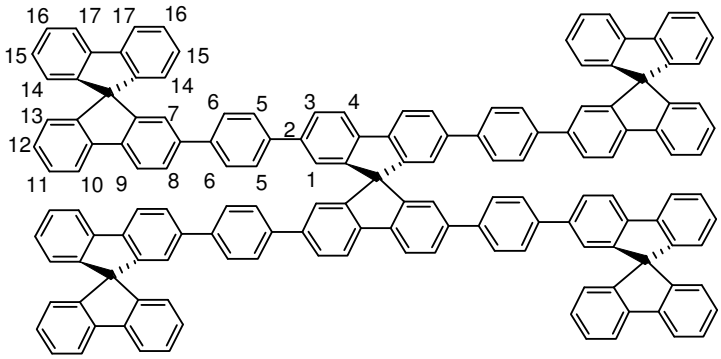

In a Young flask, containing a magnetic stirrer, 0.111 g (0.177 mmol) 2,2';7,7'-tetrabromo-9,9'-spirobifluorene, 0.74 g (1.42 mmol) 4-(9,9'-spirobifluorene-2-yl)-phenyl boronic acid and 0.20 g (1.42 mmol) K_2CO_3 were taken. Then, 15 mL toluene, 10 mL THF and 5 mL water were added to it. A pipette was dipped into the mixture to blow nitrogen gas into the solution for an hour. After that, 0.26 g (16 mol%) palladium(0)tetrakis(triphenylphosphine) was added in nitrogen gas atmosphere and then the flask was evacuated and refluxed at 80 °C for about

17 hours. The reaction mixture remained light yellow as it was in the beginning, indicating that the catalyst was not destroyed by air contamination. The reaction was monitored by TLC. For complexation and separation of the catalyst metal, about 1 g of KCN was added to the reaction and again stirred the mixture for about 2 hours. The mixture became colourless. Organic and aqueous phases were separated and the aqueous phase was washed with dichloromethane (2 times 50 mL) and all the organic phases were united. They were dried over sodium sulphate and subjected to the rotary evaporator to remove the solvent. Purification of the product was followed by column chromatography with DCM/*n*-hexane eluant.

$C_{149}H_{88}$ (1878.36 g/mol)

Yield: 0.26 g (0.14 mmol, 79 %) colourless amorph.

^{1}H-NMR (500 MHz; $CDCl_3$) (δ [ppm])

7.85-7.81 (m, 4x5H), 7.56-7.49 (m, 4x2H), 7.38-7.26 (m, 4x7H), 7.12-7.02 (m, 4x3H), 6.92 (pd, *J* = 1.26, 4x1H), 6.86 (pd, *J* = 1.25, 4x1H), 6.73-6.70 (m, 4x3H).

^{13}C-NMR (125.7 MHz; $CDCl_3$) (δ [ppm])

149.73, 149.33, 148.89, 142.03, 142.02, 142.01, 141.99, 141.61, 141.28, 141.26, 140.90, 140.63, 140.54, 139.95, 128.15, 128.13, 128.08, 128.00, 127.97, 127.45, 127.43, 127.41, 126.88, 124.36, 124.27, 122.79, 120.48, 120.27, 120.22, 66.12, 66.23.

Elemental Analysis:	Found (%)	Calculated (%)
	C: 94.32	C: 95.28
	H: 4.93	H: 4.72

7.2.13 2,2',7,7'-Tetrakis(4''-trimethylsilyl-phenyl-1-yl)-9,9'-spirobifluorene (19)

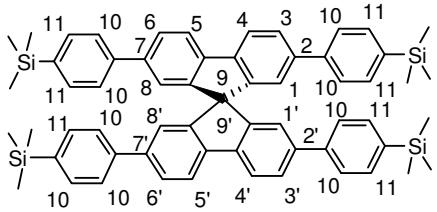

From 1.35 g (2.14 mmol) 2,2',7,7'-tetrabromo-9,9'-spirobifluorene, 2.00 g (10.30 mmol) 4-trimethylsilylphenyl boronic acid, 2.37 g (17.16 mmol) K_2CO_3 and 0.95 g (16 mol%) palladium(0)tetrakis-(triphenylphosphine), the expected product was synthesized according to procedure **7.2.12**.

$C_{61}H_{64}Si_4$ (909.53 g/mol)

Yield: 1.40 g (1.54 mmol, 90 %), colourless crystal.

MS (MALDI): *m/z* (%) = 908.39 (100) [M^+].

^{1}H-NMR (500 MHz; $CDCl_3$) (δ [ppm])

7.91 (d, *J* = 7.90 Hz, 4H, H4, H4', H5, H5'), 7.6 (d, *J* = 7.95, 4H, H3, H3', H6, H6'), 7.49-7.37 (m, 16H, H10, H11), 6.99 (s, 4H, H1, H1', H8, H8'), 0.20 (s, 36H, -CH_3).

^{13}C-NMR (125.7 MHz; $CDCl_3$) (δ [ppm])

149.64, 141.37, 140.95, 140.71, 139.10, 133.79, 133.58, 128.72, 127.29, 127.14, 126.94, 126.41, 123.02, 120.32, 66.12, -1.17.

7.2.14 2,2',7,7'-Tetrakis(4-iodophenyl)-9,9'-spirobifluorene (20)

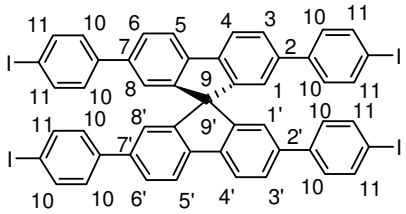

From 0.20 g (0.22 mmol) of 2,2',7,7'-tetrakis(4-trimethylsilylphenyl)-9,9'-spirobifluorene, 050 g (1.05 mmole) of iodine monochloride, the expected product was synthesized according to procedure **7.2.8**.

$C_{49}H_{28}I_4$ (1124.39 g/mol)

Yield: 0.17 g (0.15 mmol, 70 %), colourless crystal.

MS (MALDI): *m/z* (%) = 1123.81 (100) [M^+].

^{1}H-NMR (500 MHz; $CDCl_3$) (δ [ppm])

7.92 (d, *J* = 7.92 Hz, 4H, H4, H4', H5, H5'), 7.66-7.56 (m, 12H, H3, H3', H6, H6', H10), 7.19-7.12 (m, 8H, H11), 6.91 (s, 4H, H1, H1', H8, H8').

7.2.15 2,2',7,7'-Tetrakis[(9,9´-spirobifluorene-2-yl)-4,1'-biphenyl-4'-yl]-9,9'-spirobifluorene (21)

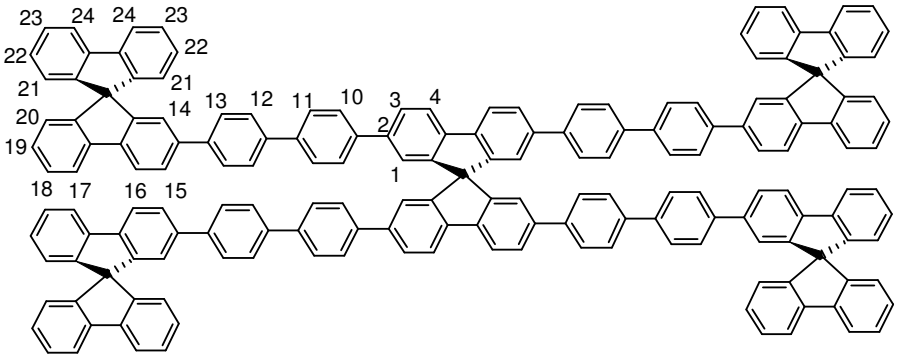

In a Young flask, containing a magnetic stirrer, 0.07 g (0.06 mmol) 2,2',7,7'-tetraiodo-9,9'-spirobifluorene, 0.13 g (0.29 mmol) 4-(9,9'-spirobifluorene-2-yl)-phenyl boronic acid, 0.07 g (0.48 mmol) K_2CO_3 were taken. Then, 45 mL toluene, 30 mL THF and 15 mL water were added to it. A pipette was dipped into the mixture to blow nitrogen gas into the solution for an hour. After that, 0.05 g (16 mol%) palladium(0)tetrakis(triphenylphosphine) was added in nitrogen gas atmosphere and then the flask was evacuated and refluxed at 70 ^{o}C for about 34 hours. Rest of the workout was followed as in **7.2.12**.

$C_{173}H_{104}$ (2182.76 g/mol)

Yield: 0.045 g (0.02 mmol, 35 %), white amorph.

MS (MALDI): *m/z* (%) = 2180.71 (100) [M^+].

^{1}H-NMR (500 MHz; NMP:$CDCl_3$; 3:2) (δ [ppm])

7.91 (d, *J* = 7.78 Hz, 4X1H, H4), 7.88 (d, *J* = 7.91 Hz, 4X1H, H16), 7.84-7.82 (m, 4X3H, H17, H24), 7.68-7.32 (m, 4X13H, H3, H15, H13, H12,H11, H18, H23, H10), 7.13-7.06 (m, 4X3H, H19, H22), 7.02 (s, 4X1H, H1), 6.92 (s, 4X1H, H14), 6.75 (dd, *J* = 7.94, 4.08 Hz, 4X2H, H21), 6.71 (d, *J* = 7.71 Hz, 4X1H, H20).

^{13}C-NMR (125.7 MHz; NMP:$CDCl_3$; 3:2) (δ [ppm])

149.51, 149.08, 148.63, 141.76, 141.75, 141.73, 141.34, 141.32, 141.07, 140.45, 140.27, 140.26, 139.81, 139.37, 139.33, 132.12, 132.04, 131.94, 128.53, 128.43, 127.82, 127.73, 127.70, 127.40, 127.34, 127.08, 126.62, 124.12, 124.10, 124.01, 122.56, 120.27, 120.02, 119.97, 65.97.

Elemental Analysis:	Found (%)	Calculated (%)
	C: 92.89	C: 95.20
	H: 4.97	H: 4.80

7.2.16 2,7-Dibromofluorene-9-one (23)

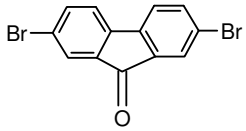

In a three necked 1 L r. b. flask with a stirrer, a dropping funnel and a reflux condenser, 32.43 g (0.18 mol) fluorenone, 800 mL water, few drops of surfactant and sulfuric acid were placed and stirred to mix. By adding 21.20 mL (0.414 mol) bromine into the mixture, the reaction was started. After the reaction had been conducted at 94 °C for 24 h, unreacted bromine was decomposed with an aqueous solution of sodium hydrogen sulfite. The reaction product, which was a dark yellow solid, was filtered off. The crude product was dissolved in toluene and was subsequently washed with water and a sodium hydrogencarbonate aqueous solution. The organic phase was dried using anhydrous magnesium sulfate. After filtration, the liquid was concentrated and then allowed to stand at 0 °C. A yellow solid precipitated. The precipitate was filtered and subsequently washed with toluene, followed by drying. Thus a yellow solid product was obtained which was purified by crystallization from conc. acetic acid (700 mL)

$C_{13}H_6Br_2O$ (338.00 g/mol)
Yield: 37.65 g (0.11 mol, 60 %), yellow crystal.
^{1}H-NMR (500 MHz; $CDCl_3$) (δ [ppm])
7.74 (pd, *J* = 1.80 Hz, 2H), 7.60 (dd, *J* = 7.91, 1.85 Hz, 2H), 7.36 (d, *J* = 7.91 Hz, 2H).
^{13}C-NMR (125.7 MHz; $CDCl_3$) (δ [ppm])
190.93, 142.23, 137.45, 135.23, 127.82, 123.28, 121.82.

7.2.17 2,7-Dibromo-9,9'-spirobifluorene (24)

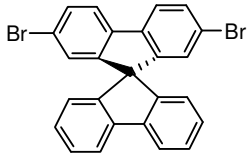

From 22.5 g (96.50 mmol) 2-bromobiphenyl, 4.70 g (193 mmol) magnesium and 32.62 g (96.50 mmol) 2,7-dibromofluorene-9-one, the expected product was synthesized according to procedure **7.2.2**.

$C_{25}H_{14}Br_2$ (474.20 g/mol)

Yield: 25.6 g (54.04 mmol, 56 %), white amorph.

Melting point: 336 °C.

^{1}H-NMR (500 MHz; $CDCl_3$) (δ [ppm])

7.83 (d, *J* = 7.66 Hz, 2H), 7.65 (d, *J* = 8.16 Hz, 2H), 7.47 (dd, *J* = 8.16, 1.81 Hz, 2H), 7.39 (t, *J* = 7.47, 7.47 Hz, 2H), 7.13 (t, *J* = 7.49, 7.49 Hz, 2H), 6.82 (pd, *J* = 1.78 Hz, 2H), 6.70 (d, *J* = 7.59 Hz, 2H).

^{13}C-NMR (125.7 MHz; $CDCl_3$) (δ [ppm])

150.55, 147.06, 141.70, 139.64, 131.13, 128.29, 128.09, 127.34, 124.05, 121.89, 121.39, 120.28, 65.61.

IR (ATR) $\bar{\nu}$ (cm^{-1}) = 3057, 3014, 1598, 1571, 1443, 1401, 1250, 1169, 1119, 1061, 1007, 949, 872, 857, 807, 753, 729, 668, 633.

7.2.18 2,7-Dibromo-2'-nitro-9,9'-spirobifluorene (25)[53]

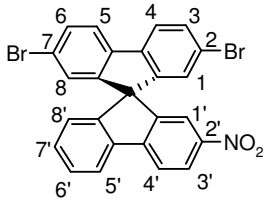

In a 100 mL three necked r. b. flask, fitted with a reflux condenser the 14.73 g (32.19 mmol) 2,7-dibromo spirobifluorene was dissolved and 5 mL (67.6 mmol) thionyl chloride was added. Then, 14.78 g (8.06 mmol) bismuth subnitrate (79 %) was added to the mixture. The reaction mixture became yellow. After 2 hours, TLC was done with dichloromethane:*n*-hexane (1:1). It showed the formation of product with some still reactant remaining. It was left to stir overnight, still showed remaining reactant. Then it was refluxed for 1 hour, but still some reactant was left. The reaction mixture was filtered to remove inorganic precipitates. The residue seemed to contain the expected product too, but was only sparingly soluble in CH_2Cl_2. The filtrate was washed with dilute HCl and then with water. The organic phase was dried with Na_2SO_4 and the solvent was removed by rotary evaporator. A column chromatography was carried out for purification. An analogous synthesis is explained in Muathen et. al. [53]

$C_{25}H_{13}Br_2NO_2$ (519.20 g/mol)

Yield: 7.65 g (14.74 mmol, 77 %), yellow crystal.

MS (MALDI): *m/z* (%) = 519.24 (100) [M^+].

^{1}H-NMR (500 MHz; NMP:$CDCl_3$; 3:2) (δ [ppm])

8.31 (dd, *J* = 8.44, 2.10 Hz, 1H, H3'), 7.94 (d, *J* = 8.43 Hz, 1H, H4'), 7.92 (d, *J* = 7.69 Hz, 1H, H5'), 7.70 (d, *J* = 8.18 Hz, 2H, H4, H5), 7.57-7.50 (m, 3H, H3, H6, H1'), 7.47 (t, *J* = 7.49, 7.49 Hz, 1H, H6'), 7.27 (t, *J* = 7.54, 7.54 Hz, 1H, H7'), 6.79-6.78 (m, 3H, H1, H8, H8').

^{13}C-NMR ($CDCl_3$) (δ [ppm])

148.57, 148.52, 148.48, 147.88, 14.62, 139.74, 139.20, 131.80, 130.27, 128.92, 127.14, 124.55, 124.49, 122.13, 121.81, 121.66, 120.48, 119.68, 65.34.

7.2.19 Phenylboronic acid (26)

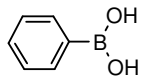

To a suspension of 5.35 g (220 mmol) magnesium in 110 mL THF, a solution of 31.4 g (200 mmol) bromobenzene in 110 mL THF was added dropwise. After complete addition of the mixture, the reaction mixture was refluxed for about 6 hours. Then it was cooled down to 0 °C. The cooled solution was added dropwise via a thin channel to the -78 °C cooled solution of 24.94 g (240 mmol) trimethylborate in 140 mL THF (1M). It was left to warm up to room temperature and stirred overnight (20 h). The reaction was quenched with the addition of 300 mL 1N HCl. It was left to stir for 2 h at RT and at the end extracted with ethylacetate, washed with dilute NaHCO3 solution, dried, filtered and the solvent was removed by rotary evaporator. Finally, it was recrystallized from toluene.

$C_6H_7BO_2$ (121.93 g/mol)

Yield: 17.31 g (142 mmol, 71 %), white powder.

^{1}H-NMR (500 MHz; NMP:$CDCl_3$; 3:2) (δ [ppm])

8.24 (d, *J* = 7.83 Hz, 2H), 7.60-7.57 (m, 1H), 7.52-7.49 (m, 2H).

^{13}C-NMR ($CDCl_3$) (δ [ppm])

135.61, 132.67, 127.95.

7.2.20 2,7-Diphenyl-2'-nitro-9,9'-spirobifluorene (27)

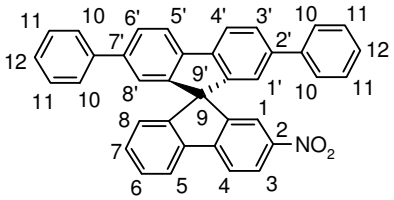

In a two necked flask, one neck with a screw cap and the next neck to allow the stream of inert gas (N_2 or Ar) containing a magnetic stirrer, 5.00 g (0.63 mmol) 2,7-dibromo-2'-nitro-9,9'-spirobifluorene, 3.52 g (28.89 mmol) phenylboronic acid, 19.96 g (144.45 mmol) K_2CO_3 were taken. Then, 85 mL toluene, 50 mL THF and 35 mL water were added to it. A pipette was dipped into the mixture to blow nitrogen gas into the solution for an hour. After that, 2.00 g (6 mol%) palladium(0)tetrakis-(triphenylphosphine) was added in nitrogen gas atmosphere and then the flask was evacuated and refluxed at 80 °C for about 17 hours in the nitrogen gas atmosphere. Rest of the workout was followed as in **7.2.12**.

$C_{37}H_{23}NO_2$ (513.60 g/mol)

Yield: 87 %, white amorph.

MS (MALDI): *m/z* (%) = 513.47 (100) [M^+].

^{1}H-NMR (500 MHz; $CDCl_3$) (δ [ppm])

8.30 (d, *J* = 8.53 Hz, 1H, H3), 7.96-7.93 (m, 4H, H4, H5, H4', H5'), 7.71-7.62 (m, 3H, H1, H3', H6'), 7.49-7.37 (m, 5H, H6, H10), 7.31 (t, *J* = 7.52, 7.52 Hz, 4H, H11), 7.24-7.22 (m, 3H, H7,H12), 6.90-6.89 (m, 3H, H8,H1',H8').

^{13}C-NMR (125.7 MHz; $CDCl_3$) (δ [ppm])

150.24, 150.14, 148.10, 147.78, 147.57, 141.29, 140.70, 140.65, 139.28, 130.09, 128.63, 128.41, 127.58, 127.31, 127.00, 124.67, 124.09, 122.48, 121.43, 120.74, 120.24, 119.85, 65.91.

Crystal data and structure refinement for i0186 (MDS0118)

Identification code	i0186	
Empirical formula	$C_{37}H_{23}NO_2$	
Formula weight	513.56	
Temperature	153(2) K	
Wavelength	0.71073 A	
Crystal system	monoclinic	
Space group	P 21/c	
Unit cell dimensions	a = 15.2874(11) A	alpha = 90°
	b = 29.8888(13) A	beta = 108.029(5)°
	c = 14.0229(9) A	gamma = 90°
Volume	6092.8(6) A^3	
Z	8	
Density (calculated)	1.120 Mg/m^3	
Absorption coefficient	0.069 mm^{-1}	
F(000)	2144	
Theta range for data collection	1.36 to 25.00°	
Index ranges	-18<=h<=18, -33<=k<=35, -16<=l<=16	
Reflections collected	39312	
Independent reflections	10729 [R(int) = 0.0540]	

Reflections observed	6119
Refinement method	Full-matrix least-squares on F^2
Data / restraints / parameters	10729 / 0 / 721
Goodness-of-fit on F^2	1.068
Final R indices [I>2sigma(I)]	R1 = 0.0990, wR2 = 0.2897
R indices (all data)	R1 = 0.1426, wR2 = 0.3164
Largest diff. peak and hole	2.458 and -0.417 e.A^{-3}

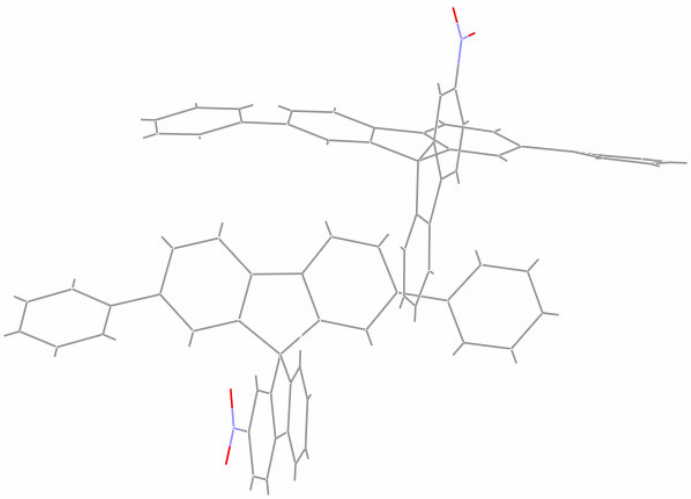

7.2.21 2',7'-Diphenyl-9,9'-spirobifluorene-2-yl amine (29)

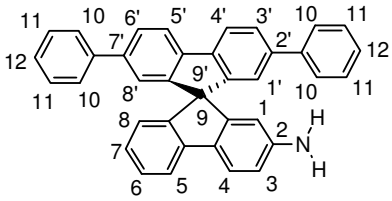

In a 250 mL three necked r. b. flask, connected with a dropping funnel, reflux condenser, and a magnet stirrer, 0.66 g (1.3 mmol) 2-nitro-2',7'-diphenyl-9,9'-spirobifluorene was added to 50 mL ethanol in nitrogen gas atmosphere and stirred. As the reactant was not completely soluble in ethanol, the whole system was kept in an ultrasonic bath and the temperature was controlled not to exceed 50 °C. As the solution became transparent, 500 mg activated carbon (palladium/carbon) suspended in 5 mL of ethanol were added. It was then refluxed for 30 minutes and 10 mL of hydrazine hydrate were added within 10 minutes. After 1h, a transparent solution of the amine was formed which was left to stir overnight at room temperature in N_2 atmosphere. The amine precipitated and was dissolved again by warming

the solution. The mixture was filtered through a layer of about 2 cm celite in N_2 atmosphere to separate the Pd/C. The celite was washed 2 times with warm ethanol. Filtrates were united and the solvent was removed by rotary evaporator which yielded the product as colourless crystals.

$C_{37}H_{25}N$ (483.62 g/mol)

Yield: 0.44 g (0.91 mmol, 78 %), colourless crystal.

MS (MALDI): *m/z* (%) = 483.32 (100) [M^+].

^{1}H-NMR (500 MHz; $CDCl_3$) (δ [ppm])

7.91 (d, *J* = 7.91 Hz, 2H, H4', H5'), 7.71 (d, *J* = 7.63 Hz, 1H, H5), 7.63 (dd, *J* = 7.91, 1.67 Hz, 3H, H6, H3', H6'), 7.45 (d, *J* = 7.86 Hz, 4H, H10), 7.32 (t, *J* = 7.56, 7.56 Hz, 5H, H11, H7), 7.28-7.21 (m, 2H, H12), 7.01- 6.99 (m, 3H, H8, H1', H8'), 6.76 (d, *J* = 7.57 Hz, 1H, H4), 6.67 (dd, *J* = 8.14, 2.02 Hz, 1H, H3), 6.12 (d, *J* = 1.73 Hz, 1H, H1), 3.53 (d, *J* = 0.46 Hz, 2H, -NH_2).

^{13}C-NMR (125.7 MHz; $CDCl_3$) (δ [ppm])

150.42, 150.30, 147.65, 146.50, 142.31, 140.85, 140.81, 140.46, 132.72, 128.53, 127.62, 127.09, 127.01, 126.75, 126.12, 123.95, 122.81, 120.84, 120.16, 118.67, 114.75, 110.68, 65.86.

7.2.22 2-(3,3-Diethyltriazenyl)-2',7'-diphenyl-9,9'-spirobifluorene (30)[79]

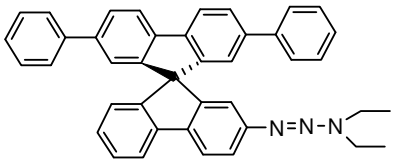

To a flask charged with 0.63 g (1.30 mmol) 2',7'-diphenyl-9,9'-spirobifluorene-2-amine, 1.69 mL conc. HCl and 10 mL H_2O were added. To this mixture, cooled with an ice bath and stirred, a solution of 0.76 g (11.04 mmol) sodium nitrite in 4 mL H_2O was added dropwise. The reaction mixture was allowed to stir at 0 °C for 30 min., transferred into a solution containing 0.07 g (0.49 mmol) K_2CO_3, Et_2NH, 58.60 mL acetonitrile and 9 mL H_2O and the mixture was cooled in an ice bath. The reaction mixture was then stirred for 30 min at room temperature. 125 mL H_2O were added supplementary. The precipitate was a heterogeneous brown mixture. The aqueous phase was discarded and the brown mass was dried in rotary evaporator. However, the crude product was subjected to the following reaction. An analogous synthesis is explained in Peng et. al. [79]

$C_{41}H_{35}N_3$ (569.76 g/mol)

7.2.23 2-Iodo-2',7'-diphenyl-9,9'-spirobifluorene (31)

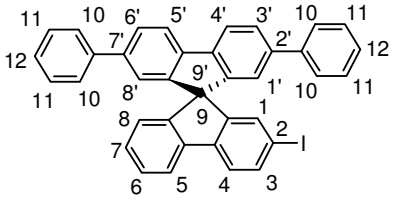

A sealed tube was charged with crude 2-(3,3-diethyltriazenyl 2,7-diphenyl-9,9'-spirobifluorene and 2.3 mL (37.62 mmol) methyl iodide. The mixture was cooled in liquid nitrogen, degassed with nitrogen and heated to 120 °C in an oil bath for 5 h. The residue was purified by column chromatography using dichloromethane and *n*-hexane (1:1) as eluent to afford the product as a white solid. An analogous synthesis is explained in Peng et. al. [79]

$C_{37}H_{23}I$ (594.50 g/mol)

Yield: 0.13 g (0.22 mmol, 20 %), white amorph.

MS (MALDI): *m/z* (%) = 594.68 (100) [M^+].

^{1}H-NMR (500 MHz; $CDCl_3$) (δ [ppm])

7.91 (d, *J* = 7.96 Hz, 2H, H3', H6'), 7.82 (d, *J* = 7.66 Hz, 1H, H3), 7.69 (d, *J* = 8.01 Hz, 1H, H5), 7.63 (d, *J* = 7.87, 2H, H4', H5'), 7.59 (d, *J* = 8.03 Hz, 1H, H4), 7.43 (d, *J* = 7.48 Hz, 4H, H10), 7.37 (t, *J* = 7.61, 7.61 Hz, 1H, H7), 7.31 (t, *J* = 7.58, 7.58 Hz, 4H, H11), 7.27-7.21 (m, 2H, H12), 7.17-7.10 (m, 2H, H1, H6), 6.91 (s, 2H, H1', H8'), 6.79 (d, *J* = 7.47 Hz, 1H, H8)

^{13}C-NMR (125.7 MHz; $CDCl_3$) (δ [ppm])

140.89, 140.87, 140.49, 128.54, 127.66, 127.11, 127.05, 126.81, 123.98, 122.82, 120.89, 120.20, 118.82, 92.45, 62.77.

7.2.24 2,2',7,7'-Tetrakis (pinacol)-9,9'-spirobifluorenyl tetraboronate (32)

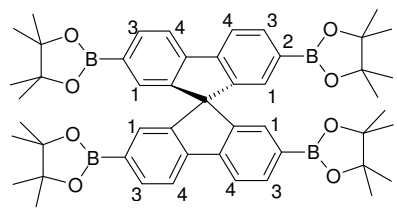

In a three necked 100 mL r. b. flask provided with a magnetic stirrer and a reflux condenser, 2.0 g (3.16 mmol) 2,2',7,7'-tetrabromo-9,9'-spirobifluorene, 3.85 g (15.17 mmol) bis(pinacolato)diboron, 0.063 g (0.23 mmol) tricyclohexyl phosphane and 1.86 g (18.96 mmol) water-free KOAc base were dissolved in 20 mL absolute dioxane. The catalyst 0.043 g (1.5 mol%) tris(dibezylideneacetone)dipalladium(0) ($C_{51}H_{42}O_3Pd_2$ MP=135°C) was added to it in nitrogen gas atmosphere. At first, the reaction mixture turned into violet colour. After heating at about 71 °C for about 20 minutes, it turned into gray color. The reaction mixture was stirred for about half an hour and was refluxed at 80 °C over night. The mixture was poured to a r. b. flask and the solvent was removed from the rotary evaporator and dissolved in CH_2Cl_2. It was then extracted through silica gel (celit on the top) with ethyl acetate and dichloromethane (1:1) as eluent. The solvent was removed and the residue was recrystallized from dichloromethane and hexane. An analogous synthesis is explained in Ishiyama et. al. [81]

$C_{49}H_{60}B_4O_8$ (820.26 g/mol)

Yield: 2.54 g (3.09 mmol, 98 %), colourless amorph.

MS (MALDI): *m/z* (%) = 820.28 (100) [M^+].

^{1}**H-NMR** (500 MHz; $CDCl_3$) (δ [ppm])

7.92-7.77 (m, 8H, H3, H4), 7.08 (s, 4H, H4), 1.2 (s, 48H, -CH_3).

^{13}**C-NMR** (125.7 MHz; $CDCl_3$) (δ [ppm])

148.16, 144.67, 134.53, 130.43, 128.83, 119.66, 83.64, 65.85, 24.78.

7.2.25 2,2',7,7'-Tetrakis(2',7'-diphenyl-9,9'-spirobifluorene-2-yl)-9,9'-spirobifluorene (33)

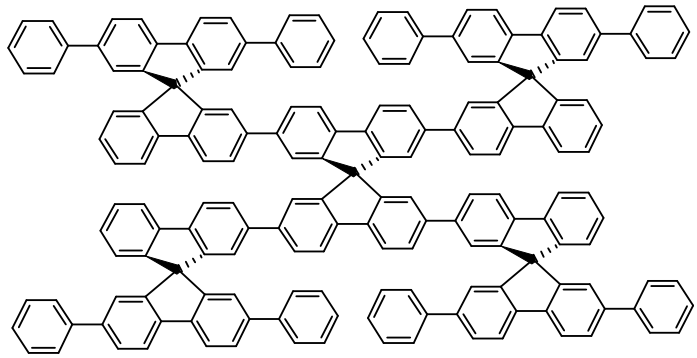

In a two necked flask, one neck with a screw cap and the next neck to allow the stream of inert gas (N_2 or Ar) containing a magnetic stirrer, 0.23 g (0.28 mmol) 2,2',7,7'-

tetrakis(boronic pinacolate)-9,9'-spirobifluorene, 0.80 g (1.34 mmol) 2',7'-diphenyl-2-iodo-9,9'-spirobifluorene, 2.22 g (16.08 mmol) K_2CO_3 were taken. Then, 25 mL toluene, 40 mL THF and 20 mL water were added to it. A pipette was dipped into the mixture to blow nitrogen gas into the solution for an hour. After that, 0.25 g (0.21 mmol) palladium(0)tetrakis(triphenylphosphine) was added in nitrogen gas atmosphere and then the flask was evacuated and refluxed at 70 °C for about 18 hours. Rest of the workout was followed as in **7.2.12**.

$C_{173}H_{104}$ (2182.76 g/mol)

Yield: 0.53 g (0.24 mmol, 87 %), white amorph.

MS (MALDI): *m/z* (%) = 2180.78 (100) [M^+].

^{1}**H-NMR** (500 MHz; $CDCl_3$) (δ [ppm])

7.85 (d, *J* = 7.95 Hz, 4x2H), 7.76 (d, *J* = 7.68 Hz, 4x1H), 7.64 (d, *J* = 8.01 Hz, 4x2H), 7.57 (dd, *J* = 7.96, 1.59 Hz, 4x2H), 7.42-7.29 (m, 4x6H), 7.29-7.21 (m, 4x5H), 7.21-7.14 (m, 4x2H), 7.07 (t, *J* = 7.47, 7.47 Hz, 4x1H), 6.93 (d, *J* = 1.23 Hz, 4x1H), 6.88 (d, *J* = 1.53 Hz, 4x2H), 6.79 (d, *J* = 1.20 Hz, 4x1H), 6.74 (d, *J* = 7.66 Hz, 4x1H).

^{13}**C-NMR** (125.7 MHz; $CDCl_3$) (δ [ppm])

149.64, 149.39, 149.13, 148.84, 141.19, 140.89, 140.81, 140.76, 140.58, 140.54, 140.39, 128.49, 127.75, 127.65, 127.26, 127.15, 127.05, 126.99, 126.88, 124.01, 122.72, 122.67, 122.42, 122.32, 120.26, 120.06, 120.04, 119.95, 66.17, 66.07.

Elemental Analysis: Found (%)	Calculated (%)
C: 94.81	C: 95.20
H: 5.16	H: 4.80

7.2.26 2-Acetyl-2',7'-dibromo-9,9'-spirobifluorene (34)

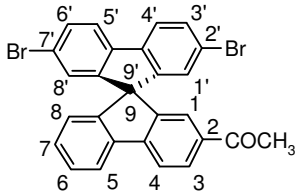

A 500 mL three necked r. b. flask provided with 8 g (16.9 mmol) 2,7-dibromo-9,9'-spirobifluorene was connected with a reflux condenser, a gas outlet, a KPG-stirrer and a dropping funnel. The compound was dissolved in 100 mL carbon disulphide solution. 4.3 g (32.2 mmol) aluminium chloride was added to it then a solution of 1.3 g (16.9 mmol) acetyl

chloride in 10 mL carbon disulphide was added drop wise to the reaction mixture within 0.5 h. After the complete addition, the mixture was refluxed for 1.5 h. At the end, the solvent was removed by rotary evaporator. The black residue was hydrolysed in 300 mL ice water/HCl overnight then the precipitate was separated. The raw product was dissolved in 20 mL dichloromethane and a column chromatography was carried out in silica gel using dichloromethane as eluent.

$C_{27}H_{16}Br_2O$ (516.24 g/mol)

Yield: 6.35 g (12.30 mmol, 73 %), white amorph.

MS (MALDI): *m/z* (%) = 516.11 (100) [M^+].

^{1}H-NMR (500 MHz;$CDCl_3$) (δ [ppm])

8.03 (dd, *J* = 8.09, 1.54 Hz, 1H, H3), 7.91 (m, 2H, H4, H5), 7.69 (d, *J* = 8.17 Hz, 2H, H4', H5'), 7.51 (dd, *J* = 8.17, 1.82 Hz, 2H, H3', H6'), 7.44 (td, *J* =7.45, 0.72 Hz, 1H, H6), 7.32 (d, *J* = 1.45 Hz, 1H, H8), 7.22 (td, *J* = 7.45, 0.90 Hz, 1H, H7), 6.80 (d, *J* = 1.81 Hz, 2H, H1', H8'), 6.75 (d, *J* = 7.63 Hz, 1H, H1), 2.50 (s, 3H, -CH_3).

^{13}C-NMR (125.7 MHz; $CDCl_3$) (δ [ppm])

197.40, 149.57, 148.36, 147.57, 146.39, 140.27, 139.76, 136.88, 131.43, 129.45, 128.59, 127.24, 124.27, 123.87, 121.99, 121.64, 121.24, 120.16, 65.48, 26.72.

IR (ATR) $\bar{\nu}$ (cm^{-1}) = 3057, 2972, 1740, 1682, 1667, 1605, 1574, 1455, 1416, 1355, 1281, 1258, 1216, 1170, 1127, 1061, 1007, 949, 872, 826, 803, 760, 733, 695, 675, 664, 613, 513.

7.2.27 2-Acetoxy-2',7'-dibromo-9,9'-spirobifluorene (35)

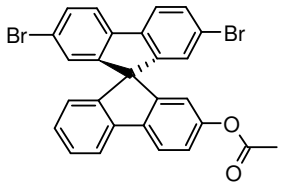

A solution of 1.24 g (2.4 mmol) 2-acetyl-2',7'-dibromo-9,9'-spirobifluorene and 0.83 g (4.8 mmol) 3-chloroperbenzoic acid (MCPBA) in 29 mL chloroform was stirred for 72 h in dark. The reaction mixture was washed with 20% NaOH solution, 2N $NaHCO_3$ solution and finally with water. It was then dried over sodium sulphate and subjected to the rotary evaporator to remove the solvent. Purification of the product was followed by recrystallization (CH_2Cl_2/hexane). An analogous synthesis is explained in Diederich et al [84].

$C_{27}H_{16}Br_2O_2$ (532.24 g/mol)

Yield: 0.93 g (1.75 mmol, 73%), white amorph.

MS (MALDI): *m/z* (%) = 532.52 (100) [M^+].

^{1}H-NMR (500 MHz; $CDCl_3$) (δ [ppm])

7.82-7.78 (m, 2H, H5), 7.65 (d, *J* = 8.14 Hz, 2H, H3', H6'), 7.48 (d, *J* = 8.15 2H, H4', H5'), 7.38 (t, *J* = 7.51, 7.51 Hz, 1H, H6), 6.84 (m, 2H, H3, H7), 6.83 (s, 2H, H1', H8'), 6.76 (d, *J* = 7.68 Hz, 1H, H1), 6.44 (s, 1H, H1), 2.14 (s, 3H, -CH_3).

IR (ATR) $\bar{\nu}$ (cm^{-1}) = 2921, 2851, 1682, 1398, 1257, 1059, 949, 804, 731.

7.2.28 Biphenyl-4-yl boronic acid (36)

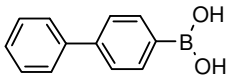

Biphenyl-4-yl boronic acid was prepared from Grignard reagent of 9.2 g (38.61 mmol) 4-bromobiphenyl following the similar procedure as in **7.2.19**.

$C_{12}H_{11}BO_2$ (198.03 g/mol)

Yield: 5.06 g (25.55 mmol, 67 %) white amorph.

MS: *m/z* (%) = 198.33 (100) [M^+].

^{1}H-NMR (500 MHz; $CDCl_3$) (δ [ppm])

8.10 (s, 2H), 7.88 (d, *J* = 8.15 Hz, 2H), 7.67 (d, *J* = 7.25 Hz, 2H), 7.63 (d, *J* = 8.17 Hz, 2H), 7.45 (t, *J* = 7.66, 7.66 Hz, 2H), 7.36 (t, *J* = 7.35, 7.35 Hz, 1H).

^{13}C-NMR (125.7 MHz; $CDCl_3$) (δ [ppm])

141.61, 140.14, 134.81, 128.96, 127.59, 126.73, 125.68.

7.2.29 2-Acetoxy-2',7'-bis(1,1'-biphenyl-4-yl)-9,9'-spirobifluorene (37)

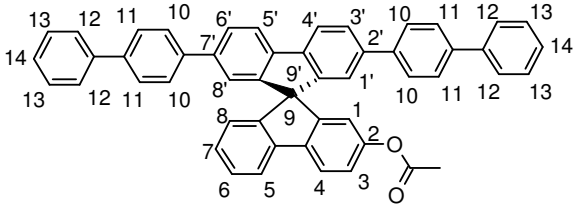

In a Young flask, containing a magnetic stirrer, 0.79 g (1.50 mmol) 2'-acetoxy-2,7-dibromo-9,9'-spirobifluorene, 0.71 g (3.60 mmol) biphenyl-4-yl boronic acid, 0.83 g (6.00 mmol) K_2CO_3 were taken. Then, 5 mL toluene, 15 mL THF and 10 mL water were added to it. A

pipette was dipped into the mixture to blow nitrogen gas into the solution for an hour. After that, 0.08 g (4.8 mol%) palladium(0)tetrakis(triphenylphosphine) was added in nitrogen gas atmosphere and then the flask was evacuated and refluxed at 80 °C for about 17 hours. The rest workout was followed as in **7.2.12**.

$C_{51}H_{34}O_2$ (678.84 g/mol)

Yield: 0.74 g (1.1 mmol, 73 %), white amorph.

MS (MALDI): *m/z* (%) = 678.28 (100) [M^+].

^{1}H-NMR (500 MHz; $CDCl_3$) (δ [ppm])

7.93 (d, *J* = 7.91 Hz, 2H, H4', H5'), 7.86 (d, *J* = 8.30 Hz, 1H, H5), 7.83 (d, *J* = 7.79 Hz, 1H, H4), 7.68 (d, *J* = 7.93 Hz, 2H, H3', H6') , 7.56-7.50 (m, 12H, H10, H11, H12), 7.41 (t, *J* = 7.65, 7.65 Hz, 4H, H13), 7.37 (t, *J* = 7.53, 7.53 Hz, 1H, H6), 7.32 (t, *J* = 7.31, 7.31 Hz, 2H, H14), 7.16 (dd, *J* = 8.30, 2.13 Hz, 1H, H3), 7.11 (t, *J* = 7.40, 7.40 Hz, 1H, H7), 7.00 (s, 2H, H1', H8'), 6.81 (d, *J* = 7.55 Hz, 1H, H8), 6.58 (pd, *J* = 1.99 Hz, 1H, H1), 2.15 (s, 3H, -CH_3).

^{13}C-NMR (125.7 MHz; $CDCl_3$) (δ [ppm])

169.53, 150.70, 150.33, 149.58, 149.00, 141.19, 140.88, 140.79, 140.28, 139.95, 139.77, 128.99, 128.18, 128.11, 127.67, 127.57, 127.52, 127.22, 124.49, 122.92, 121.72, 120.85, 120.66, 120.22, 117.73, 66.27.

7.2.30 2'-Hydroxy-2,7-bis(1,1'-biphenyl-4-yl)-9,9'-spirobifluorene (39)

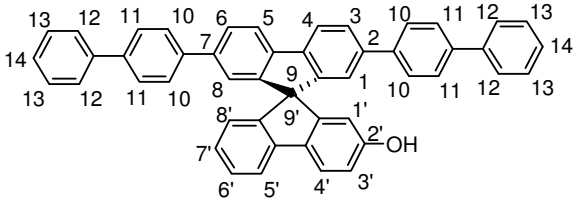

To the solution of 1 g (1.5 mmol) 2-acetoxy-2',7'-bis(biphenyl-4-yl)-9,9'-spirobifluorene in THF, a solution of 0.12 g (3 mmol) NaOH in water was added dropwise to it. The reaction mixture was heated for an hour and left to stir over night. After adding 2 N HCl, it was extracted with ethyl acetate and dried over Na_2SO_4. Then the solvent was removed by rotary evaporator. An analogous synthesis was explained in Wuest et. al work where MeOH was taken as solvent.[62] In this case, instead of MeOH, THF was taken because of the sparingly solubility of the compound in MeOH.

$C_{49}H_{32}O$ (636.80 g/mol)

Yield: 0.95 g (100 %), white amorph.

MS (MALDI): *m/z* (%) = 636.27 (100) [M^+].

^{1}H-NMR (500 MHz; deuteriated DMSO at 60 °C) (δ [ppm])

9.22 (s, 1H, -OH), 8.15 (d, *J* = 7.94 Hz, 2H, H4, H5), 7.87 (d, *J* = 7.52 Hz, 1H, H5'), 7.83 (d, *J* = 8.32 Hz, 1H, H4'), 7.801 (d, *J* = 7.94 Hz, 2H, H3, H6), 7.63 (t, *J* = 8.60, 8.60 Hz, 8H, H11, H12), 7.54 (d, *J* = 8.25 Hz, 4H, H10), 7.44 (t, *J* = 7.51, 7.51 Hz, 4H, H13), 7.38-7.31 (m, 3H, H6', H14), 7.05 (t, , *J* = 7.73, 7.73 Hz, 1H, H7'), 6.89 (s, 2H, H8, H1), 6.82 (d, *J* = 8.40 Hz, 1H, H3'), 6.69 (d, *J* = 7.66 Hz, 1H, H8'), 6.13 (pd, *J* = 1.88 Hz, 1H, H1').

7.2.31 2',7'-Bis(biphenyl-4-yl)-9,9'-spirobifluorene-2-yl trifluoromethanesulfonate (40)

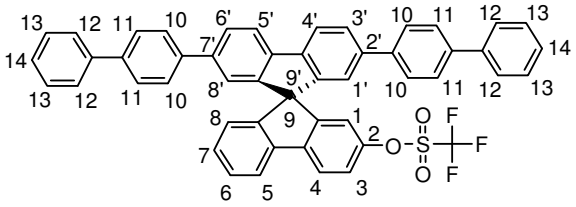

A solution of 0.95 g (1.49 mmol) 2,7-bis(biphenyl)-2'-hydroxy-9,9'-spirobifluorene in 35 mL pyridine and 15 mL dichloromethane was stirred at -20 °C in N_2 atmosphere and treated drop wise with the solution of $(CF_3SO_2)_2O$ in 5 mL dichloromethane. The mixture was stirred at -20 °C for 1 h and at 25 °C for 24 h. The mixture was then diluted with water and extracted with CH_2Cl_2. The organic layer was washed with water and brine, dried over $MgSO_4$, and filtered. Volatiles were then removed under reduced pressure, and the residue was dissolved in the minimum amount (~ 1.5 mL) of $CHCl_3$. It gave crystals after 48 h.

$C_{50}H_{31}F_3O_3S$ (768.86 g/mol)

Yield: 0.94 g (1.22 mmol, 82%), colourless crystal.

MS (MALDI): *m/z* (%) = 768.20 (100) [M^+].

^{1}H-NMR (500 MHz; $CDCl_3$) (δ [ppm])

7.95 (d, *J* = 7.92 Hz, 2H, H4', H5'), 7.91 (d, *J* = 8.47 Hz, 1H, H4), 7.86 (d, *J* = 7.73 Hz, 1H, H5), 7.70 (dd, *J* = 7.97, 1.44 Hz, 2H, H3', H6'), 7.55 (d, *J* = 8.12 Hz, 8H, H11, H12), 7.49 (d, *J* = 8.27 Hz, 4H, H10), 7.42-7.38 (m, 5H, H3, H13), 7.35-7.29 (m, 3H, H6, H14), 7.17 (t, *J* = 7.54, 7.54 Hz, 1H, H7), 6.95 (pd, *J* = 1.45 Hz, 2H, H1', H8'), 6.85 (d, *J* = 7.61 Hz, 1H, H8), 6.72 (pd, *J* = 2.28 Hz, 1H, H1).

^{13}C-NMR (125.7 MHz; $CDCl_3$) (δ [ppm])

151.08, 149.01, 148.94, 148.43, 142.04, 140.74, 140.62, 140.56, 140.16, 139.77, 139.62, 128.80, 128.75, 128.18, 127.45, 127.42, 127.37, 127.34, 127.31, 126.96, 124.39, 122.41, 121.25, 121.12, 120.66, 120.46, 117.57, 66.03.

IR (ATR) $\bar{\nu}$ (cm^{-1}) = 3031, 1599, 1420, 1207, 1138, 974, 864, 762, 694.

Crystal data and structure refinement for I0316 (MDS0160)

Identification code	i0316	
Empirical formula	C51 H32 Cl3 F3 O3 S	
Formula weight	888.18	
Temperature	133(2) K	
Wavelength	0.71073 A	
Crystal system	Triclinic	
Space group	P -1	
Unit cell dimensions	a = 11.0339(15) A	alpha = 70.675(12)°
	b = 13.228(2) A	beta = 85.194(12)°
	c = 15.356(2) A	gamma = 77.394(12)°
Volume	2064.0(5) A^3	
Z	2	
Density (calculated)	1.429 Mg/m^3	
Absorption coefficient	0.332 mm^{-1}	
F(000)	912	
Crystal size	0.28 x 0.19 x 0.02 mm	
Theta range for data collection	1.41 to 25.00°	
Index ranges	-13<=h<=11, -15<=k<=15, -18<=l<=18	
Reflections collected	13474	
Independent reflections	6861 [R(int) = 0.0906]	
Reflection observed	2508	
Absorption correction	Integration	
Max. and min. transmission	0.9923 and 0.9614	
Refinement method	Full-matrix least-squares on F^2	
Data / restraints / parameters	6861 / 0 / 550	
Goodness-of-fit on F^2	0.739	
Final R indices [I>2sigma(I)]	R1 = 0.0670, wR2 = 0.1537	
R indices (all data)	R1 = 0.1590, wR2 = 0.1790	
Largest diff. peak and hole	0.543 and -0.712 $e.A^{-3}$	

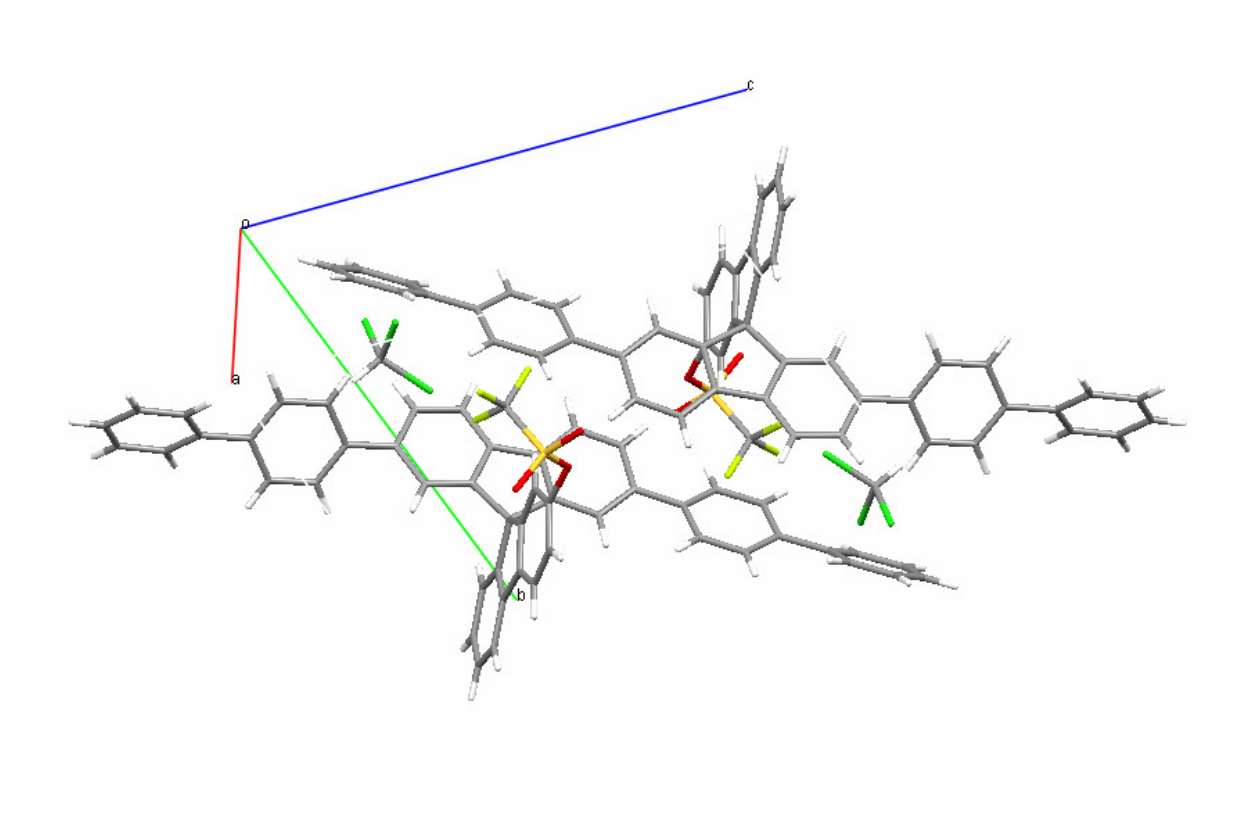

7.2.32 2-[2',7'-Bis(biphenyl-4-yl)-9,9'-spirobifluorene-2-yl]-4,4,5,5-tetramethyl-1,3,2-dioxyborolane (41)

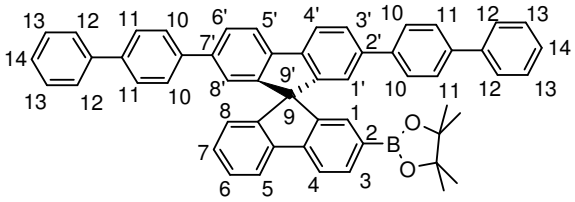

An r. b. flask assembled with a magnetic stirring bar, a septum inlet, and a condenser was charged with 0.03 g (0.03 mmol) $Pd_2(dba)_3$ and 0.04 g (0.16 mmol) tricyclohexylphosphine and flushed with nitrogen. Dioxane was added and the resulting mixture was then stirred for 30 minutes at room temperature. 0.9 g (3.39 mmol) bis(pinacolato)diboron, 0.33 g (3.39 mmol) KOAc, and 1.74 g (2.26 mmol) 2,7-bis(biphenyl-4-yl)-9,9'-spirobifluorene-2'-yl-trifluoromethanesulfonate were added successively. After being stirred at 80 °C for 16 h the reaction mixture was treated with water at room temperature. The product was extracted with toluene, washed with brine, and dried over $MgSO_4$. Column chromatography gave an analytically pure sample. An analogous synthesis is explained in Ishiyama et al. [81]

$C_{55}H_{43}BO_2$ (746.77 g/mol)

Yield: 1.46 g (1.95 mmol, 87%), white amorph.

MS (MALDI): *m/z* (%) = 746.09 (100) [M^+].

^{1}H-NMR (500 MHz; $CDCl_3$) (δ [ppm])

7.93 (d, *J* = 7.94 Hz, 2H, H4', H5'), 7.88 (m, 3H, H5, H4, H3), 7.68 (d, *J* = 7.94 Hz, 2H, H3', H6'), 7.55-7.49 (m, 12H, H10, H11, H12), 7.41-7.34 (m, 5H, H1, H13), 7.33-7.26 (m, 3H, H6, H14), 7.12 (t, *J* = 7.84, 7.84 Hz, 1H, H7), 6.96 (s, 2H, H1', H8'), 6.78 (d, *J* = 7.66 Hz, 1H, H8), 1.22 (s, 12H, -CH_3).

^{13}C-NMR (125.7 MHz; $CDCl_3$) (δ [ppm])

149.69, 149.55, 147.53, 144.96, 141.32, 140.87, 140.63, 140.23, 139.94, 139.80, 134.87, 130.37, 128.72, 128.42, 127.71, 127.34, 127.29, 127.24, 126.95, 126.72, 124.16, 122.69, 120.43, 120.40, 119.39, 83.71, 66.03, 24.79.

7.2.33 2,2',7,7'-Tetrakis[2',7'-bis(1,1'-biphenyl-4-yl)-9,9'-spirobifluorene-2-yl]-9,9'-spirobifuorene (42)

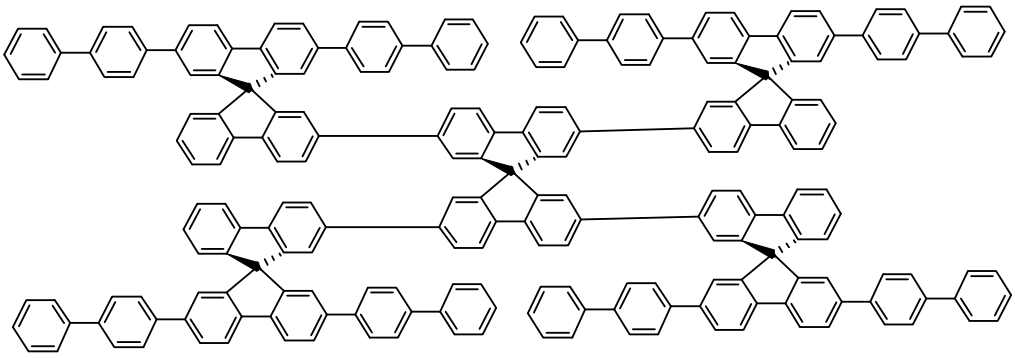

In a Yound flask, containing a magnetic stirrer, 0.12 g (0.20 mmol) 2,2'7,7'-tetrabromo-9,9'-spirobifluorene, 0.61 g (0.82 mmol) pinacol 2',7'-bis(biphenyl-4-yl)-9,9'-spirobifluorene -2-yl borane, 0.22 g (1.63 mmol) K_2CO_3 were taken. Then, 25 mL toluene, 15 mL THF and 10 mL water were added to it. A pipette was dipped into the mixture to blow nitrogen gas into the solution for an hour. After that, 0.02 g (2.4 mol%) palladium(0)tetrakis(triphenylphosphine) was added in nitrogen gas atmosphere and then the flask was evacuated and refluxed at 80 °C for about 21 hours. The rest workout was followed as in **7.2.12**.

$C_{221}H_{136}$ (2791.55 g/mol)

Yield: 0.38 g (0.13 mmol, 68%), white amorph.

MS (MALDI): *m/z* (%) = 2791.03 (100) [M^+].

^{1}H-NMR (500 MHz; $CDCl_3$) (δ [ppm])

7.75 (d, *J* = 7.75 Hz, 4x2H), 7.67 (d, *J* = 8.02 Hz, 4x2H), 7.69-7.58 (m, 4x2H), 7.54-7.47 (m, 4x6H), 7.45 (d, *J* = 8.27 Hz, 4x4H), 7.40-7.31 (m, 4x8H), 7.27-7.24 (m, 4x3H), 7.20 (d, *J* = 8.16 Hz, 4x1H), 7.03 (t, *J* = 8.08, 8.08 Hz, 4x1H), 6.87 (d, *J* = 6.48 Hz, 4x3H), 6.74 (s, 4x1H), 6.70 (d, *J* = 7.57 Hz, 4x1H).

^{13}C-NMR (125.7 MHz; $CDCl_3$) (δ [ppm])

149.67, 141.16, 140.89, 140.80, 140.59, 140.24, 139.82, 139.67, 128.71, 127.34, 127.22, 127.19, 126.91, 122.56, 120.32, 120.31, 120.07, 120.00, 66.05.

Elemental Analysis: Found (%) Calculated (%)

C: 94.13 C: 94.86

H: 5.07 H: 5.14

7.2.34 2-(4-Methoxyphenyl)-4,4,5,5-tetramethyl-1,3,2-dioxaborolane

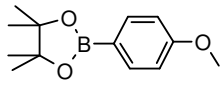

Into an ether solution of 3g (19.7 mmol) 4-methoxyphenyl boronic acid and boroxine contanined in it, some amount of dilute HCl was added making the pH of the solution about 2, some water and 4.68 g (39.4 mmol) pinacol was added into it. The reaction mixture was left to stir over night. Then the aqueous and the organic phases were separated. The organic phase was dried over Na_2SO_4 and then the solvent was removed by rotary evaporator.

$C_{13}H_{19}BO_3$ (234.11 g/mol)

Yield: 3.88 g (16.57 mmol, 84%), yellow liquid.

^{1}H-NMR (500 MHz:$CDCl_3$) (δ [ppm])

7.77 (d, *J* = 7.96 Hz, 2H), 6.89 (d, *J* = 8.25 Hz, 2H), 3.80 (s, 3H), 1.34 (s, 12H).

^{13}C-NMR (125.7 MHz; $CDCl_3$) (δ [ppm])

162.05, 136.41, 113.19, 83.39, 54.91, 24.75.

IR (ATR) $\bar{\nu}$ (cm^{-1}) = 2978, 1606, 1518, 1467, 1361, 1278, 1215, 1144, 1092.

7.2.35 2-Bromo-4'-methoxybiphenyl (45)

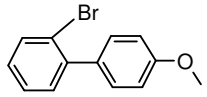

In a Young flask, containing a magnetic stirrer, 5 g (17.6 mmol) 1-bromo-2-iodobenzene, 3.41 g (14.6 mmol) pinacol 4-methoxyphenyl borane, 4.03 g (29.20 mmol) K_2CO_3 were taken. Then, 30 mL toluene, 20 mL THF and 15 mL water were added to it. A pipette was dipped into the mixture to blow nitrogen gas into the solution for an hour. After that, 0.50 g (3 mol%) palladium(0)tetrakis(triphenylphosphine) was added in nitrogen gas atmosphere and then the flask was evacuated and refluxed at 80 °C for about 17 hours. The rest workout was followed as in **7.2.12**.

$C_{13}H_{11}BrO$ (263.14 g/mol)

Yield: 2.38 g, (9.05 mmol, 62%), colourless liquid.

MS (APCI): *m/z* (%) = 262.93 (100) [M^+].

^{1}H-NMR (500 MHz; $CDCl_3$) (δ [ppm])

7.73 (d, *J* = 7.76 Hz, 1H), 7.47-7.36 (m, 4H), 7.27-7.21 (m, 1H), 7.04 (d, *J* = 8.76 Hz, 2H), 3.92 (s, 3H).

^{13}C-NMR (125.7 MHz; $CDCl_3$) (δ [ppm])

158.98, 142.09, 140.24, 133.43, 133.01, 131.27, 130.47, 129.35, 128.32, 127.28, 122.81, 113.28, 55.17.

IR (ATR): $\bar{\nu}$ (cm^{-1}) = 3009, 2839, 1603, 1479, 1288, 1036, 806, 721.

7.2.36 2,7-Dibromo-2'-methoxy-9,9'-spirobifluorene (46)

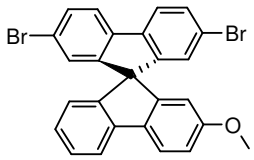

To a solution of 7.20 g (27.36 mmol) 2-bromo-4'-methoxy-biphenyl in 136 mL THF (0.2M), 1.34 g (21.89 mmol) n-BuLi solution was added dropwise slowly at -80 °C. After the complete addition, the reaction mixture was left to stir for about an hour at the same temperature. Then, at the same temperature, a solution of 7.39 g (21.89 mmol) 2,7-dibromofluorene-9-one in 145.7 mL THF were added dropwise to the reaction mixture. It was left to stir at room temperature for 20 h. The reaction was quenched with the addition of 100

mL water. It was left to stir for 2 h at RT and concentrated by rotary evaporator. The reaction mixture was then treated with ethylacetate, washed with 1 N HCl. The white precipitate alcohol was filtered and washed quickly with *n*-heptane. It was then treated with a mixture conc. acetic acid (1.75 mmL/mmol) and 2.5 mL conc. HCl and then refluxed for two hours. Due to the presence of MeO in meta position, it needs a drastic condition for the ring closing. It means excess of conc. HCl was added. The residue was filtered off and slowly stirred with water and dried.

$C_{26}H_{16}Br_2O$(504.22 g/mol)

Yield: 6.40 g (12.69 mmol, 58%), white amorph.

^{1}H-NMR (500 MHz; $CDCl_3$) (δ [ppm])

7.73 (d, *J* = 8.35 Hz, 2H), 7.65 (d, *J* = 8.19 Hz, 2H), 7.47 (dd, *J* = 8.15, 1.77 Hz, 2H), 7.35 (t, *J* = 7.50, 7.50 Hz, 1H), 7.05 (t, *J* = 7.50, 7.50 Hz, 1H), 6.93 (dd, *J* = 8.39, 2.39 Hz, 1H), 6.84 (d, *J* = 1.71 Hz, 2H), 6.66 (d, *J* = 7.57 Hz, 1H), 6.21 (d, *J* = 2.36 Hz, 1H), 3.66 (s, 3H).

^{13}C-NMR (125.7 MHz; $CDCl_3$) (δ [ppm])

159.97, 150.65, 148.78, 146.61, 141.62, 139.53, 134.50, 131.09, 128.21, 127.36, 126.85, 123.84, 121.87, 121.35, 121.02, 119.41, 114.20, 109.46, 65.54, 55.42.

7.2.37 1,1',4',1''-Terphenyl-4''-trimethylsilane (50)

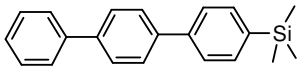

In a Young flask, containing a magnetic stirrer, 20 g (85.79 mmol) 4-bromobiphenyl, 16.98 g (87.50 mmol) 4-trimethylsilylphenyl boronic acid, 24.18 g (175.00 mmol) K_2CO_3 were taken. Then, 55 mL toluene, 45 mL THF and 30 mL water were added to it. A pipette was dipped into the mixture to blow nitrogen gas into the solution for an hour. After that, 2.42 g (2.4 mol%) palladium(0)tetrakis(triphenylphosphine) was added in nitrogen gas atmosphere and then the flask was evacuated and refluxed at 80 °C for about 17 hours. The rest workout was followed as in **7.2.12**.

$C_{21}H_{22}Si$ (302.50 g/mol)

Yield: 11.75 g (mmol, 45 %), colourless crystal.

MS (MALDI): *m/z* (%) = 302.27 (100) [M^+].

^{1}H-NMR (500 MHz; $CDCl_3$) (δ [ppm])

7.67 (d, 2H), 7.65-7.59 (m, 6H), 7.45 (t, *J* = 7.61, 7.61 Hz, 2H), 7.35 (t, *J* = 7.38, 7.38 Hz, 3H), 0.30 (s, 9H).

^{13}C-NMR (125.7 MHz; $CDCl_3$) (δ [ppm])

141.02, 140.66, 140.15, 140.01, 139.33, 133.85, 128.78, 127.47, 127.31, 127.02, 126.34, -1.09.

IR (ATR): $\bar{\nu}$ (cm^{-1}) = 2953, 1597, 1252, 1113, 814, 754.

7.2.38 1,1',4',1''-Terphenyl-4''-boronic acid (47)

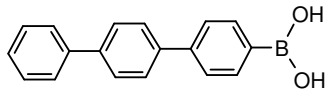

1 g (3.30 mmol) 1,1',4',1''-terphenyl-4''-trimethylsilane was dissolved in 26 ml dichloromethane. To this solution, 1.24 g (4.95 mmol) boron tribromide in 16 ml of dichloromethane was added over a period of 15 min. After stirring this solution for 3 h, 13 ml of water was added. The layers were separated, the aqueous layer was washed twice with dichloromethane (2x5 ml) (sparingly soluble) and the combined organic layers were washed twice with water (2x20 ml). The compound remained insoluble in aqueous and organic phase. Hence, it was filtered and dried. An analogous synthesis is explained in Schlüter et. al. [87]

$C_{18}H_{15}BO_2$ (274.13 g/mol)

Yield: 0.27 g (mmol, 30 %), white amorph.

MS (MALDI): *m/z* (%) = 274.12 (100) [M^+].

^{1}H-NMR (500 MHz; Deuteriated, DMSO) (δ [ppm])

8.12 (s, 2H), 7.91 (d, *J* = 8.17 Hz, 2H), 7.81-7.74 (m, 4H), 7.70 (t, *J* = 7.80, 7.80 Hz, 4H), 7.47 (t, *J* = 7.67, 7.67 Hz, 2H), 7.37 (t, *J* = 7.37, 7.37 Hz, 1H).

^{13}C-NMR (125.7 MHz; Deuteriated, DMSO) (δ [ppm])

206.57, 206.55, 140.98, 139.58, 139.27, 139.07, 134.86, 129.01, 127.57, 127.22, 127.19, 126.58, 125.54, 30.71.

IR (ATR): $\bar{\nu}$ (cm^{-1}) = 2980, 1609, 1358, 1142, 743, 654.

7.2.39 2,7-Bis(1,1',4',1''-terphenyl-4''-yl)-2'-methoxy-9,9'-spirobifluorene (48)

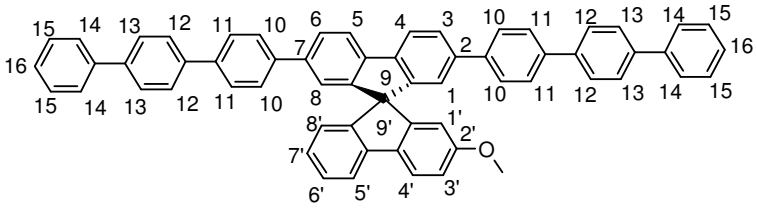

In a Young flask, containing a magnetic stirrer, 2.74 g (5.44 mmol) 2',7'-dibromo-2-methoxy-9,9'-spirobifluorene, 4.65 g (13.06 mmol) 1,1',4',1''-terphenyl-4''-boronic acid, 3.61 g (26.12 mmol) K_2CO_3 were taken. Then, 25 mL toluene, 50 mL THF and 30 mL water were added to it. A pipette was dipped into the mixture to blow nitrogen gas into the solution for an hour. After that, 0.46 g (3 mol%) palladium(0)tetrakis(triphenylphosphine) was added in nitrogen gas atmosphere and then the flask was evacuated and refluxed at 80 °C for about 17 hours. The rest workout was followed as in **7.2.12**. The product seemed to be precipitated out from the reaction mixture. It was sparingly soluble in toluene and chloroform. Hence, it was difficult to extract the organic phase. The precipitate was filtered off. The filtrate was dried with Na_2SO_4 and then the organic solvent was removed by rotary evaporator. The remained solid was united with the precipitate and refluxed in toluene for 1 h, then filtered and dried.

$C_{62}H_{42}O$ (803.03 g/mol)

Yield: 3.27 g (4.08 mmol, 75%), white amorph.

MS (MALDI): *m/z* (%) = 802.12 (100) [M^+].

^{1}H-NMR (500 MHz; $CDCl_3$) (δ [ppm])

7.94 (d, *J* = 7.79 Hz, 2H, H4, H5), 7.77 (d, *J* = 7.95 Hz, 2H, H3, H6), 7.69 (d, *J* = 7.88 Hz, 2H, H4', H5'), 7.64-7.57 (m, 16H, H13, H14, H11, H12), 7.53 (d, *J* = 7.97 Hz, 4H, H10), 7.44 (t, *J* = 7.53, 7.53 Hz, 4H, H15), 7.34 (t, *J* = 6.78, 6.78 Hz, 3H, H6', H16), 7.05 (t, *J* = 7.65, 7.65 Hz, 1H, H7'), 7.01 (s, 2H, H1, H8), 6.93 (d, *J* = 8.54 Hz, 1H, H8'), 6.78 (d, *J* = 7.54 Hz, 1H, H3'), 6.36 (s, 1H, H1'), 3.65 (s, 3H, -CH_3).

^{13}C-NMR (125.7 MHz; $CDCl_3$) (δ [ppm])

129.05, 128.78, 128.20, 127.75, 127.63, 127.49, 127.43, 127.29, 127.18, 127.00, 126.22, 126.00, 125.84, 124.07, 122.91, 122.64, 122.63, 120.83, 120.80, 120.38, 120.36, 119.25, 119.21, 113.90, 113.86, 109.62, 109.60, 66.10, 55.43.

7.2.40 2',7'-Bis(1,1',4',1''-terphenyl-4''-yl)-2-hydroxy-9,9'-spirobifluorene (51)

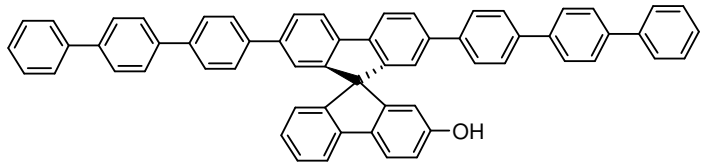

To a solution of 0.20 g (0.25 mmol) 2-methoxy-2',7'-bis(1,1',4',1''-terphenyl-4''-yl)-9,9'-spirobifluorene in absolute CH_2Cl_2, 0.17 g (0.67 mmol) BBr_3 was added at 0 °C, the mixture was stirred at room temperature for 16 h. 100 ml water were added, the organic layer was separated and evaporated to dryness which became grayish amorph. The crude product was sparingly soluble in CH_2Cl_2 and $CHCl_3$. An analogous synthesis is explained in Bo et. all [88]

$C_{61}H_{40}O$ (789.00 g/mol)

Yield: 0.19 g (0.24 mmol, 100%), white amorph.

MS (MALDI): *m/z* (%) = 788.11 (100) [M^+].

M. Pt.: 399 °C

^{1}H-NMR (500 MHz; Deuteriated DMSO) (δ [ppm])

Poor solutbility of this compound gave a spectrum of very bad resolution.

^{13}C-NMR (125.7 MHz; Deuteriated DMSO) (δ [ppm])

65.51.

7.2.41 2',7'-Bis(1,1',4',1''-terphenyl-4''-yl)-9,9'-spirobifluorene-2-yl trifluoromethyl sulfonate (52)

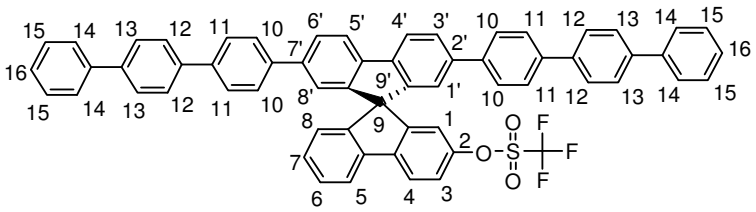

A solution of 0.20 g (0.25 mmol) 2',7'-bis(1,1',4',1''-terphenyl-4''-yl)-2-hydroxy-9,9'-spirobifluorene in 20 mL pyridine and 10 mL dichloromethane was stirred at -20 °C in N_2 atmosphere and treated dropwise with the solution of 0.10 g (0.37 mmol) $(CF_3SO_2)_2O$ in 10 mL dichloromethane. The mixture was stirred at -20 °C for 1 h and at 25 °C for 24 h. The mixture was then diluted with water and extracted with CH_2Cl_2. The organic layer was

washed with water and brine, dried over $MgSO_4$, and filtered. Volatiles were then removed under reduced pressure, and the residue was sparingly soluble in chloroform. To purify the product column chromatography was carried out using DCM /*n*-hexane as eluent.

$C_{62}H_{39}F_3O_3S$ (921.06 g/mol)

Yield: 0.19 g (0.21 mmol, 85%), white amorph.

MS (MALDI): *m/z* (%) = 920.55 (100) [M^+].

^{1}H-NMR (500 MHz; $CDCl_3$) (δ [ppm])

7.96 (d, *J* = 7.97 Hz, 2H, H4', H5'), 7.92 (d, *J* = 7.34 Hz, 1H, H5), 7.87 (d, *J* = 7.79 Hz, 1H, H4), 7.72 (d, *J* = 7.88 Hz, 2H, H3', H6'), 7.64-7.59 (m, 16H, H11, H12, H13, H14), 7.52-7.50 (m, 4H, H10), 7.44 (t, *J* = 7.55, 7.55 Hz, 5H, H3, H15), 7.35-7.32 (m, 3H, H6, H16), 7.21-7.15 (m, 1H, H7), 6.97 (s, 2H, H1', H8'), 6.85 (d, *J* = 7.80 Hz, 1H, H8), 6.74 (s, 1H, H1).

^{13}C-NMR (125.7 MHz; $CDCl_3$) (δ [ppm])

151.09, 151.04, 149.01, 148.96, 148.50, 148.46, 148.43, 142.06, 141.44, 141.26, 140.73, 140.65, 140.60, 140.25, 140.19, 139.92, 139.78, 139.70, 139.60, 139.42, 129.12, 128.87, 128.79, 128.19, 127.64, 127.58, 127.50, 127.47, 127.43, 127.35, 127.29, 127.25, 127.18, 127.00, 126.15, 125.87, 124.40, 124.37, 122.68, 122.40, 121.31, 121.27, 121.13, 120.73, 120.69, 120.52, 120.48, 117.59, 66.05.

7.2.42 2,2',7,7'-Tetrakis[2',7'-bis(1,1',4',1''-terphenyl-4''-yl)-9,9'-spirobifluorene-2-yl]-9,9'-spirobifluorene (53)

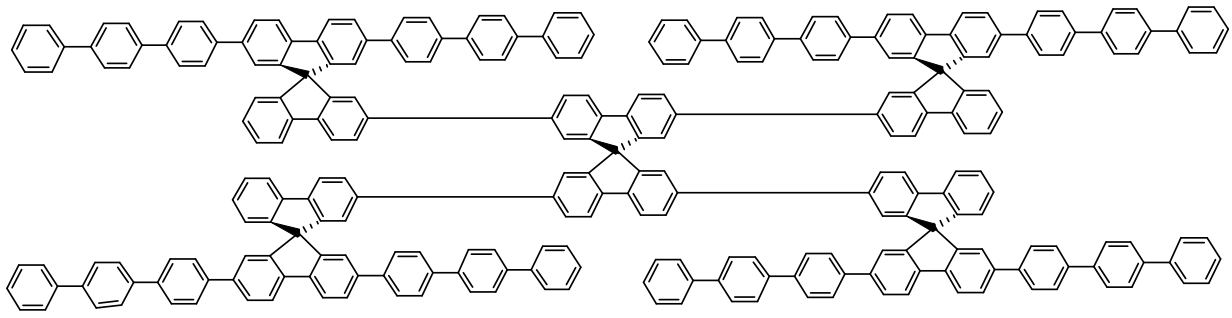

In a Young flask, containing a magnetic stirrer, 0.62 g (0.67 mmol) 2',7'-bis(1,1',4',1''-terphenyl-4''-yl)-9,9'-spirobifluorene-2-yl trifluoromethyl sulfonate, 0.13 g (0.16 mmol) 2,2',7,7'-tetrakis(boronicpinacolate)-9,9'-spirobifluorene, 0.26 g (1.89 mmol) K_2CO_3 were taken. Then, 30 mL toluene, 7 mL THF and 5 mL water were added to it. A pipette was

dipped into the mixture to blow nitrogen gas into the solution for an hour. After that, 0.02 g (10 mol%) palladium(0)tetrakis(triphenylphosphine) was added in nitrogen gas atmosphere and then the flask was evacuated and refluxed at 80 °C for about 48 hours in the nitrogen gas atmosphere. During the reaction, there was the formation of product in precipitate form which was insoluble into the reaction mixture. The solid was separated by filtration. The filtrate was treated as in **7.2.12**.

$C_{269}H_{168}$ (3400.34 g/mol)

Yield: 1.57 g (0.46 mmol, 69%), white amorph.

MS (MALDI): *m/z* (%) = 3399.93 (100) [M^+].

^{1}H-NMR (500 MHz; $CDCl_3$) (δ [ppm])

7.74 (d, *J* = 6.81 Hz, 4x2H), 7.17 (d, *J* = 7.04 Hz, 4x1H), 7.64-7.30 (m, 4x32H), 7.04 (d, *J* = 7.18 Hz, 4x1H), 6.90 (t, *J* = 3.59, 3.59 Hz, 4x1H), 6.72 (d, *J* = 7.89 Hz, 4x3H), 6.78 (s, 4x1H), 6.72 (d, *J* = 6.88 Hz, 4x1H).

^{13}C-NMR (125.7 MHz; $CDCl_3$) (δ [ppm])

66.13, 66.10.

Elemental Analysis:	Found (%)	Calculated (%)
	C: 91.17	C: 94.93
	H: 5.26	H: 5.07

7.2.43 2'-Methoxy-2,7-diphenyl-9,9'-spirobifluorene (54)

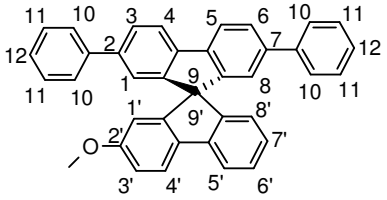

In a Young flask, containing a magnetic stirrer, 4.4 g (8.72 mmol) 2,7-dibromo-9,9'-spirobifluorene 2.55 g (20.93 mmol) phenyl boronic acid, 5.80 g (41.86 mmol) K_2CO_3 were taken. Then, 80 mL toluene, 60 mL THF and 30 mL water were added to it. A pipette was dipped into the mixture to blow nitrogen gas into the solution for an hour. After that, 0.61 g (2.5 mol%) palladium(0)tetrakis(triphenylphosphine) was added in nitrogen gas atmosphere and then the flask was evacuated and refluxed at 80 °C for about 17 hours. The rest workout was followed as in **7.2.12**.

$C_{38}H_{26}O$ (498.63 g/mol)

Yield: 3.69 g (7.41 mmol, 85%), colourless crystal.

MS (MALDI): *m/z* (%) = 499.87 (100) [M^+].

^{1}H-NMR (500 MHz; $CDCl_3$) (δ [ppm])

7.92 (d, *J* = 7.93 Hz, 2H, H4, H5), 7.76 (d, *J* = 8.14 Hz, 2H, H4', H5'), 7.64 (dd, *J* = 7.94, 1.62 Hz, 2H, H3, H6), 7.50-7.41 (m, 4H, H10), 7.38-7.28 (m, 5H, H11, H6'), 7.25-7.22 (m, 2H, H12), 7.04 (t, *J* = 7.50, 7.50 Hz, 1H, H7'), 6.97 (d, *J* = 0.86 Hz, 2H, H1, H8), 6.93 (dd, *J* = 8.42, 2.38 Hz, 1H, H3'), 6.78 (d, *J* = 7.51 Hz, 1H, H8'), 6.35 (d, *J* = 2.14 Hz, 1H, H1'), 3.64 (s, 3H, -CH_3).

^{13}C-NMR (125.7 MHz; $CDCl_3$) (δ [ppm])

159.88, 150.41, 149.97, 148.25, 141.70, 140.87, 140.85, 140.54, 134.70, 128.55, 127.69, 127.12, 127.00, 126.86, 126.69, 124.02, 122.74, 120.74, 120.26, 119.16, 113.88, 109.52, 66.05, 55.38.

Crystal data and structure refinement for I0457 (MDS2061)

Identification code	i0457	
Formula weight	1235.91T	
Temperature	153 K	
Wavelength	0.71073 A	
Crystal system	Triclinic	
Space group	P-1	
Unit cell dimensions	a = 9.9172(16) A	alpha = 71.736(11) deg.
	b = 14.962(2) A	beta = 89.067(12) deg.
	c = 22.281(3) A	gamma = 81.704(12) deg.
Volume	3105.3(8) A^3	
Z	2	
Density (calculated)	1.322 Mg/m^3	
Absorption coefficient	0.326 mm^{-1}	
F(000)	1280	
Crystal size	0.33 x 0.29 x 0.11 mm	
Theta range for data collection	1.45 to 25.00 deg.	
Index ranges	-11<=h<=11, -17<=k<=17, -26<=l<=26	
Reflections collected	20307	
Independent reflections	10296 [R(int) = 0.1454]	
Reflections observed	2473	
Absorption correction	Integration	
Max. and min. transmission	0.9650 and 0.9000	
Refinement method	Full-matrix least-squares on F^2	
Data / restraints / parameters	10296 / 0 / 777	
Goodness-of-fit on F^2	0.695	
Final R indices [I>2sigma(I)]	R1 = 0.0907, wR2 = 0.2024	
R indices (all data)	R1 = 0.2431, wR2 = 0.2503	
Largest diff. peak and hole	0.461 and -0.626 $e.A^{-3}$	

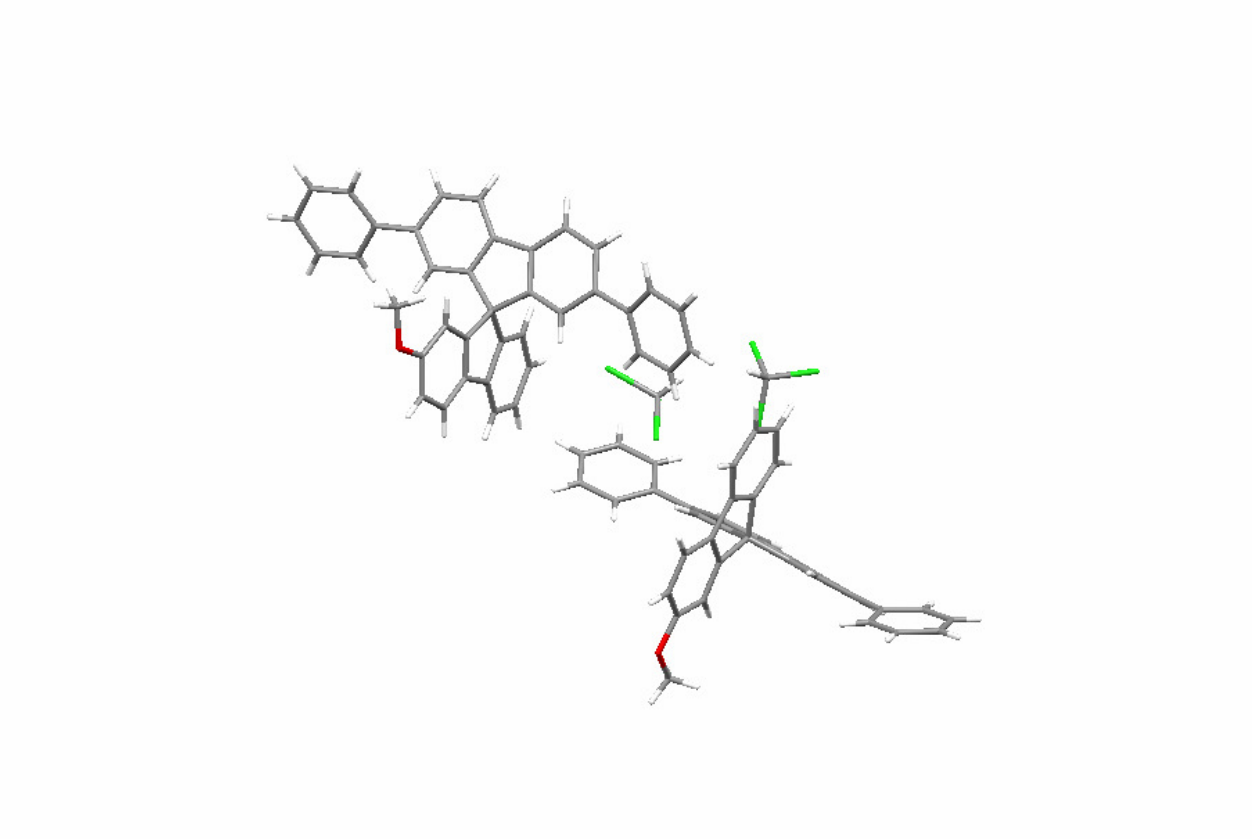

7.2.44 2'-Hydroxy-2,7-diphenyl-9,9'-spirobifluorene (55)

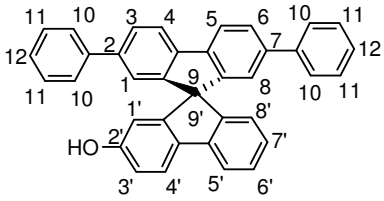

To a solution of 3.27 g (6.55 mmol) 2-methoxy-2',7'-diphenyl-9,9'-spirobifluorene in dried CH_2Cl_2, 1.5 mL (13.10 mmol) BBr_3 was added at 0 °C, the mixture was stirred at room temperature for 16 h. Water (100 ml) was added, the organic layer was separated. The organic phase was milky white. It was extracted with chloroform. Then the organic phase was dried by Na_2SO_4 and evaporated to dryness which gave white amorphous solid.

$C_{37}H_{24}O$ (484.60 g/mol)

Yield: 2.78 g (mmol, 88%), white amorph.

^{1}H-NMR (500 MHz; $CDCl_3$) (δ [ppm])

8.28 (s, 1H, -OH), 8.11 (d, *J* = 7.98 Hz, 2H, H4, H5), 7.87 (d, *J* = 7.60 Hz, 1H, H4'), 7.84 (d, *J* = 8.27 Hz, 1H, H5'), 7.75 (dd, *J* = 7.98, 1.66 Hz, 2H, H3, H6'), 7.47-7.45 (m, 4H, H10), 7.40-7.31 (m, 5H, H11, H6'), 7.27-7.24 (m, 2H, H12), 7.05 (dt, *J* = 7.50, 7.50, 0.96 Hz, 1H, H7'), 6.98 (d, *J* = 1.17 Hz, 2H, H1, H8), 6.91 (dd, *J* = 8.29, 2.26 Hz, 1H, H3'), 6.73 (d, *J* = 7.60 Hz, 1H, H8'), 6.25 (d, *J* = 2.18 Hz, 1H, H1').

^{13}C-NMR (125.7 MHz; $CDCl_3$) (δ [ppm])

As the compound was sparingly soluble in $CDCl_3$, ^{13}C was not interpretable.

7.2.45 2',7'-Diphenyl-9,9'-spirobifluorene-2-yl trifluoromethyl sulfonate (56)

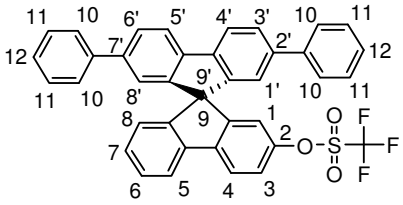

A solution of 2.71 g (5.59 mmol) 2-hydroxy-2',7'-diphenyl-9,9'-spirobifluorene in 50 mL pyridine and 50 mL dichloromethane was stirred at -20 °C in N_2 atmosphere and treated dropwise with the solution of 2 g (6.71 mmol) $(CF_3SO_2)_2O$ in 50 mL dichloromethane. The mixture was stirred at -20 °C for 1 h and at 25 °C for 24 h. The mixture was then diluted with water and extracted with CH_2Cl_2. The organic layer was washed with water and brine, dried over $MgSO_4$, and filtered. Volatiles were then removed under reduced pressure.

$C_{38}H_{23}F_3O_3S$ (616.66 g/mol)

Yield: 3.30 g (5.35 mmol, 96%), white amorph.

^{1}H-NMR (500 MHz; $CDCl_3$) (δ [ppm])

7.93 (d, *J* = 7.96 Hz, 2H, H4', H5'), 7.90 (d, *J* = 8.42 Hz, 1H, H4), 7.84 (d, *J* = 7.71 Hz, 1H, H5), 7.65 (dd, *J* = 7.96, 1.61 Hz, 2H, H3', H6'), 7.44-7.36 (m, 4H, H10), 7.33-7.30 (m, 5H, H11, H3), 7.25-7.22 (m, 3H, H6, H12), 7.115 (t, *J* = 7.49, 7.49 Hz, 1H, H7), 6.90 (d, *J* = 1.16 Hz, 2H, H1', H8'), 6.82 (d, *J* = 7.68 Hz, 1H, H8), 6.70 (d, *J* = 2.21 Hz, 1H, H1).

^{13}C-NMR (125.7 MHz; $CDCl_3$) (δ [ppm])

151.11, 149.03, 148.93, 148.34, 142.02, 141.26, 140.75, 140.54, 139.75, 128.76, 128.62, 128.14, 127.45, 127.27, 127.01, 124.37, 122.53, 121.21, 121.08, 120.57, 120.43, 117.54, 66.01.

7.2.46 2-[2',7'-Diphenyl-9,9'-spirobifluorene-2-yl]-4,4,5,5-tetramethyl-1,3,2-dioxaborolane

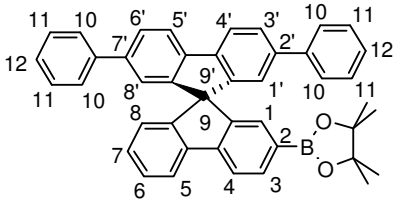

A flask assembled a magnetic stirring bar, a septum inlet, and a condenser was charged with 0.07 g (1.5% mmol) $Pd_2(dba)_3$ and 0.10 g (0.36 mmol) tricyclohexylphosphine and flushed with nitrogen. Dioxane was added and resulting mixture was then stirred for 30 min at room temperature. 1.92 g (7.54 mmol) Bis(pinacolato)diboron, 0.74 g (7.54 mmol) KOAc, and 3.10 g (5.03 mmol) 2',7'-diphenyl-9,9'-spirobifluorene-2-yl trifluoromethyl sulfonate were added successively. After being stirred at 80 °C for 16 h, the reaction mixture was treated with water at room temperature. The product was extracted with toluene washed with brine, and dried over $MgSO_4$. Column chromatography gave an analytically pure sample. An analogous synthesis is explained in Ishiyama et. al. [81]

$C_{43}H_{35}BO_2$ (594.57 g/mol)

Yield: 2.77 g (mmol, 93%), white amorph.

^{1}H-NMR (500 MHz; $CDCl_3$) (δ [ppm])

7.93 (d, *J* = 7.95 Hz, 2H, H4', H5'), 7.89-7.88 (m, 3H, H4, H5, H1), 7.65 (dd, *J* = 7.94, 1.68 Hz, 2H, H3', H6'), 7.47-7.41 (m, 4H, H10), 7.37 (dt, *J* = 7.51, 7.53, 0.96 Hz, 1H, H6), 7.33-7.28 (m, 5H, H11, H3), 7.27-7.23 (m, 2H, H12), 7.13 (dt, *J* = 7.54, 7.47, 1.00 Hz, 1H, H7), 6.94 (d, *J* = 1.18 Hz, 2H, H1', H8'), 6.79 (d, *J* = 7.62 Hz, 1H, H8), 1.27 (s, 12H, -CH_3).

^{13}C-NMR (125.7 MHz; $CDCl_3$) (δ [ppm])

149.61, 149.58, 147.56, 144.94, 141.30, 140.89, 140.78, 140.76, 134.83, 130.35, 128.54, 128.39, 127.67, 127.08, 126.99, 126.83, 124.14, 122.79, 120.40, 120.31, 119.35, 83.69, 66.02, 24.78.

7.2.47 2,2',7,7'-Tetrakis(2',7'-diphenyl-9,9'-spirobifluorene-2-phenyl-4''-yl)-9,9'-spirobifluorene (58)

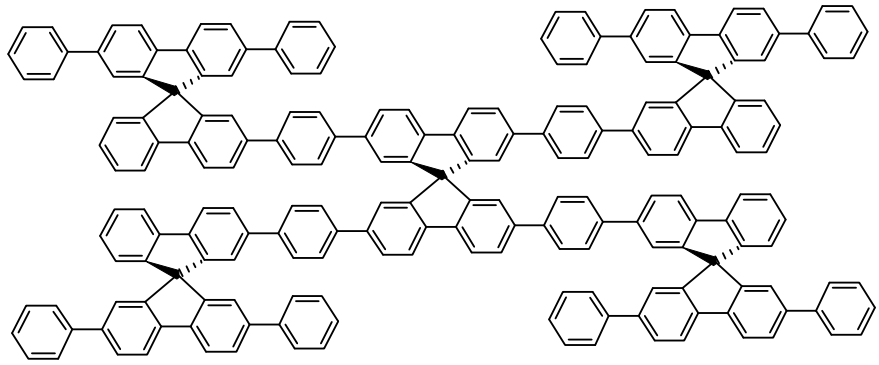

In a Young flask, containing a magnetic stirrer, 0.49 g (0.44 mmol) 2,2'7,7'-tetrakis(4-iodophenyl)-9,9'-spirobifluorene, 1.41 g (2.37 mmol) pinacol 2',7'-diphenyl-9,9'-spirobifluorene-2-yl borane, 0.65 g (4.74 mmol) K_2CO_3 were taken. Then, 20 mL toluene, 30 mL THF and 15 mL water were added to it. A pipette was dipped into the mixture to blow nitrogen gas into the solution for an hour. After that, 0.07g (2.5 mol%) palladium(0)tetrakis(triphenylphosphine) was added in nitrogen gas atmosphere and then the flask was evacuated and refluxed at 80 °C for about 17 hours. The rest workout was followed as in **7.2.12**.

$C_{197}H_{120}$(2487.15 g/mol)

Yield: 0.57 g (0.22 mmol, 52%), white amorph.

^{1}H-NMR (500 MHz; $CDCl_3$) (δ [ppm])

7.88 (d, *J* = 7.94 Hz, 4x2H), 7.85 (d, *J* = 3.89 Hz, 4x2H), 7.84 (d, *J* = 3.58 Hz, 4x1H), 7.80 (d, *J* = 7.98 Hz, 4x1H), 7.59 (d, *J* = 7.94 Hz, 4x2H), 7.52 (d, *J* = 8.05 Hz, 4x1H), 7.49 (d, *J* = 8.10 Hz, 4x1H), 7.38-7.34 (m, 4x5H), 7.32-7.23 (m, 4x8H), 7.19 (d, *J* = 7.30, 4x1H), 7.10 (t, *J* = 7.47, 7.47 Hz, 4x1H), 6.94 (s, 4x3H), 6.87 (s, 4x1H), 6.80 (d, *J* = 7.56 Hz, 4x1H).

^{13}C-NMR (125.7 MHz; $CDCl_3$) (δ [ppm])

149.66, 149.34, 148.92, 141.38, 140.96, 140.89, 140.83, 140.57, 140.35, 139.62, 139.60, 128.50, 127.80, 127.16, 127.14, 127.07, 127.00, 126.92, 126.68, 124.22, 122.71, 122.66, 120.28, 120.03, 66.08 (Central core Spiro-C), 66.04 (Terminal Spiro-C).

Elemental Analysis:	Found (%)	Calculated (%)
	C: 94.77	C: 95.14
	H: 5.16	H: 4.86

7.2.48 2',7'-Diphenyl-2-(4-bromophenyl)-9,9'-spirobifluorene (59)

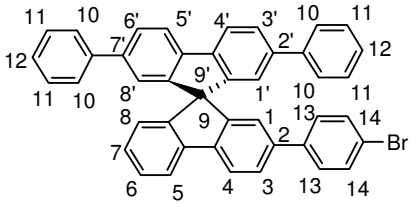

In a Young flask, containing a magnetic stirrer, 2.0 g (3.36 mmol) 2-iodo-2',7'-diphenyl-9,9'-spirobifluorene, 1.43 g (5.05 mmol) pinacol 4-bromophenyl borane, 1.40 g (10.10 mmol) K_2CO_3 were taken. Then, 25 mL toluene, 50 mL THF and 30 mL water were added to it. A pipette was dipped into the mixture to blow nitrogen gas into the solution for an hour. After that, 0.17 g (3 mol%) palladium(0)tetrakis(triphenylphosphine) was added in nitrogen gas atmosphere and then the flask was evacuated and refluxed at 80 °C for about 17 hours in the nitrogen gas atmosphere. The rest workout was followed as in **7.2.12**.

$C_{43}H_{27}Br$ (623.60 g/mol)

Yield: 2.19 g (mmol, 84%), white amorph.

MS (MALDI): *m/z* (%) = 624.29 (100) [M^+].

^{1}H-NMR (500 MHz; NMP:$CDCl_3$; 3:2) (δ [ppm])

7.96-7.86 (m, 4H, H3', H6', H5, H4), 7.65 (dd, *J* = 7.94, 1.59 Hz, 2H, H4', H5'), 7.58 (dd, *J* = 7.99, 1.63 Hz, 1H, H3), 7.49-7.18 (m, 16H, H10, H7, H13, H11, H12, H14, H6), 7.14 (t, *J* = 7.55, 7.55 Hz, 1H, H1), 6.98 (pd, *J* = 1.62 Hz, 2H, H1', H8'), 6.83 (d, *J* = 7.91 Hz, 1H, H8).

^{13}C-NMR (125.7 MHz; $CDCl_3$) (δ [ppm])

149.59, 149.47, 149.00, 141.42, 141.17, 140.95, 140.85, 140.80, 140.61, 139.77, 139.68, 131.58, 131.55, 131.50, 131.26, 130.93, 128.66, 128.61, 128.57, 128.07, 127.87, 127.17, 127.00, 126.78, 124.24, 122.71, 122.56, 121.32, 120.43, 120.37, 120.14, 66.10.

7.2.49 2-(4-Bromophenyl)-4,4,5,5-tetramethyl-[1,3,2]dioxaborolane (60)

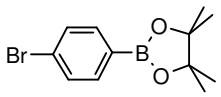

Into an ether solution of 9.8 g (48.8 mmol) 4-bromophenyl boronic acid and boroxine contanined in it, some amount of dilute HCl was added making the pH of the solution about 2

and some water and 11.50 g (97.6 mmol) pinacol was added into it. The reaction mixture was left to stir overnight. Then, aqueous and organic phases were separated. The organic phase was dried over Na_2SO_4 and then organic solvent was removed by rotary evaporator. Further purification was done by column chromatography (DCM:*n*-Hexane). Colourless liquid was isolated which later on became white solid with fiber-like structure.

$C_{12}H_{16}BBrO_2$ (282.98 g/mol)

Yield: 8.00 g (28.27 mmol, 58%), white amorph.

MS (EI)**:** *m/z* 282 (M_+),

267, 253, 239, 225, 204, 196, 183, 161, 146, 129, 117, 103, 85, 77, 69, 59, 41.

^{1}H-NMR (500 MHz; $CDCl_3$) (δ [ppm])

7.64 (d, *J* = 8.25 Hz, 2H), 7.49 (d, *J* = 8.33 Hz, 2H), 1.33 (s, 12H).

IR (ATR): $\bar{\nu}$ (cm^{-1}) = 2974, 1590, 1356, 1090, 820, 730, 620.

7.2.50 2-(2',7'-Diphenyl-9-9'-spirobifluorene-2-phenyl-4''-yl)-4,4,5,5-tetramethyl-1,3,2-dioxaborolane (63)

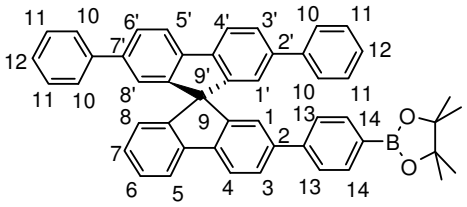

A flask assembled a magnetic stirring bar, a septum inlet, and a condenser was charged with 0.02 g (0.01 mmol) $Pd_2(dba)_3$ and 0.02 g (0.06 mmol) tricyclohexylphosphine and flushed with nitrogen. Dioxane was added and resulting mixture was then stirred for 30 min at room temperature. 0.33 g (1.29 mmol) bis(pinacolato)diboron, 0.13 g (1.29 mmol) KOAc, and 2',7'-diphenyl-2-(4-bromophenyl)-9,9'-spirobifluorene were added successively. After being stirred at 80 °C for 16 h, the reaction mixture was treated with water at room temperature. The product was extracted with toluene washed with brine, and dried over $MgSO_4$. Column chromatography gave an analytically pure sample. An analogous synthesis is explained in Ishiyama et. al.[81]

$C_{49}H_{39}BO_2$ (670.67 g/mol)

Yield: 0.20 g (0.30 mmol, 35%), white amorph.

MS (MALDI): *m/z* (%) = 670.26 (100) [M^+].

^{1}H-NMR (500 MHz; $CDCl_3$) (δ [ppm])

7.92 (t, *J* = 8.41, 8.41 Hz, 3H, H3', H6', H5), 7.87 (d, *J* = 7.49 Hz, 1H, H4), 7.73 (d, *J* = 7.88 Hz, 2H, H4', H5'), 7.64 (t, *J* = 6.92, 6.92 Hz, 3H, H3, H13), 7.49-7.40 (m, 6H, H10, H14), 7.38 (t, *J* = 7.59, 7.59 Hz, 1H, H7), 7.29 (t, *J* = 7.59, 7.59 Hz, 4H, H11), 7.26-7.21 (m, 2H, H12), 7.11 (t, *J* = 7.43, 7.43 Hz, 1H, H6), 7.04 (s, 1H, H1), 6.97 (s, 2H, H1', H8'), 6.81 (d, *J* = 7.55 Hz, 1H, H8), 1.31 (s, 12H, -CH_3).

^{13}C-NMR (125.7 MHz; $CDCl_3$) (δ [ppm])

149.68, 149.25, 149.10, 143.55, 141.38, 141.29, 140.93, 140.86, 140.76, 140.64, 135.04, 128.55, 127.96, 127.80, 127.12, 127.03, 126.96, 126.34, 124.20, 122.91, 122.77, 120.33, 120.31, 120.10, 83.71, 66.13, 24.79.

IR (ATR): $\bar{\nu}$ (cm^{-1}) = 2923, 1609, 1358, 1144, 858, 821, 765, 651.

7.2.51 4-Bromo-4'-methoxybiphenyl (65)

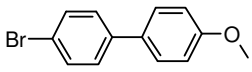

115.20 mL (162.40 mmol) dimethyl sulfate, 26.96 g (108.22 mmol) 4-bromo-4'-hydroxybiphenyl and 6.82 g (162.40 mmol) $LiOH.H_2O$ were suspended in 180 mL THF and heated at 70 °C for 1 h. The resulting mixture was partitioned between 1 M KOH and Et_2O. The organic layer was dried over $MgSO_4$ and concentrated in vacuo.[113]

$C_{13}H_{11}BrO$(263.14 g/mol)

Yield: 27.25 g (103.55 mmol, 96%), colourless crystal.

^{1}H-NMR (500 MHz; $CDCl_3$) (δ [ppm])

7.52 (m, 2H), 7.47 (m, 2H), 7.40 (m, 2H), 6.96 (m, 2H), 3.83 (s, 3H).

^{13}C-NMR (125.7 MHz; $CDCl_3$) (δ [ppm])

159.35, 139.68, 132.43, 131.75, 128.26, 127.94, 120.74, 114.28, 103.33, 55.33.

7.2.52 2-Bromophenylboronic acid (67)

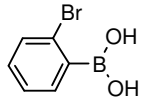

To a solution of 4.8 g (25 mmol) 1,2-dibromobenzene in ether (20 mL), 1.6 g (25 mmol) *n*-BuLi solution was added dropwise slowly at -78 °C. After the complete addition, the reaction mixture was left to stir for about an hour and warm up to -10 °C. Then it was again cooled down up to -78 °C and 2.6 g (25 mmol) $B(OMe)_3$ was added dropwise to the reaction mixture at -78 °C. Then, it was left to stir at room temperature for 20 h. The reaction was quenched with the addition of 100 mL 1 N HCl. It was left to stir for 2 h at RT and at the end the mixture was extracted in ethyl acetate, washed with dilute $NaHCO_3$ solution, dried, filtered and the solvent was removed by rotary evaporator. Recrystallization from water gave white solid product. [114]

$C_6H_6BBrO_2$ (200.83 g/mol)

Yield: 3.51 g (17.5 mmol, 70%), colourless needles.

MS (EI): *m/z* (%) = 547 (39) 469 (6), 410 (13), 281 (8), 200 (91)[M+•], 156 (57), 130 (42), 103 (7), 77 (100), 50 (33).

^{1}H-NMR (500 MHz; $CDCl_3$) (δ [ppm])

7.52 (m, 2H), 7.30 (m, 2H,).

^{13}C-NMR (125.7 MHz; $CDCl_3$) (δ [ppm])

135.09, 132.31, 131.16, 126.94, 126.38.

7.2.53 2-Bromo-4''-methoxy-1,1',4',1''-terphenyl (68)

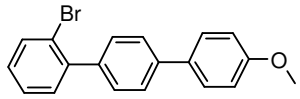

In a Young flask, containing a magnetic stirrer, 2.74 g (10.4 mmol) 4-bromo-4'-methoxy-1,1'-biphenyl, 2.50 g (12.48 mmol) 2-bromophenylboronic acid, 2.87 g (20.8 mmol) K_2CO_3 were taken. Then, 25 mL toluene, 50 mL THF and 30 mL water were added to it. A pipette was dipped into the mixture to blow nitrogen gas into the solution for an hour. After that, 0.28 g (2.4 mol%) palladium(0)tetrakis(triphenylphosphine) was added in nitrogen gas atmosphere and then the flask was evacuated and refluxed at 80 °C for about 17. The rest workout was followed as in **7.2.12**.

$C_{19}H_{15}BrO$ (339.23 g/mol)

Yield: 1.81 g (5.33 mmol, 52%), colourless liquid.

MS (MALDI): *m/z* (%) = 340.09 (100) [M^+].

^{1}H-NMR (500 MHz; $CDCl_3$) (δ [ppm])

7.67 (d, *J* = 8.01 Hz, 1H), 7.60 (d, *J* = 8.19 Hz, 2H), 7.58 (d, *J* = 8.75 Hz, 2H), 7.46 (d, *J* = 8.23 Hz, 2H), 7.36 (d, *J* = 4.20 Hz, 2H), 7.22-7.17 (m, 1H), 6.98 (d, *J* = 8.74 Hz, 2H), 3.85 (s, 3H).

^{13}C-NMR (125.7 MHz; $CDCl_3$) (δ [ppm])

159.20, 142.18, 139.97, 139.34, 133.15, 131.29, 129.75, 128.66, 128.12, 127.39, 126.18, 122.59, 114.20, 55.32.

7.2.54 2-Bromo-2',7,7'-triiodo-9,9'-spirobifluorene (70)

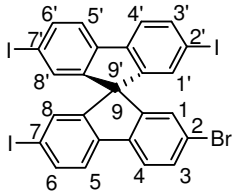

In a 250 mL three necked r. b. flask charged with a dropping funnel, N_2 stream and a strongly stirred solution of 6.20 g (15.7 mmol) 2-bromo-9,9'-spirobifluorene and 8.03 g (31.6 mmol) iodine in 35 mL $CHCl_3$, a suspension of 14.6 g (34.0 mmol) bis(trifluoroacetoxy)iodobezene in 70 mL $CHCl_3$ was added dropwise within 1 h, where the temperature was maintained at 0-5 °C. The solution was left stirred at the same temperature for 1 h and at RT overnight. The product formed was dissolved in 500 mL $CHCl_3$ and the solution was made alkaline by adding $NaHCO_3$ and aqueous Na_2SO_3 solution. After separating the organic phase, it was washed with distilled water and dried over Na_2SO_4 then the solvent was removed by rotary evaporator.

$C_{25}H_{12}BrI_3$ (772.99 g/mol)

Yield: 9.10 g (11.8 mmol, 75%), white amorph.

MS (MALDI): *m/z* (%) = 773.3 (100) [M^+].

^{1}H-NMR (500 MHz; $CDCl_3$) (δ [ppm])

7.71 (m, 3H, H6, H3', H6'), 7.66 (d, *J* = 8.16 Hz, 1H, H3), 7.56-7.53 (m, 3H, H5, H4', H5'), 7.51 (dd, *J* = 8.17, 1.79 Hz, 1H, H4), 7.00-6.96 (m, 3H, H8, H1', H8'), 6.79 (d, *J* = 1.77 Hz, 1H, H1).

^{13}C-NMR (125.7 MHz; $CDCl_3$ (δ [ppm])

148.82, 148.66, 148.62, 140.22, 140.14, 139.58, 137.57, 137.55, 133.07, 133.00, 131.69, 127.24, 122.28, 121.97, 121.94, 121.69, 93.76, 93.62, 64.81.

7.2.55 2-Bromo-2',7,7'-triphenyl-9,9'-spirobifluorene (71)

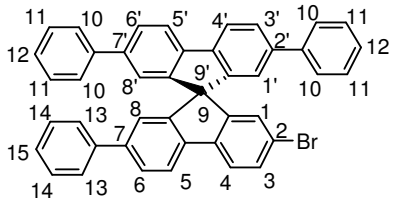

In a Young flask, containing a magnetic stirrer, 3.40 g (4.40 mmol) 2-bromo-2',7,7'-triiodo-9,9'-spirobifluorene, 1.61 g (13.20 mmol) phenyl boronic acid, 3.65 g (26.40 mmol) K_2CO_3 were taken. Then, 30 mL toluene, 20 mL THF and 15 mL water were added to it. A pipette was dipped into the mixture to blow nitrogen gas into the solution for an hour. After that, 0.37 g (2.4 mol%) palladium(0)tetrakis(triphenylphosphine) was added in nitrogen gas atmosphere and then the flask was evacuated and refluxed at 80 °C for about 17 hours in the nitrogen gas atmosphere. The rest workout was followed as in **7.2.12**.

$C_{43}H_{27}Br$ (623.60 g/mol)

Yield: 1.48 g (2.37 mmol, 54%), white amorph.

MS (MALDI): *m/z* (%) = 623.84 (100) [M^+].

^{1}H-NMR (500 MHz; $CDCl_3$) (δ [ppm])

7.94 (d, *J* = 7.99 Hz, 2H, H4', H5'), 7.89 (d, *J* = 7.92 Hz, 1H, H5), 7.74 (d, *J* = 8.11 Hz, 1H, H4), 7.67-7.62 (m, 3H, H3', H6', H3), 7.51 (dd, *J* = 8.14, 1.79 Hz, 1H, H6), 7.48-7.40 (m, 6H, H10, H11), 7.35-7.26 (m, 6H, H11, H14), 7.25-7.20 (m, 3H, H12, H15), 7.02 (d, *J* = 1.32 Hz, 1H, H8), 6.98 (d, *J* =5.33 Hz, 2H, H1', H8'), 6.95 (d, *J* = 1.67 Hz, 1H, H1).

^{13}C-NMR (125.7 MHz; $CDCl_3$) (δ [ppm])

151.00, 149.11, 148.87, 141.47, 141.12, 140.74, 140.66, 140.56, 140.39, 139.86, 131.06, 128.59, 128.57, 127.38, 127.25, 127.23, 127.15, 127.05, 122.87, 122.74, 121.51, 121.41, 120.48, 120.40, 65.95.

7.2.56 2,2',7,7'-Tetrakis(2',7,7'-triphenyl-9,9'-spirobifluorene-2-yl)-9,9'-spirobifluorene (72)

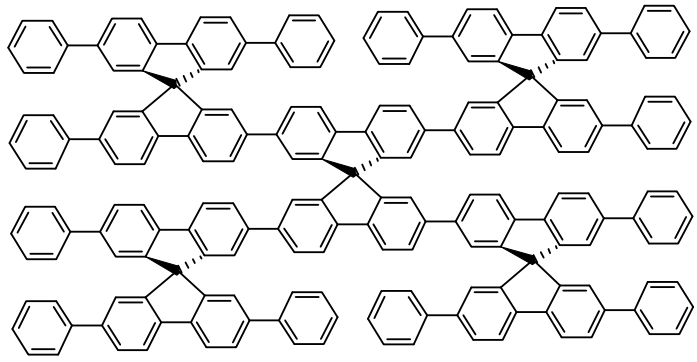

In a Young flask, containing a magnetic stirrer, 1.00 g (1.60 mmol) 2-bromo-2',7,7'-triphenyl-9,9'-spirobifluorene, 0.31 g (0.38 mmol) 2,2',7,7'-tetrakis(boronic pinacolate)-9,9'-spirobifluorene, 0.44 g (3.20 mmol) K_2CO_3 were taken. Then, 50 mL toluene, 60 mL THF and 30 mL water were added to it. A pipette was dipped into the mixture to blow nitrogen gas into the solution for an hour. After that, 0.04 g (2.5 mol%) palladium(0)tetrakis(triphenylphosphine) were added in nitrogen gas atmosphere and then the flask was evacuated and refluxed at 80 °C for about 48 hours. The rest workout was followed as in **7.2.12**.

$C_{197}H_{120}$ (2487.15 g/mol)

Yield: 0.33 g (0.13 mmol, 35%), white amorph.

MS (MALDI): *m/z* (%) = 2486.93 (100) [M^+].

^{1}H-NMR (500 MHz; $CDCl_3$) (δ [ppm])

7.83 (d, *J* = 7.95 Hz, 4x2H), 7.79 (d, *J* = 7.99 Hz, 4x1H), 7.63 (d, *J* = 8.01 Hz, 4x2H), 7.58-7.53 (m, 4x3H), 7.40-7.29 (m, 4x8H), 7.29-7.12 (m, 4x10H), 6.92-6.87 (m, 4x3H), 6.77 (d, *J* = 1.05 Hz, 4x1H).

^{13}C-NMR (125.7 MHz; $CDCl_3$) (δ [ppm])

149.83, 149.58, 149.41, 149.22, 140.87, 140.84, 140.78, 140.59, 140.56, 140.51, 140.46, 128.72, 128.59, 128.50, 127.33, 127.21, 127.20, 127.16, 127.13, 127.06, 127.02, 126.95, 122.75, 122.64, 122.42, 120.30, 120.24, 120.10, 66.13.

Elemental Analysis: Found (%) Calculated (%)

C: 93.68	C: 95.14
H: 5.00	H: 4.86

7.2.57 2-Bromo-9-(4'-methoxy-biphenyl-2-yl)-fluoren-9-ol

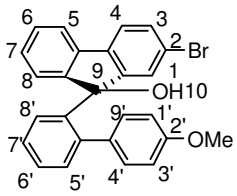

To a solution of 2.41 g (9.15 mmol) 2-bromo-4'-methoxy-biphenyl in 50 mL THF, 0.90 g (13.72 mmol) *n*-BuLi solution was added dropwise slowly at –80 °C. After the complete addition, the reaction mixture was left to stir for about an hour at the same temperature. Then, at the same temperature, a solution of 2.41 g (9.15 mmol) 2-bromofluoren-9-one in 100 mL THF was added dropwise to the reaction mixture. It was left to stir at room temperature for 20 h. The reaction was quenched with the addition of 100 mL water. It was left to stir for 2 h at RT and concentrated by rotary evaporator. The reaction mixture was then treated with ethyl acetate, washed with 1 N HCl. The organic phase was dried over Na_2SO_4 and concentrated by rotary evaporator.

$C_{26}H_{19}BrO_2$ (443.34 g/mol)

Yield: 3.24 g (7.32 mmol, 80%), colourless crystal.

MS (MALDI): *m/z* (%) = 443.83 (100) [M^+].

^{1}H-NMR (500 MHz; $CDCl_3$) (δ [ppm])

8.46 (d, *J* = 7.92 Hz, 1H, H5), 7.58 (t, *J* = 7.77, 7.77 Hz, 1H, H6), 7.40-7.33 (m, 3H, H3, H2, H6'), 7.26 (m, 4H, H7, H7', H5', H1), 7.10 (d, *J* = 8.54 Hz, 1H, H8'), 6.97 (dd, *J* = 7.45, 1.28 Hz, 1H, H8), 6.31-6.23 (m, 1H, H9'), 6.20-6.18 (m, 1H, H1'), 6.12-6.05 (m, 1H, H3'), 5.96-5.84 (m, 1H, H4'), 3.71 (s, 3H, -OCH_3), 2.31 (s, 1H, -OH).

^{13}C-NMR (125.7 MHz; $CDCl_3$) (δ [ppm])

157.16, 152.59, 150.31, 140.52, 139.36, 139.16, 139.04, 132.76, 131.65, 131.54, 128.90, 128.30, 127.64, 127.21, 127.16, 126.20, 124.33, 121.42, 121.28, 120.08, 111.88, 111.87, 111.86, 82.27, 55.20.

Crystal data and structure refinement for I0363 (MDS0189)

Identification code	i0363
Empirical formula	$C_{26}H_{19}BrO_2$
Formula weight	443.32
Temperature	133(2) K
Wavelength	0.71073 A
Crystal system	Monoclinic
Space group	P 21/n

Unit cell dimensions	a = 8.7395(8) A	alpha = 90 deg.
	b = 16.2171(18) A	beta = 92.120(7) deg.
	c = 13.9863(13) A	gamma = 90 deg.
Volume	1980.9(3) A^3	
Z	4	
Density (calculated)	1.486 Mg/m^3	
Absorption coefficient	2.095 mm^{-1}	
F(000)	904	
Theta range for data collection	1.92 to 25.00 deg.	
Index ranges	-10<=h<=10, -19<=k<=19, -14<=l<=16	
Reflections collected	12726	
Independent reflections	3489 [R(int) = 0.0923]	
Reflections observed	2806	
Refinement method	Full-matrix least-squares on F^2	
Data / restraints / parameters	3489 / 0 / 264	
Goodness-of-fit on F^2	0.994	
Final R indices [I>2sigma(I)]	R1 = 0.0475, wR2 = 0.1158	
R indices (all data)	R1 = 0.0580, wR2 = 0.1199	
Largest diff. peak and hole	0.923 and -1.350 $e.A^{-3}$	

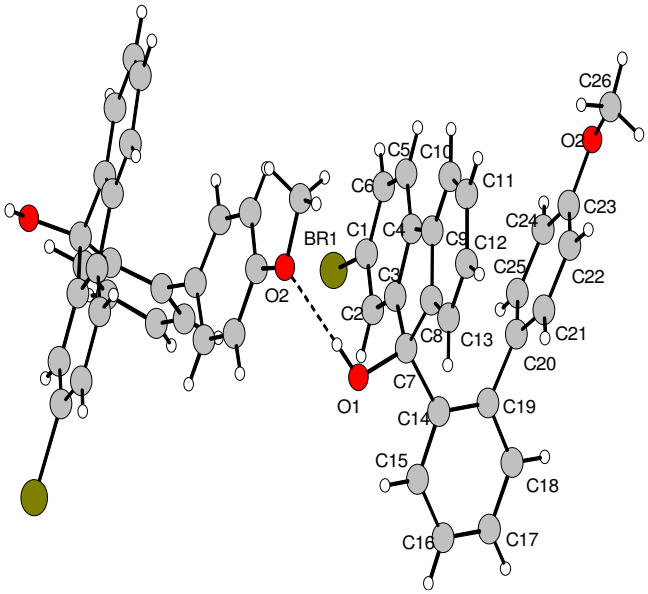

7.2.58 2-Bromo-2'-methoxy-9,9'-spirobifluorene (73)

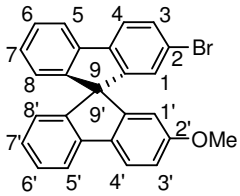

3.24 g (7.32 mmol) 2-bromo-9-(4'-methoxy-biphenyl-2-yl)-fluoren-9-ol was dehydrolysed with a mixture 25 mL conc. acetic acid and 5 mL conc. HCl, then refluxed for two hours. It was filtered and slowly stirred with water and dried.

$C_{26}H_{17}BrO$ (425.33 g/mol)

Yield: 2.92 g (6.86 mmol, 75%), white amorph.

MS (MALDI): *m/z* (%) = 426.04 (100) [M^+].

^{1}H-NMR (500 MHz; $CDCl_3$) (δ [ppm])

7.80 (d, *J* = 7.62 Hz, 1H, H5), 7.74 (d, *J* = 8.34 Hz, 2H, H4, H3), 7.70 (d, *J* = 8.12 Hz, 1H, 5'), 7.48 (dd, *J* = 8.12, 1.77 Hz, 1H, H4'), 7.39-7.30 (m, 2H, H7, H7'), 7.13 (t, *J* = 7.57, 7.57 Hz, 1H, H6'), 7.05 (t, *J* = 7.55 Hz, 1H, H6), 6.93 (dd, *J* = 8.40, 2.39 Hz, 1H, H3'), 6.88 (d, *J* = 1.70 Hz, 1H, H1), 6.75 (d, *J* = 7.61 Hz, 1H, H8'), 6.68 (d, *J* = 7.57 Hz, 1H, H8), 6.25 (d, *J* = 2.31 Hz, 1H, H11) 3.64 (s, 3H, -OCH_3).

^{13}C-NMR (125.7 MHz; $CDCl_3$) (δ [ppm])

159.89, 150.92, 149.62, 148.63, 147.46, 141.62, 140.63, 140.52, 134.56, 130.84, 128.23, 127.90, 127.86, 127.28, 126.70, 124.12, 123.80, 121.38, 121.26, 120.84, 119.98, 119.25, 114.05, 109.32, 65.73, 55.36.

7.2.59 2-(9,9'-Spirobifluorene-2-yl)-4,4,5,5-tetramethyl-1,3,2-dioxaborolane (74)

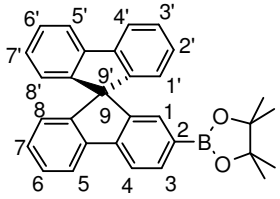

A flask assembled a magnetic stirring bar, a septum inlet, and a condenser was charged with 0.06 g (1.5% mmol) $Pd_2(dba)_3$ and 0.09 g (0.32 mmol) tricyclohexylphosphine and flushed with nitrogen. Dioxane was added and resulting mixture was then stirred for 30 min at room temperature. 1.37 g (5.40 mmol) bis(pinacolato)diboron, 0.66 g (6.75 mmol) KOAc, and 2.00 g (5.05 mmol) 2-bromo-9,9'-spirobifluorene were added successively. After being stirred at 80 °C for 16 h, the reaction mixture was treated with water at room temperature. The product was extracted with toluene washed with brine, and dried over $MgSO_4$. Column chromatography gave an analytically pure sample.[81]

$C_{31}H_{27}BO_2$ (442.37 g/mol)

Yield: 1.52 g (3.43 mmol, 68%), white amorph.

^{1}H-NMR (500 MHz; $CDCl_3$) (δ [ppm])

7.90-7.87 (m, 5H, H4, H3, H4', H5'), 7.45-7.36 (m, 3H, H6, H3', H6'), 7.30 (s, 1H, H1), 7.18-7.10 (m, 3H, H7, H2', H7'), 6.78-6.71 (m, 3H, H1', H8', H8), 1.30 (s, 12H, $-CH_3$).

^{13}C-NMR (125.7 MHz; $CDCl_3$) (δ [ppm])

149.65, 148.54, 147.63, 144.87, 141.87, 141.27, 134.75, 130.22, 128.29, 127.72, 127.60, 124.11, 124.06, 123.92, 120.35, 119.97, 119.93, 119.30, 83.66, 65.87, 24.77.

IR (ATR): $\bar{\nu}$ (cm^{-1}) = 2977, 1310, 1416, 1356, 1142, 858, 725, 632.

7.2.60 2'-Methoxy-2-(9,9'-spirobifluorene-2-yl)-9,9'-spirobifluorene (75)

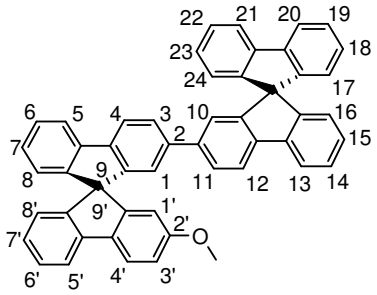

In a Young flask, containing a magnetic stirrer, 1.86 g (4.37 mmol) 2-bromo-2'-methoxy-9,9'-spirobifluorene, 2.12 g (4.80 mmol) pinacol 9,9'-spirobifluorene-2-yl borane, 1.33 g (9.60 mmol) K_2CO_3 were taken. Then, 80 mL toluene, 60 mL THF and 30 mL water were added to it. A pipette was dipped into the mixture to blow nitrogen gas into the solution for an hour. After that, 0.14 g (2.5 mol%) palladium(0)tetrakis(triphenylphosphine) was added in nitrogen gas atmosphere and then the flask was evacuated and refluxed at 80 °C for about 17 hours. The rest workout was followed as in **7.2.12**.

$C_{51}H_{32}O$ (660.82 g/mol)

Yield: 1.87 g (2.84 mmol, 65%), white amorph.

MS (MALDI)**:** *m/z* (%) = 660.16 (100) [M^+].

Melting Point: 366 °C

^{1}H-NMR (500 MHz; $CDCl_3$) (δ [ppm])

7.83 (d, *J* = 7.58 Hz, 2H, H20, H21), 7.78-7.75 (m, 2H, H4', H5'), 7.74-7.70 (m, 4H, H4, H5, H12, H13), 7.41-7.27 (m, 7H, H7, H15, H18, H23, H6', H19, H22), 7.08-7.03 (m, 4H, H8, H16, H17, H24), 6.99 (t, *J* = 7.48, 7.48 Hz, 1H, H7'), 6.92-6.83 (m, 3H, H8', H1, H10), 6.71

(dd, *J* = 7.35, 2.89 Hz, 2H, H3, H11), 6.67-6.63 (m, 3H, H3', H6, H14), 6.22 (d, *J* = 1.79 Hz, 1H, H1'), 3.59 (s, 3H, -OCH_3).

^{13}C-NMR (125.7 MHz; $CDCl_3$) (δ [ppm])

159.81, 150.40, 149.37, 149.19, 149.17, 149.01, 148.64, 148.28, 141.72, 141.71, 141.66, 141.15, 141.08, 140.97, 140.90, 140.82, 140.81, 134.64, 127.81, 127.73, 127.71, 127.67, 127.61, 127.14, 127.10, 126.60, 124.11, 123.91, 123.83, 122.63, 122.53, 120.72, 120.02, 119.99, 119.98, 119.95, 119.91, 119.12, 113.96, 109.25, 65.95, 55.34.

IR (ATR): $\bar{\nu}$ (cm^{-1}) = 3038, 1445, 1269, 826,765, 605.

7.2.61 2'-Hydroxy-2-(9,9'-spirobifluorene-2-yl)-9,9'-spirobifluorene (76)

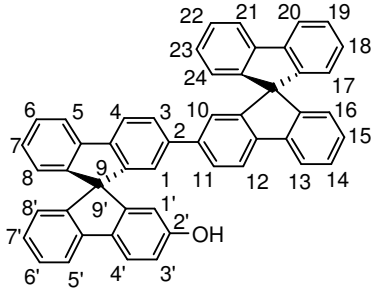

To a solution of 1.88 g (2.84 mmol) 2-methoxy-2'-(9,9'-spirobifluorene-2-yl)-9,9'-spirobifluorene in absolute 75 mL CH_2Cl_2, 2.14 g (8.52 mmol) BBr_3 was added at 0 °C, the mixture was stirred at room temperature for 16 h. 100 mL water were added, the organic layer was separated and evaporated to dryness which became grayish amorphous powder.

$C_{50}H_{30}O$ (646.80 g/mol)

Yield: 1.65 g (2.55 mmol, 90%), grayish amorphous powder.

MS (MALDI): *m/z* (%) = 646.12 (100) [M^+].

^{1}H-NMR (500 MHz; $CDCl_3$) (δ [ppm])

7.82 (d, *J* = 7.65 Hz, 2H, H20, H21), 7.80-7.64 (m, 6H, H4', H5', H4, H5, H12, H13), 7.42-7.26 (m, 7H, H7, H15, H18, H23, H6', H19, H22), 7.08-7.03 (m, 4H, H8, H17, H24), 7.00 (t, *J* = 7.47, 7.47 Hz, 1H, H7'), 6.86 (d, *J* = 7.23 Hz, 2H, H1, H10), 6.81 (dd, *J* = 8.23, 2.33 Hz, 1H, H8'), 6.71 (d, *J* = 7.58 Hz, 2H, H3, H11), 6.69-6.61 (m, 3H, H3', H6, H14), 6.13 (d, *J* = 2.21 Hz, 1H, H1'), 5.28 (s, 1H, -OH).

^{13}C-NMR (125.7 MHz; $CDCl_3$) (δ [ppm])

155.53, 150.71, 149.22, 149.19, 149.04, 148.64, 148.04, 141.72, 141.63, 141.14, 141.05, 141.00, 140.88, 140.85, 140.79, 134.75, 127.81, 127.73, 127.68, 127.63, 127.17, 127.13,

126.69, 124.12, 124.11, 123.97, 123.90, 123.83, 122.63, 122.57, 121.01, 120.01, 119.97, 119.95, 119.93, 119.13, 115.04, 111.10, 65.95, 65.79.

7.2.62 2'-(9,9'-Spirobifluorene-2-yl)-9,9'-spirobifluorene-2-yl trifluoromethyl sulfonate (77)

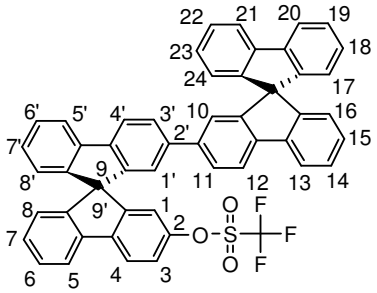

A solution of 2.09 g (3.23 mmol) 2-hydroxy-2'-(9,9'-spirobifluorene-2-yl)-9,9'-spirobifluorene in 50 mL pyridine and 50 mL dichloromethane was stirred at -20 °C under N_2 and treated dropwise with the solution of 2.27 g (8.07 mmol) $(CF_3SO_2)_2O$ in 50 mL dichloromethane. The mixture was stirred at -20 °C for 1 h and at 25 °C for 24 h. The mixture was then diluted with water and extracted with CH_2Cl_2. The organic layer was washed with water and brine, dried over $MgSO_4$, and filtered. Volatiles were then removed under reduced pressure.

$C_{51}H_{29}F_3O_3S$ (778.86 g/mol)

Yield: 2.20 g (2.82 mmol, 88%), white amorph.

MS (MALDI)**:** *m/z* **(%) =** 777.68 (100) [M^+].

^{1}H-NMR (500 MHz; $CDCl_3$) (δ [ppm])

7.86 (d, *J* = 8.45 Hz, 2H, H20, H21), 7.84-7.81 (m, 2H, H4', H5'), 7.81-7.77 (m, 2H, H12, H13), 7.74 (dd, *J* = 7.95, 4.20 Hz, 2H, H4, H5), 7.38-7.29 (m, 7H, H6', H19, H22, H7', H15, H18, H23), 7.27 (dd, *J* = 8.43, 2.24 Hz, 1H, H3), 7.14-7.01 (m, 5H, H8, H8', H16, H17, H24), 6.85 (s, 1H, H10), 6.82 (s, 1H, H11), 6.74-6.67 (m, 3H, H3', H11, H7), 6.65-6.62 (m, 2H, H6', H14), 6.58 (d, *J* = 2.17 Hz, 1H, H1).

^{13}C-NMR (125.7 MHz; $CDCl_3$) (δ [ppm])

151.08, 149.19, 149.11, 149.06, 148.87, 148.61, 147.70, 147.67, 141.98, 141.71, 141.15, 141.12, 141.09, 140.87, 140.63, 139.72, 128.66, 128.14, 128.03, 127.97, 12.83, 127.79, 127.78, 127.70, 127.69, 127.65, 127.63, 127.05, 124.24, 124.12, 124.07, 123.85, 123.72,

122.54, 122.39, 121.14, 121.01, 120.40, 120.25, 120.22, 120.07, 119.97, 119.96, 117.43, 65.96, 65.92.

IR (ATR): $\bar{\nu}$ (cm^{-1}) = 3064, 1420, 1205, 1200, 858, 760, 603.

7.2.63 2'-[2-(9,9'-spirobifluorene-2-yl)-9,9'-spirobifluorene-2-yl]-4,4,5,5-tetramethyl-1,3,2-dioxaborolane (78)[81]

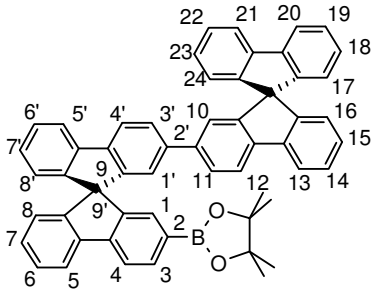

A flask assembled a magnetic stirring bar, a septum inlet, and a condenser was charged with 0.04 g (0.04 mmol) $Pd_2(dba)_3$ and 0.06 g (0.20 mmol) tricyclohexylphosphine and flushed with nitrogen. Dioxane was added and resulting mixture was then stirred for 30 min at room temperature. 1.07 g (4.23 mmol) bis(pinacolato)diboron, 0.41 g (4.23 mmol) KOAc, and 2.20 g (2.82 mmol) 2'-(9,9'-spirobifluorene-2-yl)-9,9'-spirobifluorene-2-yl trifluoromethyl sulfonate were added successively. After being stirred at 80 °C for 16 h, the reaction mixture was treated with water at room temperature. The product was extracted with toluene washed with brine, and dried over $MgSO_4$. Column chromatography gave an analytically pure sample. An analogous synthesis is explained in Ishiyama et. al. [81]

$C_{56}H_{41}BO_2$ (756.76 g/mol)

Yield: 1.25 g (1.66 mmol, 59%), white amorph.

MS (MALDI)**:** *m/z* (%) = 756.55 (100) [M^+].

^{1}H-NMR (500 MHz; $CDCl_3$) (δ [ppm])

7.83-7.81 (m, 5H, H4', H5', H12, H13, H3), 7.77 (d, *J* = 7.55 Hz, 2H, H20, H21), 7.72 (d, *J* = 8.00 Hz, 2H, H4, H5), 7.39-7.27 (m, 7H, H6, H19, H22, H7', H15, H18, H23), 7.16 (s, 1H, H1), 7.09-7.00 (m, 5H, H8, H8', H16, H17, H24), 6.84 (dd, *J* = 12.27, 1.12 Hz, 2H, H1', H10), 6.74-6.67 (m, 2H, H6', H14), 6.66-6.59 (m, 3H, H3, H11, H7), 1.23 (s, 12H, -CH_3).

^{13}C-NMR (125.7 MHz; $CDCl_3$) (δ [ppm])

149.60, 149.22, 149.03, 149.02, 148.84, 148.65, 148.62, 147.56, 144.88, 141.71, 141.32, 141.26, 141.17, 141.12, 140.94, 140.81, 140.68, 134.75, 130.27, 128.32, 127.82, 127.79,

127.73, 127.66, 127.60, 127.57, 127.11, 127.05, 124.11, 124.09, 124.02, 123.96, 123.82, 122.65, 122.49, 120.37, 120.00, 119.97, 119.93, 119.33, 83.67, 65.96, 65.93, 24.78.

IR (ATR): $\bar{\nu}$ (cm^{-1}) = 2976, 1354.

7.2.64 2,2',7,7'-Tetrakis[2'-(9,9'-spirobifluorene-2-yl)-9,9'-spirobifluorene -2-yl]-9,9'-spirobifluorene (79)

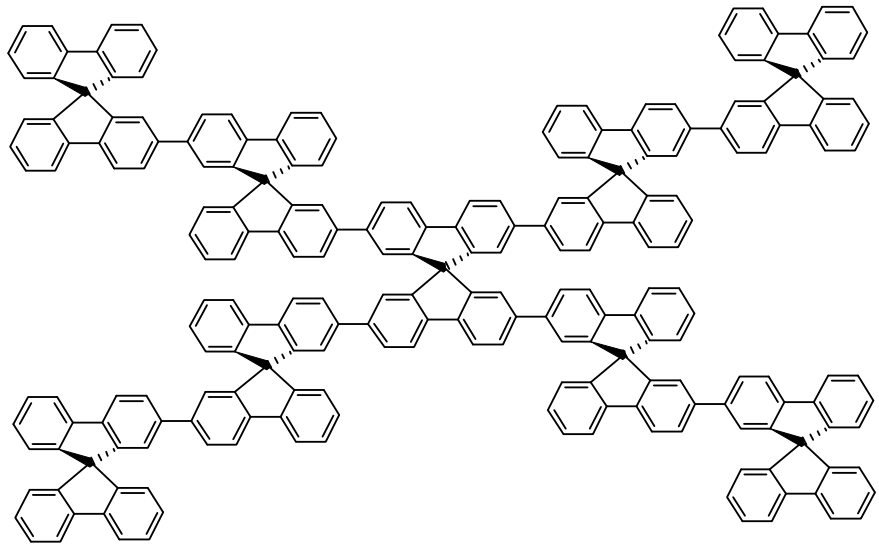

In a Young flask, containing a magnetic stirrer, 0.20g (0.32 mmol) 2,2',7,7'-tetrabromo-9,9'-spirobifluorene, 0.99 g (1.30 mmol) pinacol 2'-(9,9'-spirobifluorene-2-yl)-9,9'-spirobifluorene-2-yl borane, 0.36 g (2.60 mmol) K_2CO_3 were taken. Then, 80 mL toluene, 60 mL THF and 30 mL water were added to it. A pipette was dipped into the mixture to blow nitrogen gas into the solution for an hour. After that, 0.03 g (2.5 mol%) palladium(0)tetrakis(triphenylphosphine) was added in nitrogen gas atmosphere and then the flask was evacuated and refluxed at 80 °C for about 48 hours. The rest workout was followed as in **7.2.12**.

$C_{225}H_{128}$ (2831.53 g/mol)

Yield: 0.48 g (0.17 mmol, 54%), white amorph.

^{1}H-NMR (500 MHz; $CDCl_3$) (δ [ppm])

7.89 (d, *J* = 7.98 Hz, 4x1H), 7.84 (d, *J* = 7.60 Hz, 4x1H), 7.82 (d, *J* = 7.67 Hz, 4x2H), 7.78 (t, *J* = 7.59, 7.59 Hz, 4x2H), 7.74-7.71 (m, 4x2H), 7.61 (dd, *J* = 7.96, 1.61 Hz, 4x1H), 7.41-7.18 (m, 4x10H), 7.10-7.02 (m, 4x5H), 6.91 (d, *J* = 5.55 Hz, 4x2H), 6.87 (s, 4x1H), 6.73-6.68 (m, 4x4H), 6.64 (d, *J* = 7.55 Hz, 4x1H).

^{13}C-NMR (125.7 MHz; $CDCl_3$) (δ [ppm])

149.33, 149.20, 149.15, 149.02, 148.98, 148.64, 141.71, 141.35, 141.18, 141.15, 140.99, 140.98, 140.85, 140.81, 140.80, 128.51, 127.81, 127.76, 127.73, 127.70, 127.66, 127.61, 127.17, 127.15, 127.08, 127.00, 126.82, 124.11, 123.95, 123.83, 122.74, 122.63, 122.53, 120.26, 120.03, 120.01, 119.99, 119.97, 119.94, 66.03, 65.96.

Elemental Analysis: Found (%)	Calculated (%)
C: 94.78	C: 95.44
H: 4.86	H: 4.56

7.2.65 2'-Methoxy-2,7-bis(9,9'-spirobifluorene-2-yl)-9,9'-spirobifluorene (80)

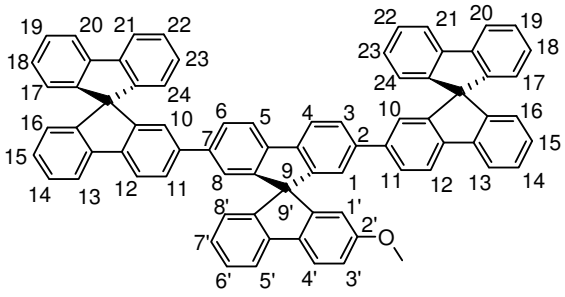

In a Young flask, containing a magnetic stirrer, 2.74 g (5.43 mmol) 2,7-dibromo-2'-methoxy-9,9'-spirobifluorene, 5.28 g (11.95 mmol) pinacol 9,9-spirobifluuorene-2-yl borane, 3.30 g (23.90 mmol) K_2CO_3 were taken. Then, 30 mL toluene, 20 mL THF and 15 mL water were added to it. A pipette was dipped into the mixture to blow nitrogen gas into the solution for an hour. After that, 0.35 g (2.4 mol%) palladium(0)tetrakis(triphenylphosphine) was added in nitrogen gas atmosphere and then the flask was evacuated and refluxed at 80 °C for about 48 hours. The rest workout was followed as in **7.2.12**.

$C_{76}H_{46}O$ (975.21 g/mol)

Yield: 3.75 g (3.85 mmol, 71%), white amorph.

MS (MALDI)**:** *m/z* (%) = 974.06 (100) [M^+].

^{1}H-NMR (500 MHz; $CDCl_3$) (δ [ppm])

7.82 (d, *J* = 7.63 Hz, 4H, H20, H21), 7.76 (d, *J* = 7.67 Hz, 2H, H4, H5), 7.72-7.69 (m, 4H, H12, H13), 7.66 (dd, *J* = 8.15, 3.26 Hz, 2H, H4', H5'), 7.39-7.26 (m, 11H, H15, H18, H19, H22, H23, H6'), 7.07-7.02 (m, 6H, H16, H17, H24), 6.96 (t, *J* = 7.43, 7.43 Hz, 1H, H7'), 6.87 (dd, *J* = 8.43, 2.38 Hz, 1H, H8'), 6.84 (d, *J* = 1.18 Hz, 2H, H1, H8), 6.80 (d, *J* = 1.16 Hz, 2H,

H10), 6.71-6.69 (m, 4H, H3, H6, H11), 6.64-6.61 (m, 3H, H3', H14), 6.20 (d, *J* = 2.31 Hz, 1H, H1'), 3.57 (s, 3H, -OCH_3).

^{13}C-NMR (125.7 MHz; $CDCl_3$) (δ [ppm])

159.78, 150.31, 149.67, 149.18, 149.01, 148.63, 141.71, 141.70, 141.67, 141.15, 140.96, 140.79, 140.74, 140.33, 134.63, 127.80, 127.70, 127.66, 127.61, 127.10, 127.06, 126.61, 124.11, 124.01, 123.83, 122.51, 122.47, 120.75, 119.96, 119.94, 119.15, 114.03, 109.30, 65.95, 55.33.

IR (ATR): $\bar{\nu}$ (cm^{-1}) = 3060, 1607, 1446, 1265, 815, 743, 629.

7.2.66 2'-Hydroxy-2,7-bis(9,9'-spirobifluorene-2-yl)-9,9'-spirobifluorene (81)

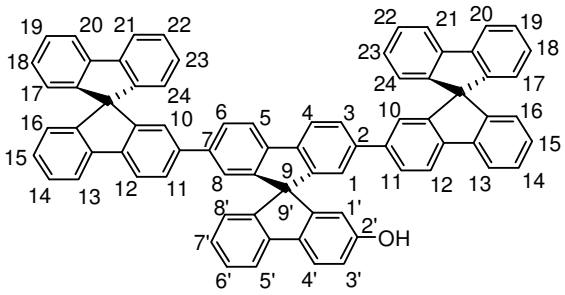

To a solution of 2-methoxy-2',7'-bis(9,9'-spirobifluorene-2-yl)-9,9'-spirobifluorene in absolute CH_2Cl_2, 2.38 g (9.51 mmol) BBr_3 was added at 0 °C, the mixture was stirred at room temperature for 16 h. 100 mL water were added, the organic layer was separated and evaporated to dryness which gave grayish amorph which was subjected to recrystallization (THF/*n*-propanol) for purification.

$C_{75}H_{44}O$ (961.19 g/mol)

Yield: 2.83 g, (2.94 mmol, 84%), white amorph.

MS (MALDI)**:** *m/z* (%) = 960.09 (100) [M^+].

Melting Point: 444 °C

^{1}H-NMR (500 MHz; $CDCl_3$) (δ [ppm])

7.81 (d, *J* = 7.63 Hz, 4H, H20, H21), 7.76 (d, *J* = 7.633 Hz, 2H, H4, H5), 7.72-7.63 (m, 6H, H12, H13, H4', H5'), 7.37-7.26 (m, 11H, H15, H18, H19, H22, H23, H6'), 7.07-7.02 (m, 6H, H16, H17, H24), 6.97 (t, *J* = 7.44, 7.44 Hz, 1H, H7'), 6.84-6.77 (m, 5H, H1, H8, H8', H10), 6.73-6.67 (m, 4H, H3, H6, H11), 6.64 (d, *J* = 7.59 Hz, 3H, H3', H14), 6.11 (d, *J* = 2.27 Hz, 1H, H1').

^{13}C-NMR (125.7 MHz; $CDCl_3$) (δ [ppm])

155.61, 150.57, 149.54, 149.17, 149.01, 148.62, 147.96, 141.70, 141.69, 141.67, 141.14, 140.97, 140.79, 140.77, 140.27, 134.65, 127.84, 127.80, 127.71, 127.66, 127.62, 127.11, 127.09, 126.66, 124.11, 124.10, 124.07, 124.06, 123.83, 122.55, 122.47, 121.03, 119.99, 119.95, 119.14, 115.10, 111.21, 65.94, 65.81.

IR (ATR): $\bar{\nu}$ (cm^{-1}) = 3920, 1446, 1262, 850, 727.

7.2.67 2',7'-Bis(9,9'-spirobifluorene-2-yl)-9,9'-spirobifluorene-2-yl trifluoromethyl sulfonate (82)

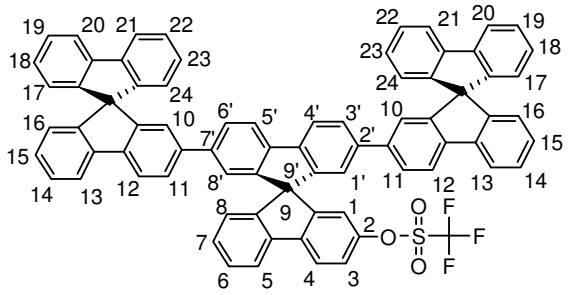

A solution of 2-hydroxy-2',7'-bis(9,9'-spirobifluorene-2-yl)-9,9'-spirobifluorene in 100 mL pyridine and 50 mL dichloromethane was stirred at -20 °C under N_2 and treated dropwise with the solution of 1.88 g (6.67 mmol) $(CF_3SO_2)_2O$ in 50 mL dichloromethane. The mixture was stirred at -20 °C for 1 h and at 25 °C for 24 h. The mixture was then diluted with water and extracted with CH_2Cl_2. The organic layer was washed with water and brine, dried over $MgSO_4$, and filtered. Volatiles were then removed under reduced pressure.

$C_{76}H_{43}F_3O_3S$ (1093.25 g/mol)

Yield: 2.27 g, (2.08 mmol, 78%), white amorph.

MS (MALDI): *m/z* (%) = 1091.68 (100) [M^+].

^{1}H-NMR (500 MHz; $CDCl_3$) (δ [ppm])

7.86 (d, *J* = 8.41 Hz, 1H, H5), 7.82 (dd, *J* = 7.66, 3.99 Hz, 4H, H20, H21), 7.79-7.75 (m, 3H, H4, H4', H5'), 7.73 (d, *J* = 8.04 Hz, 2H, H12), 7.68 (d, *J* = 8.05 Hz, 2H, H13), 7.38-7.28 (m, 11H, H15, H18, H19, H22, H23, H6), 7.27 (d, *J* = 2.25 Hz, 1H, H3), 7.08-7.03 (m, 7H, H16, H17, H24, H7), 6.82 (s, 2H, H1', H8'), 6.75 (s, 2H, H10), 6.73-6.61 (m, 7H, H3', H5', H11, H8, H14), 6.57 (d, *J* = 2.10 Hz, 1H, H1).

^{13}C-NMR (125.7 MHz; $CDCl_3$) (δ [ppm])

150.94, 149.17, 149.09, 148.96, 148.86, 148.58, 148.10, 142.00, 141.70, 141.10, 141.08, 141.06, 140.60, 140.31, 139.71, 128.67, 128.03, 127.82, 127.77, 127.68, 127.67, 127.65, 127.60, 127.02, 124.30, 124.11, 124.06, 123.85, 122.51, 122.26, 121.24, 121.07, 120.46, 120.24, 120.05, 119.96, 119.94, 117.47, 65.94, 65.92.

7.2.68 2-[2',7'-Bis(9,9'-spirobifluorene-2-yl)-9,9'-spirobifluorene-2-yl]-4,4,5,5-tetramethyl-1,3,2-borolane (83)

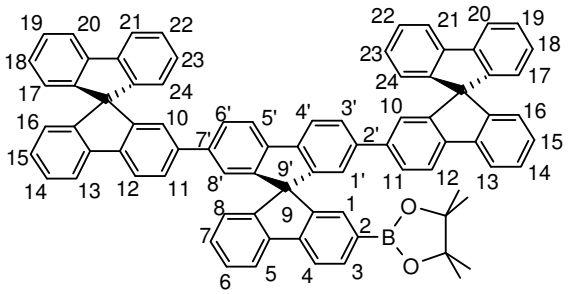

A flask assembled a magnetic stirring bar, a septum inlet, and a condenser was charged with 0.002 g (0.27 mmol) $Pd_2(dba)_3$ and 0.003 g (0.30 mmol) tricyclohexylphosphine and flushed with nitrogen. Dioxane was added and resulting mixture was then stirred for 30 min at room temperature. 0.07 g (0.27 mmol) bis(pinacolato)diboron, 0.03 g (0.30 mmol) KOAc, and 0.20 g (0.18 mmol) 2',7'-bis(9,9'-spirobifluorene-2-yl)-9,9'-spirobifluorene-2-yl trifluoromethyl sulfonate were added successively. After being stirred at 80 °C for 16 h the reaction mixture was treated with water at room temperature. The product was extracted with toluene washed with brine, and dried over $MgSO_4$. Column chromatography gave an analytically pure sample. An analogous synthesis is explained in Ishiyama et. al. [81]

$C_{81}H_{55}BO_2$ (1071.15 g/mol)

Yield: 0.13 g (0.12 mmol, 69%), white amorph.

MS (MALDI)**:** *m/z* (%) = 1071.23 (100) [M^+].

^{1}H-NMR (500 MHz; $CDCl_3$) (δ [ppm])

7.83-7.80 (m, 7H, H20, H21, H5, H4, H3), 7.76 (d, *J* = 7.62 Hz, 2H, H4', H5'), 7.70 (d, *J* = 8.04 Hz, 2H, H12), 7.65 (d, *J* = 8.02 Hz, 2H, H13), 7.36-7.26 (m, 11H, H15, H18, H19, H22, H23, H6), 7.14 (s, 1H, H1), 7.09-7.00 (m, 7H, H16, H17, H24, H7), 6.83 (s, 2H, H1', H8'), 6.76 (s, 2H, H10), 6.72-6.65 (m, 4H, H3', H6', H11), 6.64-6.60 (m, 3H, H14, H8), 1.22 (s, 12H, -CH_3).

^{13}C-NMR (125.7 MHz; $CDCl_3$) (δ [ppm])

149.53, 149.33, 149.20, 149.02, 148.63, 148.61, 147.48, 144.90, 141.74, 141.70, 141.24, 141.16, 140.92, 140.78, 140.62, 140.55, 134.75, 130.32, 128.37, 128.34, 127.87, 127.86, 127.81, 127.78, 127.67, 127.64, 127.59, 127.07, 127.01, 124.12, 124.11, 124.08, 123.82, 122.49, 122.46, 120.40, 120.04, 119.99, 119.96, 119.92, 119.37, 83.67, 65.96, 65.94, 24.78.

7.2.69 2,2',7,7'-Tetrakis[2',7'-bis(9,9'-spirobifluorene-2-yl)-9,9'-spirobifluorene-2-yl]-9,9'-spirobifluorene (84)

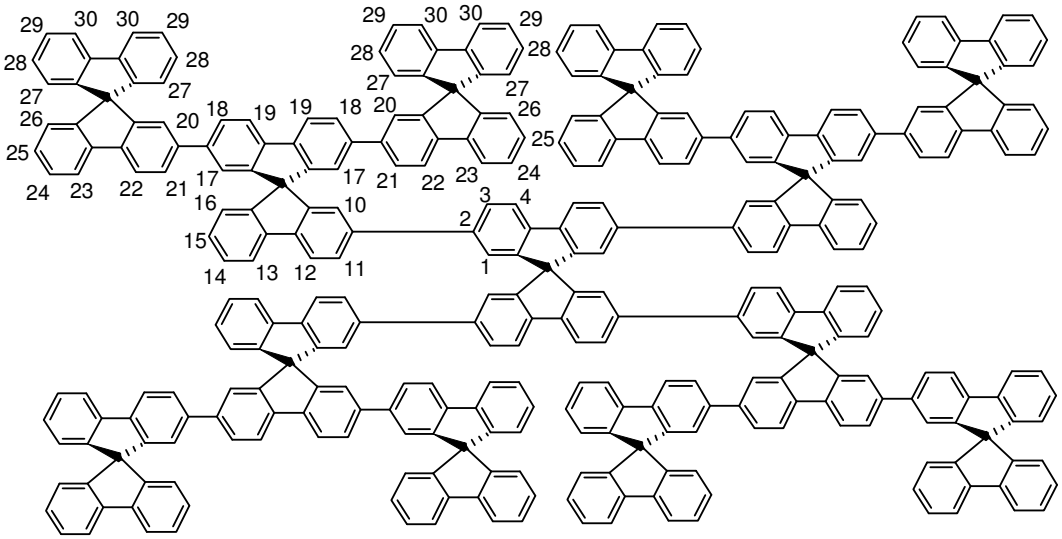

In a Young flask, containing a magnetic stirrer, 0.12 g (0.19 mmol), 2,2',7,7'-tetrabromo-9,9'-spirobifluorene, 0.92 g (0.86 mmol) pinacol 2',7'-bis(9,9'-spirobifluorene-2-yl)-9,9'-spirobifluorene-2-yl borane, 0.24 g (1.72 mmol) K_2CO_3 were taken. Then, 10 mL toluene, 20 mL THF and 25 mL water were added to it. A pipette was dipped into the mixture to blow nitrogen gas into the solution for an hour. After that, 0.02 g (2.5 mol%) palladium(0)tetrakis(triphenylphosphine) was added in nitrogen gas atmosphere and then the flask was evacuated and refluxed at 80 °C for about 48 hours. The rest workout was followed as in **7.2.12**.

$C_{325}H_{184}$ (4089.09 g/mol)

Yield: 0.16 g (2.08 mmol, 21%), white amorph.

^{1}H-NMR (500 MHz; $CDCl_3$) (δ [ppm])

7.81-7.76 (m, 4x4H, H30), 7.65 (d, *J* = 7.51 Hz, 4x1H, H4), 7.62 (d, *J* = 8.21 Hz, 4x1H, H12), 7.56 (d, *J* = 7.61 Hz, 4x2H, H23), 7.53 (d, *J* = 8.07 Hz, 4x1H, H13), 7.49 (d, *J* = 8.07 Hz, 4x2H, H22), 7.31 (d, *J* = 8.08 Hz, 4x2H, H19), 7.27 (t, *J* = 7.56, 7.56 Hz, 4x2H, H25),

7.23-7.15 (m, 4x8H, H28, H29), 7.12-7.08 (m, 4x2H, H14, H15), 7.03-6.95 (m, 4x6H, H26, H27), 6.89 (t, *J* = 7.41, 7.41 Hz, 4x2H, H24), 6.79 (s, 4x2H, H17), 6.77 (s, 4x1H, H10), 6.71 (s, 4x2H, H20), 6.66-6.60 (m, 4x7H, H18, H21, H3, H11, H1), 6.56 (d, *J* = 7.44 Hz, 4x1H, H16).

^{13}C-NMR (125.7 MHz; $CDCl_3$) (δ [ppm])

149.31, 149.20, 149.18, 148.93, 148.72, 148.58, 141.68, 141.66, 141.15, 140.88, 140.85, 140.50, 140.40, 140.28, 127.91, 127.89, 127.79, 127.72, 127.71, 127.67, 127.63, 127.06, 124.16, 124.08, 123.78, 122.27, 120.14, 120.06, 119.95, 66.00, 65.94.

Elemental Analysis: Found (%) Calculated (%)

C: 95.08 C: 95.46

H: 4.88 H: 4.54

8 Formulae

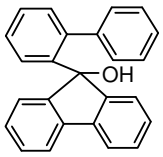

3

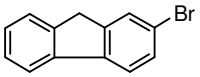

5

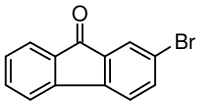

6

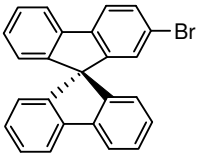

7

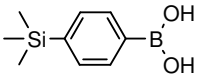

8

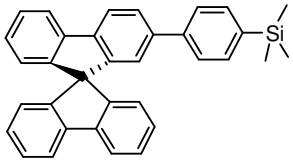

9

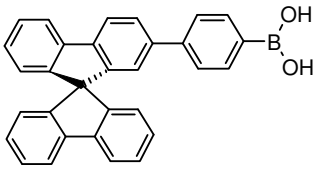

10

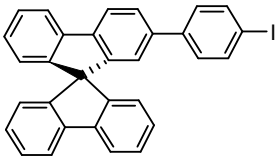

11

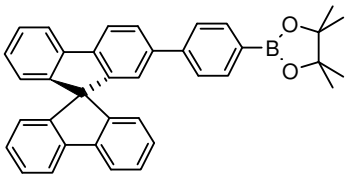

12

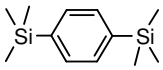

15

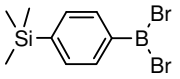

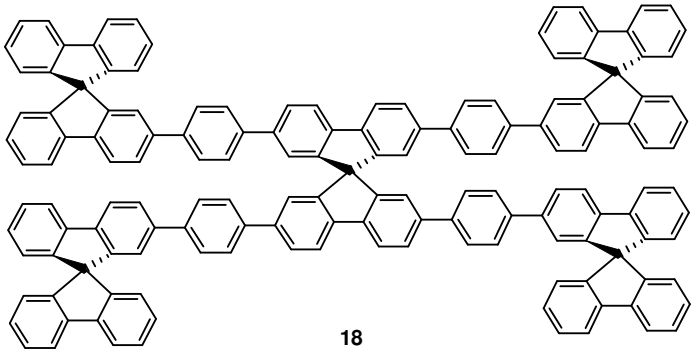

18

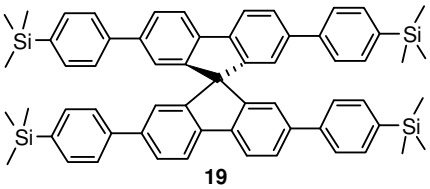

19

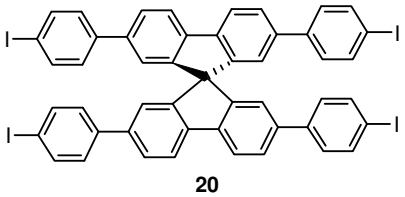

20

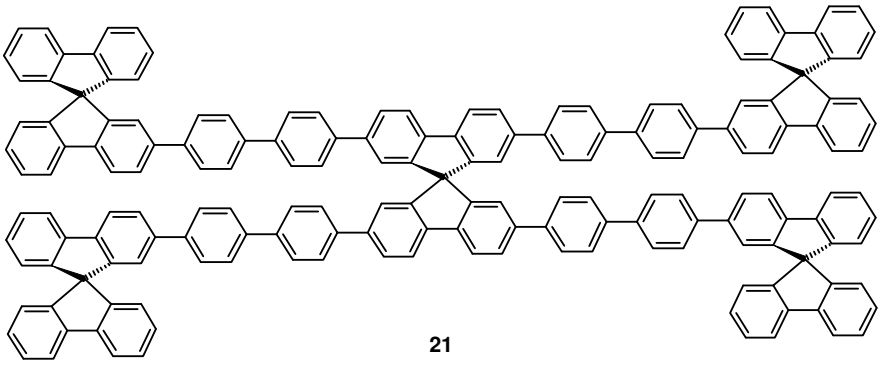

21

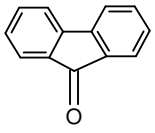

22

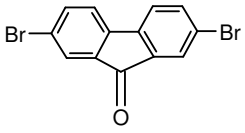

23

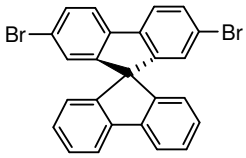

24

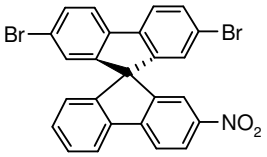

25

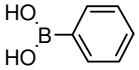

26

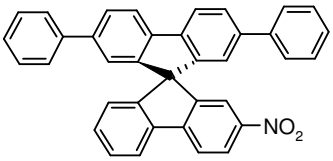

27

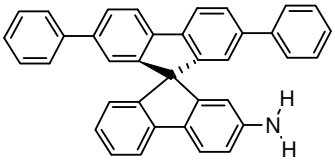

29

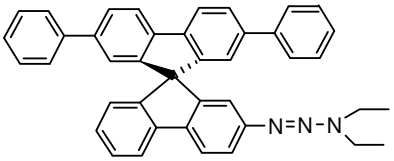

30

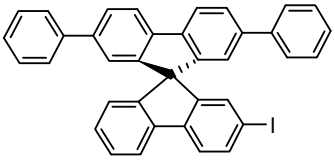

31

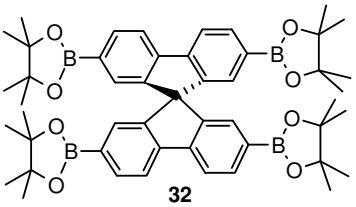

32

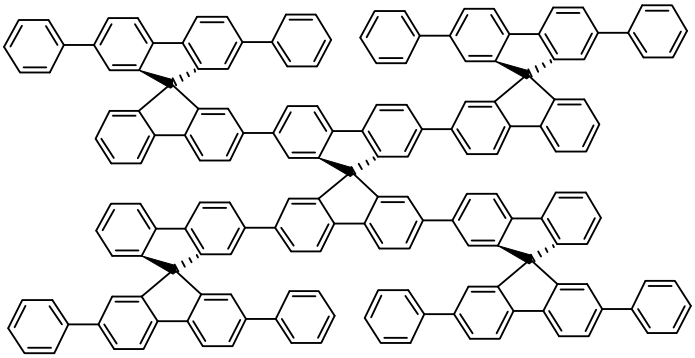

33

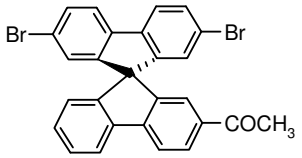

34

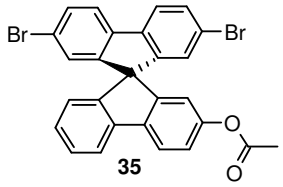

35

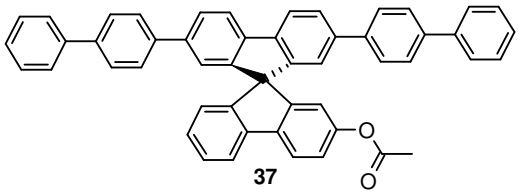

37

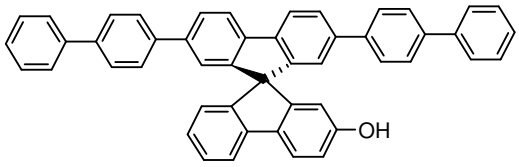

39

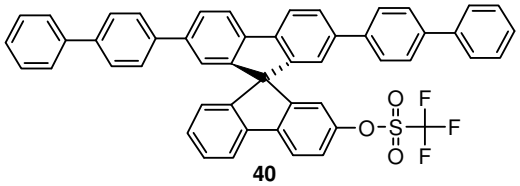

40

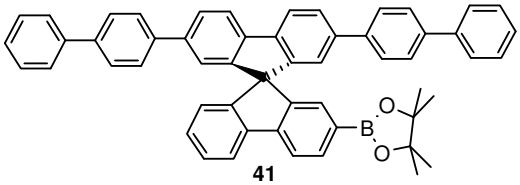

41

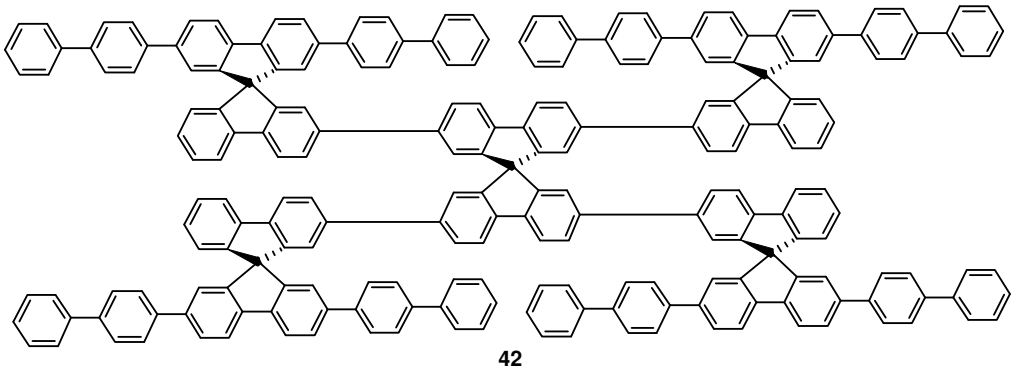

42

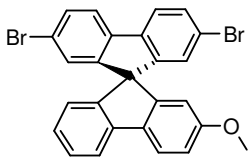

46

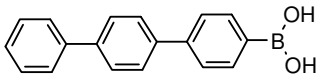

47

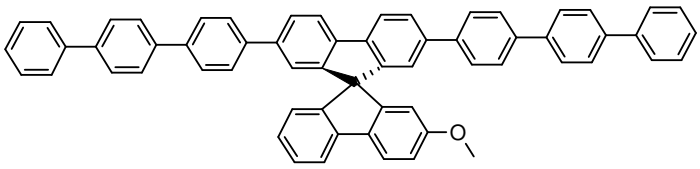

48

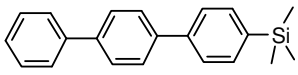

50

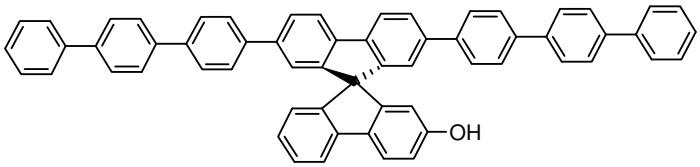

51

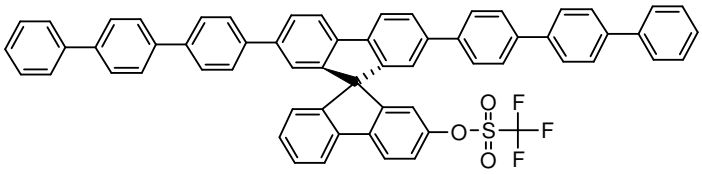

52

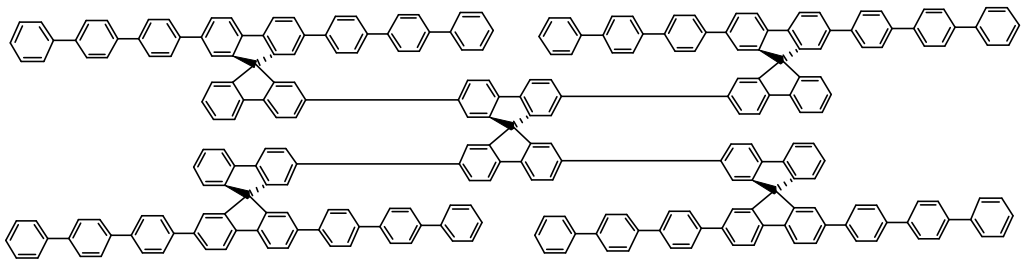

53

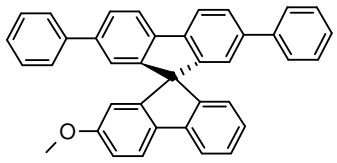

54

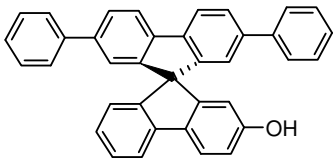

55

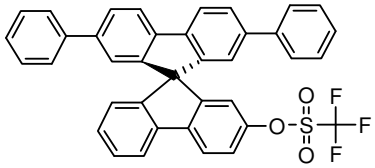

56

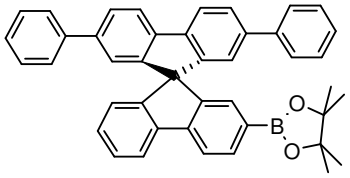

57

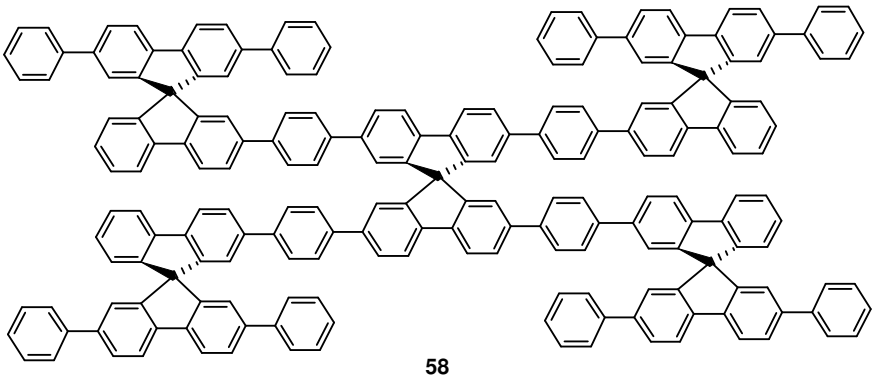

58

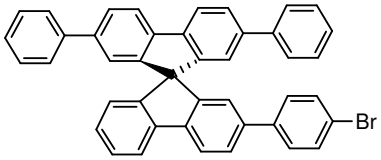

59

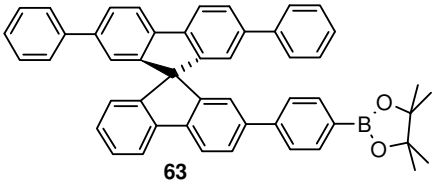

63

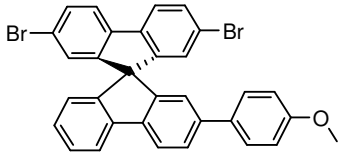

64

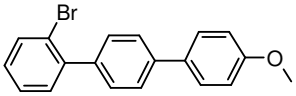

68

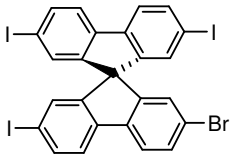

70

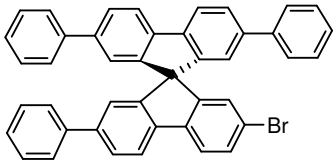

71

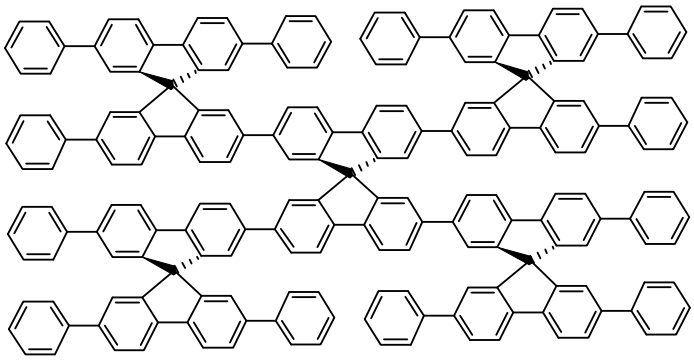

72

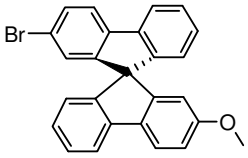

73

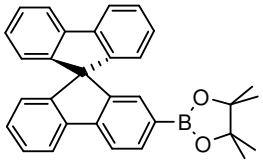

74

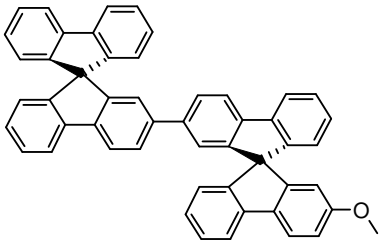

75

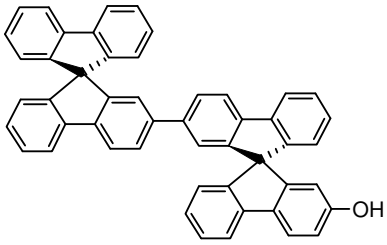

76

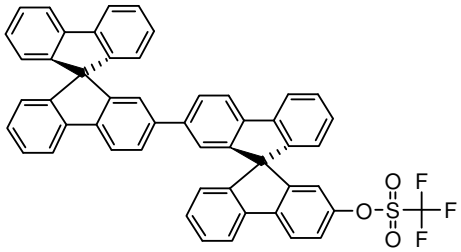

77

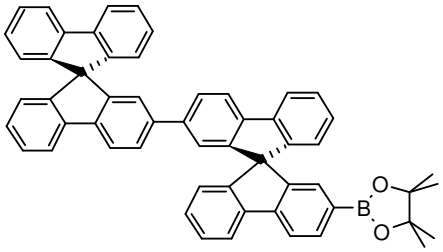

78

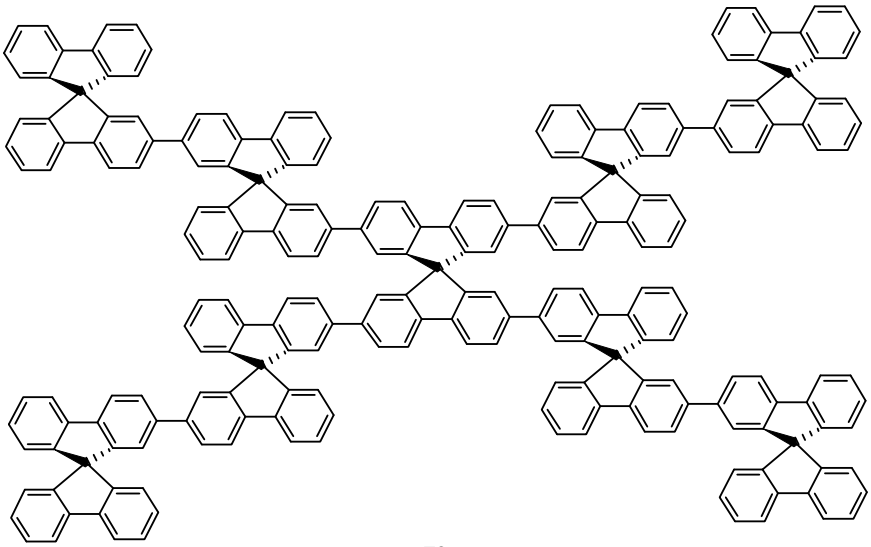

79

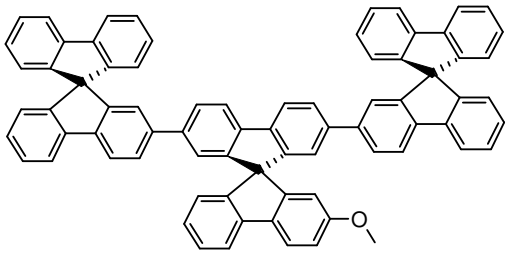

80

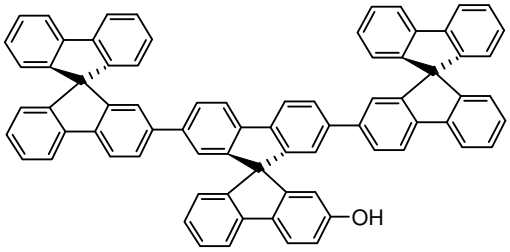

81

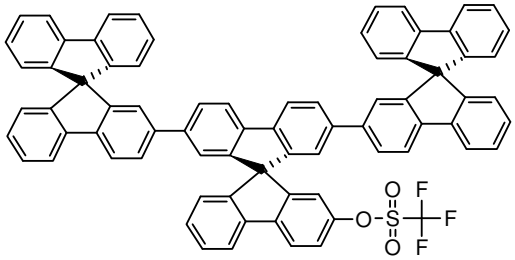

82

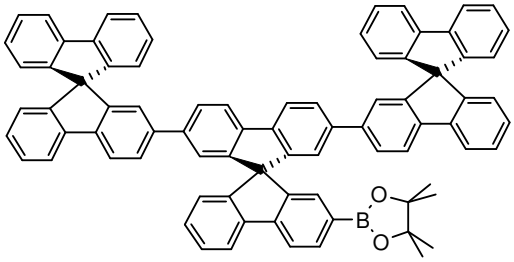

83

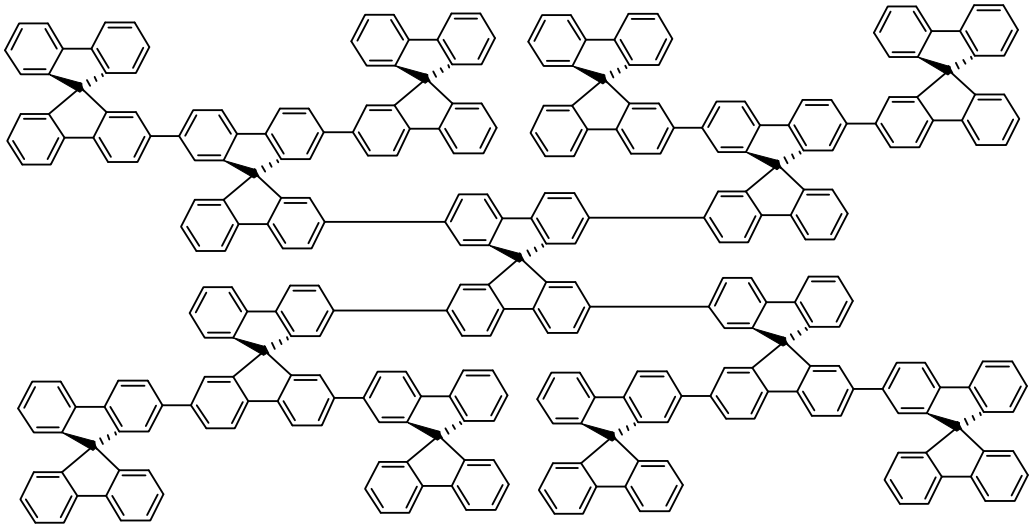

84

9 References

1. S. R. Forrest, Chem. Rev. **1997**, 97, 1793.
2. C. W. Tang, S. A. van Slyke, Appl. Phys. Lett. **1987**, 51, 913.
3. J. Salbeck, in Proc. Symp. Org. Electroluminescence (EL 1996), Eds : R H Mauch, H E Gumlich, Wissenschaft und Technik Berlin, 243, **1996**.
4. U. Bach, D. Lupo, P. Compte, J. E. Moser, F. Weissoertel, J. Salbeck, H. Spreitzer, and M. Graetzel, Nature (London) 395, 583, **1998**.
5. J. Salbeck, N. Yu, J. Bauer, F. Weissoertel, and H. Bestgen, Synth. Met. 91, 209, **1997**.
6. F. Steuber, J. Staudigel, M. Stössel, J. Simmerer, A. Winnacker, H. Spreitzer, F. Weissoertel, and J. Salbeck, Adv. Mat. 12, 130, **2000**.
7. P. Maslak, A. Chopra, C. Moylan, R. Wortmann, S. Lebus, A. Rheingold, G. Yap, J. Am. Chem. Soc., **1996**, 118, 1471.
8. Ullmanns Encyklopädie der technischen Chemie, 4. Aufl., Verlag Chemie, Weinheim, Bd. 18, 686 **1974**.
9. J. R. Lawrence, G. A. Turnbull, I. D. W. Samuel, G. J. Richards, P. L. Burn, Opt. Lett. **2004**, 29, 869.
10. N. Tessler, AdV. Mater. **1999**, 11, 363.
11. M. D. McGehee, A. J. Heeger, Adv. Mater. **2000**, 12, 1655.
12. I. D. W. Samuel, G. A. Turnbull, Mater. Today **2004**, 7 (9), 28.
13. M. Quillec, Materials for Optoelectronics, **1996**, Kluwer Academic Publishers, Massachusetts USA Examples of optoelectronic components include photocells, solar cells, light-emitting diodes, laser diodes etc.
14. http://www.math.ucr.edu/home/baez/physics/General/Glass/glass.html
15. J. Wong, C. A. Angell, Glass structure by Spectroscopy, **1976**, Madison Aveneue, NY
16. W. Kauzmann, Chem. Rev. **1948**, 43, 219.
17. R. G. Beaman, J. Polym. Sci. **1952**, 9, 470.
18. Pure and Applied Chem. **1985**, vol 57, 1737-1740.
19. (a) H. K. Cammenga, W. Eysel, E. Gmelin, W. Hemminger, G. W. H. Höhne, S. M. Sarge, Thermochim. Acta **1993**, 219, 333.
    (b) G. W. Höhne, H. K. Cammenga, W. Eysel, E. Gmelin, W. Hemminger, Thermochim. Acta **1990**, 160, 1

20. E. Pella, M. Nebuloni, J. Thermal Anal., 3, **1971**, 229.

21. (a) K. Naito, A. Miura, J. Phys. Chem, 97, **1993**, 6240
(b) K. Naito, Chem. Mater, 6, **1994**, 2343.

22. H. O. Wirth, Angew. Makromol. Chem. **1991**, 185/186, 329.

23. W. Kern, H. Wirth, Kunststoffe, Plastics **1959**, 6, 12.

24. V. Baeyer A., Ber. **1900**, 33, 3771.

25. A. Aviram, J. Am. Chem. Soc. **1988**, 110, 5687.

26. M. Hess, H. Meier, B. Zeej, Spektrokopische Methoden in der Organishen Chemie, Georg Thieme Verlag, Stuttgart **1991**,4.

27. W. A. Benjamin, Molecular Photochemistry, New York **1965**.

28. Prof. Dr. B. Valeur, Molecular Fluorescence, **2001** Wiley-VCH Verlag GmbH

29. M. Klessinger, J. Michel, Lichtabsorption und Photochemie organischer Moleküle, VCH, Weinheim, New York, **1990**.

30. S. J. Strickler, R. A. Berg, J. Chem. Phys. **1962**, 37, 814.

31. I. B. Berlman, Mol. Cryst. **1968**, 4, 157.

32. H. O. Wirth, F. U. Herrmann, G. Herrmann, W. Kern, Mol. Cryst. **1968**, 4, 321.

33. A. E. Gillam, D. H. Hey, J. Chem. Soc. **1939,** 1170.

34. P. W. Atkins, Physical Chemistry, Oxford University, Press **2006**.

35. Monatati, Credi, Prode, Gandolfi, Hand Book of Photochemistry, **2006**, CRC Group, Taylor & Francis Group.

36. J. B. Birks, Rep. Prog. Phys. **1975**, 38, 903-974.

37. (a) C. H. Hamann, W. Vielstich, Elektrochemie, Wiley-VCH, 4, **2005**.
(b) V. S. Bagotsky, Fundamentals of Electrochemistry, Wiley-Interscience, 2, **2006**.
(c) P. H. Rieger, Electrochemisty, Chapman & Hall, 2, **1993**.

38. S. Sklenak, J. Dedecek, C. Li, B. Wichterlov, V. G. Vendula, M. Sierka and J. Sauer Angew. Chem. **2007**, 119, 7424 –7427

39. http://www.bza.org/zeolites.html

40. T. Ishiyama, M. Murata, and N. Miyaura, J. Org. Chem., **1995**, 60, 7508.

41. J. Takagi, K. Takahashi, T. Ishiyama, N. Miyaura, J. Am. Chem. Soc., **2002**, 124, 8001.

42. J. J. Li, Name Reactions A Collection of Detailed Reaction Mechanisms, Springer-Verlag Gmbh, **2006**.

43. http://www.organic-chemistry.org/namedreactions/negishi-coupling.shtm

44. http://www.organic-chemistry.org/namedreactions/kumada-coupling.shtm

45. http://www.organic-chemistry.org/namedreactions/stille-coupling.shtm

46. S. P. Stanforth, Tetrahedron, **1998**, 54, 263

47. N. Miyaura, A. Suzuki, Chem. Rev., **1995**, 95, 2457

48. R. Heidenreich, K.Köhler, J. G. E. Krauter, J. Pietsch. Synlett 7, **2002** 1118.

49. A. V. Kramer, J. A. Osborn, J. Am. Chem. SOC. **1974**, 96, 7832.

50. V. Farina, B. Krishnan, J. Am. Chem. SOC. **1991**, 113, 9585.

51. (a) K. Schofield, Aromatic Nitration, Cambridge Univ. Press, **1980**
(b) G. A. Olah, R. Malhorta, S. C. Narang, Nitration-Methods and Mechanism, VCH: New York, **1989**

52. H. Harold, Organische Chemie, Weinheim: Wiley-VCH, **2007**

53. H. A. Muathen, Molecules **2003**, 8, 593-598

54. H. Becker, Organikum-Organisch-chemisches Grundpraktikum, Dt. Verl. der Wiss., Leipzig-Berlin-Heidelberg, **1993**.

55. T. Laue, Namen- und Schlagwort-Reaktionen der Organischen Chemie, Stuttgart : Teubner, **1995**.

56. (a) J. K. Kochi **1957**. "The Mechanism of the Sandmeyer and Meerwein Reactions". J.Am. Chem. Soc. 79 (11): 2942–2948.
(b) H. H. Hodgson **1947**. "The Sandmeyer Reaction". Chem. Rev. 40 (2): 251–277.

57. (a) [1] M. P. Doyle, B. Siegfried and J. F. Dellaria **1977**. "Alkyl nitrite-metal halide deamination reactions. [2] Substitutive deamination of arylamines by alkyl nitrites and copper(II) halides. A direct and remarkably efficient conversion of arylamines to aryl halides". J. Org. Chem. **2000**, 42 (14): 2426–2431.
(b) N. Suzuki, et al. Perkins Trans. I **1987**, 645.

58. W. Huang et al, Org. Lett. **2006**, vol. 8, 2, 203-205.

59. Z. Zhu, J. S. Moore, J. Org. Chem. **2000**, 65, 116.

60. J. S. Moore, E. J. Weinstein, and Z. Wu, Tetrahedron Letters. Vo1.32. No.22 pp 2465-2466.**1991**.

61. A. Siebert, Dissertation, 2009, University Kassel.

62. J. H. Fournier, T. Maris, and J. D. Wuest, J. Org. Chem. **2004**, 69, 1762-1775.

63. R. G. Clarkson, M. Gomberg, J. Am. Chem. Soc., 52, **1930**, 2881.

64. (a) F. K. Sutcliffe, H. M. Shahidi, D. Patterson, J. Soc. Dyers Colour., **1978**, 94, 306
(b) J. Salbeck, D. Lupo, Patent EP 0676461 A2, **1995**.

65. G. Ihlein, F. Schüth, O. Krauß, U. Vietze, F. Laeri, Adv. Mater. **1998**, 10, 1117.

66. (a) M. Bredol, U. Kynast, C. Ronda, Adv. Mater. **1991**, 3, 361.
(b) S. Engel, U. Kynast, K. K. Unger, F. Schüth, Stud. Surf. Sci. Catal. **1994**, 84, 477.
67. I. Braun, M. Bockstette, G. Schulz-Ekloff, D. Wöhrle, Zeolites **1997**, 19, 128.
68. J. Caro, G. Finger, J. Kornatowski, J. Richter-Mendau, L. Werner, B. Zibrowius, Adv. Mater. **1992**, 4, 273.
69. K. Hoffmann, F. Marlow, J. Caro, Adv. Mater. **1997**, 9, 567.
70. F. Weissörtel, Dissertation, 1999, University of Regensburg.
71. O. Diels, Ber. **1901**, 34, 1758.
72. B. W. Werner, F. Diederich, V. Gramlich, Helv. Chim. Acta **1996**, 79, 1338.
73. D. Kaufmann, Chem. Ber. 120, 901-905 **1987**.
74. B. H. Ye, Y. Naruta, Tetrahedron 59, **2003**, 3593–3601.
75. J. M. Tour, R. Wu, J. S. Schumm, J. Am. Chem. Soc. **1990**, 112, 5662.
76. T. P. I. Saragi, T. Spehr, A. Siebert, T. Fuhrmann-Lieker, and J. Salbeck, Chemical Reviews, **2007**, 107, 4.
77. N. Kitamura, H. Mori, T. Yasuda, European Patent Bulletin, **2003**.
78. J. H. Weisburger, E. K. Weisburger, F. E. Ray, J. Am. Chem. Soc., **1950**, 72, 4253
79. K. Wong, Y. L. Liao, Y. C. Peng, C. C. Wang, S. Y. Lin, C. H. Yang, S. M. Tseng, G. H. Lee, and S. M. Peng. Crystal Growth & Design, **2005**, vol. 5, No. 2, 667-671.
80. (a) M. Murata, T. Oyama, S. Watanabe, Y. Masuda, J. Org. Chem. **2000**, 65, 164.
(b) M. Murata, S. Watanabe, Y. Masuda, J. Org. Chem. **1997**, 62, 6458.
81. T. Ishiyama et al. Tetrahedron 57, **2001**, 9813-9816.
82. V. Prelog, G. Haas, Helv. Chim. Acta, 52, **1969**, 1202.
83. L. Mattiello, G. Fioravanti, Synth. Commun., 31, **2001**, 2645.
84. Diederich, Israel Journal of Chemistry, **1992**, Vol 32, pp. 69-77.
85. Prelog, **1979**, Helv. Chim. Acta, 62, 7, 234, 2285, Chirale-Spiros.
86. X. Cheng et al. Tetrahedron 62, **2006**, 8077-8082.
87. V. Hensel, A. D. Schlüter **1997**, Short Communication.
88. Z. Bo, Org. Lett., 6, 20, **2004**, 3485-3487.
89. D. A. Tomalia, V. Berry, M. Hall, D. M. Hedstrand, Macromolecules **1987**, 20, 1164.
90. D. A. Tomalia, A. M. Naylor, W. A. Goddard III, Angew. Chem. **1990**, 102, 119.
91. G. R. Newkome, Z. Yao, G. R. Baker, V. K. Gupta, J. Org. Chem. **1985**, 50, 2004.
92. K. Onken, Dissertation, **2007**, University of Kassel.
93. T. Spehr, Dissertation, **2007**, University of Kassel.

94. K. H. Weinfurtner, F. Weissörtel, G. Harmgarth, J. Salbeck, Proc.SPIE-Int. Soc. Opt. Eng. **1998**, 3476, 40.

95. H. Suzuki, Bull. Chem. Soc. Jap. **1960**, 33, 109.

96. I. B. Berlman, H. O. Wirth, O. J. Steingraber, J. Phys. Chem. **1971**, 75, 318.

97. N. I. Nijegorodov, W. S. Downey, J. Phys. Chem. **1994**, 98, 5639.

98. M. J. S. Dewar, J. Chem. Soc. **1952**, 3544.

99. J. N. Murrell, H. C. Longuet-Higgins, J. Chem. Soc. **1955**, 2552.

100. J. Londenberg, Dissertation, **2008**, University of Kassel.

101. A. G. Salbeck, Unpublished Result.

102. F. T. Wallenberger, Angew. Chem. **1964**, 76, 484.

103. (a) G. K. Noren, J. K. Stille, Macromolec. Review **1971**, 5, 385.
(b) J. G. Speight, P. Kovacic, F. W. Koch, J. Macromol. Sci.-Revs. Macromol. Chem. **197**1, C5, 295.
(c) P. Kovacic, M. B. Jones, Chem. Rev. **1987**, 87, 357.

104. M. Matsumoto, T. Nakazawa, V. A. Mallia, N. Tamaoki, R. Azumi, H. Sakai, M. Abe, J. Am. Chem. Soc. **2004**, 126, 1006.

105. (a) J. Salbeck, Inorganic and Organic Electroluminescence /EL96, Berlin, R.H., Mauch, H.E Gumlich, Eds, Wissenschaft und Technik, Verlag: Berlin, Germany, **199**6, p 243.
(b) J. Salbeck, F. Weissöertel, J. Bauer, Macromol. Symp. **1997**, 125, 121.
(c) J. Salbeck, M. Schörner, T. Fuhrmann, Thin Solid Films **2002**, 417, 20.

106. T. Spehr, A. Siebert, T. Fuhrmann-Lieker, J. Salbeck, T. Rabe, T. Riedl, H. H. Johannes, W. Kowalsky, J. Wang, T. Weimann, P. Hinze. Appl. Phys. Lett. **2005**, 87, 161103.

107. T. Hertzsch, J. Hulliger, E. Weber, P. Sozzani, Encyclopedia of Supramolecular Chemistry (eds: J. L. Atwood, J.W. Steed), arcel Dekker, New York, **2004**, 996; D. V. Soldatov, J. A. Ripmeester, Stud. Surf. Sci. Catal. (eds: M. Jaroniec, A. Sayari), **2005**, 156, 37.

108. L. Barbour, L. Dobrzan´ska, O. G. Lloyd, 23rd European Crystallographic Meeting, ECM23, Leuven, **2006** Acta Cryst., 2006. A62, 74.

109. U. Vietze, O. Krauß, and F. Laeri, 81, 21, Phy. Review Lett., **1998**, The American Physical Society.

110. Potential Hydrogen-storage Compound Could Fuel Hydrogen-Powered Cars http://www.sciencedaily.com/releases/2008/04/080402100010.htm

111. J. Pei, J. Ni, X. H. Zhou, X. Y. Cao, and Y. H. Lai Journal of Organic Chemistry, 67, 14, 4924-4936, **2002**.

112. T. M. Miller, T. X. Neenan, R. Zayas, H. E. Bair, Journal of the American Chemical Society, **1992**, 114, 1018-1025.

113. A. C. Spivey, C. M. Diaper, and H. Adams, J.Org.Chem. **2000**, 65, 5253-5263.

114. H. F. Bettinger, Royal Society of Chemistry, Org. Biomol. Chem., **2008**, 6, 1201-1207.